UNIVERSITY OF SOUTHAMPTON

FACULTY OF MEDICINE

Human Development and Health

PLACENTA SENSING OF, AND RESPONSES TO THE MATERNAL ENVIRONMENT

by

Mildrey Mosquera Escudero

Thesis for the degree of Doctor of Philosophy

September 2016

UNIVERSITY OF SOUTHAMPTON

ABSTRACT

FACULTY OF MEDICINE

Human Development and Health

Thesis for the degree of Doctor of Philosophy

PLACENTA SENSING OF, AND RESPONSES TO THE MATERNAL ENVIRONMENT

Mildrey Mosquera Escudero

The placenta's ability to sense the maternal environment may be necessary for adapting placental function to meet the needs of the growing fetus. The broader aim of this study was to identify mechanisms that could be involved in sensing which may act in addition to, or in conjunction with, established mechanisms such as the mTOR pathway. This was explored in two systems, a mouse model of maternal high-fat diet and metformin treatment and placentas from human cohorts.

In the mouse model of maternal high-fat diet and metformin treatment, the two conditions were shown to have distinct effects on the placenta, indicating that they were acting via independent sensing pathways. RNA sequencing data demonstrated that maternal metformin treatment affected metabolic and transport pathways in the mouse placenta.

To explore whether the effects of maternal metformin treatment on the placenta were direct, or mediated via effects on the mother, an in vitro model of metformin exposure was developed. Effects of metformin in vitro showed marked differences from those observed in vitro raining question about whether the effects observed in vitro were direct.

Expression of the fat mass and obesity associated (FTO) gene was shown to be related to birth weight in placentas from the Southampton Women's Survey, but FTO expression was not altered in SGA babies compared to controls. To investigate whether FTO acted via regulation of microRNA, knock down experiments were performed followed by microRNA sequencing.

Placental adaptation to the maternal environment is a complex process that is mediated by different sensing pathways in the placenta. Future studies need to distinguish between direct and indirect effects on the placenta and to focus on specific pathways via which signals may be mediated.

Table of Contents

List of Tables

List of Figures

DECLARATION OF AUTHORSHIP

I, Mildrey Mosquera Escudero

declare that this thesis and the work presented in it are my own and has been generated by me as the result of my own original research.

"PLACENTA SENSING OF, AND RESPONSES TO MATERNAL ENVIRONMENT"

I confirm that:

1. This work was done wholly or mainly while in candidature for a research degree at this University;
2. Where any part of this thesis has previously been submitted for a degree or any other qualification at this University or any other institution, this has been clearly stated;
3. Where I have consulted the published work of others, this is always clearly attributed;
4. Where I have quoted from the work of others, the source is always given. With the exception of such quotations, this thesis is entirely my own work;
5. I have acknowledged all main sources of help;
6. Where the thesis is based on work done by myself jointly with others, I have made clear exactly what was done by others and what I have contributed myself;
7. Part of this work have been published as:
   Barton, S. J., Mosquera, M., Cleal, J. K., Fuller, A. S., Crozier, S. R., Cooper, C., Godfrey, K. M. (2016). Relation of FTO gene variants to fetal growth trajectories: Findings from the Southampton Women's survey. *Placenta, 38*, 100-106.

Signed: .....

Date: .....

Acknowledgements

These PhD has been possible thanks to my family, friends and colleges that helped me in different ways during this period.

I would like to thank my supervisors Dr. Rohan Lewis and Dr. Jane Cleal for your constant support and patience. For putting some humour in the difficult meetings and helped me when I was stuck in the writing. I really appreciate it.

To David Wilson for being my adviser and friend specially in the most difficult moments, coffee will usually sort everything out.

Para mi familia, a mi mamá que me llamó día a día por 4 años, esas llamadas me iluminaron los días y me ayudaron a poner todo en perspectiva, hablar contigo me permitía pensar en voz alta y darme cuenta que podía hacer, gracias por entenderme tanto y saber que en ocasiones no había necesidad de consejos sino presencia. A mi papá que me mantenía concentrada y me recordaba siempre la razón de estar acá especialmente por aconsejarme que mantuviera la calma cuando realmente lo necesitaba. A Mayra, Maritza, Serge y Michelle, las conversaciones cortas o largas, los mandados o encartes, los mensajes, los chistes, los chocolates, las fotos, cada uno de ellos contribuyó a mantenerme fuerte y contenta en la distancia.

To my friends, the new ones and the old ones, getting your messages, your calls, seeing you once in while was an extra source of energy, thanks for being there.

To my colleges from the placenta lab, all the help, advice and funny stories made my PhD easier.

Lastly, I would like to thanks Colciencias and the Universidad del Valle for their funding.

Definitions and Abbreviations

Abbreviation	Definition
$25(OH)D_3$	25-hydroxy vitamin D
AC	Abdominal circumference
AMP	Adenosine monophosphate
AMPK	5'adenosine monophosphate-activated protein kinase
BM	Basal plasma membrane
BMC	Bone mineral content
BMI	Body mass index
BPD	Biparietal diameter
cDNA	Complementary DNA
Cp	Crossing point
CRF	Corticotropin-releasing factor
CRF-BP	CRF-binding protein
CRL	Crown to rump length
Ct	Cycle threshold
DMEM	Dulbecco's modified Eagle's media
DMSO	Dimethyl sulfoxide
DNA	Deoxyribonucleic acid
DNTM	DNA methyltransferase
DOHaD	Developmental origins of health and disease
DXA	Dual X-ray absorptiometry
ER	Endoplasmatic reticulum
FA	Fatty acid
FABPpm	Fatty acid binding protein
FAME	Fatty acid methyl esters
FAT/CD36	Fatty acid translocase
FATP	Fatty acid transporter protein
FBS	Fetal bovine serum
FGF	Fibroblast growth factor
FL	Femur length
FTO	Fat mass and obesity associated gene
GH	Growth hormone
GH-RH	Growth hormone-releasing hormone
GM	Geometrical mean
GnRH	Gonadotropin releasing-hormone
HC	Head circumference
hCG	Human chorionic gonadotropin
HEK 293	Human embryonic kidney cells 293
HMGR	3-hydroxy-3-methyl-glutaryl Coa reductase

hPL	Human placental lactogen
h	Hours
ICM	Inner cell mass
IGF	Insulin-like growth factor
IGF-BP	IGF-binding protein
IL	Interleukin
Insig1	Insulin-induced gene 1
IUGR	Intrauterine growth restriction
LGA	Large for gestational age
LPL	Lipoprotein lipase
m^6A	N6-methyladenosine
M-MLV-RT	Moloney murine leukemia virus reverse transcriptase
MC	Mock control
MEF	Mouse embryonic fibroblast
miRNA	Micro RNA
min	Minutes
mRNA	Messenger RNA
mTOR	Mechanistic target of rapamycin
mTORC	Mechanistic target of rapamycin complex
MVM	Microvillous plasma membrane
NAD	Nicotinamide adenine dinucleotide
NAM	Nicotinamide
NC	Negative control
NCX1	Sodium-calcium exchanger protein 1
NEC	No enzyme control
NEFA	Non-esterified fatty acid
nt	Nucleotides
NTC	No template control
PBS	Phosphate-buffered saline
PC	Positive control
PCR	Polymerase chain reaction
PGH	Placental growth hormone
PL	Phospholipids
PMCA	ATPase plasma membrane Ca2+ transporting
PTH-rp	Parathyroid hormone-related peptide
qPCR	Quantitative polymerase chain reaction
rMEF	Radiated mouse embryonic trophoblast
RNA	Ribonucleic acid
RNAse	Ribonuclease
rRNA	Ribosomal RNA
RT	Room temperature
RT-PCR	Reverse transcription polymerase chain reaction

RXRα	Retinoid X receptor alpha
sec	Seconds
Scap	SREP cleavage-activating protein
SD	Standard deviation
SEM	Standard error of the mean
SGA	Small for gestational age
siRNA	Small interfering RNA
SIRT	Sirtuin
SNP	Single nucleotide polymorphism
SPE	Solid phase extraction
SREPB	Sterol regulatory element binding protein
SWS	Southampton Women's survey
TBE	Tris borate EDTA buffer
TGF-β	Transforming growth factor-β
TG	Triglycerides
TNF-α	Tumour necrosis factor alpha
TS	Trophoblast stem cells
TXNIP	Thioredoxin interacting protein
UTC	Untransfected cells
UV	Ultraviolet
V	Volts
VDR	Vitamin D receptor
VEGF	Vascular endothelial growth factor

CHAPTER 1 INTRODUCTION

1.1 INTRODUCTION

Placental function is a key determinant of fetal growth, which has lifelong health consequences. The placenta is believed to respond to both maternal and fetal signals in order to regulate fetal growth. Maternal signals are thought to reflect the mother's capacity to support the pregnancy while fetal signals may represent fetal growth potential. What these signals are and how they are identified by the placenta are not well understood. How the placenta develops and functions during normal pregnancy has been partially characterised and some of the mechanisms that are involved in the regulation of placental function have been identified. How the placenta senses changes to the environment via these mechanisms as well as potential new pathways involved in the regulation of placental function needs to be investigated.

The placenta acts as a barrier between the maternal and fetal circulation and mediates endocrine and transport functions [1]. During pregnancy, fetal development depends on the placenta's ability to transfer nutrients, oxygen and hormones to the fetus from the maternal circulation while exchanging waste products in the opposite direction. The placenta also needs to respond to the modifications in the maternal environment and the plasticity of the placenta is an important feature of a successful pregnancy. Understanding how the placenta adapts to maternal and fetal cues could help to improve maternal and fetal health during the pregnancy.

Epidemiological studies have shown that during pregnancy exposure to nutrient restriction could increase the probability of developing a chronical non-communicable disease in adult life [2]. Also during pregnancy exposure to other situations such as smoking, exercise or diseases could affect fetal development and have an effect later on during adult life. This theory known as developmental origins of health and disease (DOHaD) proposes that certain diseases have their origins during gestation [3]. The DOHaD theory suggests that early exposure to negative situations could change the structure, function and metabolism of the body producing the first cue for the development of a chronical disease [4]. The possibility that the risk of developing a disease is established during the early stages of development has a great impact on

public health strategies. The development of new interventions to reduce negative exposures during pregnancy in order to improve fetal and maternal health could have a lifelong impact [2,5].

The design of interventions involves the understanding of the associations between the intrauterine environment during pregnancy and its subsequent effects on the fetus during adult life [5]. Pregnancy is a complex process where the mother must meet the demands for nutrients and oxygen of both herself and her fetus; the placenta is the organ responsible for fulfilling this function. Sensing both the maternal environment and fetal demands and then adapting itself accordingly is the main aim of the placenta (Figure 1.1).

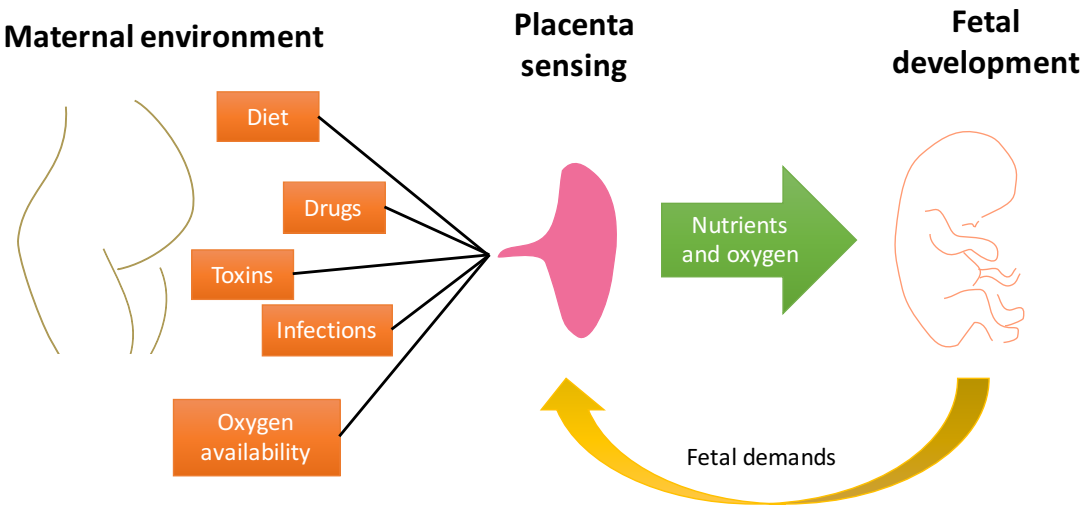

Figure 1.1 Placental function and fetal development

During pregnancy, the placenta has to respond to maternal and fetal signals. The placenta receives the fetal requirements and also senses the maternal nutrients and oxygen availability (as well as the factors that can modify that availability). With that information the placenta modifies its function in order to assure that the fetal supply of nutrients is stable without affecting the maternal ability to provide them.

Placental development and function will be discussed in this chapter. Additionally, the importance of the placenta during pregnancy and fetal growth in the context of the DOHaD hypothesis will be addressed. This chapter aims to outline what is already known about how the placenta senses maternal signals in order to regulate its function.

1.2 DEVELOPMENTAL ORIGINS OF HEALTH AND DISEASE

An altered environment during fetal life can adversely affect the future health of an individual. This hypothesis is known as the DOHaD concept, it proposes that during pregnancy exposure to over or under nutrition, maternal diseases, smoking and stress can increase the risk of developing a non-communicable disease later in life [4,5]. Fetal development can be altered in terms of modified tissue growth, hormonal signalling and tissue function, amongst others. These modifications may initially be to protect the fetus from the external environment when inside the womb. However, such adaptations could have a lifelong effect, especially if during the life course the individual is exposed to unhealthy conditions such as a high fat diet, sedentary behaviour or a high sugar diet. The DOHaD hypothesis also suggests that early intervention has the potential to have a major impact on lifelong health (Figure 1.2) [5-7].

1.2.1 Epidemiological studies

The associations between fetal development and non-communicable disease were first found in retrospectives observational studies. Human cohort studies of people born during the early and middle 1900's showed associations between infant mortality rate and ischaemic heart disease prevalence in adults [8]. These studies also found associations between birth weight and coronary heart disease [9], hypertension[10], glucose intolerance [11] and type 2 diabetes [12] which led to the development of the DOHaD hypothesis. The placenta has also been implicated in the fetal programming as these studies described an association between placenta size and development of hypertension in adult life [10]. These associations have been shown across the normal birth range in different populations from both developed and developing countries [13].

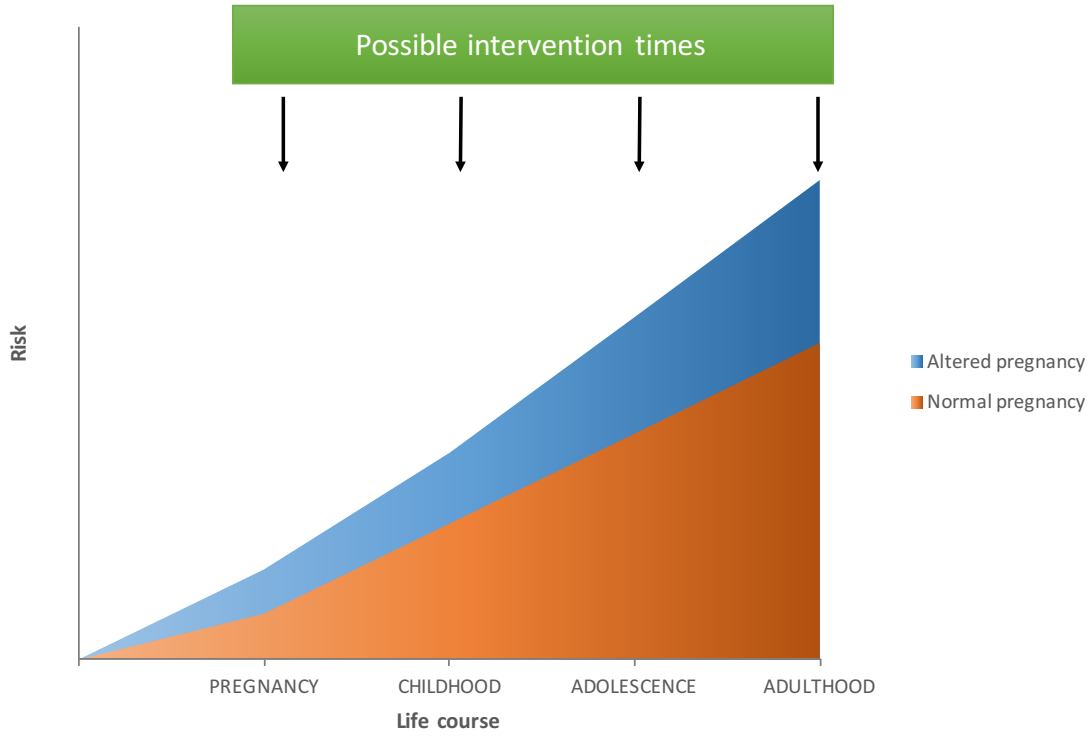

Figure 1.2 Life course approach to development of chronic diseases

The risk of developing a non-communicable disease increases across the life course. An "altered pregnancy" can be one where the nutrients supplied are inadequate or where the mother is exposed to a disease. If an individual is exposed to an unhealthy in utero environment the risk of developing a non-communicable disease is increased across the life course. Early interventions have increased benefits from the preventive point of view since the organism has higher plasticity and the accumulated damage is lower [5].

Demonstration of the relationship between nutritional challenge during fetal development and health in adulthood was the Dutch Hunger Winter 1944-1945. In the Netherlands, during the Second World War, there was a restriction of food availability for over 5 months due to a ban on food transport by the Germans as a reprisal for the support to the allied offensive. Adult populations had access to less than 800 calories per day and pregnant women were unable to cover their nutrient requirements. Nevertheless, professional obstetric care was provided and detailed records of the course of pregnancy and delivery, size and health of the baby were kept [14]. This information formed the basis of a retrospective cohort study of people that were exposed to the famine while in the womb. The studies of this period showed how *in utero* exposure to famine during different periods of the pregnancy produced different effects on the offspring. For example, a lower percentage of boys were born alive in

the whole cohort, especially in the group that was exposed to the famine in late gestation. Whereas, exposure to the famine in middle and late gestation caused a reduction in the weight, length and head circumference of the babies along with a reduction in the placental weight [15].

The exposure to famine during fetal development was also associated with long term consequences in terms of adult health. People exposed to the famine in early gestation showed a higher prevalence of cardiovascular disease in later life [16]. Atherogenic lipid profile, breast cancer and altered blood coagulation were also increased in people exposed to the famine in early gestation [14]. Famine exposure during mid and early gestation had effects on adult health, such as increased risk of obstructive airways disease and glucose intolerance [17,18]. These studies show association between inadequate nutrition during pregnancy, birth weight and lifelong effects. However, they also show that the alterations that occurred during pregnancy are not always associated with birth weight as it was the case of the group that was early exposed to famine. This suggests that birthweight alone is not a good predictor of adulthood disease risk due to fetal adaptations.

Other studies have investigated the effects of maternal nutrition on fetal programming. A similar study was carried out with people that were subjected to nutrient deprivation during the siege of Leningrad (1941-1944). In this study, people that were born in Leningrad before the siege (Childhood exposure) were compared with people born during the siege (Intrauterine exposure) as well as to people born in the same period of time but outside of the siege area (Unexposed group). No differences were found in glucose tolerance, insulin concentration, blood pressure and lipid concentration between the groups [19]. The different results between the Netherlands famine and the Leningrad study might be explained by the differences in the duration of the starvation period, while in the Netherlands the reduction in rations lasted 5 months and adequate diet was established soon after it ended, in Leningrad the siege lasted 28 months. So in Leningrad, people exposed to malnutrition in early and mid-gestation were exposed to a postnatal malnutrition as well. Meanwhile, in the Netherlands famine postnatal nutrition was normal [19].

Short periods of fasting have been also studied in pregnant women during the Ramadan. In Muslim populations, there is an annual period of day-time fasting during a month for religious reasons (Ramadan). Studies of pregnancies that occurred during the Ramadan period have shown an increase in maternal cortisol levels during the fasting period [20]. There is also a decrease in placental weight and placenta/birth weight ratio in pregnancies that went through Ramadan during the second or third trimester of the pregnancy [21] and a reduction in fetal growth during the fasting period [22]. These studies showed how nutrient restriction can affect placental and fetal growth and have a later effect in life. Additionally, these studies provide evidence that the timing of the exposure during pregnancy has differential effects on fetal development.

This current study utilizes data from The Southampton Women's Survey (SWS), which is a prospective cohort that has been established to examine how the maternal and intrauterine factors interact with the offspring's genes and postnatal environment [23]. The study collected data of non-pregnant female patients between 1998 and 2002 and characterised the initial population and the women who then became pregnant. The children from this study have subsequently been followed up also. This cohort study has helped to establish relationships between maternal nutrient status, before and during pregnancy, intrauterine development and child development and health [23]. In the SWS cohort, maternal plasma polyunsaturated fatty acid levels in late pregnancy were positively associated with fat mass in the offspring at 4 years and 6 years [24]. Decreased maternal vitamin D levels were associated with a reduction in fat mass in the offspring at birth and with an increased of fat mass later in childhood (4 and 6 years) [25]. This suggests a relationship between offspring body composition and maternal nutrient status. Other evidence indicates that neonatal body composition can be established during pregnancy. For example, late intrauterine growth could act as a predictor of skeletal growth and mineralisation at birth and that early intrauterine growth could help to predict skeletal status at 4 years of age [26,27]. These findings indicate a potential mechanism for how fetal growth could be affected during pregnancy by maternal conditions.

In order to understand how fetal development was influenced by maternal conditions, the relationships between placental size and function and fetal growth were investigated in the SWS. This showed that placental volume at the beginning of the pregnancy was associated with neonatal bone mass [28]. Interestingly, it was also found that placental amino acid gene transporter expression was positively correlated with maternal serum vitamin D levels [27]. All these associations suggested a potential mechanism of how placental adaptations to the maternal environment could modify fetal development and subsequent health.

1.2.2 Animal models and DOHaD

Animal models have been developed to investigate the mechanisms linking an altered maternal environment to the offspring phenotype in the context of the DOHaD hypothesis. Maternal nutrient restriction in pregnant rats produced vascular dysfunction and hypertension in a sex-related manner in the offspring [29,30]. In mice chronic protein restriction during pregnancy affected fetal growth and produced a smaller placental junctional zone [31]. Whereas exposure to a high fat diet during pregnancy in mice up-regulated nutrient transport in the placenta and increased fetal growth [32]. Modification of nutrient availability during pregnancy has been associated with alterations in the offspring including changes in expression of key genes, methylation patterns, birth weight, and cardiovascular function [33]. These associations have been used to help understand fetal programming and the effects that different exposures might have on placental function and fetal development [34].

The maternal environment has a strong influence on fetal development and placental function. Understanding how the placenta adapts to maternal conditions in order to sustain the pregnancy will help to design specific interventions aimed at preventing altered fetal development and improving the health of mother and baby. This information will also lead to the identification of potential biomarkers that highlight those exposed to adaptations during pregnancy and therefore at increased risk of disease during postnatal life.

1.3 EMBRYONIC AND FETAL DEVELOPMENT

Normal human gestation lasts between 38 to 41 weeks. Fertilisation usually occurs in the oviduct and the fertilised ovum is transported to the uterus where it implants and continues its development. Pregnancy has two stages the embryonic stage that lasts around 8 weeks and the fetal stage from 8 weeks until birth [35].

1.3.1 Embryonic stage

During the embryonic stage, the embryo is mainly increasing the cell mass. Cells differentiation is driven by paracrine signalling [3,36]. At day 4 of pregnancy, the embryo has reached the uterus and the implantation starts. At that point the embryo is in the morula stage, cells are polarised, with a small group of internal cells (inner cell mass) that will produce the fetus and the external cells that become the trophoblast that will produce the placenta (placental development will be addressed later on in this chapter). The origin of the different mammalian tissues is shown in Figure 1.3. The inner cell mass (ICM) forms the hypoblast layer that will produce the yolk sac. The remaining ICM is the epiblast layer. The epiblast will generate the amnionic ectoderm and the embryonic epiblast (Figure 1.3) [37]. Initially, the embryo and later the fetus will go through periods of rapid growth during pregnancy, however it is difficult to predict when these periods will happen in the pregnancy [38].

1.3.2 Fetal stage

In the fetal stage, the growing fetus will undergo periods of development where specific tissues are developing and growing. Cell division depends on nutrient and oxygen availability. Therefore, a decreased rate of cell division during pregnancy can be produced by nutrient deficiency or by altered concentration of growth factors and hormones [39]. If a decrease in fetal nutrient and oxygen delivery occurs during a period when a specific tissue is developing it can, in theory, alter the rate of cell production and therefore reduce the amount or type of cells in that specific tissue.

In utero modifications of fetal growth can produce changes in the distribution of cell types, in the hormonal feedback, or metabolic pathway activity and organ structure [40].

Determining tissue alterations during fetal development is not easy. Ultrasound measurements during pregnancy to monitor fetal growth and anthropometric measures after birth are the most common methods that are used to diagnose modifications in fetal development but it has a low capacity to detect tissue-specific alterations [41]. Small for gestational age (SGA), large for gestational age (LGA) and intrauterine growth restriction (IUGR) are three of the terms used to describe alterations in fetal development.

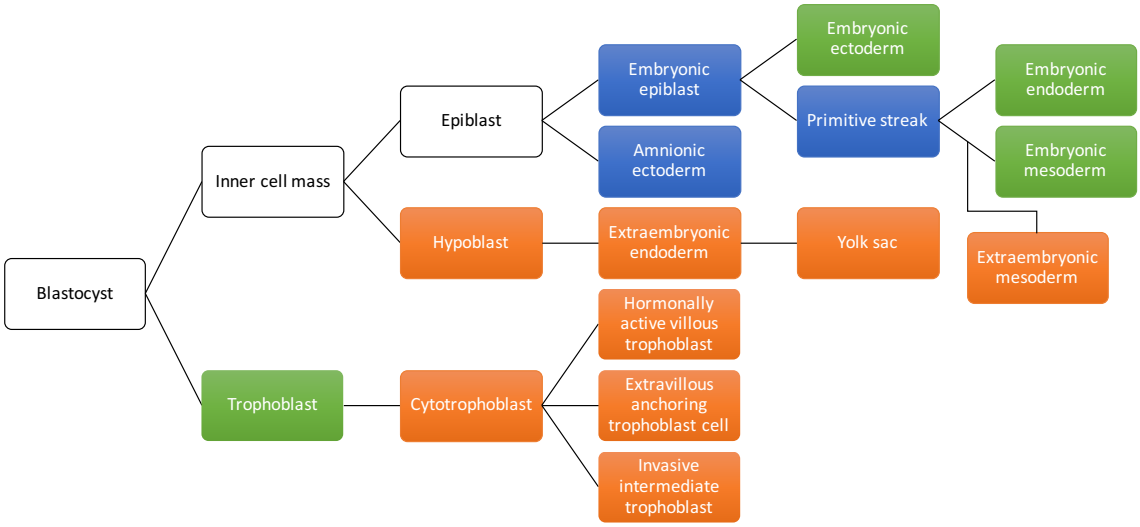

Figure 1.3 Derivation of tissues from the human blastocyst

The blastocyst will produce all the cell lines that form the extraembryonic tissues (orange boxes) such as the placenta and the yolk sac and also produce the embryonic tissues (green boxes), ectoderm, endoderm and mesoderm that will form the fetus. Modified from [37].

1.3.3 Altered fetal development

Since birth weight is relatively easy to measure and it marks several aspects of fetal development, it has become the primary indicator of fetal growth when combining with gestational age [42]. Birth weight percentiles charts have been produced to assess whether an infant is appropriately grown for its gestational age [43]. Pregnancy can be classified according to its duration as preterm (less than 37 weeks), term (between 37 weeks to 41 weeks) and post-term (more than 41 weeks). Birth weight, length, head and abdominal circumference are used with the percentiles charts in order to determine a retardation in fetal development during pregnancy [42,43]. However, birth weight and other growth measures might just reflect genetic factors, environmental or

maternal conditions instead or pathological process and they can be SGA babies that have a lower risk of developing complications. The distinction between SGA and IUGR babies is usually made when indications of a pathological process during the pregnancy can be established [43].

1.3.3.1 Intrauterine growth restriction

IUGR refers to a reduction in fetal growth rate compared with the rate estimated for that specific infant. IUGR it can also be defined as a situation where a fetus does not reach its genetic growth potential [41]. Factors that have been related to the development of IUGR are listed in Table 1.1. [38]. Prevalence of IUGR varies between 5% to 55% around the world with higher prevalence in the poorer countries. Identification of an IUGR baby is not always easy and is made using birth weight combined with others anthropometrical measures such as biparietal diameter, head and abdominal circumference. Nevertheless, some cases of IUGR can be misdiagnosed as SGA babies [38,44].

Altered fetal development has been shown to influence the development of the heart and the vascular tree [45,46]. It has also been associated with alterations in glucose transporter expression or activity and insulin metabolism in different tissues [39,47]. Prevention of IUGR could help to improve the success of the pregnancy and adulthood health.

1.3.3.2 Large for gestational age

Infants with a birth weight higher than the 90th percentile for their gestational age or more than 4000 g are considered LGA babies. LGA or macrosomia classification is still difficult to determine since it can include children that are just genetically predisposed to be big [48]. Factors such as maternal pre-gravid weight, maternal obesity, age and parity and diabetes mellitus, have been associated with LGA [48]. LGA is associated with several complications in the pregnancy such as prolonged labour, emergency caesarean section and post-partum haemorrhage [49]. LGA has been associated with obesity, insulin resistance, and impaired glucose tolerance [50,51].

In this context, placental adaptations to the environment can have deleterious effects on the fetus. An excess in nutrient supply has detrimental consequences to the baby's health and later on in adult life.

Table 1.1 Common causes of intrauterine growth restriction

IUGR origin	Most common causes
Maternal	Smoking
	Age
	Substance abuse
	Height and weight
	Parity
	Inter-pregnancy interval
	Assisted reproductive technologies
	Malnutrition
	Pregnancy-related pathological conditions (preeclampsia, gestational diabetes)
Environmental	Altitude
	Poverty
	Developing countries
Placental	Placental dysfunction
	Abnormal uteroplacental vasculature
	Decidual or spiral arteries arteritis
	Avascular villi
	Placental hemangioma
	Single umbilical artery
	Chronic inflammatory lesions
	Placental infections
Fetal/genetic	Chromosomal abnormalities
	Genetic syndromes
	Major congenital abnormalities
	Multiple gestation
	Congenital infections
	Metabolic disorders

IUGR: Intrauterine growth restriction. From [38,44,47]

1.3.4 Regulation of fetal growth

Fetal growth is regulated by the baby's genetic potential, the mother's ability to support the pregnancy and placental function. A combination of all of these factors will act via signals, such as hormones, to assure and regulate the supply of nutrients and oxygen to the fetus without affecting the mother. Fetal growth, as indicated by birth weight, can also be limited by different maternal and uteroplacental factors such as; maternal size, under or over-nutrition, infections and alcohol/cigarettes consumption [52]. Fetal growth is regulated by constitutional factors such as genes, hormones and uterine constraint among others [48].

Fetal growth is genetically determined by factors such as fetal genotype and sex [53]. Male babies are on average heavier than females babies and usually, have larger placentas [54]. Other constitutional factors are maternal size, with the maternal height being positively correlated with birth weight [55]. Maternal parity is also related to fetal size, with mothers who deliver LGA or SGA babies in a previous pregnancy showing a stronger possibility of having another child with the same condition [48].

Additionally, fetal growth is control by hormonal regulation. Placental and fetal hormones are directly involved in the control of fetal growth. Whereas, maternal hormones indirectly influence fetal growth by ensuring adequate nutrient levels, maintaining cardiovascular homoeostasis and adequate uteroplacental blood flow [56]. The fetus is mainly autonomous from the hormonal point of view as most of the maternal hormones are unable to cross the placenta [56]

1.3.4.1 Insulin

Insulin is one of the most important fetal hormones related to intrauterine growth [56]. Fetal insulin deficiency caused by pancreatectomy reduced the body weight, limb length and crown to rump length in sheep by approximately 40%. This growth restriction could be restored to normal with an insulin replacement treatment [57]. There is also a positive correlation between plasma insulin levels and fetal weight in several species such as pig, sheep, rat. Insulin effects in the prenatal period are different to the effects during the postnatal period. In the fetus, glucose levels are kept

relatively constant producing a pancreatic insensitivity to the glucose concentrations and a major sensitivity to amino acid levels, in the postnatal period, the pancreas release insulin as a respond to glucose levels [56]. Fetal insulin as an anabolic hormone contributes directly to fetal growth by activation of synthesis pathways within the cells, but also indirectly by stimulating others growth factors such as IGF-I [56].

1.3.4.2 Thyroid and fetal growth hormone

Thyroid hormones are essential for normal fetal growth [58]. During pregnancy, thyroid hormones are produced by the fetus and they can also be transported by the placenta which can contribute to the fetal levels [58]. In humans, thyroid hormone levels are associated with birth weight and length [59]. In the equine fetus a partial thyroidectomy produced an alteration in the development of the bones and locomotor skills [60]. In sheep, a maternal or fetal thyroidectomy affected body, heart and lung weight and also altered fetal brain development [61]. Indicating that they are essential for normal fetal development.

Fetal growth hormone (GH) levels are higher during pregnancy than after birth with a peak at 20-24 weeks of pregnancy. In rats, fetal GH was shown to increase insulin-like factor binding protein-2 activity and expression in lung epithelial culture suggesting a potential involvement in lung development [62].

1.3.5 Placental regulation of fetal growth

The placenta is the organ that senses the maternal environment and transports nutrients and oxygen to the fetus and it has a central role in fetal programming [2]. The placenta acts as an interface between the mother and the fetus, and as a provider of nutrients and oxygen to the fetus, it is essential to the normal development of the baby [63]. The placenta senses the maternal environment and receives and transmits endocrine signals between the mother and fetus. The way the placenta senses the maternal environment and controls nutrient transport could help to understand how fetal growth is altered during pregnancy. The growing placenta generates hormones for the maternal adaptation to the pregnancy and regulates the nutrient transport

from the maternal circulation to the fetal circulation [64]; these functions will continue until the end of the pregnancy.

An altered maternal environment affects the placenta's ability to transfer nutrients to the fetus. This requires further investigation in order to determine how the placenta adapts to the maternal cues and to the fetal demand so as to maintain a healthy pregnancy. In the following sections, placental development and function and its involvement in fetal development will be addressed.

1.4 PLACENTAL DEVELOPMENT AND STRUCTURE

To support fetal growth, the placenta needs to develop a highly specialised structure. In the following sections the development of human and mouse placenta will be discussed and the placental transport units for both species will be compared.

1.4.1 Human placental development

The development of the placenta is a complex process that starts when the blastocyst implants in the endometrium (day 6 after fertilisation). At that point, the blastocyst has two different cell types, the outer single layer of trophoblast cells that will form the placenta and fetal membranes and an ICM that will form the embryo (Figure 1.4 A). The outer layer of cells in the blastocyst produce the trophoblast stem cells that differentiate into the cytotrophoblast (Figure 1.3). Trophoblast stem cells differentiate into villous or extravillous trophoblast. Villous cytotrophoblast can further differentiate into syncytiotrophoblast. The extravillous trophoblast can become anchoring trophoblast or junctional trophoblast that are involved in the attachment of the placenta to the uterus or invasive intermediate trophoblast that invade the decidua and remodel the uterine spiral arteries [65]. Each type of trophoblast produces a different range of cytokines and proteins that help them to fulfil their function [66].

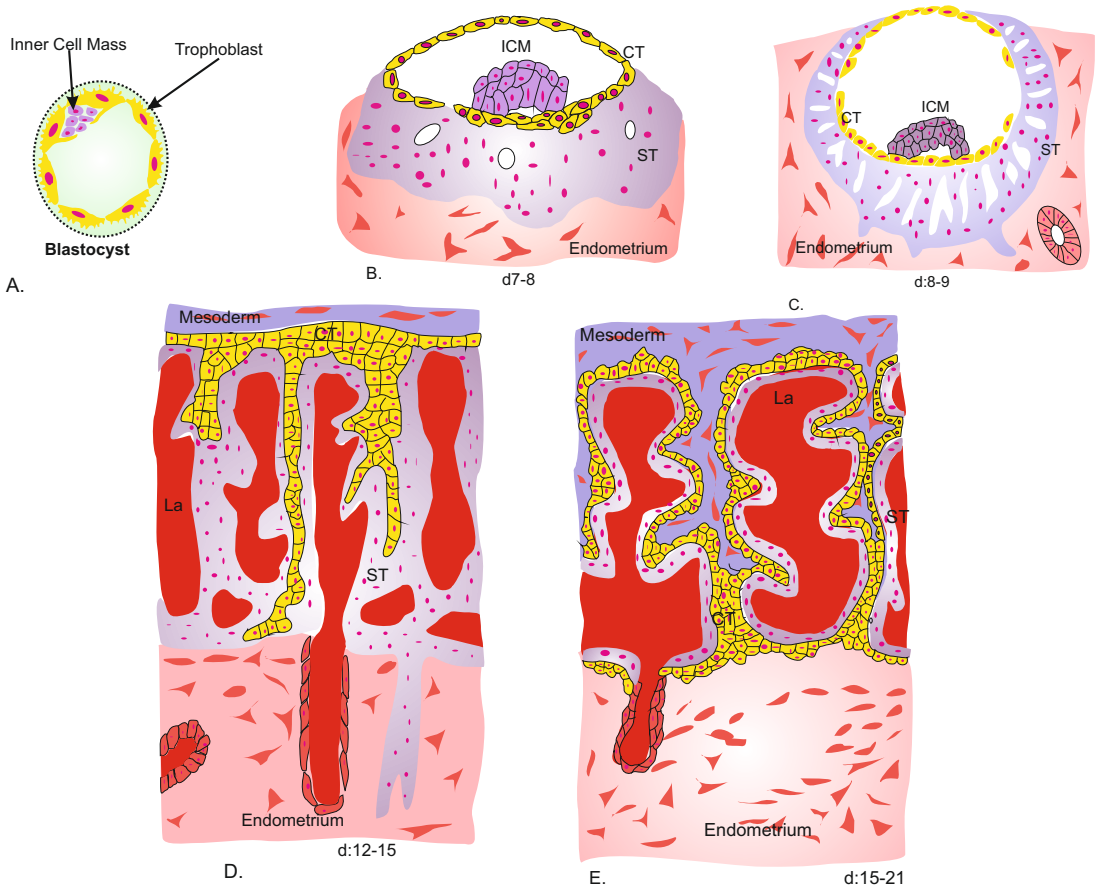

Figure 1.4 Human placental development

A. Blastocyst 6 days post-fertilisation has developed two different cell types, the outer single layer of trophoblast cells that will form the placenta and fetal membranes and an inner cell mass (ICM) that will form the embryo. B. Implantation occurs around 7 days post-fertilisation, the blastocyst attaches to the endometrium and the trophoblast stem cells differentiate into cytotrophoblast (CT) and subsequently to multinucleated syncytiotrophoblast (ST). C. The syncytiotrophoblast forms a layer and spaces (the lacunae or sinuses) begin to form. D. 12 to 13 days post fertilisation, the lacunae fill with maternal blood from the spiral arteries and the syncytiotrophoblast becomes trabecular with the enlargement of the lacunae. E. 15 to 21 days post fertilisation, the formation of the secondary and tertiary villi occur together with the vascularization of the mesoderm. (Modified from Physiology of Reproduction [65]).

Placental formation starts with a pre-lacunar stage at the beginning of the implantation. The trophoblast stem cells differentiate into both cytotrophoblasts that surrounds the ICM of the blastocyst and into a multinucleated syncytiotrophoblast that is in contact with the maternal tissue. The cytotrophoblast rapidly divides and the cells fuse to produce more syncytiotrophoblast to continue to expand into the maternal endometrium (Figure 1.4 B). Around day 8 of pregnancy, the syncytiotrophoblast mass start to develop spaces that will increase in size and fuse

together to produce the lacunae or sinuses that are separated by columns or trabeculae of syncytiotrophoblast (Figure 1.4 C). Day 12 after conception, implantation is considered over and at that stage, the ICM has transformed and the extraembryonic mesoderm has been derived from that cell mass (Figure 1.3). The extraembryonic mesoderm covers the inner part of the cytotrophoblast layer and forms the chorion (Figure 1.4 D) [65].

During the implantation process, the mantle of growing syncytiotrophoblast reaches the maternal capillaries and the venous plexus. The trophoblast cells induce the vessels to dilate and a continue flow of blood is produced between the vessels and the lacunae. After the placenta has reached the lacunar stage (12 days after conception), cells for the primary chronic plate penetrate the trabeculae (Figure 1.4 D), and come into direct contact with the endometrium. These cytotrophoblasts are called extravillous cytotrophoblasts because of their location and function and they migrate into the endometrial stroma between the spiral arteries and uterine glands. These cytotrophoblasts become the interstitial and endovascular trophoblast that helps the spiral arteries to dilated to assure an adequate supply of maternal blood to the placenta [65].

Around day 13 post implantation, the trabeculae start to produce branches that invade the lacunae (Figure 1.4 E), these are the primary villi, and afterwards, the extraembryonic mesoderm invades the trabeculae and the primary villi transforming it into the secondary villi. At day 21 of gestation, fetal capillaries differentiate within the villi mesoderm and signal the formation of tertiary villi. Tertiary villi mass makes up the bulk of the placental tissue. During the first trimester growth of the villous tree is fast, but during the third trimester villi formation and maturation is reduced [65,67].

In humans, the syncytiotrophoblast is the primary barrier for nutrient transport across the placenta and nutrients must be transported across both the maternal facing microvillous plasma membrane (MVM) and the fetal facing basal plasma membrane (BM). All the transport that happens in the placenta will depend on the transporters available in the MVM and BM (Figure 1.5) [68].

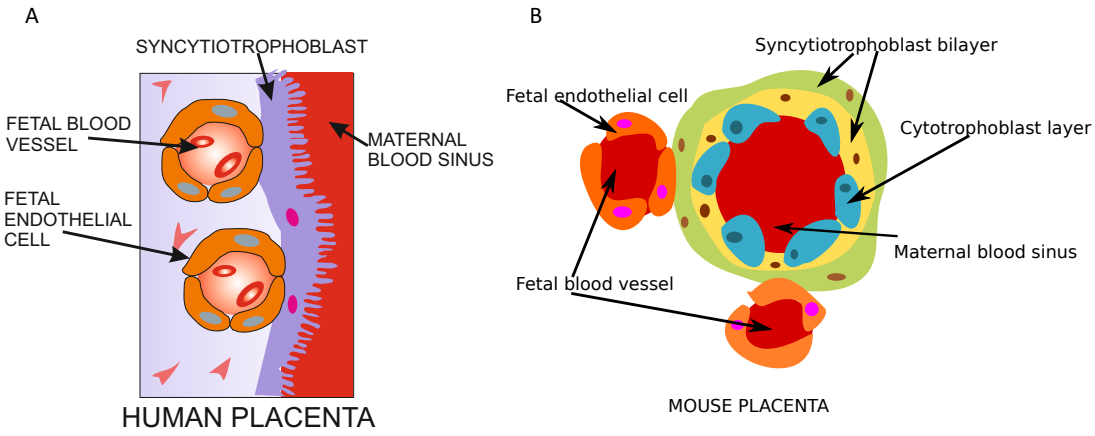

Figure 1.5 Human and mouse placenta exchange unit between the mother and the fetus

A. In human placenta the syncytiotrophoblast and the vascular fetal endothelium layer are the barriers that separate the maternal blood from the fetal blood. B. In mouse placenta, the exchange unit has four layers: vascular fetal endothelium layer, one cytotrophoblast layer and two syncytiotrophoblasts layers that separate the maternal from the fetal blood [69,70].

1.4.2 Mouse placental development

The overall structure and molecular mechanisms involved in the development of human and mouse placenta share some similarities which allows the use of the mouse as a model to study placental function [71,72]. The development of the mouse placenta starts when the blastocyst implants in the endometrium (embryonic day 4.5). At implantation the blastocyst has two cell lineages: the outer trophectoderm epithelium that will form the placenta and the ICM that is inside and will form the embryo [71,73].

In the mouse blastocyst the trophectoderm layer hast two parts, the mural trophectoderm as the layer that is furthest from the ICM and the polar trophectoderm that is closest to the ICM. The mural trophectoderm consists of polyploid cells, the primary trophoblast giant cells (analogous to human extravillous cytotrophoblast cells); these mediate the implantation and invasion processes. Later in pregnancy, the giant cells will produce the hormones and cytokines that help with the physiological adaptation to the pregnancy [73,74]. The polar trophectoderm proliferates as a response to the fibroblast growth factor 4 (FGF4) produced by the ICM and produces diploid extra-embryonic ectoderm and the ectoplacental cone. The extra-embryonic ectoderm

will become the trophoblast cells of the chorion layer and later the labyrinth area of the mouse placenta. The labyrinth development is supported by the spongiotrophoblast that is the layer produced from the ectoplacental cone. The spongiotrophoblast corresponds to the column cytotrophoblast of the human placenta and is a compact layer between the labyrinth and the outer giant cells. Later in gestation, glycogen trophoblast cells differentiate within the spongiotrophoblast and invade the uterine wall [72].

The extra-embryonic mesoderm (allantois) will produce the vascular portion of the placenta (embryonic day 8.5). The allantois extends from the posterior end of the embryo and joins the chorion (chorioallantoic attachment). After that, the chorion begins to fold and produce the villi within the space for the fetal blood vessels to grow from the allantois. The chorionic cells then differentiate into multinucleated syncytiotrophoblast (produced by the fusion of trophoblast cells) that surround the fetal capillaries and mononuclear trophoblast cells that surround the maternal blood sinuses. Inside the labyrinth the fetal vasculature and the trophoblast generate the branched villi similar to that of the human placenta. The placenta will continue growing becoming larger until birth (embryonic day 18.5-19.5) [71,72].

In mice, the transport of molecules between the mother and the fetus occurs through two layers of syncytiotrophoblast cells and an additional layer of mononuclear cells in the maternal blood sinuses (Figure 1.5) [72].

1.5 PLACENTAL FUNCTION

During pregnancy, the placenta is responsible for facilitating the bidirectional transport of nutrients and waste between the mother and the fetus. The placenta also produces hormones to help the mother to adjust to the pregnancy and to help the embryo to develop. It provides defence against the maternal immune system and acts as a structural barrier between maternal and fetal cell traffic [75,76]. In this section, the main processes underlying placental function will be discussed.

1.5.1 Placental nutrient transport

The fetus depends on the placenta for the transfer of nutrients such as glucose, amino acids and lipids from the maternal circulation. The transport of nutrients across the placenta can be by facilitated diffusion, active and passive transport and can be reliant on specific nutrient transport proteins. Nutrient transport across the placenta can be regulated by the availability of nutrients in the maternal circulation, in the placenta and in the fetal circulation [34,77]. Nutrient transport can also be affected by other factors such as transporter number, maternal and fetal blood flow, exchange area and placental metabolism [78].

1.5.1.1 Placental glucose transport

Glucose is the main source of energy for the placenta and the fetus [79]. Glucose is transported from the mother to the fetus by facilitated diffusion using transporters in the MVM and BM of the syncytiotrophoblast [79]. During early gestation the fetus is not able to synthesise glucose, making the maternal supply necessary for the survival of the fetus. Later on in the pregnancy fetal demand for glucose is increased; especially in the third trimester when there is an increase in fetal growth [79]. Glucose transporter proteins (GLUTs) are highly expressed in the MVM and they allow a rapid glucose uptake into the syncytiotrophoblast, however, they are expressed at a lower level in the BM. This difference in expression between both membranes indicates that the BM transport of glucose might be the rate-limiting step in the placental glucose transfer [68,80,81].

In the human placenta, the primary glucose transporter GLUT1 has been found in both membranes of the syncytiotrophoblast [80,82]. GLUT3 is primarily expressed during early gestation in the syncytiotrophoblast [82,83]. Other glucose transporters that have been reported in human placenta are GLUT4 [84], GLUT8 [85], GLUT9 [86] and GLUT10 [87]. Glucose transfer will be limit by the amount of glucose that is transported by the BM to the fetus. It is therefore necessary that the glucose concentration inside the syncytiotrophoblast is similar to the levels in maternal blood [80,81].

1.5.1.2 Placental amino acid transport

Placental amino acid transport is a complex process that involves the exchange of amino acids between the mother, the placenta, and fetus to assure a net flux of amino acids to the fetus to fulfil its demand [88]. In the maternal blood the amino acid concentrations are lower than in fetal blood [89], therefore amino acids are transported against a concentration gradient by an active process. Amino acid transporters are classified into three classes: facilitative transporters, accumulative transporters and exchangers according to the type of transport mechanism they use. All three classes are present in the placenta and together they provide all the amino acids that the fetus needs [88].

Facilitative transporters can transport amino acids in both directions across the membrane and net transport is concentration gradient-dependant. In the human placenta, these transporters are thought to be in the BM [77], and this group of transporters includes TAT1, LAT3 and LAT4 (Table 1.2). The expression of these transporters has been positively correlated with fetal growth [77].

Accumulative transporters increase the concentration of amino acid inside the cell. These transporters are able to actively transport amino acids into the cell coupling it to Na^+ transport. Accumulative transporters have been reported in the MVM and BM of the placenta [90] and include the SNATs and EAATs (Table 1.2). The reduction of activity of system A (SNATs transporters) has been associated with fetal growth restriction [91].

The amino acid exchangers are the third type of amino acid transporter expressed in the placenta. These transporters switch an amino acid inside the cell for another molecule outside the cell, which means that they do not alter the osmotic concentration inside the cells. This group includes LAT1, LAT2, ASCT1 and ASCT2 among others (Table 1.2) [92].

Table 1.2 Placental amino acid transporters

Gene name	Protein name	Evidence in the placenta
	Facilitative transporters	
SLC16A10	TAT1	mRNA and protein BM
SLC43A1	LAT3	mRNA and protein BM
SLC42A2	LAT4	mRNA and activity in BM [77]
	Accumulative transporters	
SLC1A1	EAAT3	Activity MVM and BM
SLC1A2	EAAT2	Activity MVM and BM
SLC1A3	EAAT1	Activity MVM and BM
SLC1A6	EAAT4	Activity [93]
SLC1A7	EAAT5	Activity [94]
SLC7A1	CAT1	Protein BM
SLC7A2	CAT2	Activity in MVM and BM and mRNA
SLC7A3	CAT3	Activity in MVM and BM and mRNA
SLC38A1	SNAT1	mRNA
SLC38A2	SNAT2	Activity MVM and BM
SLC38A3	SNAT3	mRNA [94]
SLC38A4	SNAT4	mRNA
SLC38A5	SNAT5	Protein MVM [94]
	Exchange transporters	
SLC1A4	ASCT1	Activity BM
SLC1A5	ASCT2	Activity BM
SLC7A5	LAT1	Activity MVM and BM
SLC7A6	y^+LAT2	Activity MVM and BM, mRNA
SLC7A7	y^+LAT1	Activity MVM and BM, mRNA
SLC7A8	LAT2	Activity MVM and BM
SLC7A10	Asc1	mRNA
SLC7A11	xCT	Protein MVM [95]

Localisation is from Cariappa *et al* [96], Cleal *et al* [88] and Kudo *et al* [97] unless otherwise stated.

The amino acid transporters in the placental syncytiotrophoblast are asymmetrically distributed with exchange and accumulative transporters in both membranes and facilitated transporters in the BM. The specificity of the amino acid transporters require that some of the amino acids are used to assure the passage of others into the placenta (Figure 1.6) [77]. Amino acid transport to the fetus involves the transfer through the MVM by the accumulative transporters and exchangers [88]. Amino acids transported by the accumulative transporters can be used by the exchangers in order to get other amino acids inside the syncytiotrophoblast. Amino acids inside the syncytiotrophoblast can be used by the placenta for protein synthesis, metabolism and also they can be transported to the fetal blood in order for the fetus to use them in metabolism [94]. The transport of amino acids to the fetus is mediated by facilitated transporters and exchangers [77]. In the BM there are also accumulative transporters that take amino acids from the fetal blood into the placenta. Another function of specific amino acids inside the placenta is to provide a chemical gradient across the membranes that can drive uptake of other substances by exchange. This function has been recently described for glutamate which has a high concentration inside the placenta and it acts as a counter ion to drive uptake of other substances such as other amino acids, oestrogen substrates or waste products by exchange [95,98].

1.5.1.3 Placental fatty acid transport

Fatty acids are a source of energy, a major constituent of the cell membranes and required for the biosynthesis of bioactive compounds such as the eicosanoids and prostaglandins. Essential fatty acids and long-chain polyunsaturated fatty acid are required for fetal development, they are components of fetal membranes and precursors of eicosanoids that are necessary for brain development [99]. The fatty acids that are transferred to the fetus come from two main sources in the maternal blood, non-esterified fatty acids (NEFA) and esterified fatty acids in triglycerides (TGs). Due to their hydrophobic nature, TGs are transported in lipoproteins [79]. Lipoproteins interact with the lipoprotein lipase (LPL) present on the MVM, this enzyme hydrolyses TGs releasing the NEFAs to cross the membrane [100].

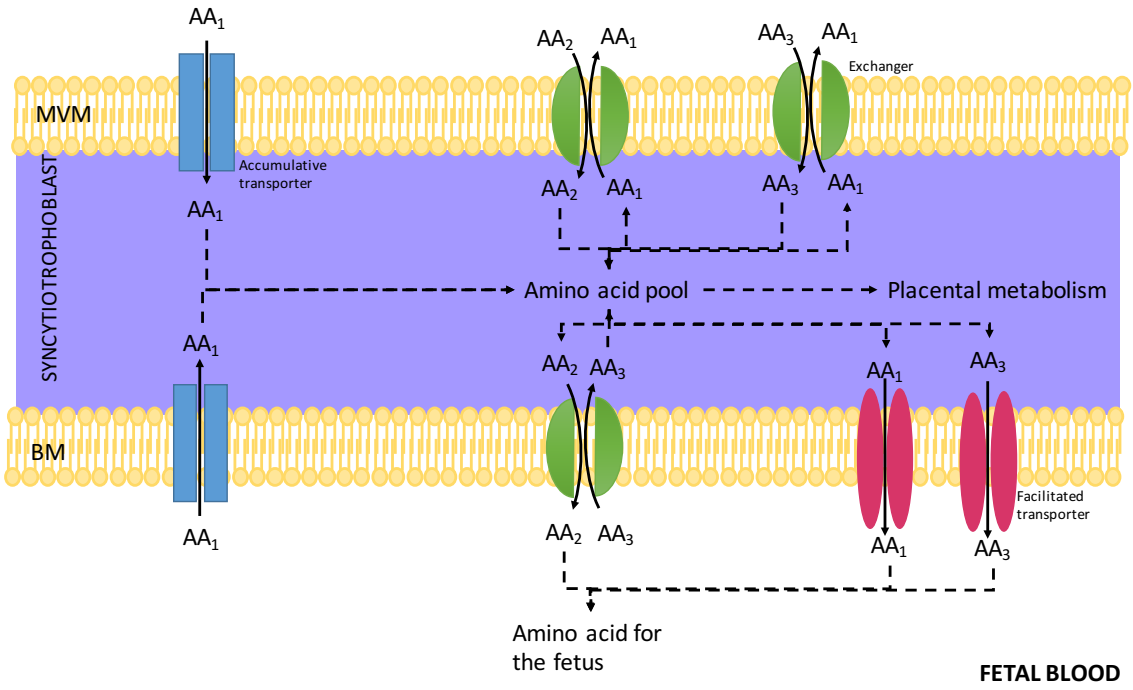

Figure 1.6 Amino acid transport in the placenta

The placental amino acid transfer involves the transport of amino acids through the microvillous membrane (MVM) and the basal membrane (BM). In the MVM, accumulative (blue) and exchanger (green) transporters are able to transport amino acid across the syncytiotrophoblast where they can be used by the placenta or be transported to the fetus across the BM by exchangers and facilitated transporters.

Specific proteins mediate fatty acid transport across the placental membranes. Fatty acid transporter proteins (FATP) is a family of the solute carriers (SLC27) that include six members and its expression has been shown in different tissues including placenta [101]. The fatty acid translocase (also known as CD36) and the fatty acid binding protein (FABPpm) also transport fatty acids across the membranes [102]. Initially, it was thought that fatty acids crossed the membranes by diffusion but now it is known that transport of fatty acid is mediated by these proteins [103].

In the placenta, FAT/CD36 and FATP have been found on the MVM and the BM. Cytoplasmic binding proteins are also expressed in the syncytiotrophoblast. The presence of FAT/CD36 and FATP in both membranes indicate bi-directional transport of fatty acids between the maternal and fetal circulation with the net transport of fatty

acids to the fetus (Figure 1.7) [104]. Fatty acid transport by the placenta is affected by the presence of binding proteins such as albumin in the maternal and in the fetal blood [105].

The transport of fatty acid to the fetus has been shown to be preferential, essential fatty acid and docosahexaenoic acid have a higher rate of transfer compare with the non-essential fatty acids, this preferential transport is to assure the polyunsaturated fatty acid supply that the fetus needs [106]. Differential levels of fatty acid in the umbilical vein and artery also shows specific lipid pools in the fetal circulation that might help to direct the supply of fatty acid to the fetal tissues [107].

Placental nutrient transport is a complex process that is not still fully understood. Its importance in determining fetal growth has been widely accepted; however, how nutrient transport is regulated by the placenta is still not completely clear.

1.5.2 Placental function as barrier and as a suppressor of the immune response

In human placenta, the syncytiotrophoblast is a continuous layer that separates the maternal circulation from the fetal circulation. In the syncytiotrophoblast the apical MVM is in contact with the maternal blood and the BM is facing the fetal circulation (Figure 1.5) [65]. The syncytiotrophoblast is a physical barrier and the molecules can pass between the two circulations through two different routes. The transcellular route involves the transfer of the molecules across the two membranes and the cytosol of the syncytiotrophoblast. There is also a paracellular route that has been described as an extracellular water-filled pathway [108]. The transcellular route is in charge of the nutrient and waste transport between mother and the fetus and will be described later in this chapter.

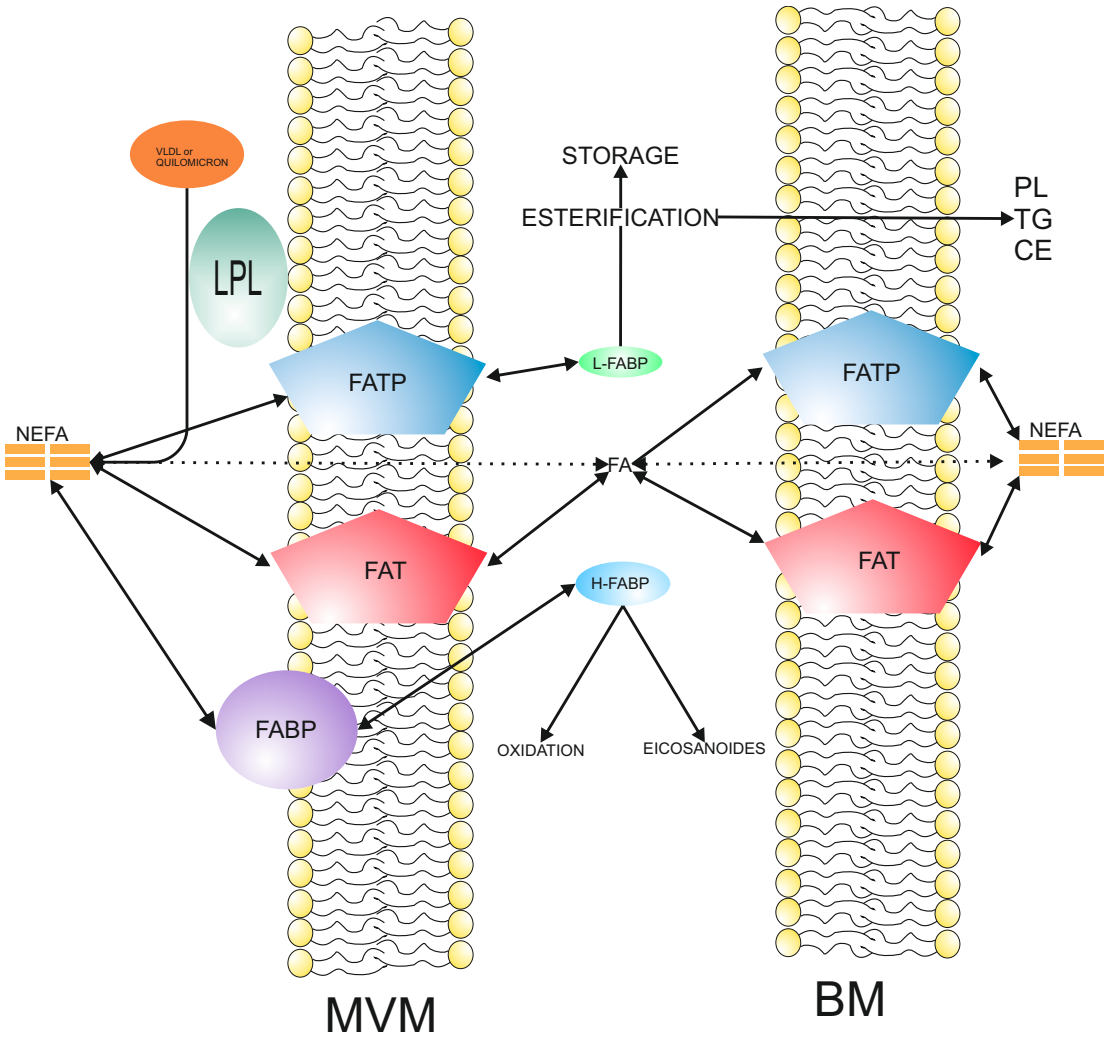

Figure 1.7 Placental fatty acid transport

Fatty acids (FA) can be transported from the maternal to the fetal circulation with the help of fatty acid transporter proteins (FATP) that are present in the MVM and the BM. The transported fatty acids need to be distributed between the placenta and the fetus. FABP: Plasma membrane placental fatty acid binding protein. LPL: lipoprotein lipase. FAT: fatty acid transfer protein. L-FABP and H-FABP: liver and heart fatty acid binding protein. NEFA: non-esterified fatty acid. MVM: microvillus membrane. BM: Basal membrane. PL: Phospholipids. TG: triglycerides, CE: Cholesterols esters. Modified from [100]

The placenta also reduces the possibility of the mother rejecting the pregnancy. Fetal tissues express paternal histocompatibility antigens that should activate the maternal immune system and generate a reaction similar to when a tissue is rejected after a transplant. Nevertheless, that does not happen in pregnancy. Placental trophoblast does not express some of the human leukocyte antigen (HLA) antigens such as HLA-A and HLA-B that are the main stimulators of the immune response. Trophoblast cells also do no express HLA class II antigens that are the ones that stimulate the T cell

response. Placental trophoblast expresses HLA-G that has been found to inhibit CD4 T cell activation and production of different cytokines contributing to the general reduction of the maternal immune respond [76,109]. Maternal lack of or reduced immune response to the pregnancy involves not just the placenta but also the mother and the fetus. Placental production of immune suppressive molecules and the expression of others that inactivate immune cells is part of the mechanism that generates the maternal acceptance of the fetal tissue [76].

1.5.3 Placental endocrine function

One of the placenta's roles during pregnancy is the production of hormones that adapt maternal physiology to support the pregnancy. The production of hormones during the pregnancy is not just a feature of the placenta; the fetal membranes (amnion and chorion) and the maternal decidua also produce hormones. These hormones act in an autocrine and in a paracrine manner. Some of the hormones produced by the intrauterine tissues are chemically identical and biologically active as the hormones produced by other tissues such as the brain, pituitary gland and gonads among others [110]. Hormones produced by intrauterine tissues are listed in Table 1.3.

The expression of placental hormones is controlled by paracrine and autocrine mechanisms. Gonadotropin releasing hormone (GnRH) is one of the hypothalamus-like hormones produced by the placenta that controls the production of the others placental hormones necessary for the success of the pregnancy [52]. In trophoblast cell culture GnRH production increased when exposed to high concentrations of K^+ or veratridine and the effect is reversed by Ca^{2+} antagonists. GnRH production was also increased by adenosine monophosphate (AMP), prostaglandins E2 and F2 and epinephrine [111].

GnRH is also reduced by the progesterone and increased by estradiol [112]. GnRh feedback regulation shows how the placenta acts as endocrine regulator centre for the pregnancy [52]. GnRH induces the secretion of human chorionic gonadotropin (hCG) in the placenta [113]. This is a central hormone for the pregnancy and is secreted early in pregnancy and is used for the diagnosis of the pregnancy. Production of GnRH, hCG

and progesterone are also modulated by inhibin A and activin A, these also are hormones produced by the placenta [114]. Regulation of hormone production in the placenta is a complex process similar to the hypothalamus-pituitary axis in the brain (Figure 1.8) [110].

Table 1.3 Hormones produced by intrauterine tissues

Hormone type	Name
Hypothalamus-like hormones	Gonadotropin-releasing hormone (GnRH)
	Corticotropin-releasing factor (CRF)
	Urocortin
	CRF-binding protein (CRF-BP)
	Growth hormone-releasing hormone (GH-RH)
	Somatostatin
Pituitary-like hormones	Human chorionic gonadotropin (hCG)
	Placental growth hormone (PGH)
	Human placental lactogen (hPL)
Growth hormones	Transforming growth factor-β (TGF-β)
	Activin A
	Follistatin
	Insulin-like growth factor (IGF)
	IGF-binding protein (IGF-BP)
	Fibroblast growth factor (FGF)
	Epidermal growth factor
	Vascular endothelial growth factor (VEGF) peptides
	Progesterone
	Estrogens
Vasoactive peptides	Adrenomedullin
	Endothelin
	Calcitonin gene-related peptide
	Parathyroid hormone-related peptide (PTH-rp)
Metabolic hormones	Leptin
	Ghrelin

From [110]

The hCG is necessary at the beginning of the pregnancy in order to maintain the corpus luteum during the first 8 weeks of pregnancy. hCG is also involved in trophoblast differentiation since it induces the differentiation of cytotrophoblast into syncytiotrophoblast [66,75].

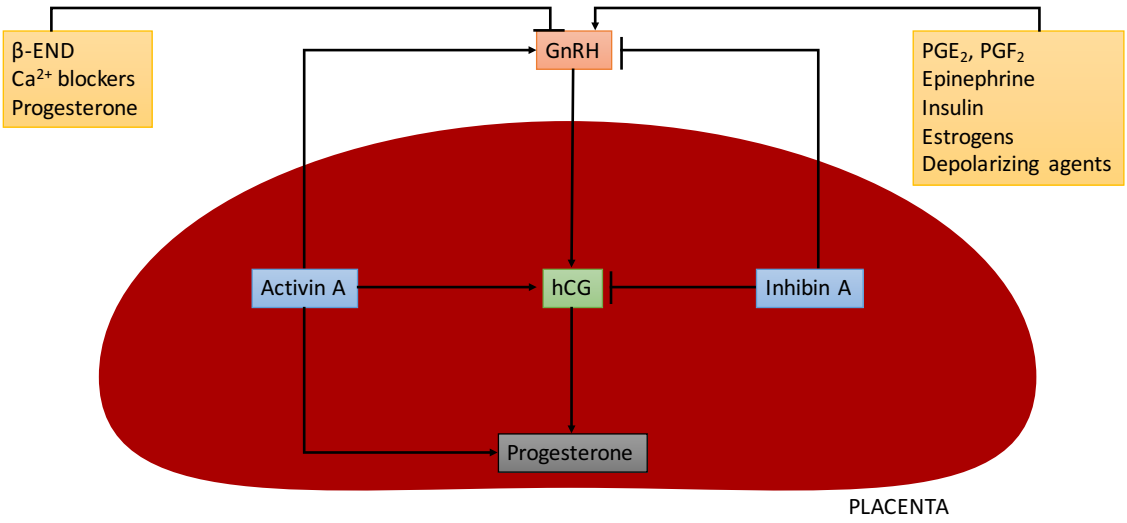

Figure 1.8 Regulation of human chorionic gonadotropin in the placenta

Placental hormonal secretion is controlled in an autocrine and paracrine manner. Gonadotropin releasing hormone (GnRH) is produced by the placenta and it actives the production of human chorionic gonadotropin (hCG) that is a central hormone for the success of the pregnancy. hCG promotes the formation of the syncytiotrophoblast, it helps to transform the ovary corpus luteum from ovary to gravid and it maintains the production of progesterone and others hormones.

Other placental hormones such as human placental lactogen (hPL), placental growth hormone (PGH) and placental growth factor (PGF) produced by the placenta help to change maternal metabolism to ensure nutrient availability to the fetus and subsequent fetal development. PGH, hPL and PGF are also involved in other physiological adaptations to the pregnancy, for example maturation of the maternal mammary ducts; preparing the uterus for the delivery and reducing the maternal immune response. Insulin-like growth factors 1 and 2 (IGF-1 and IGF-2) are peptide hormones produced by the placenta and are involved in the proliferation and differentiation of the cytotrophoblast. The placenta also synthesizes other hormones such as prolactin, relaxin and human chorionic thyrotropin [110]. Some of these hormones are produced in small concentrations and their interactions during the pregnancy are still being studied [66,75].

The placenta produces the steroid hormones progesterone and oestrogen. Progesterone is synthesized by the syncytiotrophoblast and is mainly secreted into the

maternal blood, it suppresses the maternal immune system responses and reduces the activity of the uterine smooth muscle [115]. Some of the placental progesterone is delivered to the fetus where it is converted to the adrenal steroids cortisol and dehydroepiandrosterone (DHEA). DHEA is the precursor for oestrogen synthesis. The placenta lacks 17α-hydroxylase enzyme, one of the enzymes needed to convert progesterone into DHEA, therefore, the placenta depends on the mother and the fetus to receive the precursor of oestrogen [75,116]. However, placental oestrogen synthesis is not necessary for a successful pregnancy. Aromatase deficiency has been described in patients that shown a virilisation prepartum with low levels of serum oestrogens and high levels of androgens, however, these women were able to complete the pregnancy [117,118].

1.6 PLACENTAL SENSING AND REGULATION

The placenta acts as a sensor to the maternal environment in order to respond to changes that occur during pregnancy that could affect fetal development [69]. However, the mechanisms behind this sensing process are not completely understood [69].

Placenta function is thought to respond to maternal signals, reflecting the capacity to support the pregnancy, and the fetal demand for nutrients to support its growth. The placenta can act as a nutrient sensor, receiving nutritional signals from the mother that alter the placental nutrient transport system in order to respond to the changes in nutrient availability [119]. It is not completely clear which signal (maternal or fetal) drives the placental function. It has been proposed that fetal growth will be restricted by the maternal supply and that the placental function is controlled by the fetal demand [69]. Placenta function can also be regulated by maternal constraint, which refers to the intrinsic capacity of the mother to carry out the pregnancy without affecting her own health or her future ability to reproduce [40]. Maternal and fetal signals to the placenta will be discussed and placental responses or modifications to these signal will be addressed.

1.6.1 Maternal endocrine regulation of placental function

Placental nutrient transport has been shown to respond to maternal hormones such as insulin, cortisol, leptin and IGF-I, these hormones inform the placenta about the maternal nutritional status [78]. Hormones signalling is a complex process, with maternal hormones levels being modified by circadian rhythms, nutrients levels, stress levels and diseases [52]. In pregnancy, maternal body mass index (BMI) has been positively correlated with insulin and leptin levels at the beginning and at the end of the pregnancy and negative correlated and adiponectin levels at the beginning of the pregnancy and with IGFBP-1 at the end of the pregnancy. In the same study, IGFBP-1 levels at the end of the pregnancy were negatively correlated with birth weight [120].

In rats, it had been shown that maternal undernutrition increased maternal plasma corticosterone levels with decreased placental capacity to metabolise glucocorticoids and also decreased placental glucose and amino acid transporter expression [121,122]. In mice, a high fat diet during pregnancy increased the transport of glucose and neutral amino acids in the placenta and also resulted in fetal overgrowth [32]. In humans, maternal obesity has been associated with higher birth weight [123]. In the same study, birth weight was correlated with placental mTOR signalling pathway activity, and with activity and protein expression of amino acid transporters (system A) [123]. Gestational diabetes has also been found to affect placental function, increasing system A activity [124]. Maternal age has an effect on placental function and in the outcome of the pregnancy as well, with pregnant teenagers having lower placental system A activity and lower transporter expression compared to pregnant adults [125]. Nevertheless, The mechanism behind how the placenta adapts and responds to different maternal conditions is still not completely understood [63].

Associations between a reduction in adiponectin levels and an increase in the concentration of leptin and inflammatory cytokines (e.g., IL-6 and TNF-α) have been reported in pregnancies with gestational diabetes associated to macrosomia in the babies [126]. In normal pregnancies, inflammatory factors are positively associated with maternal glucose levels and birth weight while adiponectin is negative associated [127]. Insulin, interleukin 6 (IL-6) and tumour necrosis factor (TNF)-α also have been reported to increase the activity of system A in the human placenta [128,129].

The effect of maternal hormones on placental function have been shown *in vitro.* Insulin increased the activity of system A and also increased the expression of SNAT2 in human primary trophoblast cells, while adiponectin inhibited the effect of the insulin in the same cells [130]. In term human placental villous explants, system A activity was reduced by the exposure to CRF and urocortin [131]. Human placental villous explants have also shown that system A activity is increased by leptin and insulin exposure but was not affected by cortisol [132,133]. Placental responses to different hormonal cues have been shown to involve the transcription factor STAT-3, which could indicate a common pathway in the control of placental function [78]. In mouse, corticosterone exposure during mid to late pregnancy, reduced fetal weight, reduced system A activity in late pregnancy while increasing *SNAT1* and *SNAT2* expression [134].

The above studies indicate that placental function is affected by maternal signals. The placenta needs to process these signals in order to adapt itself and the fetal nutrient supply to the new situation. Figure 1.9 shows an overview of the maternal signals that affect placental function and their effects in the placenta and in fetal development.

1.6.2 Fetal regulation of placental function

Fetal signals affecting placental function include IGF-II and fetal PTHrP [69]. Evidence of fetal signals acting on the placenta is difficult to obtain in humans and the most convincing evidence has been produced from knock out studies in mice [78].

In mice, *Igf2* has a placental-specific transcript (P0) that is exclusively expressed in the placenta. When this transcript is deleted, the fetal *Igf2* expression is not affected but it is decreased in the placenta. The effect of the P0 KO is that placental growth is reduced in mid-gestation followed by a delayed reduction in fetal growth by the end of gestation [135]. The placental specific knock out in the mouse placenta demonstrates a compensatory mechanism where, while in mid-gestation placental size is reduced its amino acid transport capacity is upregulated to compensate, and fetal growth is maintained. However, as pregnancy progress and fetal demand increases, the placenta

is unable to sufficiently upregulate nutrient transport and fetal growth becomes restricted [135].

PTHrP is a hormone produced by fetal tissues with PTH-like effects [78]. PTHrP stimulates ATP-dependent calcium transport in BM isolated from human placentas suggesting that fetal hormones can affect placental function in humans [136]. In pregnancies complicated by IUGR or insulin dependent diabetes, both PTHrP umbilical cord blood PTHRP and ATP-dependent calcium transport are reported to be increased [137].

These studies have shown how the fetus can send signals to the placenta in order to modify the placental nutrient transport as a compensatory mechanism in order to compensate for a reduction in placental function.

1.6.3 Placental regulation pathways

As shown above, the placenta needs to respond to signals sent not just by the mother but also by the fetus. Establishing how the placental intracellular pathways are activated by these signals will contribute to a better understanding of pregnancy physiology. In the placenta, the mechanistic target of rapamycin complex 1 (mTORC1), 5' adenosine monophosphate-activated protein kinase (AMPK) and the amino acid response signal transduction pathway are examples of intracellular pathways that are implicated as being part of a nutrient sensing process [34,78].

1.6.3.1 Mechanistic target of rapamycin

Mechanistic target of rapamycin (mTOR) (before mammalian TOR), is a serine/threonine kinase, it interacts with different proteins to form two different complex: mTORC1 and mTORC2. Each complex has a different response to rapamycin and different upstream effectors and downstream outputs [138]. mTORC1 is affected by rapamycin, nutrient and energy levels, oxygen, stress and growth factors. This complex regulates macromolecules synthesis (mRNA and proteins), cell growth, autophagy and metabolism. mTORC2 has been shown to be affected by growth factors but is not affected by rapamycin. mTORC2 affects cytoskeletal organisation and cell survival [138].

In the placenta, mTOR is expressed in the syncytiotrophoblast. In primary trophoblast cell culture glucose deprivation decreased the activity of one of the amino acid transporter groups (system L) and this effect was lost in the presence of rapamycin. The effect of glucose deprivation on system A amino acid transporters had two opposite responses: an upregulation that was not mediated by mTOR and a downregulation that was mTOR-dependent [139]. Insulin and IGF-I increased system A activity and insulin increased system L activity, this last effect was mTOR-dependent [139]. In primary trophoblast cells inhibition of mTOR by rapamycin reduced the activity of system A, system L and taurine amino acid transporters. mTOR inhibition also reduced the mRNA expression of *LAT1* (system L) and taurine but not the expression of the *SNAT1*, *SNAT2* or *SNAT4*, *LAT4* or *4F2HC* [140]. Any of the amino acid transporter protein expression was affected by mTOR inhibition [140].

In pregnancies complicated with IUGR, it has been shown that mTOR activation was reduced [141], while in large babies born from obese women mTOR signalling, system A activity and SNAT2 (system A) protein expression were positively correlated with birth weight [123]. Recently, it was shown that independent inhibition of both mTOR complexes decreased system A and system L activity without affecting growth factor-stimulated amino acid uptake in trophoblast primary culture [142]. Inhibition of both mTOR complexes inhibited amino acid transport activity (basal and growth factor-stimulated), additionally, inhibition of either mTORC1 or mTORC2 decreased the plasma membrane expression of SNAT2 (system A) and LAT1 (system L) but total protein expression was not modified [142]. All of this evidence supports mTOR as an important placental sensor that is able to respond to nutrient and hormone levels by modifying amino acid transporter activity and expression in the placenta (Figure 1.9).

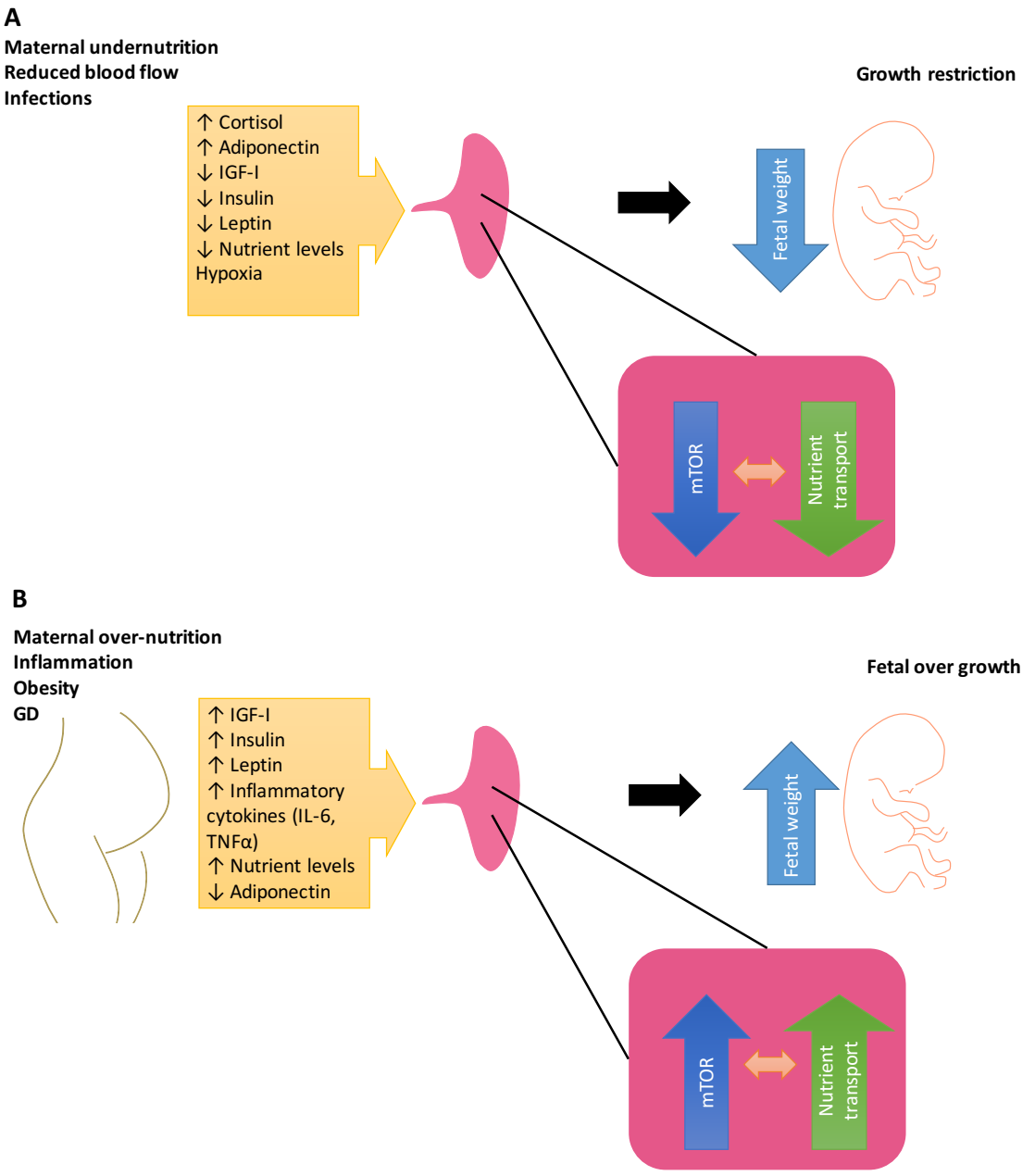

Figure 1.9 Overview of placental response to maternal signals

A. Maternal decreased nutrient supply can occur as a result of maternal undernutrition or as a result of an altered blood supply or maternal infection. Different maternal signals will be produced as a response to these situations but they will have a similar effect on placental function and fetal growth. B. Maternal overnutrition and inflammation are usually present with obesity and/or gestational diabetes (GD). They modified maternal signals to the placenta increasing nutrient supply to the fetus that can produce fetal overgrowth. Modified from [69,143].

1.6.3.2 5'-adenosine monophosphate – activated protein kinase

AMPK acts as an energy sensor in most cells in the body. It responds to the increase of AMP in the cell (that indicates a decrease of ATP, therefore energy depletion)

inhibiting the energy-consuming pathways including all the anabolic pathways. It increases the ATP production in the cells by activating the energy-producing pathways [144].

In ewes exposed to a nutrient restricted diet, fetal and placental weight was reduced, maternal levels of glucose, insulin and leptin were decreased and AMPK activity was increased in placental cotyledons [145]. In rats, placental mTORC1 activation and reduction in AMPK phosphorylation have been reported when exposed to a high fat diet during pregnancy [146]. In hypoxic mice, AMPK has been involved in vasodilatory responses in the placenta as a potential adaptive mechanism to reduce cellular energy depletion [147]. Also, placental AMPK activation was negatively correlated with birth weight in babies from obese women [123] indicating a potential role in the placental response to nutrients levels.

1.6.3.3 Amino acid response pathway

Amino acid response pathway is an adaptive mechanism in the cells in order to respond to changes in nutrients levels, especially when dietary proteins are reduced (therefore amino acids availability is reduced) [148]. Depletion of any amino acid will produce an increase in uncharged transfer RNA that bind to the general control nonderepressible 2 kinase, which phosphorylate the translation initiation factor 2 alpha (eIF2α). This reduces general protein synthesis and increases activating transcription factor 4 (ATF4) increasing the expression of genes involved in oxidative stress [148]. In rats, a protein-restricted diet during pregnancy produced increased mRNA expression of genes involved in amino acid response pathway as well as increased protein levels of ATF4 and p-eIF2α. Increase expression of the amino acid response pathway associated genes was correlated with the reduction in fetal growth and the expression of the amino acid transporter *Snat2* [149]. In humans, phosphorylated eIF2α is increased in placenta from pregnancies complicated with IUGR, but it is not clear if this response is due to an amino acid reduction response or an oxidative stress response [150].

1.6.3.4 Other sensing pathways

Other pathways possibly implicated as part of the placental sensing mechanism are the glycogen synthase-3 and the hexosamine signalling pathway [151]. Glycogen synthase-3 pathway has been shown to act as a glucose sensor and in pregnancies complicated with IUGR, glycogen synthase-3 pathway is activated in the placenta [151]. Hexosamine signalling pathway has also been shown to be activated in human placenta during the first trimester affecting IGF signalling [151]. This indicates they might be more cellular pathways that could be involve in regulation of placental function.

1.6.4 Other potential placental sensors

Placental responses to maternal and fetal signals still needs more research as maternal environmental modifications affect fetal development in different ways. A better understanding of this process will allow an improvement in maternal and fetal health as well as the long term health of the baby. Other pathways that have been found to be altered during pregnancy and/or have been described as energy or nutrient sensors in other tissues will be described below as potential regulators of placental function.

1.6.4.1 Fat Mass and obesity-associated gene (FTO)

Single nucleotide polymorphisms (SNPs) in the first intron of the *FTO* gene have shown a strong association with BMI and higher risk to developing obesity in adult humans [152]. In mouse embryonic fibroblasts, the lack of *FTO* has been associated with a decreased activation of the mTORC1 pathway [153], suggesting that the present of *FTO* is necessary for the normal sensing of amino acid levels in the mTORC1 pathway [153]. The lack of *FTO* in the cells decreased mRNA translation rates and increased autophagy, suggesting *FTO* interacts with proteins in the multi-tRNA synthase complex, however, its function in this interaction is still unclear [153]. Also, *FTO* mRNA and protein levels are reduced by amino acid deprivation in human embryonic kidney cells (HEK 293) [154]. The *FTO* product is a RNA demethylase [155] that can be involved in messenger RNA metabolism [156]. *FTO* gene expression in the human placenta has been associated with increased fetal weight and length [157]. In sheep, placental *FTO* gene is highly expressed and its expression was unaffected by maternal nutrient intake during early-to-mid gestation. However, in the same study, there was a positive correlation between FTO

mRNA abundance and fetal weight at 110 days gestation [158]. Since *FTO* has been involved as potential nutrient sensor and its placental expression has been related with birth weight, it is possible that FTO could be acting as a nutrient sensor in the placenta, and helping to control placental function.

1.6.4.2 Clock genes

Many physiological and behavioural processes in mammals are controlled by circadian rhythms. The clock genes are known to regulate energy consumption, nutrient availability and breathing frequency [159]. There are both central clocks, maintained by the suprachiasmatic nucleus (SCN) and peripheral clocks. Central clocks maintain proper phase alignment with the peripheral tissues clocks [159]. It is possible that the clock genes may play an important role in regulating placental function, either in maintaining circadian rhythms or alternatively the cellular machinery which mediate the clock system could be entrained to regulate other metabolic pathways in the placenta.

The mammalian central circadian system is controlled by the SCN in the brain, which is responsible for the peripheral oscillator systems in other tissues. The mechanisms of the circadian system in the SCN and in peripheral tissues are similar at the molecular level [160]. Briefly, in all the tissues there is a group of genes, which are the components of the core clock. They work as a network of transcriptional-translational feedback loops that regulate the circadian rhythm in the cells.

The genes *Clock* and *Bmal1* are in the first step of the feedback loop. Their products form a heterodimer that activates the transcription of the secondary proteins *Period* (*Per1*, *Per2* and *Per3*) and *Cryptochrome* (*Cry1* and *Cry2*). The PER:CRY heterodimers exert a negative feedback and repress the transcription of *Clock* and *Bmal1* [161]. In addition to activating the transcription of *Per* and *Cry,* CLOCK and BMAL1 also promote the transcription of *Rorα* and *Rev-erbα* genes. The products of *Rorα* and *Rev-erbα* have different effects over the CLOCK:BMAL1 expression; RORs protein increases the transcription of these genes but REV-ERBs act as an inhibitor of their transcription (Figure 1.10) [162].

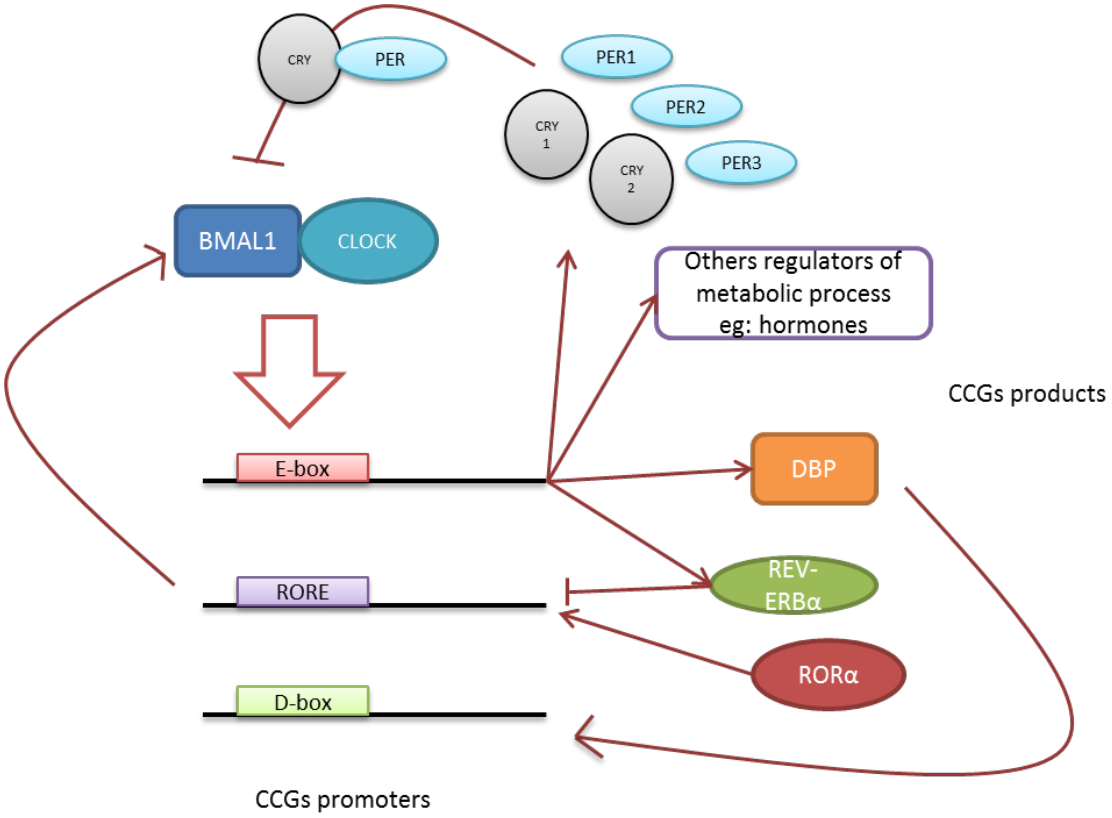

Figure 1.10 Clock gene feedback loop including the main downstream targets

The heterodimer CLOCK-BMAL1 activates genes with E-box elements in their promoters (Clock-controlled genes – CCGs). Among the CCGs are also the genes encoding CRY and PER proteins that act as negative regulators of their own transcription.

There is evidence of circadian expression of clock genes in human, mouse and rat placenta. The expression of the clock genes is different between the mother and the fetus, showing they have independent circadian rhythms [163]. It is possible that placental clock genes are independent of the maternal or fetal central clock and their regulation might be by hormones such as melatonin since it is capable of passing through the placenta [163,164].

1.6.4.3 Sirtuins

Sirtuins are nicotinamide adenine dinucleotide (NAD)-dependent deacetylases that have been associated with the regulation of longevity and lifespan in lower

organisms[165]. As sirtuins sense energy levels via NAD, they may respond to energy status to regulate placental function.

Sirtuins are highly conserved from bacteria to human and in mammals there are seven isoforms (SIRT1-7), all of them with a conserved NAD-binding and a catalytic domain. The NAD requirement of the sirtuins for their activity associates them with the metabolic state of the cell [165]. The characteristics of the sirtuins are shown in Table 1.4.

The expression of the clock genes including *BMAL, RORY, PER2* are affected by SIRT1 activity, and also SIRT1 promotes the degradation of PER2 by its deacetylation [166]. This provides a mechanism by which cellular metabolism and the circadian rhythms in the placenta are linked.

Sirtuins are the only histone deacetylases that need NAD to accomplish their function. The general deacetylation reaction catalysed by sirtuin is a two-step process. In the first part, sirtuins cleave NAD and produce nicotinamide (NAM) and in the second part, the acetyl group is transferred from the substrate to the ADP moiety of NAD to generate O-acetyl-ADP and a deacetylated substrate. Most of the sirtuins have the deacetylase activity, but SIRT4 has only an ADP-ribosyltransferase activity, and SIRT1 and SIRT6 have both activities (deacetylation and a weak ADP-ribosylation). Another characteristic of the mammalian sirtuins is the fact that in addition to targeting histones, they can deacetylate a wide variety of proteins in different subcellular compartments so they may be involved in the control of cellular function [167].

SIRT1 is the most studied member of this family, and its function has been related to a wide range of cellular processes. Cell survival and death, transcriptional suppression, mitochondrial biogenesis, fat mobilisation and utilisation, hormone release and inflammation, among others have been connected with SIRT1 function. Furthermore, the response to fasting or caloric restriction, insulin secretion and sensibility, cholesterol metabolism and fatty acid oxidation are related to SIRT1 function [165,168].

Table 1.4 Mammalian sirtuins

	Enzymatic activity	Subcellular localization	Class	Targets
SIRT1	Deacetylation	Nuclear, cytoplasmatic	I	PGC-1α, FOXO1, FOXO3, NF-κβ, AceCS1, MEF2, PCAF, histones H4K16 and H1K26, p53, p300, MyoD, TAF_I68, HIV Tat protein, Notch, LXR, FXR, SREBP1c and more.
SIRT2	Deacetylation	Cytoplasmatic, nuclear	I	Tubulin, histone H4K16, PEPCK, FOXO1, PAR3.
SIRT3	Deacetylation	Mitochondrial, Nuclear	I	LCAD, HMGCS2, GDH, OXPHOS complexes, SOD2, IDH2 and more
SIRT4	ADP-ribosylation	Mitochondrial	II	GDH
SIRT5	Deacetylation (low activity), Demalonylation, Desuccinylation	Mitochondrial	III	CPS1
SIRT6	Deacetylation ADP-ribosylation	Nuclear	IV	H3K9, H3K56
SIRT7	Unknown	Nuclear	IV	Unknown

SIRT1 deficiency in mice has been shown to promote heterochromatin formation and transcription repression and its overexpression has also been related to improvement of glucose tolerance in mice with a high fat diet and with protection against high fat diet-induced type 2 diabetes [169]. In human SIRT1 genetic variation has been correlated with obesity and type 2 diabetes [169].

SIRT1 also mediates the stress response in biological processes such as inflammation, hypoxic stress, heat shock and genotoxic stress. SIRT1 is able to deacetylate Nuclear factor kappa- beta causing is inhibition thereby inhibiting the expression of its target genes [165].

SIRT2 is mainly a cytoplasmic protein, but it can also be found in the nucleus. Its function has been related to oligodendroglia differentiation, control of the cell cycle and adipocyte differentiation among others [165].

SIRT3 is the best-characterized mitochondrial sirtuin and its function has been related to fatty acid metabolism. In knock out mice, SIRT3 deficiency has been linked to a defect in fatty acid oxidation and reduced respiration and ATP levels [165]. The other mitochondrial sirtuins, SIRT4 and SIRT5 have been correlated with control of insulin secretion and alterations in urea production, respectively. SIRT6 deficiency has been shown in mice with increased glycolysis and triglyceride synthesis in the liver, a premature ageing phenotype and genomic instability [170].

Sirtuin involvement in all these cellular processes is clear but there is little data available on the expression and regulation of sirtuins in human fetal tissues, especially in the placenta. SIRT1 has been reported as one of the molecules related to the regulation of pregnancy and parturition due to its anti-inflammatory ability.

In the placenta, SIRT1 is necessary for the primary trophoblast survival by increasing cellular resistance to hypoxia [168]. SIRT1 is also involved in the control of metabolic pathways but its role is controversial. In general, sirtuins will help to maintain gluconeogenesis in times of energy limitation [171]. Human SIRT1 and SIRT2 have been localised in different areas of the placenta. SIRT1 together with the ligand-regulated transcription factor peroxisome proliferator-activated receptor (PPAR)α coordinate the suppression of genes involved in mitochondrial function in the placenta [172]. Further investigation is needed to determinate the relation between sirtuins and placental metabolic status [165,173]. It is possible that SIRTs sense placental energy levels via NAD, and regulate placental nutrient transport to maintain these at a steady state.

1.6.4.4 Insulin-induced gene (Insig1)

Insig1 is activated by insulin, and is one of the most insulin responsive molecules in liver [174]. Insig1 expression has been shown to be decreased in the placenta of obese women when compared with lean women [175]. Insig1 could be involved in the placental

sensing mechanism as an insulin responder. Insig1 is part of a family of proteins in the endoplasmatic reticulum (ER) that are involved in the negative regulation of cholesterol synthesis. In humans, there are two Insig proteins (1 and 2) involved in the regulation of cholesterol metabolism. Insig1 is a negative target of the sterol regulatory element binding protein (SREPs). Insig1 also mediates the degradation of the 3-hydroxy-3-methyl-glutaryl Coa Reductase (HMGR) a key enzyme in the synthesis of cholesterol [176,177].

SREPs are synthesised as inactive proteins that are in the ER membrane and in there they bind the SREPB cleavage-activating protein (Scap). When the cholesterol levels decrease, SREPB:Scap complex are released by the ER in vesicles that go to the golgi where SREPBs are cleaved to their active form. Active SREPBs translocate to the nucleus and bind sterol regulatory elements, increasing the expression of HMGR and other proteins involved in cholesterol synthesis. When Cholesterol levels are elevated they bind Scap changing their conformation. Modified Scap bind Insig1, retaining the SREPB:Scap complex in the ER. Insig1 can also bind to another membrane protein (gp78). When cholesterol intermediaries such as lanosterol are increased within the cell they bind insig1 which releases gp78 that is involved in the ubiquitination and posterior degradation of HMGR [178,179].

In pregnancies complicated with hypercholesterolemia, cholesterol levels in venous cord blood and lipid content in the placenta are not different between the mothers with high blood cholesterol and the mothers with normal cholesterol levels [180]. Also the expression of the enzymes involved in cholesterol synthesis are either increased (SREPB-1) or not modified (SREPB-2 and HMGR in the hypercholesteraemic mothers with high cholesterol [180]. In mice exposed to undernutrition (50% of protein restriction) during pregnancy, *Insig1* expression was increased compared with the control mice [181]. In mice, *Insig1* expression is up-regulated in low birth weight mice that were exposed to a normal diet after weaning [181]. In placentas from pregnancies from assisted reproduction, insig1 and SREPB expression was higher and both genes had lower methylation levels than the controls [182]. These studies therefore suggest that placental regulation of lipid metabolism is affected differentially when compared

with other tissues and also that cholesterol metabolism might have an important role in implantation and early placenta development.

1.7 CELL MODELS FOR *IN VITRO* STUDY OF PLACENTAL FUNCTION

While *in vivo* studies of placental function are most physiological, there are often experimental limitations with this sort of approach. For instance, if you give a treatment to a whole animal and study the effect of the placenta it is not clear whether any changes observed are direct or indirect effects. Furthermore, the placenta contains many cell types and it is not possible to study the effect on one cell type in particular *in vivo*. For this reason, a number of placental cell culture models are used to answer particular questions. However, these cell lines are not perfect models either and their strengths and weaknesses are discussed below.

1.7.1 Primary cytotrophoblast cell culture

Primary cell lines can be obtained from the human placenta. Using digestion, a preparation of cytotrophoblast from human placenta can be extracted by a density gradient and cultured [183]. This model is used for placenta barrier function and placental transfer studies. The limitations of this model include the difficulty getting cells to form a confluent layer, it has a high rate of contamination in the culture, cells are not viable for more than a week and they are not viable for many passages [184].

1.7.2 Cell lines used as models of trophoblast

Studies of trophoblast function have been carried out with different cell lines. The use of cancer cell lines raises questions about the suitability of these models. The choice of the model needs to be related to what you want to study as some cell lines are suitable for the study of trophoblast invasion, while others are more suitable for migration or syncytialization studies. As most of the cell lines are derived from extravillous trophoblast their suitability for studying villous trophoblast also needs to be considered. In this section the most common cell lines used for placenta studies will

be described as outlined in Table 1.5. The human trophoblast cell lines can be divided into three main groups: cell lines generated from normal tissues, cell lines generated from malignant tissues and cell lines generated from embryonal carcinomas but shows evidence of trophoblast differentiation [184,185].

1.7.2.1 Trophoblast cell lines derived from normal tissues

This is a wide group of cell lines that have been reported since 1986. These cell lines have been produced by transformation of normally isolated cells from the placenta that have suffered an spontaneous transformation and become immortalised or that have been transfected with a virus which produced the immortalization [185]. Many of these cells are difficult to culture or to characterise, which made their use very limited as a trophoblast model. Attempts to characterise these cells have been done showing that their "trophoblast characteristics" are highly variable [186,187] (Table 1.5).

1.7.2.2 Trophoblast cell lines derived from malignant tissues

Choriocarcinoma derived cell lines are more commonly used in the study of trophoblast function. Choriocarcinoma cells have a similar morphology to invasive trophoblast [187] and share some of their characteristics such as molecular markers, similar proteases and adhesion molecules production and they also can produce some of the same growth factors and hormones [185,186]. The main choriocarcinoma cell lines used in placenta studies are BeWo, JAR and Jeg-3 (Table 1.5). BeWo choriocarcinoma cells growth as a monolayer and morphologically are similar to normal trophoblast. This cell line has been used in studies for nutrient and Ca-uptake, caspases gene expression and placental syncytialization. JAR and Jeg-3 cell lines are adherent cell lines used in the study of trophoblast invasion and CE uptake [187].

1.7.2.3 Trophoblast cell lines derived from embryonal carcinomas

These cell lines are the least developed and used as an *in vitro* model of trophoblast. They are able to produce some of the trophoblast hormones and markers but their usefulness in the study of the placenta still needs to be evaluated.

Table 1.5 Characteristics of cell lines used as trophoblast models

Cell line	Origin	Use	hCG production
Cell lines derived from normal tissues			
HTR-8/Svneo	HTR-8 transfected with pSV3neo	Trophoblast invasion, migration and adhesion	+
RSVT-2	HTR-8 transfected with pRSV-T		
Cell lines derived from choriocarcinoma			
BeWo	Choriocarcinoma – naturally occurring	Trophoblast invasion, syncytialization Nutrient transport	+
JEG-3	Choriocarcinoma explant –naturally occurring	Trophoblast invasion	+
JAR	Gestational choriocarcinoma – naturally occurring	Trophoblast invasion	+
AC1M-88	JEG/Term trophoblast	Trophoblast migration and adhesion	
Cell lines derived from embryonal tissues			
H9	Inner cell mass from blastocyst cultured on MEF feeder layer		+

From [185,186]

1.7.2.4 Other cell lines used in the study of placental function

Endometrial epithelial cell lines have been used for the study of the implantation process but mainly as a model of the endometrium [186]. Another cell line that has been previously reported to be used for the study of functions that occur in the placenta is human embryonic kidney 293 cells [188]. HEK 293 cells were immortalised after the transfection of human adenovirus to human embryonic kidney cells [189]. HEK 293 cells growth as a monolayer and they can be used as a model of epithelial transport. Although HEK 293 cells are not originally from an intrauterine tissue they were shown

to have a more similar gene expression profile to the placenta than BeWo cells [188]. This makes them a suitable model for the study of nutrient transport in an epithelium and its similarity with placental transporter expression allows to extrapolate certain observation within the limit of the model.

1.8 SUMMARY

Placental structure and function are key determinants of fetal growth and are important to understanding the factors that regulate placental development. Placental function is regulated by fetal and maternal signals, with evidence of how the maternal environment affects the placenta. Signalling pathways such as mTOR have been involved in the placental response to external cues, but there are still many aspects of the regulation of placental function that remain unclear. Understanding how the placenta responds to external factors and how these modifications can affect fetal growth can have an impact on maternal and fetal health during the pregnancy and could also help to design interventions to improve the outcome of the pregnancy.

1.9 AIMS

The aims of this PhD are

1. To investigate the effect of prenatal high fat diet and metformin treatment on the expression of target genes in mouse placenta.
2. To determine the effect of metformin exposure in the expression of genes related to placental function in an *in vitro* model.
3. To determine whether the association between placental FTO gene expression with birth weight can be replicated in other cohorts.
4. To determine the effect of FTO knock down on microRNA expression in an *in vitro* model.

CHAPTER 2 GENERAL METHODS

2.1 HUMAN PLACENTAS

Human term placentas were collected from different human cohorts by researchers from the University of Southampton or the University of Cardiff as part of three different cohort studies: The Southampton Women's Survey (SWS), the maternal vitamin D osteoporosis study (MAVIDOS) and the Cardiff cohort. Following is a description of the studies and data collected in each of them.

2.1.1 Ethical considerations

All of the human cohort studies that provided samples for this study were conducted according to the guidelines of the Declaration of Helsinki. The Southampton and South West Hampshire Research Ethics Committee approved all the procedures (06/Q1702/104) for the SWS and the MAVIDOS Study. The South East Wales Research Ethics Committee approved all the procedures for the Cardiff cohort (REC number: 10/WSE02/10). Written informed consent was obtained from all participating women and by parents or guardians with parental responsibility on behalf of their children.

2.1.2 Southampton Women's Survey

The SWS is a cohort study of 3158 pregnancies with information collected from the mothers before conception [23]. Non-pregnant women (12579) aged 20 to 34 years were recruited via their General Practitioners and assessment of diet, physical activity, body composition, social circumstances and lifestyle were performed by trained research nurses at study entry and then in early (11 weeks) and late (34 weeks) gestation among those women who became pregnant (3159). Maternal blood samples were collected at 11 and 34 weeks gestation, blood samples were centrifuged and an aliquot of maternal plasma was frozen at -80°C until the fatty acid analysis was performed. Neonatal anthropometry, cord blood and placental samples were collected at birth. The children were followed up at 6 months, 1, 2, 4 and 6 years of age [23].

2.1.2.1 Maternal anthropometric measures in the SWS

Before pregnancy and at 11 and 34 weeks of pregnancy, trained research nurses took maternal body size measurements. These included: height, weight and four skinfold thicknesses (triceps, biceps, subscapular and suprailiac) that were measured in triplicate to the nearest 0.1 mm on the non-dominant side using Harpenden skinfold callipers. Mid upper arm circumference was also measured using a tape measure. BMI was calculated using the formula: weight/height^2 (Units: kg/m^2). Fat mass was estimated from skinfold thickness measurements using the method of Durnin & Womersley [190]. Arm muscle area was derived using a formula ((mid arm circumference – π x triceps skinfold thickness)^2/4π) - 6.5).

2.1.2.2 Fatty acids analysis of plasma phospholipids in the SWS

In the maternal blood samples collected at 11 and 34 weeks of pregnancy, fatty acids were analysed for plasma phosphatidylcholine (PC). This analysis was performed by Dr. Charlene Sibbons, a researcher of the SWS study. Total lipid was extracted from plasma with chloroform:methanol (2:1 vol/vol) and butylated hydroxytoluene (50 mg/L) was added as an antioxidant. Plasma lipid fractions were separated and isolated by solid phase extraction (SPE) on aminopropylsilica cartridges. Cholesterol esters (CE) and triacylglycerols (TAG) were first eluted with chloroform, then PC, the major plasma phospholipid, was eluted with chloroform:methanol (60:40, vol/vol). The PC fraction was dried under nitrogen and dissolved in toluene. Fatty acid methyl esters (FAME) were formed by incubation with methanol containing 2% (vol/vol) H_2SO_4 at 50°C for 2 h. After allowing the tubes to cool, samples were neutralised with a solution of 0.25 M $KHCO_3$ and 0.5 M K_2CO_3. FAME were extracted into hexane, dried down, dissolved in a small volume of hexane, and separated by gas chromatography. Gas chromatography was performed on a Hewlett-Packard 6890 gas chromatograph fitted with a BPX-70 column (30 m x 0.22 mm x 0.25 µm). The inlet temperature was 300°C. Oven temperature was initially 115°C and this was maintained for 2 min post-injection. Then the oven temperature was programmed to increase to 200°C at the rate of 10°C/min, to hold at 200°C for 16 min, and then to increase to 240°C at the rate of 60°C/min and then to hold at 240°C for 2 min. Total run time was just over 29 min. Helium was used as the carrier gas. FAME were detected by a flame ionisation detector held at a

temperature of 300°C. The instrument was controlled by and data collected using HPChemStation (Hewlett Packard, Waldbronn, Germany). FAME were identified by comparison of retention times with those of authentic standards run previously.

2.1.2.3 Fetal, neonatal and childhood measures in the SWS

Gestational age was calculated from the combination of the mother's last menstrual period date and early ultrasound data in comparison to a reference group of pregnancies of known gestational age in relation to size. Measures of fetal size were determined at 11, 19 and 34 weeks of gestation by a research sonographer. Head circumference (HC), abdominal circumference (AC), femur length (FL) and crown-to-rump length (CRL) were measured using a high-resolution ultrasound system (Acuson 128 XP, Aspen and Sequoia).

Shortly after delivery, research midwives recorded neonatal anthropometric measures (birth weight, HC, AC, mid-upper arm circumference and CRL). Within 2 weeks of birth, a subset of infants had body composition measurements made using dual X-ray absorptiometry (DXA) with a Lunar DPX-L machine. Fat mass, fat-free mass and bone indices (bone area, bone mass content and bone mass density) were calculated from the whole-body scan by using paediatric small scan mode, v 4.7c (paediatric software). Children were followed up at 4 (n = 1076) and 6 (n = 1477) years of age and anthropometric measures were repeated. Height was measured using a Leicester height measurer and weight was measured using Seca calibrated digital scales. Whole body composition DXA was measured using a Hologic Discovery Instrument and paediatric scan mode software. Anthropometric data collection was carried out by the SWS Study Group [191].

2.1.3 Maternal Vitamin D Osteoporosis Study – The MAVIDOS Study

The MAVIDOS cohort is a randomised, double-blind, placebo-controlled trial comparing a daily oral 1000 IU cholecalciferol (Vitamin D_3) with a matched placebo in pregnant women [192]. Pregnant women at around 12 weeks of gestation were recruited during a control screening ultrasound scan appointment by a research nurse. The women were recruited at three trial centres (Southampton, Sheffield and Oxford). The

samples used in this study were collected in Southampton only. If the informed consent was signed a blood sample was taken and 25-hydroxy vitamin D ($25(OH)D_3$) was measured in maternal serum using a Diasorin Liaison radioimmunoassay on an automated platform in a central laboratory (MRC, Human Nutrition Research Centre, Cambridge, UK). Women with $25(OH)D_3$ levels between 25 and 100 nmol/L were randomised to an oral vitamin D_3 supplement (1000 UI cholecalciferol per day) or a matched placebo from 14 weeks of pregnancy until delivery of the baby. A questionnaire was administered and information about parity, demographics, smoking, alcohol intake and exercise was gathered during early (14 to 17 weeks) and late (34 weeks) pregnancy. Anthropometry was measured during early and late pregnancy and 3D ultrasound was performed at 18 to 21 weeks of pregnancy. At 14 and 34 weeks of pregnancy maternal blood was taken for serum $25(OH)D_3$ measurement (Diasorin radioimmunoassay).

Following delivery, the placenta was collected. Neonatal anthropometry (weight, CRL, subscapular and triceps skinfold thicknesses and HC, AC and mid-upper arm circumferences) was measured and neonatal DXA was carried out using a Hologic Discovery Instrument.

2.1.4 Cardiff cohort

The study participants were healthy caucasian women with singleton pregnancies and no known medical disorders. 218 women were recruited prior to delivery at University Hospital Wales, Cardiff and Royal Gwent Hospital, Newport [193]. All the babies were delivered at term (≥37 weeks) with normal birth weight. Placentas were collected within 30 min of delivery by Dr. Anna Janssen to preserve the RNA quality.

2.1.4.1 Obstetric covariates in Cardiff

Information was obtained from the participant's medical notes. Obstetric history was noted with respect to parity, previous stillbirths and previous low birth weight or macrosomic pregnancies. Information was also obtained on the current pregnancy including prescribed medication, intrauterine infection or antepartum haemorrhage. Maternal smoking, alcohol consumption and drug use before and during pregnancy

were recorded from participant's medical notes and compared with self-reported measures from the participant questionnaire. Information on birth outcomes was also obtained including mode of delivery, complications of delivery, birth weight, HC, sex and gestational age. Finally, measures of infant well-being such as Apgar scores, arterial cord blood pH and neonatal intensive care unit admission were also recorded.

2.1.4.2 Neonatal measures in Cardiff

In addition to birth weight, custom birth weight centiles were calculated based on maternal height, weight, parity and ethnicity as well as infant birth weight, gestational age and gender using the GROW bulk centile calculator (UK), version 6.7.5 [194].

2.1.5 Placental sampling in human cohorts

In the SWS study, 300 placentas were collected by Dr. Rohan Lewis from term pregnancies. In the MAVIDOS study, 74 placentas were collected by Dr. Claire Simner and in the Cardiff cohort, 218 placentas were collected by Dr. Anna Janssen. All samples were collected within 30 min of delivery to preserve RNA quality.

The placental membranes and umbilical cord were removed and the placental weight recorded. In the SWS and MAVIDOS studies, to ensure that samples collected were representative of the placentas as a whole, five villous tissue samples of ~0.5 cm^2 were selected from the maternal side using a stratified random sampling method. Samples were snap frozen in liquid nitrogen and stored at -80°C. For each placenta, the five samples were pooled and crushed in a frozen tissue press, before being aliquoted into five cryovials and stored at -80°C. In the Cardiff cohort, the placentas were weighed and dissected within 2 h of delivery. Samples from villous trophoblast were obtained at five random sites from the maternal surface of the placenta, midway between the cord and the distal edge. In order to remove the excess of blood samples were rinsed in ice-cold phosphate buffered saline (PBS) and then stored in RNAlater (Sigma, UK) at -80°C until the RNA extraction.

2.2 THE HIGH FAT DIET AND METFORMIN TREATMENT MOUSE MODEL

Mouse placentas were generated as part of project run by Dr Felino Cagampang and Hugh Thomas from the University of Southampton. All studies were conducted under UK Home Office Licence. Female C57 BL6 mice were housed under controlled conditions: room temperature (RT) 22 ± 2°C; 12 h of light/dark cycle. They were randomly assigned to independent variables 'diet': control diet (7% kcal fat) or high fat diet (45% kcal fat) for 6 weeks before conception and during pregnancy, and 'treatment': control treatment or metformin treatment (metformin in drinking water at 250 mg/kg/day) The diet was administrated for 6 weeks before conception and during pregnancy and the treatment was supplied when the conception was confirmed (Figure 2.1). The metformin treatment was calculated within the range of treatment dosage in humans [195]. On day 16 of pregnancy (mouse pregnancy is between 19 to 21 days), the mothers were sacrificed, blood samples were taken and fetal liver, heart, placenta and total weight were recorded, and complete organs were collected. All the tissues were frozen in liquid nitrogen and stored at -80°C within 30 min after collection.

2.3 CELL CULTURE

2.3.1 Thawing, culture, passaging and cryopreservation of cell lines

Media and reagents need to be pre-warmed in a water bath at 37°C before any procedure. Information about the reagents and media used in the cell culture experiments are included in Table 2.1 and Table 2.2.

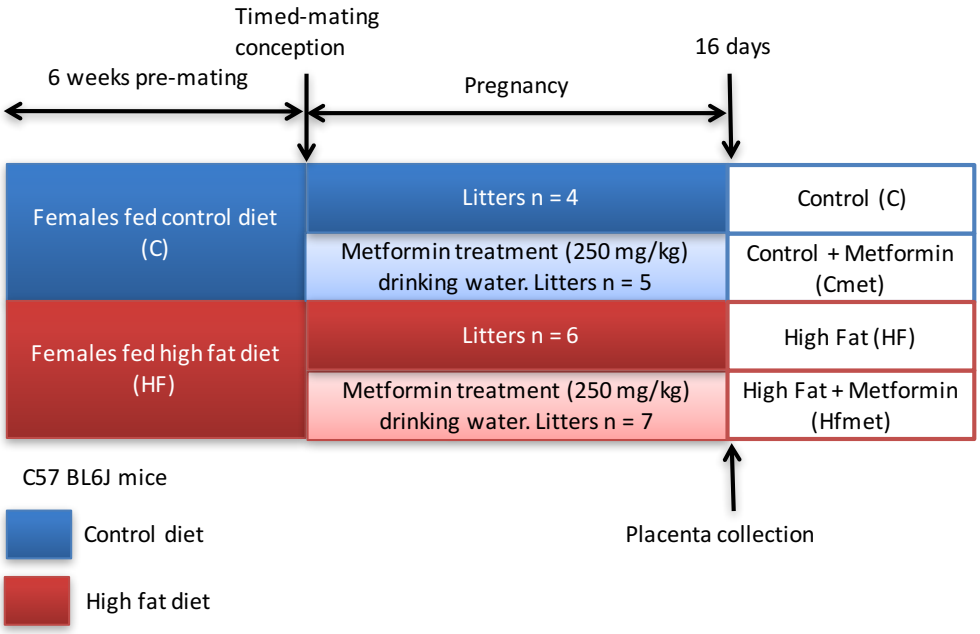

Figure 2.1 The high fat and metformin treatment study design

The dams were fed with the selected diet (control or high fat) 6 weeks before mating and during pregnancy (16 days). After the pregnancy was confirmed the diet groups were divided and two groups received metformin (250 mg/kg/day) in the drinking water. The tissues samples were collected after 16 days (normal mouse pregnancy last 21 days).

Table 2.1 Cell culture reagents

Reagent	Provider
Dulbecco's phosphate-buffered saline (PBS (-)). Calcium and magnesium free	D8537, Sigma, UK
Fibroblast growth factor 4 (FGF4)	100-31, PrepoTech, London, UK
Heparin	H3149, Sigma, UK
β-mercaptoethanol	M7522, Sigma, UK
Fetal bovine serum (FBS)	14821482, Fisher Scientific, UK
Penicillin-streptomycin solution	P4333, Sigma, UK
L-glutamine	17-605E, Lonza, Cambridge, UK
Trypsin-EDTA	T3924, Sigma UK
Sodium pyruvate	S8636, Sigma, UK
Dimethyl sulfoxide (DMSO)	D2650, Sigma, UK
Dulbecco's modified Eagle's media – high glucose. (DMEM) With 4500 mg/L glucose, l-glutamine, sodium pyruvate, and sodium bicarbonate, sterile-filtered	D6429, Sigma, UK
Dulbecco's modified Eagle's media – high glucose. AQmedia™ (DMEM AQMedia™) With 4500 mg/L glucose, l-alanyl-glutamine, and sodium bicarbonate, without sodium pyruvate, sterile-filtered,	D0819, Sigma, UK
RPMI 1640 media With l-glutamine and sodium bicarbonate, sterile-filtered,	R8758, Sigma, UK

Table 2.2 Media and reagents preparation

Media/reagent name	Preparation
FGF4 - 1000X stock solution (25 µg/ml)	Add 1 ml of PBS (-) containing 0.1% (w/v) bovine serum albumin to a vial of lyophilised human recombinant FGF4 and store at -80 in 100 µl aliquots.
Heparin - 1000X stock solution (1 mg/ml)	Re-suspend heparin in PBS (-) to a concentration of 1.0 mg/ml and store at -80°C in 100-µl aliquots.
HEK 293 cell media	DMEM – high glucose with 10% of FBS, penicillin (100 U/ml), streptomycin (100 mg/ml) and 1 mM of l-glutamine.
MEF media	DMEM AQMedia™ – high glucose with 10% of FBS, penicillin (100 U/ml), streptomycin (100 mg/ml) and 2 mM of l-glutamine.
TS media	RPMI media with 20% of FBS, 100 U/ml of penicillin, 100 mg/ml of streptomycin, 20 mM of l-glutamine, 1 mM of β-mercaptoethanol and 10 mM of sodium pyruvate.
TS + 1.5X F4H	TS media with 1.5X of FGF4 and heparin
TS + F4H	TS media with 1X of FGF4 and heparin
70CM + F4H	30% of TS media, 70% of conditioned media and 1X of FGF4 and heparin
70CM + 1.5X F4H	30% of TS media, 70% of conditioned media and 1.5X of FGF4 and heparin
70CM + 1.8X F4H	30% of TS media, 70% of conditioned media and 1.8X of FGF4 and heparin
MEF freezing media	70 % of DMEM AQMedia™ with 20% of FBS and 10% of DMSO
TS freezing media	70% TS media with 20% of FBS and 10% of DMSO
HEK 293 cell freezing media	70% of DMEM with 20% of FBS and 10% of DMSO

FGF4: Fibroblast growth factor 4, PBS: Phosphate-buffered saline, TS: Trophoblast stem cells, MEF: mouse embryonic fibroblast. Conditioned media – see section 2.3.2.2.

2.3.1.1 Thawing cell lines

Cells are quickly thawed at 37°C in a water bath. Then 9 ml of the cell media according to the cell type is added to a 50 ml tube with the cell suspension and centrifuged at 1000 rpm for 10 min. The supernatant is discarded and the cell pellet is re-suspended in 10 ml of media and transferred to a 0.75 cm^2 cell culture flask, containing 10 ml of

media. The cells are incubated at 37°C in a humidified incubator of 5% CO_2 atmosphere. Media is changed when necessary.

2.3.1.2 Passaging and counting cell lines

When the cells become confluent (approximately 90%) the media is removed and cells are washed with 10 ml PBS. In order to detach the cells 3 ml of 0.05% trypsin/0.2 mM EDTA are added to each flask and the cells are incubated for 3 min at 37°C. Trypsinisation is stopped by adding 7 ml of media to each flask. The cell suspension is collected in a 50 ml falcon tube, centrifuged for 10 min at 1000 rpm and the cell pellet re-suspended in 10 ml of media.

Before plating or splitting the cells, cell counting is carried out in order to determine the approximate amount of cells that are added to the plates or flask. Cells are counted using a Neubauer bright-line haemocytometer. The haemocytometer is cleaned with 70% ethanol and the coverslip is affixed using gentle pressure. The cell suspension is mixed gently and 1 ml is transferred to an tube before the cells have settled. 100 µl of the cell suspension is mixed with 100 µl trypan blue (for determining viability) avoiding lysing them. This is added to the chamber carefully without overfilling it. Using the 10X objective of the microscope the grid lines of the heamocytometer are visualised (Figure 2.2). The haemocytometer has four larger corner squares made up of 16 smaller squares. The number of viable cells (live cells do not take up trypan blue) in each of the four corner squares is determined. Cells touching the bottom and right side of each large corner square are not counted. The number of cells in one corner square is equivalent to the number of cell x 10^4/ml. The total number of cells is calculated as follows: Average of count from the 4 sets of 16-corner-squares/2 = number of cells x 10^4 /ml.

2.3.1.3 Freezing cell lines

After the cells have been harvested (as described in section 2.3.1.2) they are re-suspended in freezing media (Table 2.1). 1 ml of the suspension is added to a cryovial and stored overnight at -80°C in a cell freezing container (Nalgene Mr. Frosty® - Fisher

Scientific) filled with isopropanol (cooling rate of -1°C per minute). After 24 h the cells are transferred to a liquid nitrogen tank for long term storage.

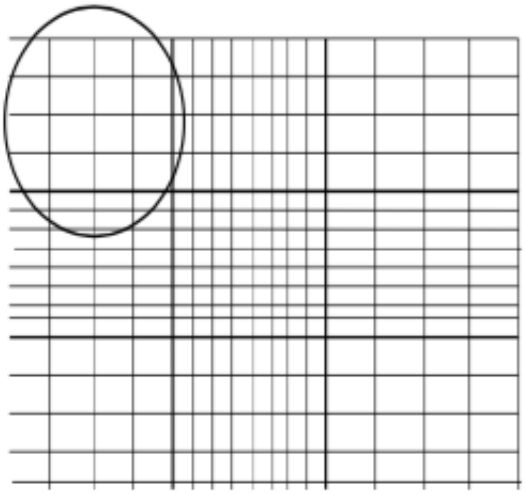

Figure 2.2 Gridlines on haemocytometer

Haemocytometer gridline, a corner of 16 squares is selected for the cells to be counted.

2.3.2 Mouse embryonic fibroblast and trophoblast stem cells culture

Mouse embryonic fibroblast (MEF) and trophoblast stem cells (TS) were kindly donated by Dr. Neil Smyth of University of Southampton. Table 2.1 includes all the reagents that were used in the culture of these cells lines. Table 2.2 includes the reagents and media preparation for the cell culture experiments. This protocol was adapted from the protocol of Tanaka [196].

2.3.2.1 Culture of Mouse embryonic fibroblast – preparation of radiated feeder cell stocks

The MEF were cultured in MEF cell culture media (Table 2.2). The cells were thawed as described in section 2.3.1.1, re-suspended in 10 ml of cell culture media and split into two 1.75 cm^2 cell culture flasks, each containing 20 ml of cell culture media. The cells were incubated at 37°C in a humidified incubator of 5% CO_2 atmosphere. Media was changed when necessary. When the cells became confluent (approximately 90%) the cells were harvested as described in section 2.3.1.2 and then re-suspended and split into eight 1.75 cm^2 cell culture flasks, each containing 20 ml of media.

The cells were incubated as described above until they were 90% confluent, harvested as described before and split into sixteen 1.75 cm^2 cell culture flasks. After the cells reached confluency they were harvested in 100 ml of media into two 50 ml falcon tubes. Cells were then radiated for 23.6 min at 50G in a Gammacell 1000 Irradiator located in the Tenovus Building in Southampton University. Radiated cells were centrifuged at 1000 rpm for 10 min and the pellet re-suspended in 16 ml of MEF freezing media (Table 2.2), and cryopreserved as described in section 2.3.1.3.

2.3.2.2 Preparation of condition media stocks

The TS cells need a bed of MEF cells to be able to grow, they also need fibroblast growth factor 4 (FGF4) and heparin (Table 2.2). In order to grow TS cells it is necessary to first produce stocks of MEF that are inactivated (to stop their division capacity) by radiation. It is also necessary to produce stocks of conditioned media that contain the factors and nutrients released by the inactivated MEF. This can be used when the TS cells are grown without the feeder layer. Table 2.2 Media and reagents preparation contains the description of the media used for TS and MEF cell culture and what they contained.

Media and reagents were pre-warmed in a 37°C water bath before any procedure. A vial of radiated MEF was quickly thawed as described in section 2.3.1.1 and the cell pellet re-suspended in 5 ml of TS cell culture media without FGF4 and heparin (Table 2.2). The cells were transferred into a 0.75 cm^2 cell culture flask containing 5 ml of TS media. They were incubated for 3 days at 37°C in a 5% CO_2 atmosphere. The media was collected and stored at -20°C. Two more batches of media were prepared with the same flask of radiated MEF before the cells were discarded. The three batches of media were combined, centrifuged for 20 min at 1000 rpm and the cell debris was removed. The conditioned media was then filtered using a 0.45 µM filter and stored at -20°C in 10 ml aliquots. The aliquots were thawed when necessary and stored at 4°C during use. Thawed stocks were not re-frozen.

2.3.2.3 Culture and passage of TS cells

The day before starting the TS cell culture a cryovial of the radiated MEF was thawed and cultured in a six well plate (approximately 5 x 10^4 cells/35-mm dish) using TS + F4H media (Table 2.2). They were incubated at 37°C in a 5% CO_2 atmosphere. The next day a vial of TS cells was thawed, the TS freezing media was removed and the TS cells were plated onto the pre-cultured radiated MEF and then incubated at 37°C in at 5% CO_2 atmosphere. TS media was changed daily.

2.3.3 Human embryonic kidney cells 293 culture

Human embryo kidney cells (from Dr. Matt Darley) were thawed as described in section 2.3.1.1. The cells were cultured using HEK 293 cell culture media (Table 2.1), in 0.75 cm^2 cell culture flasks at 37°C in a humidified incubator of 5% CO_2 atmosphere. Media was changed when necessary When cells reached 90% confluency they were split using trypsin (section 2.3.1.2), counted and plated in 24 well plates for the exposure experiments.

2.3.4 Knock down of Fat Mass and Obesity Associated gene in HEK 293 cells

HEK 293 cells were used to knock down the *FTO* gene mRNA expression using small interfering RNA (siRNA) inhibition. The transfection was performed using Lipofectamine™ RNAiMAX (Ambion-Life technologies, UK) reagent. siRNAs were obtained from Ambion-life technologies, UK (positive control, negative control and *FTO* specific siRNAs)

Initial experiments were performed using the reverse protocol, which is when the siRNA and the transfection reagent are added to the cells on the same day that they are plated. The protocol was provided by the manufacturer and an optimisation of the method was performed to determine the most reliable conditions in our lab. The protocol was tested in order to determine concentration of siRNA, time of incubation and number of cells that were necessary in order to obtain a knock down of the gene expression up to 90% for the positive control and up to 70% for the *FTO* gene. Also, the two siRNAs provided by the company were tested in order to determine which one induced the greatest reduction of *FTO* expression in the cells.

HEK 293 cells were thawed and cultured as described in section 2.3.1 until they were 80 to 90% confluent (approximately 2 days). On the day of the experiment, all the reagents were pre-warmed at 37°C. All the siRNAs (positive control-PC, negative control-NC, and *FTO* siRNA1 and *FTO* siRNA2) were diluted to a 100 µM stock solution that was aliquoted and stored at -20°C. The day of the experiment a 10 µM working solution was prepared for all the siRNA for use in the experiment. All the knock down experiments were performed in duplicate and a mock control (MC- media and lipofectamine® RNAiMAX) and untransfected cell control (UTC) were included in all the experiments.

In order to form the siRNA oligomer-lipofectamine® RNAiMAX complexes, a solution containing DMEM media without FBS or antibiotics and each siRNA was prepared. The solution was mixed gently and then the Lipofectamine® RNAiMAX was added and incubated 10-20 min at RT.

HEK 293 cells were harvested as described before in section 2.3.1, the pellet was diluted in 10 ml of DMEM without FBS or antibiotics and the amount of cells per ml was determined as described in section 2.3.1.2. The cells were platted as follows: in a 24-well cell culture plate 102 or 104 µl of the oligomer-Lipofectamine® RNAiMAX-media mixture was added to each well, then 5 x 10^4 HEK 293 cells were added to each well and finally DMEM media without FBS or antibiotics was used to complete a final volume of 600 µl per well. The cells were checked every 24 h to confirm they were growing properly; no media was changed during the duration of the experiment. When the incubation time (48 h) was finished the media was removed from the plates and 500 µl of RNAzol were added to each well. The cells were scraped and the mixture was transferred to a 1.5 ml tube and stored at -80°C until the RNA extraction was performed.

2.3.5 Metformin exposure experiment in HEK 293 cells

A vial of HEK 293 cells was thawed and the cells were cultured as described before until they were 80 to 90% confluence (approximately 2 days). A metformin stock

solution of 100 mM was previously prepared, filtered and stored at -20°C until its use. On the day of the experiment all the reagents were pre-warmed at 37°C, the cells were harvested and counted as described in section 2.3.1.2. 25 x 10^4 cells were added per well in a 6 well cell culture plate. The metformin stock solution was diluted in DMEM cell culture media (Table 2.2) and was added to the plated cells in order to reach a final concentration of 20 μM of metformin per well. The cells were incubated at 37°C in a 5% CO_2 atmosphere. After 48 h the media was removed from the plates and 1 ml of RNAzol was added to each well. The cells were detached from the well and mixed with the RNAzol; the mixture was frozen at -80°C until the RNA was extracted.

2.4 RNA AND DNA EXTRACTION

2.4.1 RNA extraction

Two methods were used for the extraction of total RNA from the tissues and cells used in this study. A column based extraction technique was used for the RNA extraction in the human samples in order to avoid the potential protein contamination that can happen with fibrous tissues as the placenta. An ethanol precipitation based technique was used with the cells and mouse placenta samples since the protein content in this samples was lower and the initial evaluation showed a good quality sample after the extraction.

2.4.1.1 RNAzol

Previously collected cell lysate, whole placentas or 30 mg of crushed mouse placenta were homogenised in 1 ml of RNAzol® (Sigma, UK) for 30 s. For the DNA, protein and polysaccharide precipitation 0.4 ml of RNAse-free water were added to the samples, they were shaken for 15 s, incubated for 15 min at RT and then centrifuged at 12000 g for 15 min at RT. The supernatant containing the RNA was transferred to a new tube, 1 ml of 70% isopropanol (Sigma, UK) was added and the samples were incubated for 10 min at RT then centrifuged at 12000 g for 10 min at RT to pellet the RNA. The supernatant was removed and 0.5 ml of 75% ethanol (Fisher Scientific, UK) were added. The samples were centrifuged at 4000 g for 3 min, this process was repeated

twice in order to remove excess of isopropanol. At the end of the second wash the ethanol was removed and without drying the RNA pellet was solubilized by adding 100 µl of RNAse-free water and shaking the samples for 5 min at RT. RNA yield and quality were assessed as described in section 2.4.2. RNA was stored at -80°C.

2.4.1.2 miRNeasy kit

The miRNeasy kit (Qiagen, Manchester, UK) was used for the RNA extraction in the human placenta following the manufacturer's instructions. Briefly, 20 to 30 mg of powdered placenta were homogenized in 0.7 ml of QIAzol Lysis reagent® for 30 sec and incubated for 5 min at RT. 140 µl of chloroform (Fisher Scientific, UK) were added and the samples were shaken for 15 sec and centrifuged for 15 min at 12000 g at 4°C. Three phases were formed and 350 µl of the aqueous phase (upper phase) containing the RNA were transferred to a new tube. Then 525 µl of 100% ethanol was added and mixed with the samples. 700 µl of the mixture was transferred into a RNeasy mini spin column and centrifuged at 8000 g for 15 sec at RT. The eluate was discarded and the rest of the mixture (≈ 200 µl) was transferred into the column, centrifuged at 8000 g for 15 sec at RT and the flow-through discarded. 350 µl of buffer RWT were added into the column and the samples were centrifuged for 15 sec at 8000 g at RT. For the DNase treatment, 80 µl of DNase I mix was added directly to the RNA (bound to the membrane in the column) and incubated for 15 min at RT. At the end of the incubation the samples were washed once with 350 µl of RWT buffer and twice with 500 µl of RPE buffer; being centrifuged at 8000 g for 1 sec at RT each time. Between each wash, the eluate was discarded. The column was transferred to a collection tube and 50 µl of RNase-free water was added into the column. The samples were centrifuged at 8000 g for 1 min at RT and the RNA recovered in the collection tube. RNA yield and quality were assessed as described below. The samples were stored at -80°C.

2.4.2 DNA extraction

A Quick-gDNA™ MiniPrep kit (Zymo Research, USA) was used to extract the genomic DNA from the samples, the procedure was according to the manufacturer instructions. Briefly, 40 µg of crushed frozen tissue was homogenised in 500 µl of Genomic Lysis Buffer at RT. After the lysate was centrifuged at 12,000 g for 5 min. The supernatant

was then transferred to a Zymo Spin Colum contained in a collection tube. The column with the sample was then centrifuged at 12,000 g for 2 min. The flow through and the collection were discarded and the column was placed in a new collection tube and a 200 µl of pre-wash buffer was added. Samples were centrifuged at the same conditions and the flow through was discarded, 500 µl of wash buffer were added and samples were centrifuged again. Tube collection with flow through were discarded and the column was placed in a new tube, 100 µl of water were added to the column and the samples were incubated at RT for 5 min and then centrifuged at 16000 g for 30 s. Samples were stored at -80°C until they were used for the sex determination of each placental sample.

2.5 NUCLEIC ACID QUANTIFICATION AND QUALITY DETERMINATION

The quality and yield of the RNA and DNA were assessed using a NanoDrop® 1000 spectrophotometer (Thermo Scientific, USA) and agarose gel electrophoresis. An extra analysis using Agilent 2100 Bioanalyser was performed for the samples that were sent to sequencing.

2.5.1 RNA and DNA quality and concentration measured by UV light

Nucleic acids and proteins absorb UV light at 260 nm and 280 respectively and there is a linear relationship between the amount of UV light absorbed and the concentration of these molecules. In a spectrophotometer, by measuring how much UV light is absorbed it is possible to calculate the amount of RNA or DNA in the sample and also the presence of contamination (proteins and/or solvents). Protein contamination was determined through the 260/280 ratio and solvent contamination using the 260/230 ratio. Ratios for RNA or DNA above 1.7 were considered to be of acceptable quality. RNA samples that did not meet these quality criteria were not used for the next experiments.

RNA and DNA concentration and quantity were assessed using a NanoDrop® 1000 spectrophotometer. Briefly, using 1 µl of RNAse-free water the machine was blanked

then 1 µl of the samples was loaded and the absorbance measured according to the manufactures instructions. The RNA and DNA concentration (ng/µl), 260/280 and 260/230 ratios were recorded for each sample.

2.5.2 RNA and DNA quality and size quantification using gel electrophoresis

This procedure is based on the capacity to separate molecules with the same charge by their size using an electric field. Electrophoresis is used to determine the size of a fragment or the extraction quality.

Gels are prepared at different concentrations depending on the size of the fragments that want to be separated (higher concentration smaller the fragments that need to be separated). The necessary amount of agarose was added to 100 ml Tris Borate EDTA (TBE; Fisher Scientific) and 7 µl of Gel Red™ (Biotium, USA) was added for the visualisation of the nucleic acid under UV light. The gel was allowed to set and the samples were loaded into the gel and run at 100 V for 45 min. The bands were visualised using UV light.

To prevent the formation of secondary structures in the RNA molecules, that can influence their migration through the gel, all gels were run under denaturing conditions by adding 2 µl formamide to the RNA samples. This method allows a qualitative analysis of the RNA by showing DNA contamination and RNA integrity. It also allows a semi-quantitative analysis based on the brightness of the bands (Figure 2.3).

For RNA samples, an agarose gel of 1% concentration was prepared as described above. The gel was allowed to set and the samples were prepared by mixing 5 µl of RNAse-free water, 2 µl of deionised formamide (Fisher Scientific, UK), 2 µl of loading dye (Promega, USA) and 3 µl of neat RNA sample (between 1.2 to 0.8 µg of RNA). The samples were loaded into the gel and run at 100 V for 45 min. The bands were visualised using UV light. For RNA samples that were not degraded, two clear bands should be observed (28S and 18S ribosomal RNA) in a relation 2:1. (Figure 2.3).

For DNA samples, an agarose gel of 1.5% was prepared as described above. The gel was allowed to set and 10 µl of DNA sample with 2 µl of loading dye (Promega, USA) were loaded into the gel and run at 100 V for 45 min. A 1000 Kb ladder (Promega, UK) was also loaded. The bands were visualised using UV light. For DNA gel electrophoresis

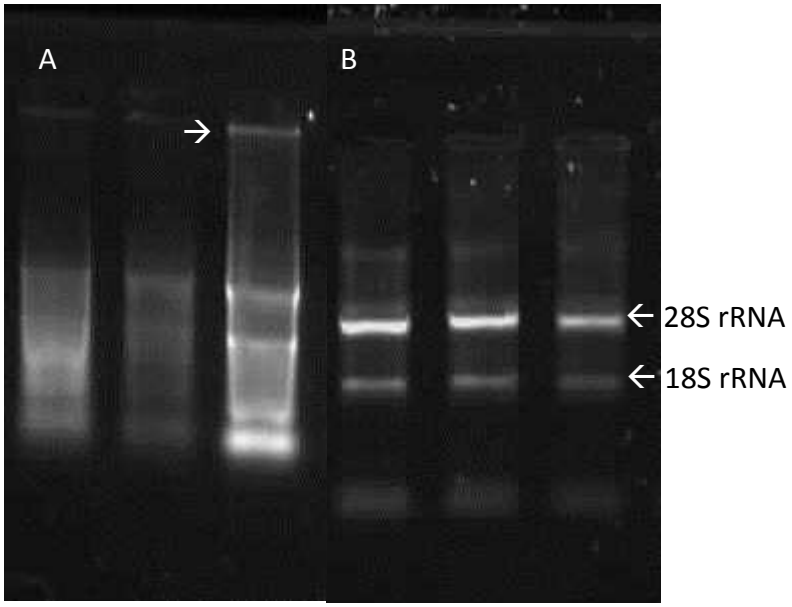

was used to determine fragment sizes when necessary.

Figure 2.3 Evaluation of RNA quality using electrophoresis

An example of RNA gel electrophoresis. A. Partially degraded RNA as indicated by indistinct 18s and 28s bands and smearing, in addition, the presence of nucleic acid in the well in lane 3 may indicate DNA contamination (arrow). B. Intact RNA with two bands 28S, 18S. The ratio between them should be approximately 2:1.

2.5.3 RNA quality and concentration measured by bioanalyser

Total RNA samples for messenger RNA (mRNA) and microRNA (miRNA) sequencing were sent to the Woelk laboratory (University of Southampton) in order to determine their quality using a bioanalyser. The bioanalyser electrophoretic assay is based on a similar principle to gel electrophoresis. The samples are loaded into a chip that contains a polymer matrix that helps to separate the molecules by size and dye molecules intercalate into the RNA forming a complex that is detected by laser-induced fluorescence. The data is transformed into gel-like images and electropherograms as is showed in Figure 2.4. The samples are compared with a ladder

of known sizes and the migration times are used to determine the size of the molecules in the samples. In the RNA assays the ribosomal ratio (28S rRNA/18S rRNA) is calculated in order to determine the RNA integrity, additionally, the RNA Integrity Number (RIN) can be utilised to estimate the integrity of total RNA samples. This number is calculated using the entire electrophoretic trace of the RNA sample and the presence/absence of degradation products. A RIN number of 10 indicated intact RNA, a RIN number of 5 indicated partially degraded RNA and a RIN number under 3 belongs to a strongly degraded RNA sample.

In order to analyse the samples, 10 µl of the diluted RNA with a concentration above 100 ng/µl were sent to the Woelk laboratory. Samples with RIN number over 8.5 were accepted as a good quality RNA. RNA samples that did not meet these quality criteria were not used for the next experiments.

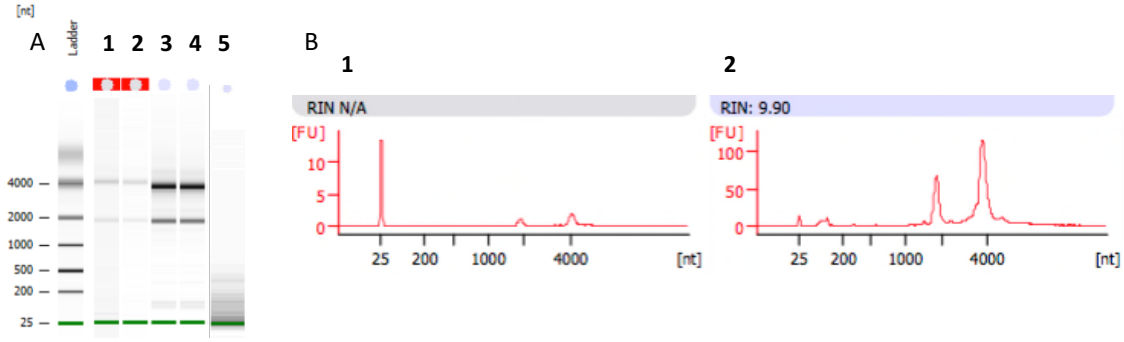

Figure 2.4 Evaluation of RNA quality by a bioanalyser

An example of bioanalyser results. A. shows the densitometry plot that is produced by the machine and is similar to a gel image, the first line is the ladder, 1 and 2 are examples of samples with not enough RNA for the analysis, lines 3 and 5 are examples of good non-degraded RNA and line 5 is an example of a degraded RNA. B. shows two examples of the electropherogram produced by the machine, number 1 is showing a sample without enough RNA and number 2 is showing a sample with non-degraded RNA.

2.6 GENE EXPRESSION QUANTIFICATION

In this study in order to quantify the expression of the genes of interest, the mRNA molecules were quantified: mRNA was converted to complementary DNA (cDNA) using

a reverse transcription polymerase chain reaction (RT-PCR) and then a quantitative PCR (qPCR) was performed for each gene that needed to be measured.

2.6.1 Reverse transcription PCR (RT-PCR)

Quantification of mRNA expression was performed in two steps; the first step was the synthesis of cDNA and the second one was the qPCR that was performed using specific primers. Standard curve, controls and experimental samples were prepared at the same time as follows:

Standard curve: 6 µg of RNA were dissolved in 30 µl of RNAse-free water (concentration: 0.2 µg/ µl) and labelled as standard 7 (S7), another 6 tubes were labelled from S6 to S1; 15 µl of RNAse-free water was added at each of them. 15 µl of the S7 was added to S6 and mixed; the same was done for all the other standards being careful to change the tip between each tube. The standards were mixed and centrifuged and reserved for the RT-PCR.

Controls: A pooled sample of neat RNA was prepared using 10 different samples and then adding 30 µl of RNAse-free water to reach a final concentration of 0.04 µg/µl.

Experimental samples: All the samples were diluted to a final volume of 25 µl (concentration: 0.04 µg/µl).

For the RT-PCR reaction 5 µl of the standards, controls (6) or experimental samples were added to a new tube, 0.5 µg of random primers (Promega, USA) were added and RNAse-free water to a final volume of 15 µl. The samples were heated at 70°C for 5 min on a Veriti® thermal cycler (Applied Biosystems). 50 nmol of triphosphate nucleotides mixture, 25 units of Recombinant RNasin® Ribonuclease Inhibitor, 200 units of Moloney Murine Leukemia Virus Reverse Transcriptase (M-MLV-RT), 5X M-MLV-RT buffer (Promega, UK) and water were added to the reaction mixture to a final volume of 25 µl. The mixture was heated at 37°C for 60 min and then 75°C for 10 min. The samples were shaken, centrifuged and diluted to 1:25 with RNA-free water. All the samples were reverse transcripted in one batch to reduce variation.

To control for genomic DNA contamination no enzyme controls (NEC) were prepared at the same time by adding the same amount of reagents and replacing the M-MLV-RT with water. Samples, standards and controls were stored at -20°C.

2.6.2 Real time quantitative PCR (qPCR)

PCR techniques are based on the ability of the DNA polymerase to synthesize specific DNA fragments using oligonucleotides (primers) that are complementary to the specific area that needs to be amplified [197]. PCR reactions require three steps: denaturation (DNA molecules are denatured by exposure to high temperatures), annealing (temperature is reduced to allow the formation of the primer-DNA template dimer) and extension (DNA polymerase recognise the dimer and amplifies the DNA template). These three steps occur during 1 cycle at the end of which two copies of the target should have been produced. Cycles are repeated several times to increase the number of copies of the fragment of interest. The reaction occurs in an exponential manner since in each cycle the number of copies is duplicated [197]. qPCR is a modification of the normal PCR, a dye substance or a target probe is added to the reaction in order to detect when the amplification has taken place [198].

Intron spanning primers and probes were designed using ProbeFinder® version 2.49 or Primer-BLAST. Primers were purchased from Eurogentec (Eurogentec, Southampton, UK), Universal Probe Library Probes were purchased from Roche (Roche, Sussex, UK), Taqman probes from (Eurogentec) and Perfect Probes from Primer design (Southampton UK), depending on the genes that were measured. The quantification of the mRNA expression was carried out using the LightCycler® 480 real time PCR system (Roche) and all the reactions were performed in a 384 well plate. Briefly: ~3 ng of cDNA, 1 µM of forward, reverse primers and probe and 2 X master mix (LightCycler® 480 probes master, 2X. Roche, UK) were added to the well for a final volume of 10 µl. The run protocol in the machine was set according to the type of probe that was used for the reaction (Table 2.3). A standard curve, set of controls, NEC and no template control (NTC) were added to each run to determine the accuracy of the measurements; all the samples were measured in triplicate. The crossing point (Cp)

value was obtained from the machine for each sample using the second derivative method as described below.

Table 2.3 Quantitative RT-PCR run protocols according to the type of probe used

Probe type	Number of cycles	Step	Time	Temp. (°C)
PerfectProbe®	1	Enzyme activation	10 min	95
	50	Denaturation	15 s	95
		Data collection	30 s	50
		Extension	15 s	72
TaqMan®	1	Enzyme activation	10 min	95
	40	Denaturation	15 s	95
		Annealing, elongation and data collection	60 s	60
Universal ProbeLibrary®	1	Enzyme activation	5 min	95
	45	Denaturation	10 s	95
		Extension	30 s	60
		Data Collection	1 s	72

2.6.2.1 Quantification of PCR product

Quantification in qPCR is based on the principle that the accumulation of an amplification product can be determined indirectly using a fluorescent measure. qPCR machines measure the fluorescence signal per cycle in each sample during a PCR run. In theory, with every PCR cycle the product amount is duplicated increasing the fluorescence signal produced until the fluorescence intensity is higher than the background signal. A graph can be plotted with the fluorescence signal (y-axis) against the number of cycles for each sample as shown in Figure 2.5. From this graph a relative quantitative value representing the fluorescence level can be calculated for each sample using two methods. The fit point method is performed by drawing a line parallel to the x-axis and within the linear phase of the real-time fluorescence intensity curve. This gives a value for when each sample crosses the line called the cycle threshold (Ct). The second method is known as second derivate, and calculates the fractional cycle where the second derivate of the real time fluorescence intensity curve reaches the maximum value; called the crossing point (Cp) [199]. Ct or Cp values can be

recorded for each sample in order to calculate the relative expression of the mRNA transcript.

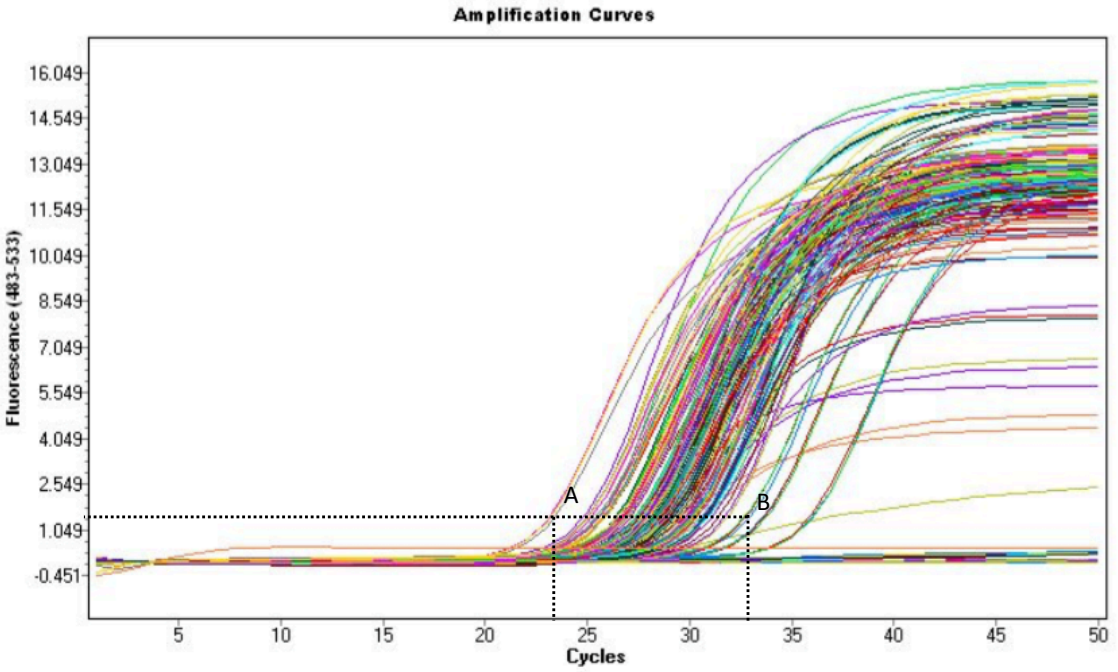

Figure 2.5 Amplification curve from a qPCR run

In a qPCR run, fluorescence can be quantified and a plot of the fluorescence vs of the cycle number can be generated. A and B show the Crossing point value (Cp Value) for two different samples. Cp is the PCR cycle at which the target amplification is first detected. Since there is a linear correlation between Cp and concentration a lower Cp value indicates a higher concentration of the product in the sample.

2.6.2.2 Relative quantification of gene expression levels

The qPCR results can be quantified by two methods: the standard curve method and the comparative threshold method (delta 2^{-Ct}). In the standard curve method, a set of seven known standards are amplified with the samples. The first standard (S7) is given the arbitrary concentration of 100 and all the samples are a double dilution in relation to this (100, 50, 25, etc.). Since the Cp values have a linear correlation with the logarithm concentration of cDNA in the starting material, a plot of log of initial target arbitrary concentration versus Cp values can be made (Figure 2.6). This is used to calculate the concentration of a sample when the Cp value of the sample is known. The Cp value of each sample and control was converted to concentration using the equation from the standard curve: $X = 10^{((y - c)/m)}$. Where X is concentration, m is the slope, c is y-intercept and y is Cp value. The triplicate results were averaged and that

value was considered the concentration of the samples. Concentration levels were then normalized to the expression of appropriate reference genes that was also measured in all the samples.

The delta 2^{-Ct} method was used for some of the experiments, the delta 2-Ct method was used for some of the experiments, when there was not enough spare RNA for prepared the standard curve. Briefly, the highest Cp/Ct value for the specific mRNA that was being quantified was subtracted from all the other Cp/Ct values, that way all the Ct values were transformed to "deltaCT value", then for each data point the equation: $2^{(-deltaCT)}$ was applied, obtaining the relative expression (relative to the lower expression of the samples). This relative expression was then divided by the expression of the reference genes and that relative expression was used for further analysis.

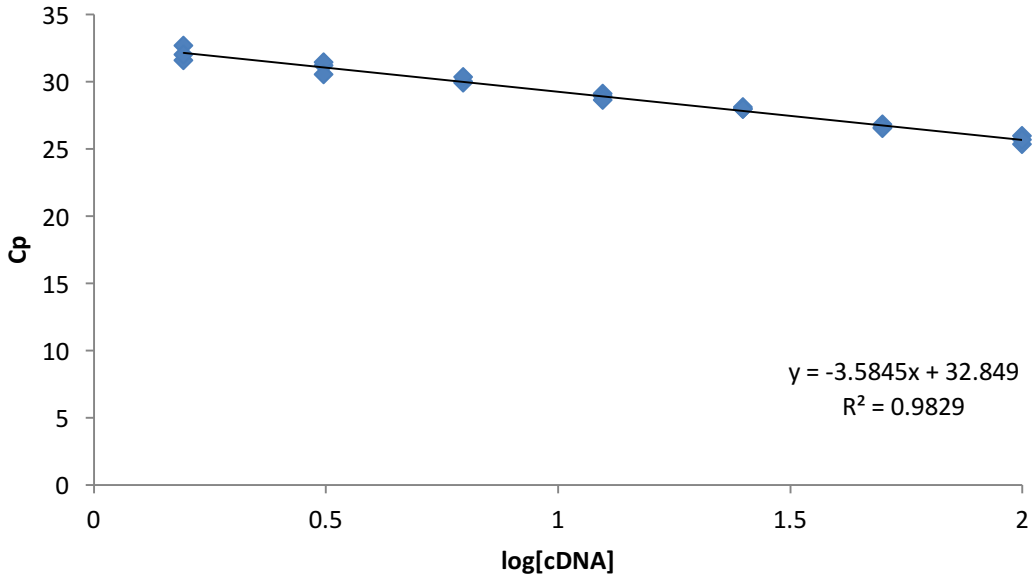

Figure 2.6 Example of standard curve

The Cp values for the seven standards were plotted against the log of cDNA concentration. The slope (-3.58 in this example) of the curve is used to calculate the efficiency and amplification for each qPCR reaction. Y-axis: Crossing point (Cp) X-axis: log of concentration of the standards.

The standard curve was used to calculate the overall efficiency of the run as well as the relative concentration of each sample and controls. Figure 2.6 shows an example of an experimental standard curve. In accordance with the general rules for qRT-PCR, during

amplification, the amount of DNA is duplicated after each cycle meaning that the efficiency in the run is perfect (efficiency value = 1) and the slope of the standard curve is -3.3, but, in experimental conditions that is not always the case so adding a standard curve to each run allows the calculation of the efficiency for each experiment improving the accuracy of the measures [200].

The accuracy of each PCR run was determined. Linear regression was used to calculate the slope of the experimental standard curve and its accuracy represented by a R^2 value; values above 0.8 were considered acceptable. The efficiency of the run was calculated using the formula: efficiency = (log -1/slope)-1 and runs with efficiency between 0.8 and 1.2 were considered acceptable for the gene expression calculation. Using the standard curve equation, the concentration of the controls was calculated and the coefficient of variation (CV) for the controls was also calculated using the equation: CV = (SD/Av)*100, where Av is the average of the concentration of the six controls and SD is the standard deviation of the six controls. A CV less than 10% was acceptable for the gene expression calculation. The NTC and the NEC were also checked for any amplification indicating contamination in the reactions.

Reference genes that are stably expressed in the specific tissue and experimental conditions (as established by geNorm® analysis) [201] were also measured. The calculation of the concentration of each reference gene was made as previously described and the geometrical mean (GM) of the measured references genes was calculated. The gene of interest expression was normalised by the GM of the references genes [200].

2.6.3 Selection of reference genes for HEK 293 cells

Internal reference genes are the most common method of normalisation for gene expression quantification and they need to be validated for particular tissues or cell types and specific experimental design [200-203]. In order to determine the reference genes that were less affected by the experimental conditions in the assays using the HEK 293 cell line a geNorm™ reference gene selection was used (Primerdesign, UK).

The determination of the less variable reference genes for HEK 293 was carried out using the LightCycler® 480 real time PCR system (Roche) and all the reactions were performed in a 384 well plate. Briefly: 3.2 ng of cDNA, 1 µM of forward, reverse primers and probe and 2X master mix (LightCycler® 480 probes master, 2X. Roche, UK) were added to the well for a final volume of 10 µl. The run protocol in the machine was set for PerfectProbe primers/probe reaction (Table 2.3). Eight control samples and eight treatment samples, NEC and NTC were added; all the samples were measured in triplicate. Cp values were determined using the second derivative method as described in section 2.6.2.1.

The results were analysed using qbase^{PLUS} data analysis software (Biogazelle, UK). The information obtained was the average expression stability value (M) of the reference genes that were evaluated, with a lower M value indicating a higher stability. The GM is used to determine relative gene expression and is calculated using the most stable reference genes. In order to establish how many references genes are necessary a V score is calculated by the software. The V score indicates how the GM changes when another gene is included in the calculation. V score of 0.15 or below indicated that the additional gene had no significant contribution to the GM (Figure 2.7) [201].

2.7 QUANTIFICATION OF miRNA

The small non-coding RNA molecules, miRNA were also quantified in this study. Similar to the mRNA quantification the miRNA molecules were reverse transcribed using miScript II RT® (Qiagen, UK) and then quantified using miScript SYBR green PCR® (Qiagen, UK) and specific primers for the miRNA of interest.

2.7.1 Reverse transcription PCR for miRNA quantification

Quantification of miRNA expression was performed in two steps; the first step was the synthesis of cDNA and the second one was the qPCR that was performed using specific primers. The samples were all reverse transcripted at the same time along with the NTC.

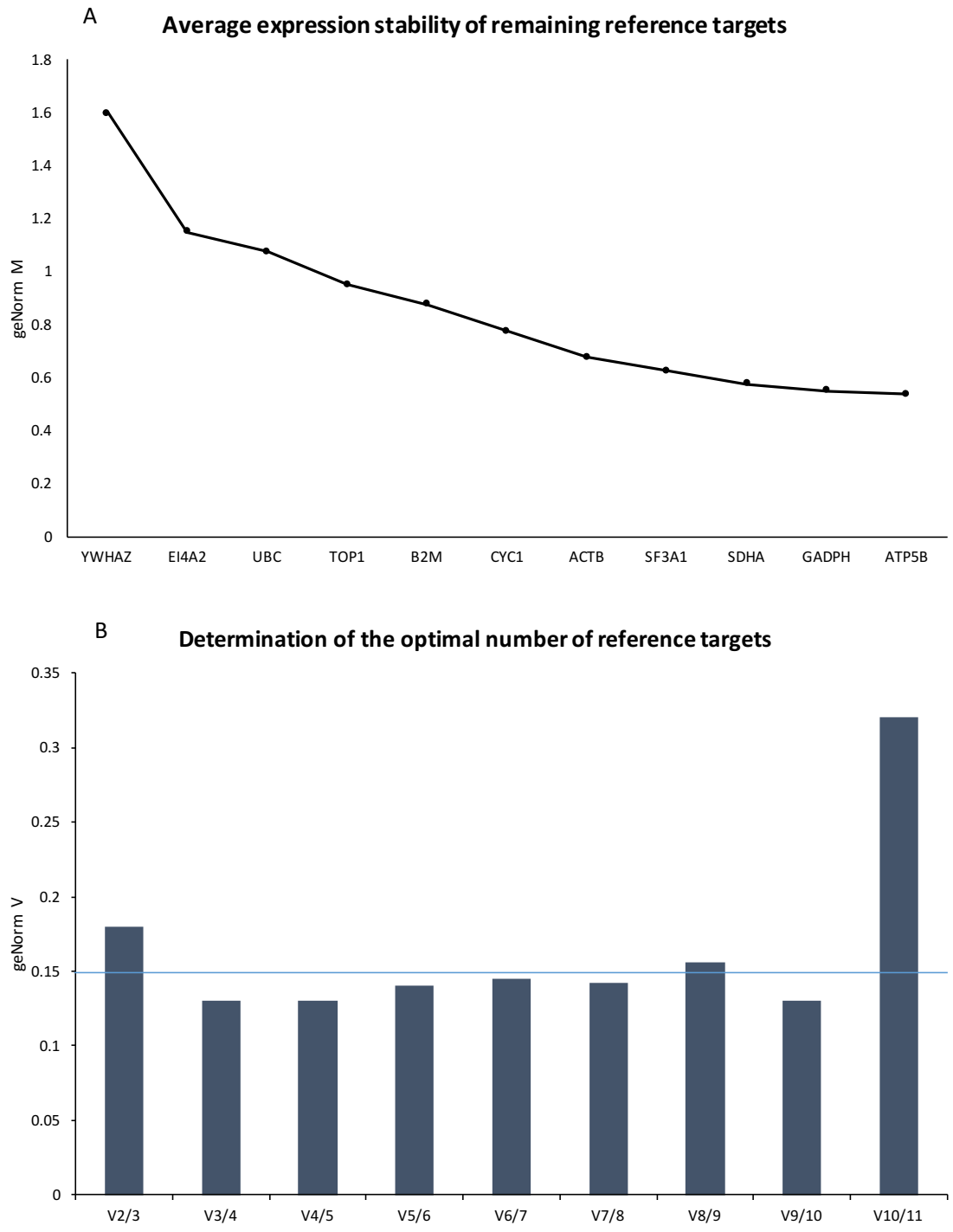

Figure 2.7 Examples of geNorm analysis results

geNorm analysis produced two types of graphs. A. Stability of the measured reference genes (M value) is plotted for each gene in this example, the most stables genes are ATP5B, GADPH and SDHA. B. V score is also calculated showing how the genes expression is affected when an extra reference gene is added to the calculation, V score of 0.15 or below indicates that additional gene has not an extra contribution to the analysis. In this example, the V-score between using 2 genes against using 3 is higher than 0.15 indicating that 3 reference genes will be optimal for that experimental situation.

Total RNA was extracted using RNAzol as described in section 2.4.1.1. Samples were diluted to a final volume of 25 µl (concentration: 0.04 µg/µl). 5 µl of the dilution was added to a new tube and then 15 µl of a mix containing 5X miScript HiSpec buffer, 10X miScript nucleics mix, miScript reverse transcriptase mix and ultrapurified water was added to the tube. All the tubes were mixed and centrifuged. The mixture was heated in a Veriti thermal cycler (Applied Biosystems) at 37°C for 60 min and then 95°C for 10 min. The samples were mixed, centrifuged and diluted 1:10 with RNA-free water before storage at -20°C.

2.7.2 Quantitative PCR for miRNA

The quantification of the miRNA expression was carried out using the LightCycler® 480 real time PCR system (Roche) and all the reactions were performed in a 384 well plate. Briefly: ~2 ng of cDNA, were mixed with QuantiTect SYBR green PCR master mix (Qiagen, UK), miScript Universal primer and miScrip primer assay (specific for each miRNA) and added to the well for a final volume of 10 µl. The run protocol was set as follow: 1 cycle (15 min at 95°C) and 45 cycles (15 sec at 94°C, 30 sec at 55°C and 30 sec at 70°C) data were collected in each cycle at the 70°C step. Samples and NTC were added to each run; all the samples were measured in triplicate.

The Cp was calculated using the second derivative method as described in section 2.6.2.1. The miRNA expression was calculated using the deltaCT method. Briefly, the highest Cp/Ct value for the specific miRNA that was being quantified was subtracted from all the other Cp/Ct values, that way all the Ct values were transformed to "deltaCT value", then for each data point the equation: $2^{(-deltaCT)}$ was applied, obtaining the relative expression (relative to the lower expression of the samples). This relative expression was then divided by the expression of the reference miRNA and that relative expression was used for further analysis.

2.8 SEX CLASSIFICATION OF MOUSE PLACENTA

In order to send the same sex mouse placenta samples for RNA sequencing, frozen mouse placentas were ground and around 40 μg of tissue was used for DNA extraction and sex classification. The rest of the sample was preserved at -80°C for RNA extraction.

2.8.1 Determination of sex in mouse placenta samples by PCR

Sry the master sex-determining gene on the Y chromosome and *Myog* (*Myogenin*) an internal control of the PCR were determined using the primers sequence and modified protocol designed by McClive and Sinclair [204]. A Veriti® thermal cycler (Applied Biosystems) was used for the PCR. All the reactions were performed in 0.2 tubes. Briefly: ~3.2 ng of DNA, 4 μM of forward, reverse primers for *Myog* and *Sry* genes (Eurogentec), master mix stock (master mix, Promega, UK) and sterile ultrapure water were added to the tube for a final volume of 25 μl. The run protocol was: 1 cycle at 94°C for 5 min, 30 cycles (94°C for 5 sec and 67°C for 40 s), 1 cycle of 72°C for 1 min. Samples were stored at -20°C until the electrophoresis was run and the bands were determined. A positive control for both gender and NTC were included in the PCR run.

Following PCR samples were run on a 1.5% agarose gel and the bands were visualised using UV light. *Myog* product was 245 bp and *Sry* product was 441 bp. The presence of both bands indicated a male sample the present of just the *Myog* band indicates a female sample. The band's size was determined against the ladder and the controls. Figure 2.8 shows an example of one of the sex classification gel.

2.9 RNA AND miRNA SEQUENCING

Samples for RNA and miRNA sequencing were sent to Expression Analysis - Q^2 Solutions (EA/Q^2 solutions - USA). The company was in charge of the sequencing and pipeline analysis of the samples as described below.

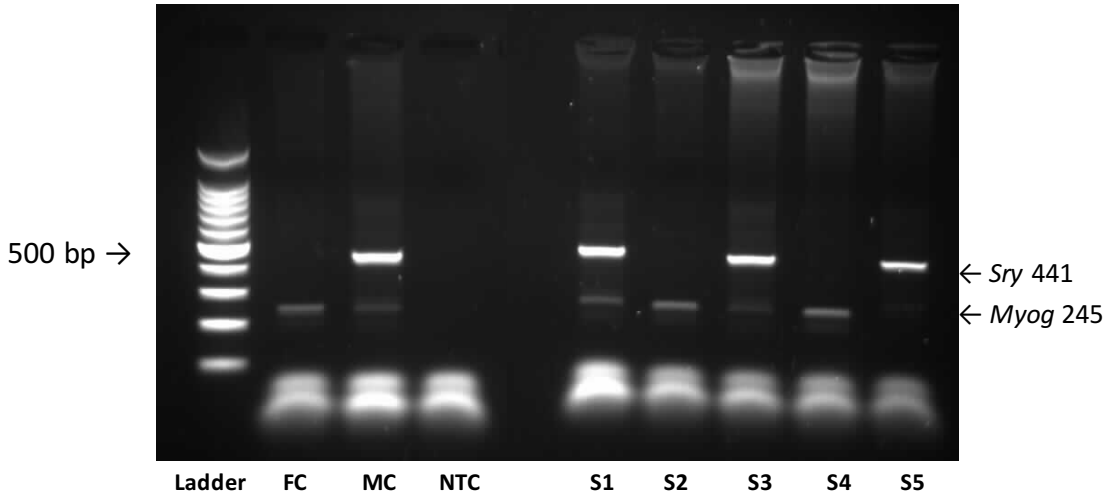

Figure 2.8 Gel electrophoresis of PCR of sex classification samples

Samples were run in a gel in order to determine the fetal sex from the placental sample. DNA Ladder: 1Kb, FC: female control, MC: male control, NTC: no template control, S1 to S5: placentas. The presence of Myog band indicates a female sample (FC, S2 and S4), the presence of both bands indicates a male sample (MC, S1, S3). When the Myog band was not clear (S5) sample was not classified.

2.9.1 Preparation of mRNA library

The cDNA libraries for the samples were built using the Illumina TruSeq™ Stranded mRNA sample preparation kit (Figure 2.9). First, total RNA samples are concentration normalised, and polyadenylated mRNAs in the samples selected using polyT oligos attached to magnetic beads. The purified mRNAs were then fragmented in the presence of divalent cations and high temperature. The fragmented RNA was then copied into the first strand of cDNA using reverse transcriptase polymerase and random primers. In order to conserve strand specificity, the second cDNA was produced using deoxyuridine triphosphate (dUTP) instead of deoxythymidine triphosphate (dTTP) in the reaction. After that, the 3'ends were adenylated and then forked adapters that include index sequences were ligated to the end of each fragment. The amplification of the fragments was performed by PCR the polymerase used was unable to continue the copy of strands that contained dUTP, assuring that only the first strand was amplified. At the end, the cDNA libraries were quantified, normalised and pooled ready to be sequenced.

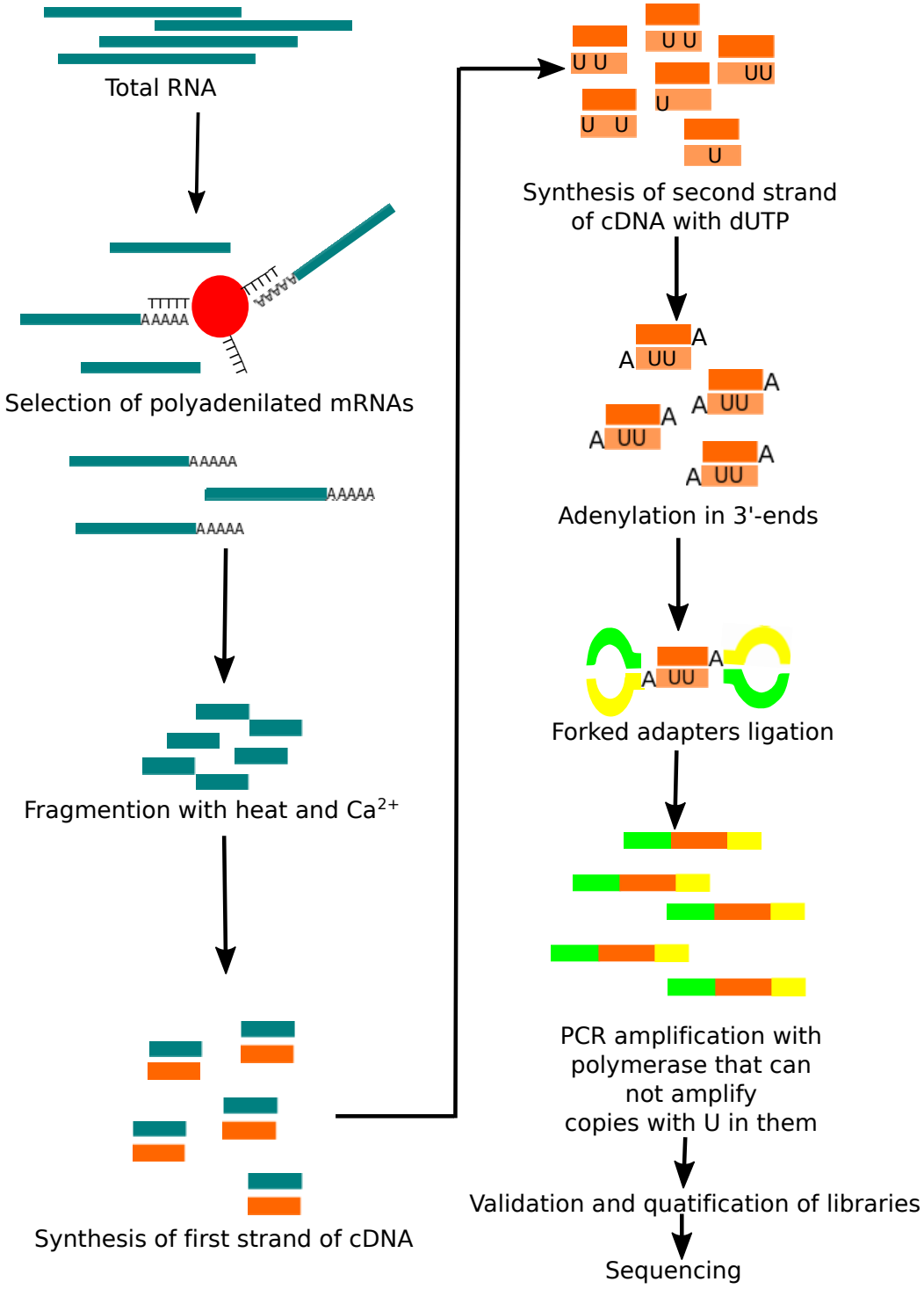

Figure 2.9 Preparation of mRNA library

Figure shows the main steps in the production of mRNA libraries for sequencing.

2.9.2 Preparation of miRNA library

Total RNA samples were converted into indexed cDNA sequencing libraries using Illumina's TruSeq Small RNA sample preparation kit (Figure 2.10). Using 1000 ng of total RNA, a single-stranded adenylated DNA adapter was added to the 3' hydroxyl group using T4 RNA ligase 2 deletion mutant. This enzyme prevented the ligation of the adapter to 5' end due to ATP absence. A 5' adapter was then added to the 5' end phosphate using T4 RNA ligase in the presence of ATP. Following the adapter ligation, single-stranded cDNA was synthesized by a reverse transcription reaction. The cDNA was then amplified by PCR using a common sequencing primer and an indexed primer that is unique to each sample. The cDNA libraries were analysed for quality and fragment size ranges using the Agilent 2200 Tapestation (D1000 Screentape, Agilent). The cDNA libraries were then size/selected, retaining fragments between 125 – 160 bp, using BluePippin (3% cassettes, Sage Sciences), resulting in a mean library size about 135 bp approximately. The final libraries were then quantitated by qPCR (KAPA library Quant Kit, KAPA Biosystems) and normalised to 2 nM in preparation for sequencing.

2.9.3 Sequencing of mRNA or miRNA libraries

The final cDNA libraries (from mRNA or miRNA) were bound to a flow cell (that contained specific oligos). A cluster of individual oligos was created for each template by clonally amplifying each bound molecule up to 1000 fold. The sequence was determined using sequencing-by-synthesis technology: fluorescence labelled nucleotides (GTP, ATP, TTP, CTP) were used, one type of the fluorescence labelled nucleotide was added to the flow cell and the polymerisation was carried out. The nucleotides (nt) were previously modified in order to stop the reaction when they were added to the nascent chain (assuring just one nucleotide will be added per cycle). After each cycle fluorescence was measured for each cluster and then the cell was washed out and a new nucleotide added and the sequencing continued. The sequence was carried out to a depth of 19 million reads. The information obtain was used for the RNA sequencing analysis.

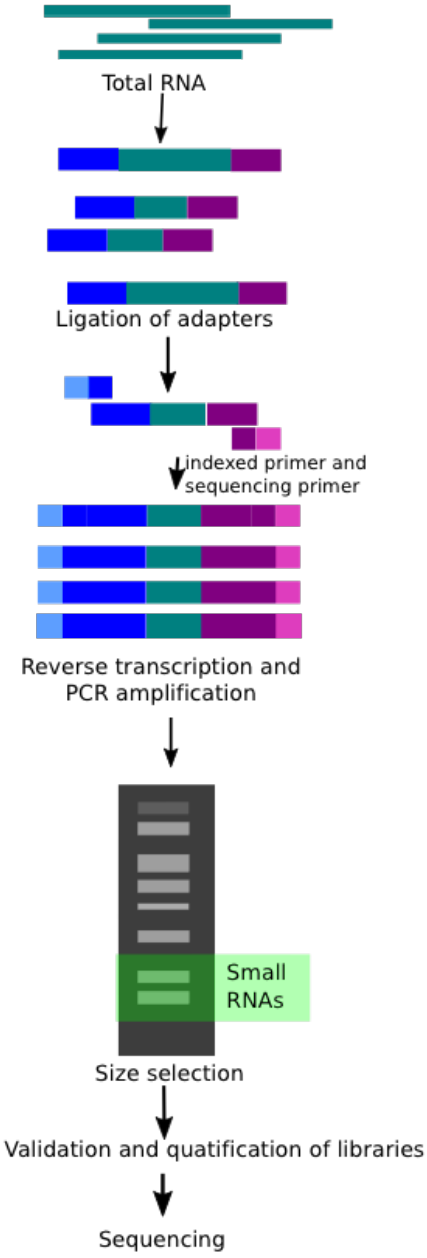

Figure 2.10 Preparation of miRNA library

Figure shows the main steps in the production of miRNA libraries for sequencing.

2.9.4 RNA sequencing analysis

The bioinformatics analysis of the RNA-seq results was carried out by Dr. Faisal Reswan of the Asthma genetics laboratory. He used the following pipeline: The raw sequence data (FASTQ) was alignment using Bowtie/TopHat (http://tophat.cbcb.umd.edu/) against the reference genome. The transcripts were compiled using Cufflink (http://cufflinks.cbcb.umd.edu/) and gene annotation was added to each identified RNA.

The differential expression between the experimental groups was then determined. These tools have gained wide acceptance and are fully documented [205]. Differentially expressed genes between groups were used for a further pathway analysis using QIAGEN's Ingenuity® Pathway Analysis (IPA® QIAGEN Redwood city, www.qiagen.com/ingenuity).

2.9.5 Analysis of miRNA sequencing data

After sequencing, the analysis was performed using a miRNA pipeline developed by EA/Q^2 Solutions that used a variety of programs developed by the company in combination with open source programs. The pipeline is designed in order to perform both quality control and miRNA quantification.

The primary sequencing output file (FASTQ) was checked after its creation to ensure the integrity of the data. The second step was performed using a fastq-mfc software developed by EA/Q^2 solutions, in this step the Illumina adapters that were added during the sample preparation were removed from the sequencing data (process is known as "clipping and trimming"), additionally, low-quality bases are also clipped from the ends of the reads. The remaining sequence must be at least 13 nt in length in order to be included in subsequent analysis. In order to quantify the miRNA the next step was collapsing unique sequence reads and then the sequence reads were aligned to the reference library (miRBase.org – University of Manchester). The alignment was performed using Bowtie version 0.12.9. Counts of miRNA were then normalised and log transformed across the samples. A principal component analysis was performed in order to determine the miRNAs that were different between the groups.

DIANA miRPath version 3.0 [206] was used to determine the target genes (and their pathways) for the differentially expressed miRNA.

2.10 STATISTICAL ANALYSIS

All the results were analysed using SPSS version 22.0 (IBM, USA). Normal distribution was determined for all the variables. Variables were logarithmic transformed when necessary and the distribution was assessed again. Summary data are presented as mean (SD) or median (inter-quartile range). For all statistical test, a p value ≤ 0.05 was considered significant.

Pearson's correlation coefficient was used to determine the partial correlation between placental gene expression and maternal, fetal and neonatal measures in the human cohorts. The correlations were adjustment by sex and gestational age when necessary. One-way ANOVA was used to determine the difference in placental FTO gene expression in the human cohorts.

A mixed model was used to determine the effects of the diet and the metformin treatment in the mouse placenta studies. Diet and metformin treatment were added as fixed factors to the model and litter was included as a random factor. A mixed model was used as well to determine the effects of the metformin exposure or the KO of *FTO* on the cells. In the first, metformin was added to the model as a fixed factor and experiment number was included as a random factor. In the second KO of FTO was added as a fixed factor and experiment number was included as a random factor.

2.10.1 Sample size

In the population study of this thesis, sample size was primarily determined by availability of sample. When necessary, retrospective sample calculations were made in order to determine whether more samples were necessary in order to answer the raised hypothesis of the study. Retrospective sample calculation was done using the online software: Sample-size.net [207]

CHAPTER 3 EFFECTS OF MATERNAL HIGH FAT DIET AND METFORMIN IN THE MOUSE PLACENTA

3.1 INTRODUCTION

The prevalence of maternal obesity, type 2 diabetes and gestational diabetes have increased in the last decade in the United Kingdom and around the world. Gestational diabetes and maternal obesity can have deleterious effects for the mother, the fetus and the lifelong health of the baby [208]. It is not clear how maternal obesity affects the fetus but the mechanism is likely to be mediated by the placenta responding to signals in the maternal circulation [209]. Gestational diabetes is developed in about 5% of pregnant women and oral hypoglycaemic agents such as metformin or glibenclamide are used to treat this condition, as they are considered safe to use during pregnancy [210-212] Since metformin is considered a non-teratogenic its use during pregnancy is quite extensive, but its effects on fetal development and placental function are not completely understood [213]. In addition, it is unknown whether the drug treatment alleviates the effects of maternal obesity on the placenta or whether there are effects independently of the maternal status. The aim of this study is therefore to determine the effects of a maternal high fat diet induced-obesity and/or metformin treatment on the placenta.

Mice provide a useful model to study the effects of maternal environment on the placenta and fetus. Maternal obesity can be induced by feeding mice with a high fat diet before pregnancy. In our laboratory, a maternal high fat diet in mice has been shown to produce maternal glucose intolerance and fetal growth restriction [214]. Furthermore, there are long term effects on the offspring including increased prevalence of non-alcoholic fatty liver disease and impaired bone development [214,215]. High fat diet-induced maternal obesity produces an increase in protein levels of amino acid and glucose transporters in the placenta suggesting that the effects of a high fat diet exposure on the offspring could be mediated by an altered placental function [32].

Metformin has been shown to affect the expression of the circadian clock genes and the metabolic rhythms in different mouse tissues [216]. Metformin treatment during pregnancy in mice increased weight gain and mesenteric fat mass in the offspring

when they were exposed to a postnatal high fat diet [217]. In addition, the male offspring developed impaired glucose tolerance with the postnatal high fat diet and the expression of the insulin-induced gene (*Insig1)* in liver was increased in the male offspring that received metformin during the pregnancy [217]. This indicates that metformin could be affecting fetal development with a later effect in adult life, however, prenatal metformin exposure needs to be investigated in order to obtain a better understanding of the effects of this drug during pregnancy.

How the placenta senses the altered levels of nutrients such as fat or the presence of drugs such as metformin is unclear. The placenta senses many maternal signals that help to regulate placental function such as nutrient transport to the fetus. In maternal undernutrition increased levels of hormones such as cortisol and adiponectin and decreased insulin, leptin and Insulin-like growth factor 1 (*Igf-1*) are some of the signals that inform the placenta about the decreased nutrient availability [68]. In addition, the decreased levels of nutrients directly affect the intracellular levels of the mTOR signalling pathway in placenta. These signals then regulate placental growth and nutrient transport to balance fetal demand with maternal capacity to maintain the pregnancy [69]. In several studies, genes such as clock genes, Insulin-induced gene 1 (*Insig1)*, Sirtuins and the fat mass and obesity-associated gene (*Fto*), have been described to be involved in cellular function or to affect cellular pathways that respond to altered nutrient levels [169,176,218,219]. Changes in circadian rhythms during pregnancy have been associated with low birth weight, glucose intolerance and insulin resistance in the offspring, as well as, morphological and physiological changes in the placenta [163] Clock genes may therefore provide a potential sensing mechanism linking the maternal metabolic environment to the fetal/placenta outcome.

The pathways involved in placental sensing of the maternal environment are not fully understood. This study, therefore, investigated the effects of a high fat diet or metformin exposure on potential sensing molecules that could be involved in placental function; such as the clock genes, sirtuins, *Fto* and *Insig1.*

3.2 AIMS

1. To determine the effect of high fat diet during pregnancy on the expression of target genes in mouse placenta.
2. To determine the effect of prenatal metformin treatment on the expression of target genes in mouse placenta.
3. To determine whether the effects of maternal high fat diet on placental gene expression and metformin treatment are likely to be sensed via common or distinct pathways.
4. To determine the effects of prenatal metformin exposure on the mouse placenta transcriptome.

3.3 METHODS

3.3.1 Mouse placentas collection

Mouse placentas were obtained from Dr Felino Cagampang and Dr Hugh Thomas from the University of Southampton as described in section 2.2. The study was conducted under UK Home Office Licence. The mice were maintained at 22 ± 2°C and 12 h of light/dark cycle. 6 weeks before conception female C57 BL6 mice were randomly assigned to a control diet (7% kcal fat) or to a high fat diet (45% kcal fat). The composition of control and high fat diet are included in Table 3.1. After mating and pregnancy confirmation, the mice were kept on the same diet and assigned to a control treatment or a metformin treatment (Figure 3.1). For half of each dietary group, metformin was added to the drinking water (250 mg/Kg/day). On day 16 of pregnancy, the mothers were sacrificed and blood and tissue samples were collected. Fetal and placental weight were recorded by Dr Hugh Thomas and the placentas were snap-frozen in liquid nitrogen within 30 min. Samples were stored at -80°C until processing.

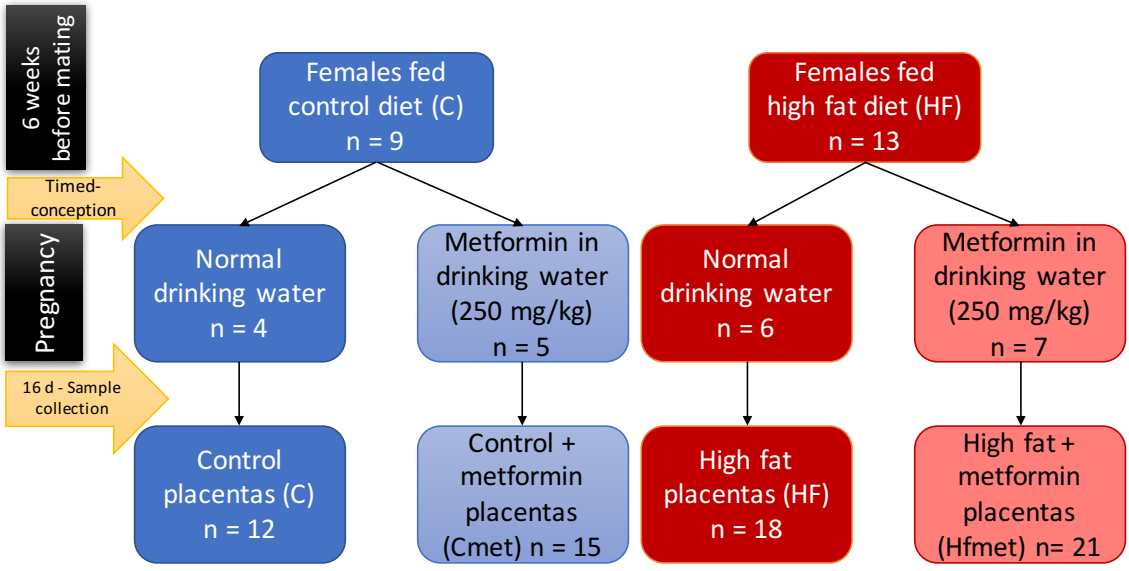

Figure 3.1 Study design

The dams were fed with the selected diet (control or high fat) 6 weeks before mating and during the pregnancy. After the pregnancy was confirmed, the diet groups were divided and two groups received metformin (250 mg/kg/day) in the drinking water. The tissues samples were collected after 16 days of pregnancy. (Pregnancy in mice is 21 days). Three placentas were selected per dam. Number of placentas per group that was used in this study are included in the bottom squares.

Table 3.1 Macronutrients composition and energy values in the control and high fat diets

	Control diet	High fat diet
Percentage weight (g)		
Carbohydrates	70.0	49.5
Protein	18.0	26.5
Lipid	10.0	22.5
Percentage of energy (kcal)		
Carbohydrates	62.9	35.0
Protein	16.5	20.0
Lipid	20.6	45.0
Fat breakdown (% AFE)		
Saturated	0.51	2.27
Monounsaturated	0.88	6.04
Polyunsaturated	0.88	6.54

AFE: Additional forms of expression. FA: Fatty acid. From [214]

3.3.2 RNA extraction of mouse placentas samples

In order to answer the first three aims of this study, three placentas per dam were selected in a non-systematic manner. The final numbers of placentas used per group are included in Figure 3.1.

Each placenta was homogenised whole in 1 ml of RNAzol® for the total RNA extraction as described in section 2.4.1.1. Briefly, Placentas were homogenised for 30 sec in RNAzol®, after 400 µl of ultrapure water were added to the samples. Samples were shaken for 15 sec and incubated for 15 min a RT, afterward, samples were centrifuged at 12000 g for 15 min at RT. Supernatant was transferred to a new tube and 1 ml of 70% isopropanol (Sigma, UK) was added to the samples. Following 10 min of incubation at RT samples were centrifuged again at 12000 g for 10 min at RT. Supernatant was removed and the RNA pellet was washed twice with 0.5 ml of 75% ethanol. After the second wash, the ethanol was removed and without drying the RNA

pellet. 100 µl of ultrapure water was added and samples were shaken for 5 min at RT to assure the solubilisation of the RNA.

RNA concentration and quality were determined using a NanoDrop® 1000 spectrophotometer and agarose gel electrophoresis as described in sections 2.5.1 and 2.5.2 respectively.

3.3.3 Gene expression quantification

Synthesis of cDNA was performed using Promega reagents as described in section 2.6.1. Briefly, 200 ng of sample were mixed with 0.5 µg of random primers to a final volume of 15 µl. The samples were heated at 70°C for 5 min on a Veriti® thermal cycler (Applied Biosystems). After, 50 nmol of triphosphate nucleotides mixture, 25 units of Recombinant RNasin® Ribonuclease Inhibitor, 200 units of M-MLV-RT, 5X M-MLV-RT buffer and water were added to the reaction mixture to a final volume of 25 µl. The mixture was heated at 37°C for 60 min and then 75°C for 10 min. The samples were mixed, centrifuged and diluted to 1:25 with RNA-free water. All the samples and NEC were reverse transcripted in one batch to reduce variation.

Reactions were performed in a 384 wells plate using a LightCycler® 480 real time PCR system (Roche). Samples, standard curve, controls, NEC and NTC were added in triplicate as follow: 3 ng of cDNA were added to a mixture containing 1 µM of forward and reverse primers and probe and 1X master mix (LightCycler® 480 probes master mix, 2X) to give a final volume of 10 µl.

Insig1, *Fto*, *Lpl*, and amino acid transporters (*Snat2, Tat1,* and *Lat1*), glucose transporters (*Glut1* and *Glut3*) and fatty acid transport protein 2 (*Fatp2*) primers and probes were designed using ProbeFinder® version 2.49 (Roche, Table 3.2). Gene expression was measured using Universal ProbeLibrary® probes and protocol. PCR run protocol was: 1 cycle at 95°C for 5 min, then 45 cycles (95°C for 10 s, 60°C for 30 sec and 72°C for 1 s). Data collection was made at 72°C step, as described in Table 2.3.

Table 3.2 Primers and probes used in gene expression measures

Gene	Gene bank accession number	Primers Sequence, 5'-3'	UPL* (No.)	Product size (bp)
Slc16a10 (Tat1)	NM_028247.4 NM_001114332.1	F: AACATGGCCTTCAAGACAGC R: GTCCGTGAAGACACTCACGA	74	87
Slc38a2 (Snat2)	NM_175121.3	F: CAATGAGATCCGTGCAAAAG R: TGCTTCCAATCATCACCACT	2	72
Slc7a5 (Lat1)	NM_011404.3	F: ATGTGGCTCCGATTCAAGA R: GGAGGGCCAGATTCACCT	78	61
Slc2a1 (Glut1)	NM_011400.3	F: CAGCCGGCACAGCTAGAG R: TCCCACAGCCAACATGAG	3	88
Slc2a3 (Glut3)	NM_011401.4	F: GGAGGAAGACCAAGCTACAGAG R: GAGCTCCAGCACAGTCACCT	2	130
Slc27a2 (Fatp2)	NM_011978.2	F: TGCTGCACTGCTTTCAATG R: CCTTTTTCAGGGTTGGAAGA	25	96
Lpl	NM_008509.2	F: CTGGTGGGAAATGATGTGG R: TGGACGTTGTCTAGGGGGTA	25	74
Insig1	NM_153526.5	F: TGGGAAACATAGGACGACAGT R: CACCCAGGACCAGTGTCTCT	38	114
Clock	NM_001289826.1	P: CGCACGCGCTCCCGTGAA F: GAGAGCGCGAAGGAAATCTG R: GCCTGTAAAAGTTTCTTCTTGTGCTT	Na	78
Cry2	NM_021117.3	P: CTTCGGCCGACGTACAGACCCCA F: CCAACAATTCTTCCACTGCTACTG R: CAGGTACCGCCGGATGTAGT	Na	82
Per2	NM_011066.3	P: CTTCCAACACTCACCCCAGCCCTG F: TGCGGATGCTCGTGGAA R: TCATCATGAGTCTGAAGGCATCA	Na	66
Arntl1 (Bmal)	NM_001243048.1 NM_007489.4	P: AGAGGTGCCACCAACCCATACACAGAA F: ATGGCTGTTCAGCACATGAAAA R: CTGATAGAAATGTTGGCTTGTAGTTTG	Na	82
Sirt3	NM_001177804.1 NM_001127351.1 NM_022433.2	P: CATCTGGGATCCCTGCCTCAAAGCT F: CATCGACGGGCTTGAGAGA R: GGTCCCGTGGGCTTCAAC	Na	64
Sirt1	NM_019812.2	F: CGGCAGCGATCGGCTA R: CACAGGAATGAAAGCCATTAGTG	Na	72
Fto	NM_011936.2	F: CACAGCCTCGGTTTAGTTCC R: AATCCAAGGTGCCTGTTGAG	53	60

* UPL: Universal Probe Library. Na. No applicable. R: Reverse, F: Forward, P: probe.

Expression of Clock genes (*Clock, Bmal, Cry2* and *Per2*), Sirtuins (*Sirt1* and *Sirt3*) and reference genes (*β-actin* and *Ywhaz*), was measured using TaqMan® primers, probes, and protocol (Table 3.2). PCR run protocol was: 1 cycle at 95°C for 10 min, then 40 cycles (95°C for 15 sec and 60°C for 60 s). Data collection was made at 60°C step, as described in Table 2.3.

Cp values were collected using the second derivate method as described in section 2.6.2.1 and arbitrary RNA concentration was calculated using the standard curve method as described section 2.6.2.2. Relative gene expression levels were calculated as a ratio between the gene of interest and the geometric mean of the two references genes (*β-actin and Ywhaz*) Another researcher in the placenta group previously determined the most appropriate reference genes for mouse placenta.

3.3.4 Placental DNA extraction and sex determination

In order to further investigate the effects of metformin treatment in the mouse placenta new placentas from the control and metformin group were selected from the tissue bank. These placentas were powdered and divided into three aliquots (40 μg for DNA extraction and sex determination, 30 mg for RNA extraction and RNA sequencing and the rest of the placenta powder that was kept in the tissue bank). In order to select samples of the same sex to be sent for RNA sequencing, sex-determination was performed in 24 placentas, 12 placentas from the control group and 12 placentas for the metformin group (3 placentas per dam).

Genomic DNA (gDNA) was extracted using the Quick-gDNA™ MiniPrep (Zymo Research, USA) according to the manufacturer instructions as described in section 2.4.2. Briefly, around 40 μg of frozen placenta were homogenised in 500 μl of Genomic Lysis Buffer at RT. Then the lysate was centrifuged at 12,000 g for 5 min. The supernatant was transferred to a Zymo-Spin Column contained in a collection tube, centrifuged at 12,000 g for 2 min at RT. Flow through and the collection tube was discarded and the column was placed in a new collection tube 200 μl of pre-wash buffer were added and samples were centrifuged at the same conditions. Flow through was discarded, 500 μl of wash buffer were added and samples were

centrifuged again. Tube collection and flow through were discarded and the column was placed in a 1.5 ml tube, 100 µl of ultrapure DNase, RNase-free water was added to the columns and samples were incubated at RT for 5 min. Samples were centrifuged at 16000 g for 30 sec at RT. Samples were stored at -80°C until they were processed.

The sex of the sample was established by determining the presence of the sex-determining region of chromosome Y (*Sry)* in the samples. Myogenin (*Myog*) was also measured in the same PCR as an internal control that should produce a band in all the samples to assure that amplification occurred during the reaction. Primers and modified protocol used were previously described by McClive and Sinclair [204]. Primer information is included in Table 3.3. PCR was performed as described in section 2.8.1, briefly, 3.2 ng of gDNA were mixed with 4 µM of forward and reverse primers for *Myog* and *Sry* genes, master mix mixture (master mix, Promega, UK) and sterile ultrapure water to a final volume 25 µl. Samples were mixed and centrifuged. The PCR protocol was: 1 cycle at 94°C for 5 min, 30 cycles (94°C for 5 sec and 67°C for 40 s), 1 cycle of 72°C for 1 min and 4°C until the samples were stored at -20°C until the electrophoresis was run.

Table 3.3 Primers used for sex classification of mouse placentas

Gene	Primers Sequence, 5'-/3'	Product size (bp)
Sry	F: TCATGAGACTGCCAACCACAG R: CATGACCACCACCACCACCAA	245
Myog	F: TTACGTCCATCGTGGACAGC R: TGGGCTGGGTGTTAGTCTTA	441

R: Reverse, F: Forward.

An 1.5% agarose gel was prepared as described in section 2.5.2. 10 µl of samples were mixed with 2 µl of loading dye (Promega, USA) and were loaded onto the gel and run at 100 V for 45 min. A 1000 Kb ladder (Promega, UK) was also loaded. The bands were visualized using UV light. *Myog* product was 245 bp and *Sry* product was 441 pb. The presence of both bands indicated a male sample, the present of just the *Myog* band indicate a female sample (Figure 2.8). The band size was determined against the ladder

and the controls. 4 same sex samples from different dams per group were selected and send for RNA sequencing.

3.3.5 RNA sequencing of mouse placentas

3.3.5.1 RNA extraction, quantification and qualification of samples for RNA sequencing

Total RNA for the samples for RNA sequencing was extracted using the miRNeasy kit (Qiagen, Manchester, UK) according to the manufacturer instructions as described in section 2.4.1.2. Briefly, 30 mg of powdered placenta were homogenized in 0.7 ml of QIAzol lysis reagent® for 30 s. Samples were incubated for 5 min at RT. 140 μl of chloroform was added to the samples which were then shaken for 15 sec and centrifuged for 15 min at 12,000 g at 4°C. 350 μl was removed from the upper phase and transferred to a new tube to which 525 μl of 100% ethanol was then added and mixed. The mixture was added to an RNeasy mini spin column and centrifuged at 8000 g for 15 sec at RT. The flow through was discarded and the rest of the mixture was added to the column and centrifuged at the same conditions. The flow through was discarded and 350 μl of RWT buffer® were added to the column. Samples were centrifuged again at the same conditions and 80 μl of DNase I mix were added directly to the membrane in the column and incubated for 15 min at RT. Samples were washed with RWT buffer and then twice with 500 μl of RPE buffer. A centrifugation at 8000 g for 1 sec at RT was performed each time. Between each washes the flow through was discarded. Finally, the column was transferred to a new collection tube and 50 μl of RNase-free ultrapure water was added to the columns which were centrifuged at 8000 g for 1 min at RT, and the eluted sample stored at -80°C.

RNA quality and quantity was assessed as described in section 2.5. Sample concentration was measured using a NanoDrop® 1000 spectrophotometer. Quality was assessed by an agarose gel as described in section 2.5.2 and by a bioanalyser as described in section 2.5.3. Briefly, for the bioanlyser the samples were loaded in a chip that separated and dyed the RNA molecules. These formed a complex that is detected by laser-induced fluorescence. Data are transformed into gel-like images and electropherograms as showed in Figure 2.4. This analysis determines the integrity of

the RNA (RNA integrity number – RIN) using the ribosomal RNA ratio (28S rRNA/18S rRNA) and the presence/absence of degradation products. 4 control and 4 metformin samples were sent for RNA sequencing, all the samples belong to male mice, had an RNA concentration ≥ 250 ng/μl and an RIN ≥ 9.5.

3.3.5.2 Library preparation and sequencing of mRNA mouse placenta samples

Total RNA samples were sent to Expression Analysis / Q^2 Solutions (EA/Q^2 solutions – USA). For RNA sequencing. The company was in charge of the sequencing and pipeline analysis of the samples. The Illumina TruSeq™ Stranded mRNA sample preparation kit was used to produce the cDNA libraries of the samples, following the manufacturer's instructions as described in section 2.9.1. Briefly, RNA concentration of the samples was normalized and polyadenylated mRNAs in the samples were selected using polythymidine oligonucleotides attached to magnetic beads. Purified mRNAs were fragmented using divalent cations and high temperatures. Fragmented RNA was copied into the first strand of cDNA. In order to conserved strand specificity, the second cDNA was produced using deoxyuridine triphosphate (dUTP) instead of deoxythymidine triphosphate (dTTP) in the reaction. After the 3'ends were adenylated a forked adapter that included index sequences was ligated to the end of each fragment. Amplification was performed using a polymerase unable to continue copy strands that contained dUTP, assuring that only the first strand was amplified. At the end, the cDNA libraries were quantified, normalized and pooled ready to be sequenced (Figure 2.9).

Sequencing of the samples was performed as described in section 2.9.3. The libraries were bound to a flow cell that contained specific oligonucleotides. A cluster of individual oligonucleotides was created for each template by clonally amplifying each bound molecule up to 1000 fold. The sequence was determined using sequencing-by-synthesis technology. Sequencing was carried out to a depth of 19 million reads. The information obtained was used for the sequencing analysis.

3.3.6 RNA sequencing analysis

The analysis of the RNA sequencing results was carried out by Dr. Faisal Rezwan of the Asthma genetics laboratory, University of Southampton. Following discussion, he used the following pipeline: The raw sequence data was alignment using Bowtie2/TopHat (software v 2.1.0) against the reference genome (In this analysis, *Mus musculus* 10 – mm10 reference genome was used). The transcripts were compiled using Cufflink (software v 2.1.1) and gene annotation was added to each identified RNA. The differential expression between the experimental groups was determined using cuff-diff (Figure 3.2).

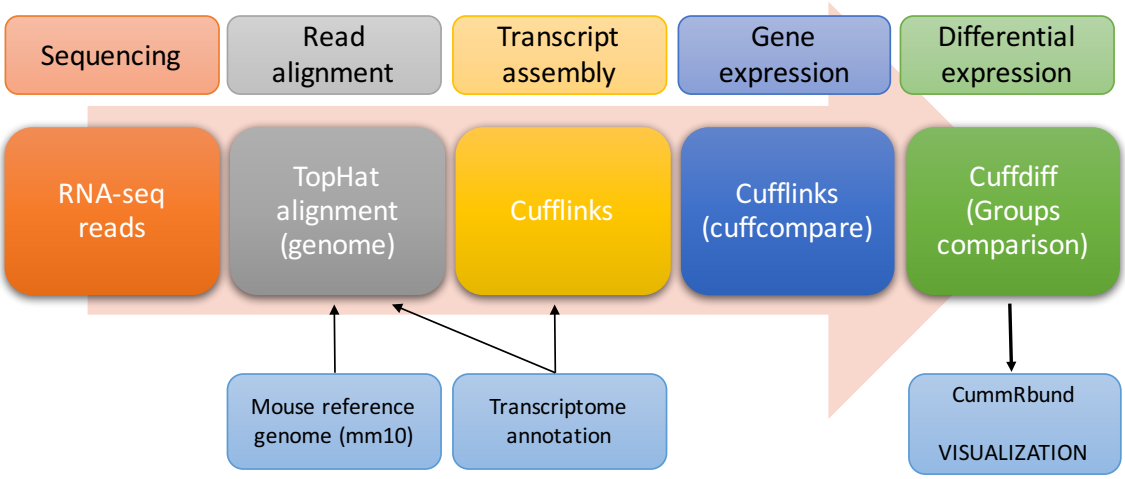

Figure 3.2 RNA sequencing analysis pipeline

Results from the RNA sequencing analysis were analysed using a pipeline designed by Institute for quantitative and Computational Biosciences.

Differentially expressed genes between groups were used for a further pathway analysis using QIAGEN's Ingenuity® Pathway Analysis (IPA® QIAGEN Redwood city, www.qiagen.com/ingenuity). IPA was used to determine which well-characterized cell signalling and metabolic pathways were affected by the metformin treatment in the mouse placenta (Canonical Pathway Analysis) and also to determine which biological and diseases-related processes were affected by the metformin treatment in the mouse placenta (Functions and Diseases Pathway Analysis) [220].

3.3.7 Statistical analysis

A mixed model was used to determine the effects of the high fat diet and the metformin treatment on the qRT-PCR gene expression in mouse placenta. The fixed factors in the model were diet, treatment, and their interaction and the random factor was litter. This model was used because it determines the effect that the fixed factors have over the population mean corrected by the covariance produced by the random factors. In this case, it allows controlling the effect of having samples that belong to the same litter and are not independent of each other.

In each experimental group correlations between the expression of different genes were determined using Pearson's correlation coefficient. A p-value ≤ 0.05 was considered significant.

For the RNA sequencing data in order to reduce the false positives in the analysis, an adjusted p-value was calculated that takes into account the false discovery rate. Differentially expressed genes were selected using an adjusted p-value ≤ 0.05. In order to validate the RNA sequencing data a t-test was performed comparing the expression of the genes that were quantified with qPCR between the control and the control metformin group. Results were compared with the unadjusted p-value of the RNA sequencing data.

3.4 RESULTS

3.4.1 Fetal and placental weight

Information about placental weight and fetal weight was not collected for all the samples. In Table 3.4 is the information about fetal and placental weight that was collected followed by the number of fetus with available information. Information about fetal and placental weight was not available for 7 samples in the control group and for 4 samples in the high fat group. Fetal weight information was not available for 4 samples in the high fat-metformin group. The high fat diet reduced fetal weight and the number of fetuses per litter and there was an interaction between metformin treatment and high fat diet that increases the number of fetus per litter. Neither the diet nor the metformin treatment has an effect on the placental weight (Table 3.4).

Table 3.4 Fetal and placental weight and total number of fetuses per dam

Group	C	Cmet	HF	HFmet	p* value 2-way ANOVA		
					Diet	Treatment	Interaction
Fetal weight (g) (# fetus)	0.61 ± 0.04 (5)	0.52 ± 0.04 (15)	0.37 ± 0.06 (14)	0.39 ± 0.02 (17)	**0.007**	0.645	0.335
Placental weight (g) (# placentas)	0.111 ± 0.007 (5)	0.110 ± 0.005 (15)	0.109 ± 0.005 (14)	0.110 ± 0.004 (21)	0.870	0.972	0.833
(# fetus/litter)	10 ± 1	9 ± 1	6 ± 2	9 ± 1	**0.010**	0.296	**0.016**

C: Control diet, **CMet:** Control diet + metformin treatment, **HF:** High fat diet and **HFMet:** High fat diet + metformin treatment. Values are mean ± SEM. *p ≤ 0.05 are in bold. **Values are mean ± SD.

3.4.2 Effects of diet and metformin treatment on placental gene expression

Metformin decreased the relative mRNA expression of both *Clock* and *Per2* and in *Clock* the control diet interacts with the metformin treatment decreasing the expression of these gene when compared with the control diet without treatment (Figure 3.3), *Insig1* relative mRNA expression was decreased by the high fat diet

(Figure 3.4). The relative mRNA expression of *Bmal*, *Cry, Fto*, *Sirt1, Sirt3* in mouse placenta was not significantly affected by diet or metformin treatment (Figure 3.3 and Figure 3.4).

The relative mRNA expression of the amino acid transporters *Snat2*, *Tat1* was reduced by maternal high fat diet (Figure 3.5). Metformin treatment decreased the expression of *Tat1* (Figure 3.5). There was an interaction between high fat diet and metformin treatment whereby metformin decreased *Lat1* expression in control placentas but increases it in high fat placentas (Figure 3.5).

Placental mRNA expression of *Glut1* and *Glut3* were reduced by maternal high fat diet and *Glut3* expression was reduced by the metformin treatment (Figure 3.6).

Placental mRNA expression of *Lpl* and *Fatp2* were reduced by the metformin treatment (Figure 3.7).

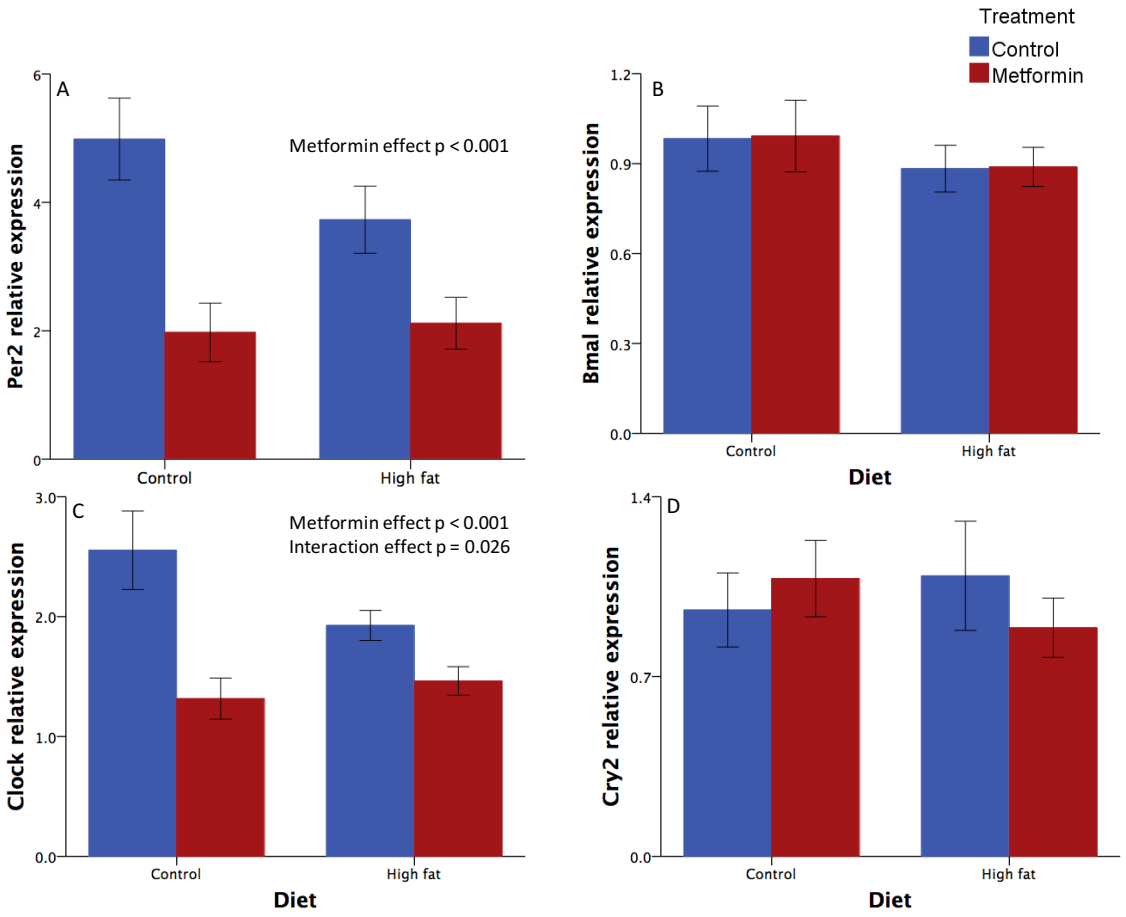

Figure 3.3 Clock genes (*Clock, Bmal, Per2* and *Cry2*) relative mRNA expression in mouse placenta

A. Relative mRNA Expression of ***Per2*** *was decreased by the metformin treatment (Diet p = 0.365,* ***treatment p = 0.001*** *and interaction p = 0.275). B.* ***Bmal*** *relative mRNA expression was not affected by the metformin or the diet (Diet p = 0.253, treatment p = 0.935 and interaction p = 0.985). C.* ***Clock*** *relative mRNA expression was decreased as an effect of the metformin treatment and as an interaction between the control diet and the metformin treatment (Diet p = 0.164,* ***treatment p < 0.001 and interaction p = 0.026****). D.* ***Cry2*** *relative mRNA expression was not affected by metformin treatment or the diet (Diet p = 0.825, treatment p = 0.798 and interaction p = 0.387). Data are mean ± SEM. (n: control: 4 dams, high fat: 6 dams, control-metformin: 5 dams and high fat-metformin: 7 dams – 3 placentas were selected per dam in all the groups).*

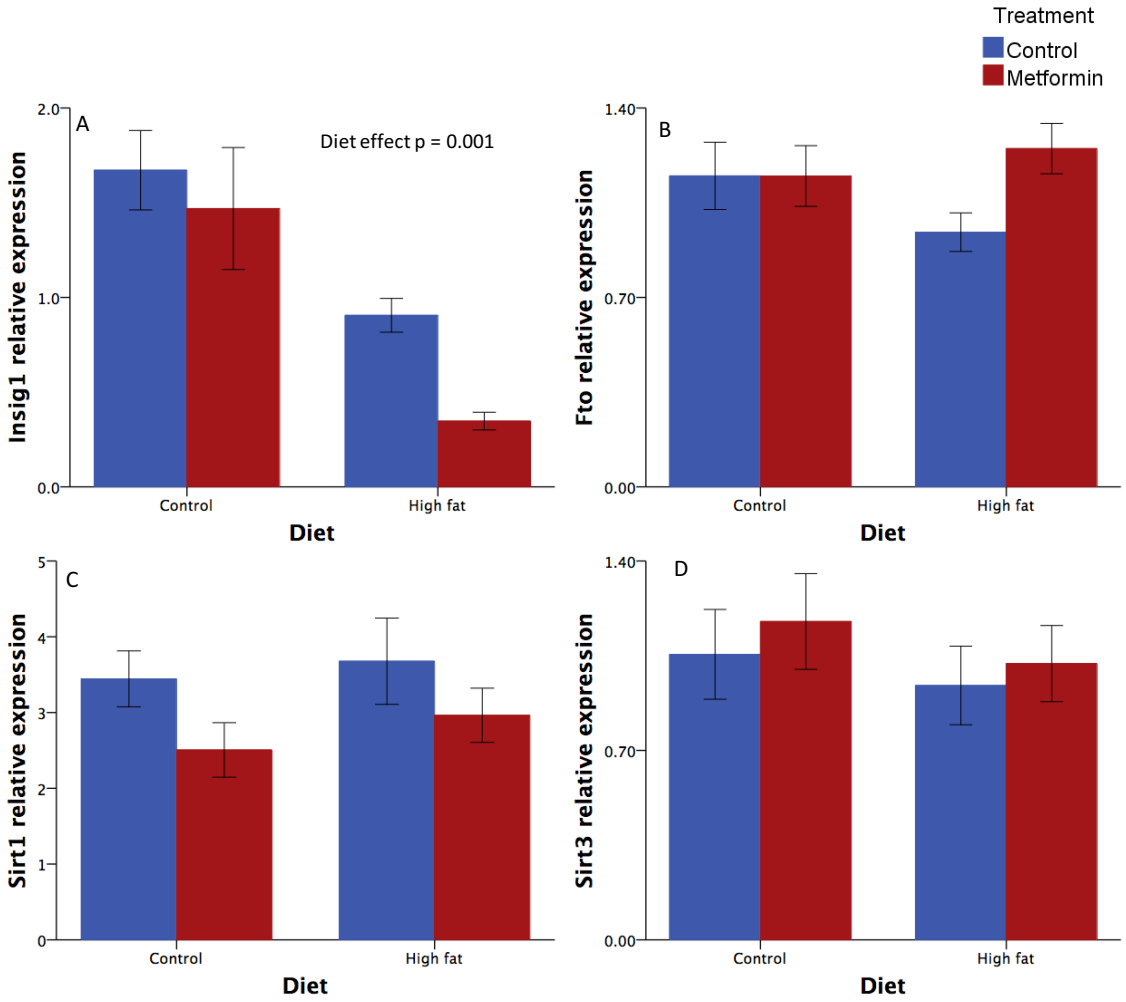

Figure 3.4 Insulin induced gene (*Insig1*), fat mass and obesity associated gene (*Fto*), Sirtuins (*Sirt1* and *Sirt3*) relative mRNA expression in mouse placenta

*A. **Insig1** relative mRNA expression was decreased by the high fat diet (**Diet p = 0.001**, treatment p = 0.272 and interaction p = 0.272). B, C and D. Relative mRNA expression of **Fto** (Diet p = 0.585, treatment p = 0.118 and interaction p = 0.116), **Sirt1** (Diet p = 0.439, treatment p = 0.067 and interaction p = 0.801) and **Sirt3** (Diet p = 0.433, treatment p = 0.643 and interaction p = 0.859) was not affected by the diet or the metformin treatment. Data are mean ± SEM. (n: control: 4 dams, high fat: 6 dams, control-metformin: 5 dams and high fat-metformin: 7 dams – 3 placentas were selected per dam in all the groups).*

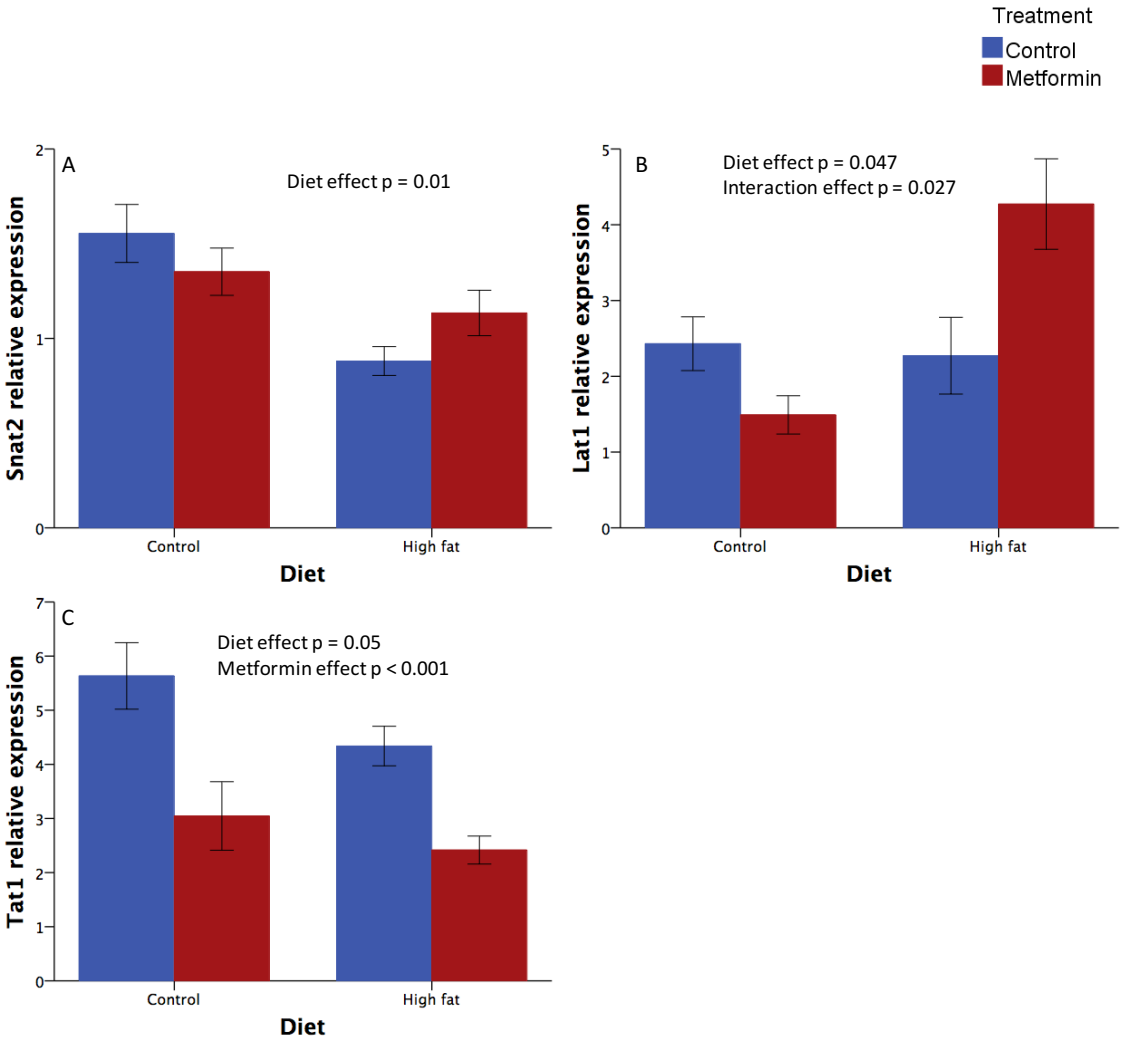

Figure 3.5 Amino acid transporters (*Snat2, Tat1* and *Lat1*) relative mRNA expression in mouse placenta

A. ***Snat2*** *relative mRNA expression was decreased by the high fat diet (****Diet p = 0.01****, treatment p = 0.843 and interaction p = 0.079). B.* ***Lat1*** *relative mRNA expression was decreased by diet but increased by the metformin treatment when interacted with the diet (****Diet p = 0.047****, treatment p = 0.41 and* ***interaction p = 0.027****). C.* ***Tat1*** *relative mRNA expression was decreased by the high fat diet and by the metformin treatment (****Diet p = 0.05****,* ***treatment p < 0.001*** *and interaction p = 0.499). Data are mean ± SEM. (n: control: 4 dams, high fat: 6 dams, control-metformin: 5 dams and high fat-metformin: 7 dams – 3 placentas were selected per dam in all the groups).*

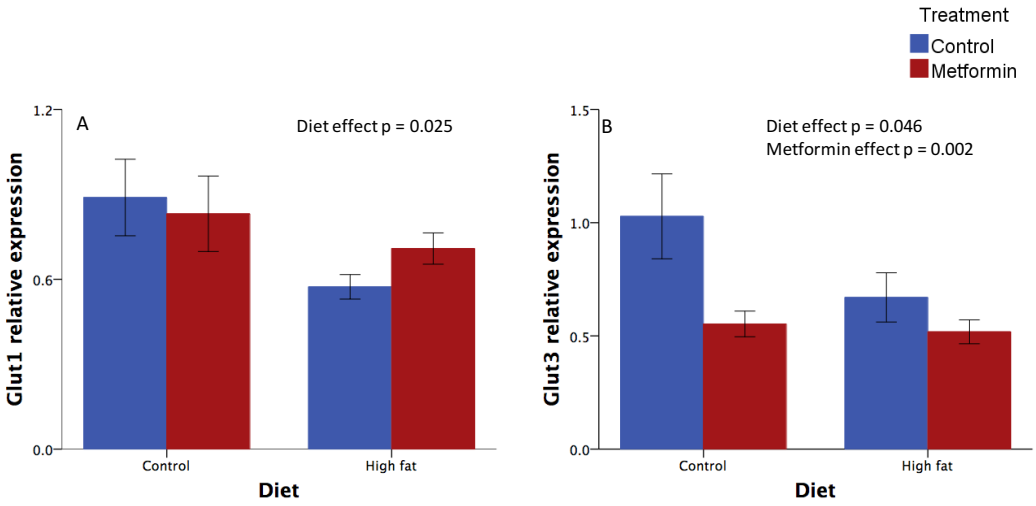

Figure 3.6 Glucose transporters (*Glut1* and *Glut3*) relative mRNA expression in mouse placenta

*A. **Glut1** relative mRNA expression was reduced by the high fat diet (**Diet p = 0.025**, treatment p = 0.649 and interaction p = 0.345). B. **Glut3** relative m RNA expression was reduced by the high fat diet and the metformin treatment (**Diet p = 0.046**, **treatment p = 0.002** and interaction p = 0.099). Data are mean ± SEM. (n: control: 4 dams, high fat: 6 dams, control-metformin: 5 dams and high fat-metformin: 7 dams – 3 placentas were selected per dam in all the groups).*

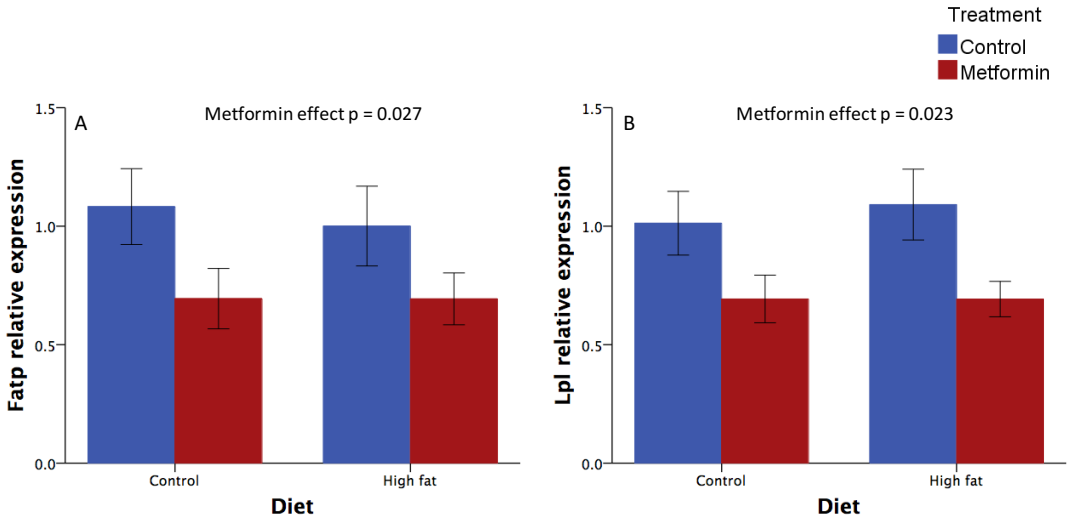

Figure 3.7 Lipoprotein lipase (*Lpl*) and fatty acid transporter (*Fatp2*) relative mRNA expression in mouse placenta

*A and B. **Fatp2** (Diet p = 0.788, **treatment p = 0.027** and interaction p = 0.796) and **Lpl** (Diet p = 081, **treatment p = 0.023** and interaction p = 0.796) relative mRNA expression were decreased by metformin treatment. Data are mean ± SEM. (n: control: 4 dams, high fat: 6 dams, control-metformin: 5 dams and high fat-metformin: 7 dams – 3 placentas were selected per dam in all the groups).*

3.4.3 RNA sequencing analysis for metformin treated placentas

Of the 12671 genes measured, 344 genes were differentially expressed between the control and the metformin samples. 150 genes have a 2 log fold change (log2FC) that is positive (genes levels increase after metformin treatment) from this list 6 genes with a log2FC $\geq$ 2 (Table 3.5). 194 genes have a log2FC that is negative (gene levels decrease after metformin treatment) with 7 genes with a log2FC $\leq$ -2 (Table 3.5).

Table 3.5 Highest and lowest expressed genes from the RNA sequencing analysis between the metformin group and the control group

Gene name	Gene symbol	Log2FC	Adjusted p-value
Genes with a log2FC $\geq$ 2 – overexpressed in control metformin group			
Aldo-keto reductase family 1, member B7	*Akr1b7*	2.10476	5×10^{-5}
Proline dehydrogenase (oxidase) 2	*Prodh2*	2.28032	5×10^{-5}
Hemoglobin Z, beta-like embryonic chain	*Hbb-bh1*	2.3056	9×10^{-4}
Hemoglobin X, alpha-like embryonic chain in Hba complex	*Hba-x*	2.41605	5×10^{-5}
Arylacetamide deacetylase (esterase)	*Aadac*	2.42798	8.5×10^{-4}
Hemoglobin Y, beta-like embryonic chain	*Hbb-y*	4.31895	5×10^{-5}
Genes with a log2FC $\leq$ -2 – under expressed in control metformin group			
Keratin 1	*Krt1*	-6.37232	0.027
Keratin 10	*Krt10*	-4.04187	0.004
Carcinoembryonic antigen-related cell adhesion molecule pseudogene 1	*Ceacam-ps1*	-3.13174	0.004
Small proline-rich protein 2A3	*Sprr2a3*	-2.83018	0.012
Diamine oxidase-like protein	*Doxl2*	-2.29173	0.004

3.4.3.1 Pathway analysis of RNA sequencing results

Canonical Pathway Analysis (which are those that have been well established and characterized in cells or tissues) was performed. This analysis shows which well-characterized signalling or metabolic cellular pathways were affected after the metformin treatment. Table 3.6 and Figure 3.8 show the 33 cellular pathways that were found to be affected by the metformin. The analysis included a ratio calculated

by dividing the number of genes affected by the metformin treatment in that pathway by the total number of genes from that pathway. The z-score that indicates if the treatment has an overall effect in the pathway (positive score: activation, negative score: inhibition).

In this analysis, it was found that metformin altered pathways such as the liver X receptor / retinoid X receptor (LXR/RXR) activation (Figure 3.9).

Function and Disease and Pathway Analysis was also carried out (Table 3.6 and Figure 3.10). In this analysis genes differentially expressed following metformin treatment and that are involved in the same function or disease were grouped in networks showing the connections between them and the function or disease. Networks that were related with metabolism or transport were selected for a further analysis.

Table 3.6 Canonical pathways affected by the metformin treatment

Canonical Pathways	-log (p-value)	Ratio	z-score	Genes affected by metformin
Acute Phase Response Signalling	4.09	0.0355		*Plg,Itih2,Saa3,Itih4,Ambp,C9*
FXR/RXR Activation	3.71	0.0397		*Lipc,Itih4,Vtn,Ambp,C9*
Cell Cycle: G2/M DNA Damage Checkpoint Regulation	2.93	0.0612		*Top2a,Ccnb2,Ccnb1*
LXR/RXR Activation	**2.76**	**0.0331**	**2.0**	***Itih4,Vtn,Ambp,C9***
DNA damage-induced 14-3-3σ Signalling	2.54	0.105		*Ccnb2,Ccnb1*
Maturity Onset Diabetes of Young (MODY) Signalling	2.45	0.0952		*Aldob,Slc2a2*
Triacylglycerol Degradation	2.3	0.08		*Aadac,Lipc*
Threonine Degradation II	2.07	0.5		*Tdh*
Retinol Biosynthesis	2.04	0.0588		*Aadac,Lipc*
Coagulation System	2.02	0.0571		*Plg,F10*
IL-17A Signalling in Fibroblasts	2.02	0.0571		*Lcn2,Mmp1*
Thyroid Hormone Metabolism II (via Conjugation and/or Degradation)	2.02	0.0571		*Ugt2b10,Dio2*
Thyronamine and Iodothyronamine Metabolism	1.9	0.333		*Dio2*
Thyroid Hormone Metabolism I (via De-iodination)	1.9	0.333		*Dio2*
Lysine Degradation II	1.68	0.2		*Aass*
Nicotine Degradation III	1.66	0.037		*Cyp3a7,Ugt2b10*
Glioma Invasiveness Signalling	1.62	0.0351		*Plg,Vtn*
Melatonin Degradation I	1.62	0.0351		*Cyp3a7,Ugt2b10*
Phospholipases	1.6	0.0345		*Lipc,Plcg2*
Urea Cycle	1.6	0.167		*Cps1*
ATM Signalling	1.59	0.0339		*Ccnb2,Ccnb1*
Superpathway of Melatonin Degradation	1.55	0.0323		*Cyp3a7,Ugt2b10*
Nicotine Degradation II	1.54	0.0317		*Cyp3a7,Ugt2b10*
NAD Biosynthesis from 2-amino-3-carboxymuconate Semialdehyde	1.53	0.143		*Qprt*
Dopamine-DARPP32 Feedback in cAMP Signaling	1.51	0.0186		*Plcg2,Kcnj16,Prkg2*
Mitotic Roles of Polo-Like Kinase	1.5	0.0303		*Ccnb2,Ccnb1*

Table 3.6 –continued

Canonical Pathways	-log (p-value)	Ratio	z-score	Genes affected by metformin
Serotonin Degradation	1.49	0.0299		*Aldh1b1,Ugt2b10*
Airway Pathology in Chronic Obstructive Pulmonary Disease	1.48	0.125		*Mmp1*
Sucrose Degradation V	1.43	0.111		*Aldob*
Hepatic Fibrosis / Hepatic Stellate Cell Activation	1.37	0.0164		*Col23a1,Col9a2,Mmp1*
Cyclins and Cell Cycle Regulation	1.37	0.0256		*Ccnb2,Ccnb1*
Mineralocorticoid Biosynthesis	1.34	0.0909		*Cyp21a2*
Glucocorticoid Biosynthesis	1.31	0.0833		*Cyp21a2*

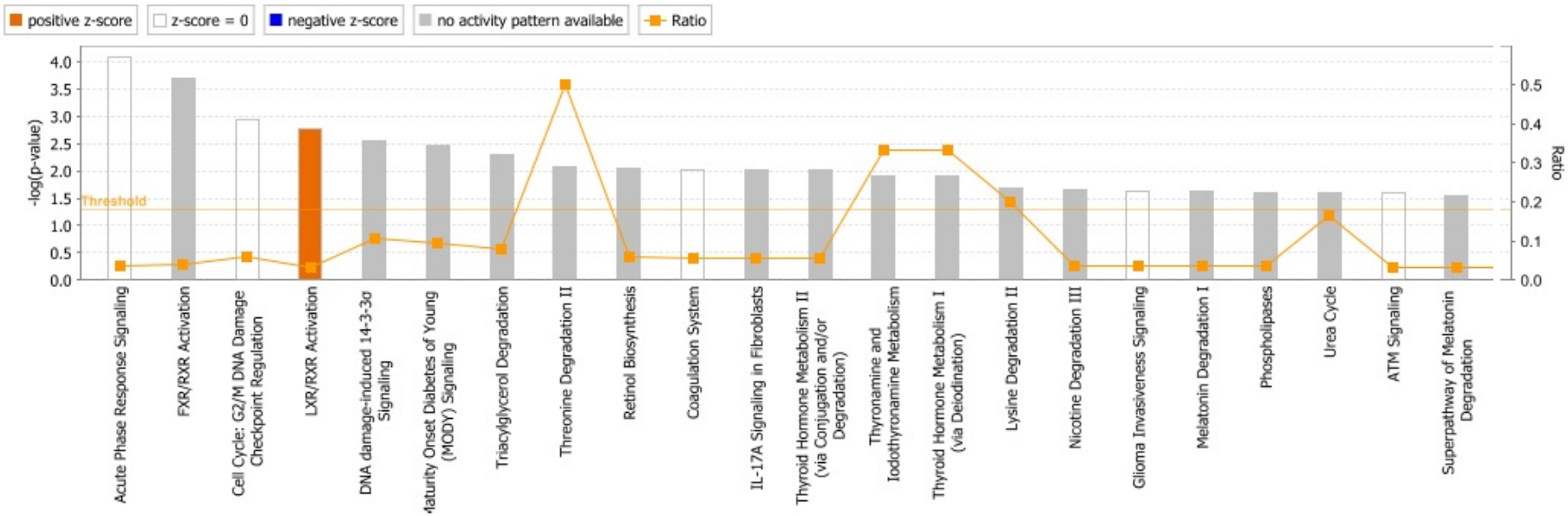

Figure 3.8 Canonical pathways affected by the metformin treatment in mouse placenta

22 most significant Canonical pathways affected for the metformin treatment. Threshold line shows the cut-off point of the significant p-value. Ratio shows the amount of genes for pathway that were affected in this experiment compared with the total amount of genes in each pathway. Bar colours shows the z-score that predicts the direction of the effect. Positive z-score indicates an activation in the pathway (orange bars) a negative z-score indicates an inhibition of that pathway (blue bars). Grey bars indicate that the directionality of the effect was not determined. (n: control and control metformin: 4 placentas each).

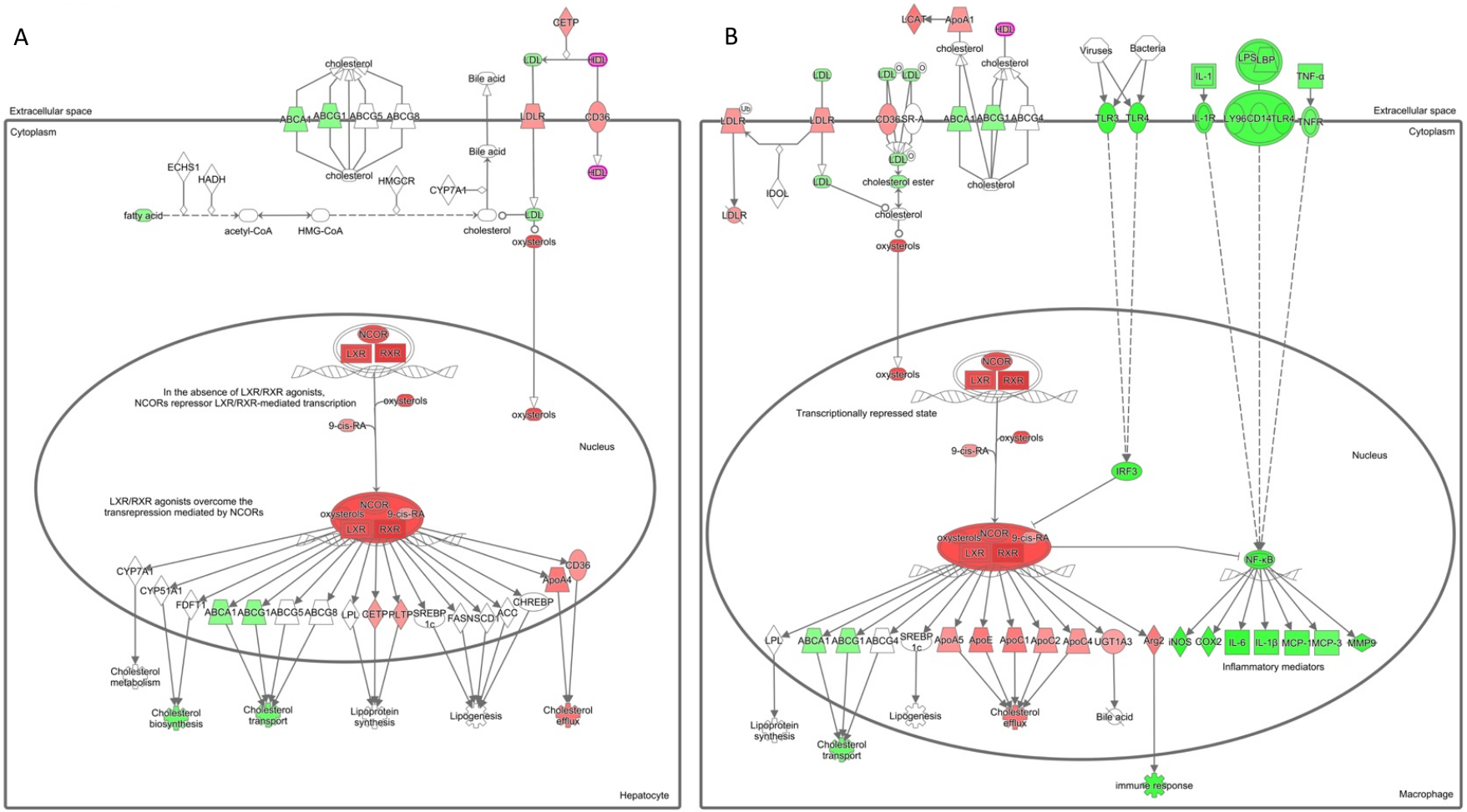

Figure 3.9 LXR/RXR activation pathway affected by the metformin treatment

This figure shows the canonical pathways of LXR/RXR activation. Figures in red show the upregulated molecules and figures on green show the downregulated molecules. Intensity of the colour indicate levels of up or down regulation. Genes without colour were not identified as differentially expressed by the metformin treatment and were integrated into the networks by the IPA. A. Shows the pathway activation in the hepatocyte and B. Shows the pathway activation in the macrophage. (n: control and control metformin: 4 placentas each).

Table 3.7 Disease and function pathways that were affected by the metformin treatment

Category	p-value	Genes affected by metformin treatment
Cancer	3.15×10^{-08} - 8.43×10^{-03}	*Cyp3a7, Lipc, Popdc3, Bmp4, Ager, Saa3, Vtn, Slc36a2, Kcnj16, Ccnb2, Slc30a3, Prkg2, Mki67, Slc22a6, Dio2, Elmod1, Magel2, Guca2b, Hbe1, Krt13, Itih2, Aldob, Itih4, Krt1, Mogat2, Mcm5, Aldh1b1, Podn, Scn9a, Fam64a, Lcn2, Kif4a, Aass, Cyp21a2, Pigr, Ccnb1, Ca7, F10, Enpp3, Pkib, Plcg2, Col23a1, Ndc80, Ly6g6c, Nek2, Cps1, Enpep, Fam107a, Spire2, Phlda2, Chrdl2, Ambp, C9, Qprt, Htr1d, Slc6a13, Krtdap, Aadac, Mfi2, Fam46b, Slc2a2, Top2a, Hsd11b2, Kif2c, Crym, Cacna2d3, Mmp1, Dpp4, Krt6b, Ugt2b10, Sox11, Prodh2, Hbg2, Plg, Clca1, Chrdl1, Col9a2*
Organismal Injury and Abnormalities	3.15×10^{-08} - 8.43×10^{-03}	*Cyp3a7, Bmp4, Popdc3, Lipc, Ager, Saa3, Slc36a2, Vtn, Kcnj16, Ccnb2, Slc30a3, Mki67, Prkg2, Dio2, Slc22a6, Magel2, Elmod1, Guca2b, Hbe1, Krt13, Itih2, Itih4, Aldob, Krt1, Mogat2, Mcm5, Aldh1b1, Podn, Proz, Scn9a, Fam64a, Kif4a, Lcn2, Aass, Cyp21a2, Pigr, Ccnb1, Ca7, Enpp3, F10, Pkib, Plcg2, Col23a1, Ndc80, Ly6g6c, Nek2, Cps1, Enpep, Fam107a, Spire2, Phlda2, Chrdl2, C9, Ambp, Qprt, Htr1d, Slc6a13, Krtdap, Aadac, Mfi2, Fam46b, Slc2a2, Top2a, Hsd11b2, Kif2c, Krt10, Crym, Cacna2d3, Mmp1, Dpp4, Krt6b, Ugt2b10, Sox11, Prodh2, Hbg2, Plg, Clca1, Chrdl1, Col9a2*
Cardiovascular Disease*	**1.37×10^{-06} - 8.43×10^{-03}**	***Dpp4, Bmp4, Lipc, Ager, Vtn, Scn9a, Lcn2, Qprt, Slc30a3, Mki67, Dio2, Guca2b, Ca7, Plg, F10, Itih4, Top2a, Hsd11b2, Mogat2, Cps1, Mmp1***
Endocrine System Disorders	2.68×10^{-06} - 8.43×10^{-03}	*Enpep, Fam107a, Bmp4, Lipc, Ager, Vtn, C9, Qprt, Ccnb2, Htr1d, Mki67, Slc22a6, Dio2, Akr1b7, Hbe1, Itih4, Slc2a2, Top2a, Hsd11b2, Mogat2, Cacna2d3, Mmp1, Dpp4, Krt6b, Scn9a, Lcn2, Aass, Sox11, Cyp21a2, Ccnb1, Plg, Ca7, F10, Clca1, Plcg2, Col23a1, Ly6g6c, Col9a2*

Table 3.7 – continued

Category	p-value	Genes affected by metformin treatment
Gastrointestinal Disease	2.68×10^{-06} - 8.43×10^{-03}	*Dpp4, Enpep, Bmp4, Lipc, Ager, Scn9a, Lcn2, Qprt, Sox11, Slc22a6, Ccnb1, Ca7, Guca2b, Plg, F10, Itih4, Pkib, Col23a1, Plcg2, Slc2a2, Hsd11b2, Ly6g6c, Col9a2, Cacna2d3, Mmp1*
Metabolic Disease*	**2.68×10^{-06} - 8.43×10^{-03}**	***Enpep, Lipc, Bmp4, Ager, Slc36a2, C9, Qprt, Slc30a3, Htr1d, Fxyd2, Slc22a6, Akr1b7, Mfi2, Aldob, Itih4, Slc2a2, Hsd11b2, Mogat2, Cacna2d3, Mmp1, Dpp4, Proz, Scn9a, Lcn2, Aass, Cyp21a2, Ccnb1, Ca7, Hbg2, Plg, F10, Col23a1, Plcg2, Ly6g6c, Col9a2, Cps1***
Hematological System Development and Function	3×10^{-06} - 8.43×10^{-03}	*Dpp4, Bmp4, Ager, Saa3, Proz, Vtn, Scn9a, C9, Ambp, Lcn2, Pigr, Plg, Clca1, F10, Shcbp1, Plcg2, Mmp1*
Organismal Functions	3×10^{-06} - 8.43×10^{-03}	*Plg, F10, Ager, Vtn, Proz, C9, Lcn2, Prkg2, Sox11, Mmp1*
Endocrine System Development and Function	5.33×10^{-06} - 8.43×10^{-03}	*Plg, Cyp3a7, Dpp4, Bmp4, Slc2a2, Vtn, Lcn2, Hsd11b2, Prkg2, Mogat2, Cyp21a2, Nppb, Dio2, Crym, Akr1b7*
Small Molecule Biochemistry	5.33×10^{-06} - 8.43×10^{-03}	*Enpep, Cyp3a7, Bmp4, Lipc, Ager, Vtn, Slc36a2, Ambp, Kcnj16, Qprt, Prkg2, Slc6a13, Dio2, Fxyd2, Slc22a6, Nppb, Magel2, Akr1b7, Guca2b, Aldob, Slc2a2, Top2a, Hsd11b2, Mogat2, Crym, Dpp4, Lcn2, Aass, Cyp21a2, Ccnb1, Plg, Enpp3, Plcg2, Cps1*
Cardiovascular System Development and Function	6.82×10^{-06} - 8.43×10^{-03}	*Plg, F10, Bmp4, Ager, Vtn, Krt1, Pigr*
Cell-To-Cell Signalling and Interaction	6.82×10^{-06} - 8.43×10^{-03}	*Enpep, Dpp4, Lipc, Bmp4, Ager, Saa3, Scn9a, Vtn, Lcn2, Ccnb2, Pigr, Ccnb1, Plg, Clca1, F10, Enpp3, Plcg2, Hsd11b2, Krt1, Mmp1*

Table 3.7 – continued

Category	p-value	Genes affected by metformin treatment
Cellular Movement	1.76×10^{-05} - 8.43×10^{-03}	*Dpp4, Bmp4, Krt6b, Ager, Saa3, Scn9a, Vtn, Lcn2, Kif4a, Cyp21a2, Pigr, Plg, F10, Plcg2, Top2a, Nek2, Mmp1*
Cell Cycle	2.42×10^{-05} - 8.43×10^{-03}	*Plg, Dpp4, Bmp4, Kif4a, Top2a, Ndc80, Ccnb2, Chrdl1, Nek2, Kif2c, Ccnb1*
Cellular Assembly and Organization	2.42×10^{-05} - 8.43×10^{-03}	*Krt6b, Ager, Vtn, Kif4a, Ccnb2, Endou, Ccnb1, Top2a, Ndc80, Kif2c, Nek2, Krt1, Krt10, Mmp1*
DNA Replication, Recombination, and Repair	2.42×10^{-05} - 7.1×10^{-03}	*Kif4a, Top2a, Ndc80, Ccnb2, Nek2, Kif2c, Ccnb1*
Cell Morphology	5.27×10^{-05} - 8.43×10^{-03}	*Plg, Hbe1, Bmp4, Hbz, Plcg2, Vtn, Kif4a, Lcn2, Nek2, Kif2c, Krt1, Krt10*
Cellular Compromise	5.27×10^{-05} - 8.43×10^{-03}	*Hbe1, Bmp4, Ager, Krt6b, Hbz, Vtn, Plcg2, Top2a, Nek2, Mmp1*
Neurological Disease	5.41×10^{-05} - 8.43×10^{-03}	*Ager, Vtn, C9, Qprt, Htr1d, Slc30a3, Mki67, Prkg2, Slc6a13, Slc22a6, Mfi2, Slc2a2, Top2a, Cacna2d3, Crym, Mmp1, Scn9a, Kif4a, Lcn2, Sox11, Ccnb1, Plg, Hbg2, Ca7, F10, Cps1*
Reproductive System Disease	7.71×10^{-05} - 8.43×10^{-03}	*Cyp3a7, Popdc3, Bmp4, Ager, Vtn, Ccnb2, Mki67, Dio2, Hbe1, Itih2, Krt13, Aldob, Itih4, Krt1, Mogat2, Mcm5, Aldh1b1, Scn9a, Lcn2, Kif4a, Aass, Cyp21a2, Ccnb1, F10, Plcg2, Col23a1, Ly6g6c, Nek2, Cps1, Enpep, Fam107a, Phlda2, Chrdl2, C9, Slc2a2, Top2a, Hsd11b2, Kif2c, Cacna2d3, Mmp1, Dpp4, Krt6b, Ugt2b10, Sox11, Prodh2, Plg, Clca1, Chrdl1, Col9a2*
Amino Acid Metabolism*	**1.05×10^{-04} - 4.22×10^{-03}**	***Enpep, Slc36a2, Aass, Slc6a13, Crym, Dio2***
Molecular Transport*	**1.05×10^{-04} - 7.64×10^{-03}**	***Bmp4, Spire2, Lipc, Ager, Slc36a2, Kcnj16, Slc30a3, Prkg2, Slc6a13, Nppb, Dio2, Fxyd2, Slc22a6, Akr1b7, Magel2, Guca2b, Slc2a2, Hsd11b2, Mogat2, Krt10, Cacna2d3, Crym, Dpp4, Scn9a, Lcn2, Sox11, Pigr, Plg, Clca1***

Table 3.7 – continued

Category	p-value	Genes affected by metformin treatment
Dermatological Diseases and Conditions	1.52×10^{-04} - 8.43×10^{-03}	*Cyp3a7, Lipc, Ager, Slc36a2, Mki67, Prkg2, Slc22a6, Dio2, Elmod1, Magel2, Hbe1, Krt13, Itih2, Aldob, Krt1, Aldh1b1, Podn, Scn9a, Lcn2, Cyp21a2, Pigr, Enpp3, F10, Plcg2, Col23a1, Nek2, Cps1, Enpep, Fam107a, Chrdl2, Ambp, C9, Htr1d, Slc6a13, Krtdap, Aadac, Mfi2, Top2a, Cacna2d3, Krt10, Mmp1, Dpp4, Krt6b, Ugt2b10, Sox11, Hbg2, Plg, Clca1, Chrdl1, Col9a2*
Cellular Function and Maintenance	1.56×10^{-04} - 8.43×10^{-03}	*Dpp4, Bmp4, Krt6b, Ager, Vtn, Scn9a, Lcn2, Kif4a, Kcnj16, Pigr, Plg, Hsd11b2, Nek2, Kif2c, Cps1*
Connective Tissue Disorders	1.68×10^{-04} - 8.43×10^{-03}	*Mcm5, Dpp4, Bmp4, Ager, Saa3, Vtn, Scn9a, Lcn2, Sox11, Slc22a6, Ccnb1, Plg, F10, Col23a1, Plcg2, Ly6g6c, Cacna2d3, Col9a2, Mmp1*
Inflammatory Disease	1.68×10^{-04} - 8.43×10^{-03}	*Mcm5, Dpp4, Bmp4, Ager, Saa3, Vtn, Scn9a, Lcn2, Pigr, Slc22a6, Ccnb1, Ca7, Plg, F10, Plcg2, Top2a, Ly6g6c, Cacna2d3, Col9a2, Mmp1*
Skeletal and Muscular Disorders	1.68×10^{-04} - 8.43×10^{-03}	*Mcm5, Dpp4, Bmp4, Ager, Saa3, Vtn, Scn9a, Lcn2, Mki67, Sox11, Slc22a6, Ccnb1, Plg, F10, Plcg2, Top2a, Ly6g6c, Cacna2d3, Col9a2, Mmp1*
Cell Death and Survival	1.75×10^{-04} - 8.43×10^{-03}	*Dpp4, Bmp4, Ager, Saa3, Vtn, Lcn2, Mki67, Sox11, Slc22a6, Ccnb1, Plg, Hbz, Slc2a2, Plcg2, Top2a, Ndc80, Mmp1*
Tumor Morphology	1.75×10^{-04} - 1.75×10^{-04}	*Bmp4, Vtn*
Nucleic Acid Metabolism*	**1.88×10^{-04} - 7.61×10^{-03}**	***Plg, Guca2b, Enpp3, Bmp4, Ager, Qprt, Nppb, Ccnb1***
Lipid Metabolism*	**2.45×10^{-04} - 8.43×10^{-03}**	***Dpp4, Cyp3a7, Bmp4, Lipc, Ager, Vtn, Slc36a2, Ambp, Prkg2, Slc6a13, Cyp21a2, Nppb, Plg, Plcg2, Hsd11b2, Mogat2, Cps1***
Vitamin and Mineral Metabolism	2.45×10^{-04} - 6.36×10^{-03}	*Plg, Cyp3a7, Bmp4, Lipc, Hsd11b2, Prkg2, Cyp21a2, Nppb*
Organismal Survival	2.62×10^{-04} - 4.22×10^{-03}	*Top2a, Ndc80*

Table 3.7 – continued

Category	p-value	Genes affected by metformin treatment
Tissue Morphology	2.62×10^{-04} - 8.43×10^{-03}	*Bmp4, Lipc, Ager, Eda, Vtn, Ambp, Lcn2, Prkg2, Sox11, Nppb, Akr1b7, Plg, Clca1, Shcbp1, Hbz, Plcg2, Hsd11b2, Mogat2*
Psychological Disorders	2.86×10^{-04} - 6.39×10^{-03}	*Ager, Scn9a, Ambp, Lcn2, C9, Htr1d, Slc30a3, Slc6a13, Prodh2, Ccnb1, Hbg2, Plg, Ca7, Mfi2, Itih4, Slc2a2, Cacna2d3, Mmp1*
Inflammatory Response	3.09×10^{-04} - 8.43×10^{-03}	*Mcm5, Dpp4, Bmp4, Ager, Saa3, Vtn, Scn9a, Ambp, Lcn2, Mki67, Slc22a6, Pigr, Ccnb1, Ca7, Plg, Clca1, F10, Shcbp1, Plcg2, Top2a, Ly6g6c, Krt1, Cacna2d3, Col9a2, Mmp1*
Hair and Skin Development and Function	4.86×10^{-04} - 4.22×10^{-03}	*Krt6b, Krt1, Krt10*
Organ Morphology	4.86×10^{-04} - 8.43×10^{-03}	*Plg, Clca1, Bmp4, Ager, Slc2a2, Lcn2, Hsd11b2, Sox11, Krt1, Cyp21a2, Krt10*
Cellular Development	6.57×10^{-04} - 8.43×10^{-03}	*Plg, Dpp4, Bmp4, Krt6b, Ager, Plcg2, Vtn, Hsd11b2, Sox11, Dio2, Nppb, Mmp1*
Cellular Growth and Proliferation	6.57×10^{-04} - 8.43×10^{-03}	*Plg, Dpp4, Enpp3, Bmp4, Ager, Vtn, Scn9a, Lcn2, Hsd11b2, Sox11, Nppb, Mmp1*
Organ Development	6.57×10^{-04} - 8.43×10^{-03}	*Guca2b, Plg, Dpp4, Bmp4, Ager, Vtn, Lcn2, Hsd11b2, Pigr, Dio2, Nppb, Mmp1*
Skeletal and Muscular System Development and Function	6.57×10^{-04} - 8.43×10^{-03}	*Plg, Dpp4, Bmp4, Ager, Saa3, Chrdl2, Vtn, Kcnj16, Hsd11b2, Prkg2, Sox11, Nppb, Mmp1*
Tissue Development	6.57×10^{-04} - 8.43×10^{-03}	*Dpp4, Bmp4, Eda, Ager, Krt6b, Vtn, Chrdl2, Lcn2, Prkg2, Endou, Sox11, Nppb, Plg, Hsd11b2, Mmp1*
Auditory and Vestibular System Development and Function	7.76×10^{-04} - 4.22×10^{-03}	*Cacna2d3, Dio2*

Table 3.7 – continued

Category	p-value	Genes affected by metformin treatment
Immune Cell Trafficking	7.81×10^{-04} - 8.43×10^{-03}	*Plg, Clca1, Dpp4, F10, Bmp4, Ager, Saa3, Plcg2, Vtn, Scn9a, Lcn2, Pigr*
Renal and Urological Disease	8.16×10^{-04} - 8.43×10^{-03}	*Enpep, Dpp4, Bmp4, Ager, Slc36a2, Lcn2, Aass, Slc22a6, Pigr, Ccnb1, Plcg2, Slc2a2, Top2a, Hsd11b2, Cps1*
Ophthalmic Disease	8.5×10^{-04} - 8.43×10^{-03}	*Plg, Ca7, F10, Bmp4, Lipc, C9, Top2a, Qprt, Chrdl1, Nek2, Col9a2*
Protein Synthesis	8.72×10^{-04} - 6.36×10^{-03}	*Enpep, Dpp4, Lipc, Vtn, Ambp, Aass, Qprt, Endou, Dio2, Slc22a6, Elmod1, Akr1b7, Plg, Hbg2, Hbe1, Hbz, Slc2a2, Mogat2, Krt1, Cps1, Mmp1*
Drug Metabolism	8.87×10^{-04} - 8.43×10^{-03}	*Plg, Cyp3a7, Bmp4, Vtn, Top2a, Hsd11b2, Cyp21a2, Dio2, Nppb, Slc22a6*
Hematological Disease	9.46×10^{-04} - 8.43×10^{-03}	*Dpp4, Lipc, Vtn, Lcn2, Aass, Qprt, Mki67, Cyp21a2, Plg, Hbg2, F10, Itih4, Top2a, Ndc80, Krt1, Kif2c, Mogat2, Cps1*
Hematopoiesis	9.46×10^{-04} - 4.22×10^{-03}	*Bmp4, Ager, Vtn, Plcg2, Lcn2*
Respiratory Disease	9.46×10^{-04} - 8.43×10^{-03}	*Aldh1b1, Podn, Krt6b, Ager, Scn9a, Lcn2, Kcnj16, Ccnb2, Mki67, Ccnb1, Hbg2, Plg, Ca7, Hbe1, F10, Itih2, Col23a1, Top2a, Cps1, Mmp1*
Nutritional Disease	9.69×10^{-04} - 4.22×10^{-03}	*Ca7, Dpp4, F10, Scn9a, Top2a, Hsd11b2, Htr1d, Cyp21a2, Mogat2, Akr1b7*
Organismal Development	1.12×10^{-03} - 8.43×10^{-03}	*Dpp4, Bmp4, Ager, Eda, Krt6b, Kcnj16, Ccnb2, Prkg2, Sox11, Dio2, Magel2, Plg, Itih4, Slc2a2, Plcg2, Hsd11b2, Krt10*
Renal and Urological System Development and Function	1.24×10^{-03} - 6.76×10^{-03}	*Guca2b, Plg, F10, Bmp4, Ager, Vtn, Lcn2, Hsd11b2, Pigr*
Hereditary Disorder	1.28×10^{-03} - 8.43×10^{-03}	*Bmp4, Proz, Slc36a2, Scn9a, C9, Kif4a, Aass, Htr1d, Sox11, Cyp21a2, Pigr, Magel2, Ca7, Hbg2, Plg, F10, Slc2a2, Plcg2, Nek2, Krt1, Crym, Cps1, Col9a2, Mmp1*

Table 3.7 – continued

Category	p-value	Genes affected by metformin treatment
Post-Translational Modification	1.33×10^{-03} - 5.32×10^{-03}	*Plg, Dpp4, Enpep, Endou, Dio2, Cps1, Mmp1*
Protein Degradation	1.33×10^{-03} - 5.32×10^{-03}	*Plg, Dpp4, Enpep, Vtn, Ambp, Endou, Cps1, Mmp1, Elmod1*
Nervous System Development and Function	1.55×10^{-03} - 8.43×10^{-03}	*Bmp4, Scn9a, Lcn2, Hsd11b2, Sox11*
Reproductive System Development and Function	2.01×10^{-03} - 8.43×10^{-03}	*Plg, Bmp4, Lipc, Hbz, Lcn2, Ambp, Ccnb2*
Connective Tissue Development and Function	2.04×10^{-03} - 8.43×10^{-03}	*Plg, Lipc, Bmp4, Hbz, Plcg2, Lcn2, Hsd11b2, Prkg2, Mogat2, Sox11, Nppb, Akr1b7*
Embryonic Development	2.04×10^{-03} - 8.43×10^{-03}	*Plg, Bmp4, Eda, Ager, Sox11, Nppb*
Infectious Diseases	2.04×10^{-03} - 8.43×10^{-03}	*Hbg2, Ca7, Hbe1, Lcn2, Top2a*
Digestive System Development and Function	2.88×10^{-03} - 6.2×10^{-03}	*Guca2b, Prkg2, Pigr*
Immunological Disease	3.19×10^{-03} - 4.22×10^{-03}	*F10, Ager, Plcg2, C9, Top2a, Ndc80, Mki67, Kif2c, Pigr*
Developmental Disorder	3.51×10^{-03} - 8.43×10^{-03}	*Bmp4, Scn9a, C9, Kif4a, Aass, Sox11, Cyp21a2, Magel2, Slc2a2, Hsd11b2, Krt1, Chrdl1, Col9a2, Cps1, Mmp1*
Auditory Disease	4.22×10^{-03} - 4.22×10^{-03}	*Top2a*
Carbohydrate Metabolism	4.22×10^{-03} - 8.43×10^{-03}	*Bmp4, Ager, Aldob, Vtn, Plcg2, Slc2a2, Dio2, Fxyd2, Akr1b7, Magel2*
Hepatic System Disease	4.22×10^{-03} - 4.22×10^{-03}	*Slc2a2*

Table 3.7 – continued

Category	p-value	Genes affected by metformin treatment
Lymphoid Tissue Structure and Development	4.22×10^{-03} - 4.22×10^{-03}	*Ager, Hsd11b2*
Respiratory System Development and Function	4.22×10^{-03} - 4.22×10^{-03}	*Pigr*
Visual System Development and Function	4.22×10^{-03} - 8.43×10^{-03}	*Bmp4, Hsd11b2*
Behaviour	4.97×10^{-03} - 4.97×10^{-03}	*Dpp4, Bmp4, Ager, Krt6b, Lcn2, Ambp, Kcnj16, Hsd11b2, Slc30a3, Mogat2, Cacna2d3, Akr1b7, Magel2*
Energy Production	7.61×10^{-03} - 7.61×10^{-03}	*Plg, Ager, Ccnb1*
Gene Expression	8.43×10^{-03} - 8.43×10^{-03}	*Krt6b*

* (bold) Pathways that were selected for further analysis

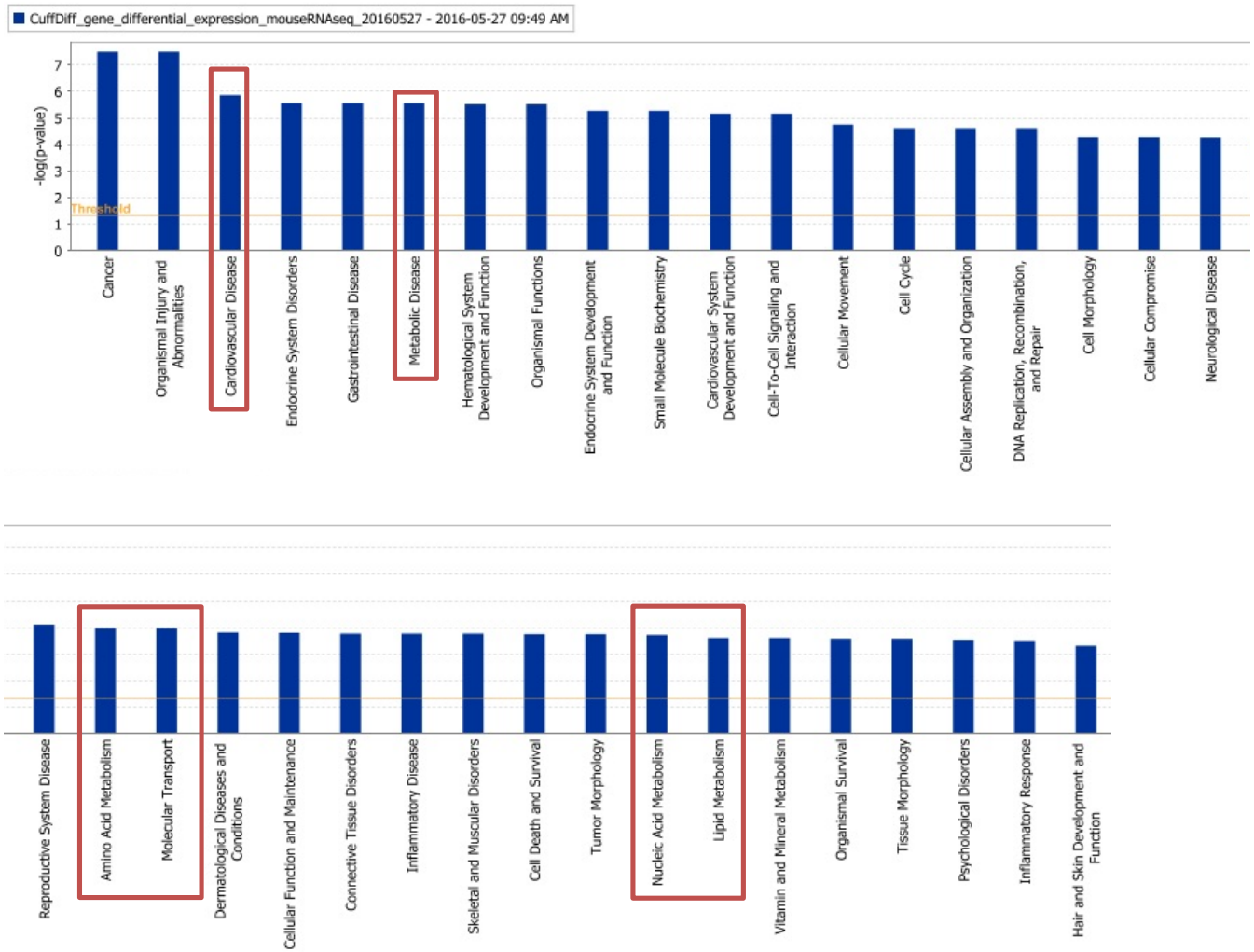

Figure 3.10 Disease and function pathways affected by metformin

This analysis shows the 37 mots significant networks that were affected by the metformin treatment. In red are the pathways that were selected for further analysis. Threshold is showing the significant cut-off point. (n: control and control metformin: 4 placentas each).

Disease and function networks interactions

Cardiovascular and metabolic disease pathways, Amino acid metabolism, Molecular transport, Nucleic acid metabolism and Lipid metabolism were selected from the previous analysis (Table 3.7) in order to determine the interaction found between the genes that were modified by the metformin treatment and the mentioned pathways. Cardiovascular disease pathway showed that venous thromboembolism, vaso-occlusion, thrombosis of vein between others were modified by the metformin treatment (Figure 3.11).

Metabolic disease pathway is shown in Figure 3.12. On the outside of the diagram are the genes that were affected by the metformin and connected to the Metabolic disease. Glucose metabolism disorders were inhibited by the metformin treatment, other metabolic diseases pathways such as hypercholesterolemia, diabetes mellitus, diabetic nephropathy, acidemia were also found in this analysis but the effect of the metformin treatment on them was not that clear.

Transport of beta-alanine, release of l-lysine, l-methionine, alanine and leucine and efflux of amino acids were components of the Amino acid metabolism pathway that were found to be altered by the genes affected by the metformin treatment (Figure 3.13).

Molecular transport showed that processes such as Concentration of hormones, Concentration of glucose and Transport of molecule were all activated by metformin treatment (Figure 3.14).

Figure 3.15 shows the Nucleic acid metabolism pathway with genes affected by metformin treatment located around the outside of the network diagram.

Lipid metabolism pathway is shown in Figure 3.16; Synthesis of lipid and Steroid metabolism were activated and Conversion of lipid was inhibited by metformin.

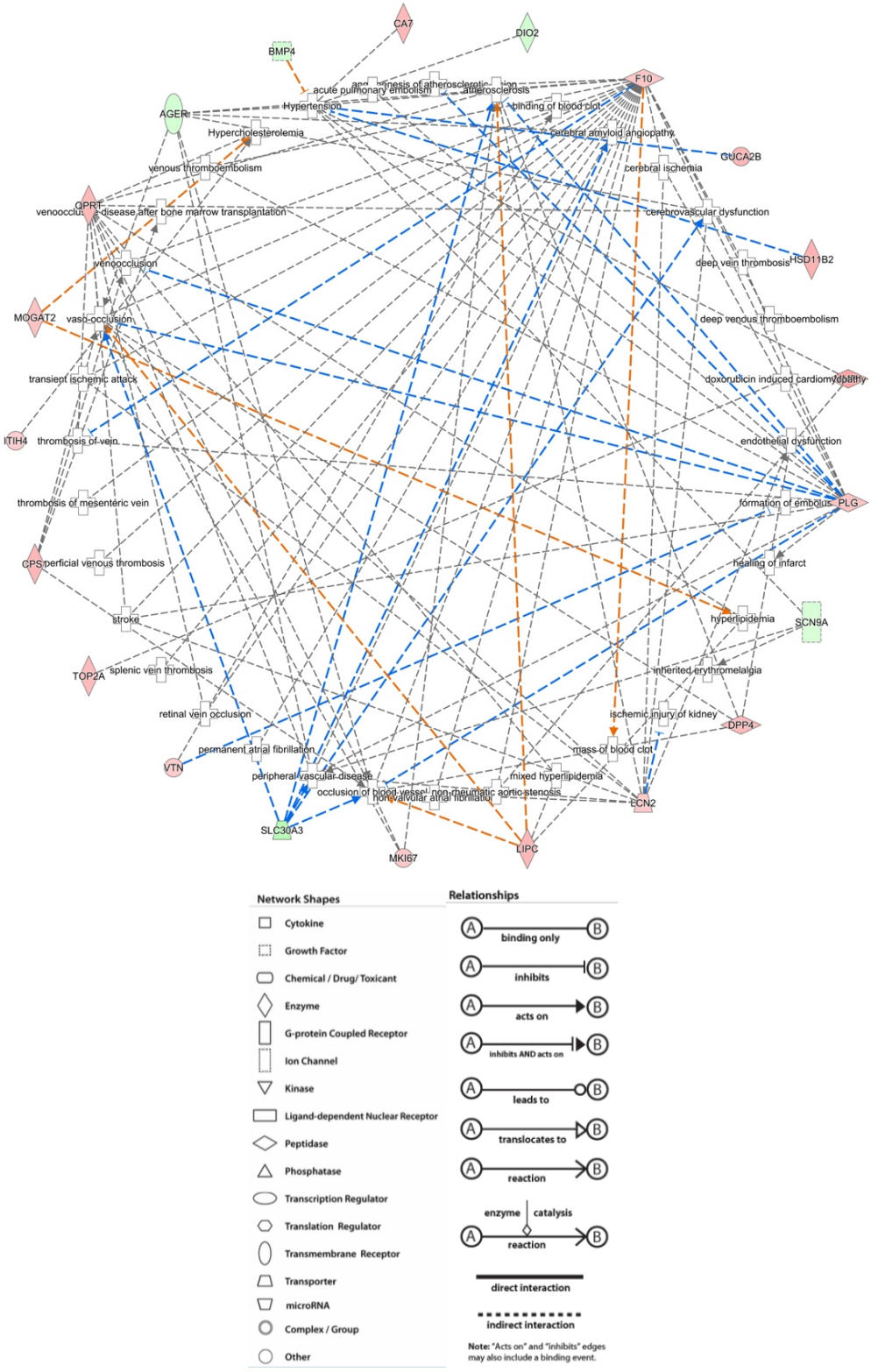

Figure 3.11 Cardiovascular disease network affected by metformin treatment

This figure shows the genes that were affected by the metformin treatment (outside) and that are related to Cardiovascular diseases (white figures inside). In green are the genes that had a decreased expression with the metformin treatment and in red are the ones with an increased expression with the treatment. Interactions were indirect. Blue lines indicate that the interaction produces an inhibition in the downstream node and oranges lines indicates an activation in the downstream node. Grey line indicates that the interaction could not be calculated. (n: control and control metformin: 4 placentas each).

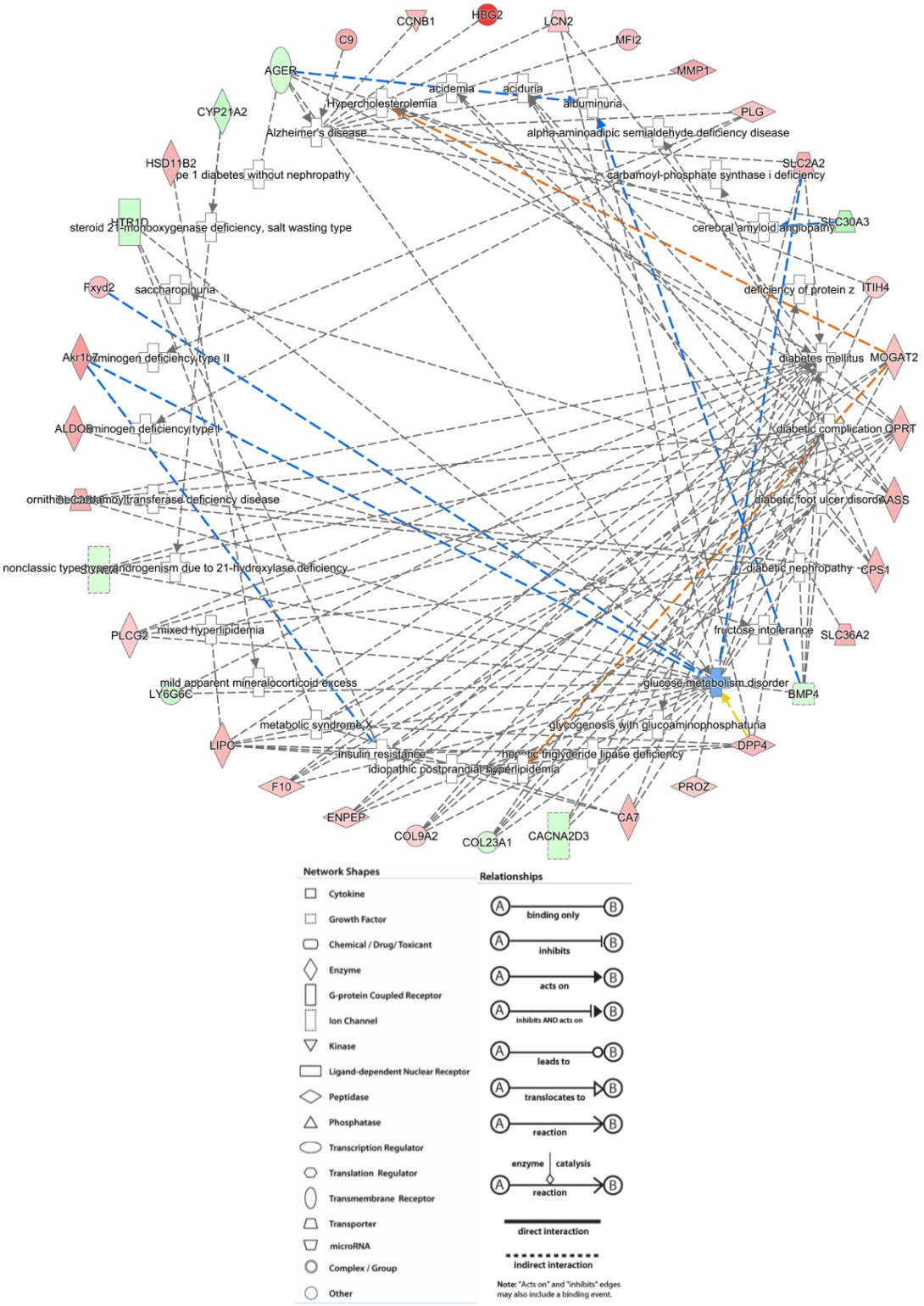

Figure 3.12 Metabolic disease pathway affected by metformin treatment

This figure shows the genes that were affected by the metformin treatment (outside) and that are related to Metabolic diseases (white figures inside). In green are the genes that had a decreased expression with the metformin treatment and in red are the ones with an increased expression with the treatment. All the interactions are indirect. Blue lines indicate that the interaction produces an inhibition in the downstream node and oranges lines indicate an activation in the downstream node. Yellow lines indicate that the findings of the analysis are inconsistent with the state of the downstream node. Grey line indicates that the interaction could not be calculated. (n: control and control metformin: 4 placentas each).

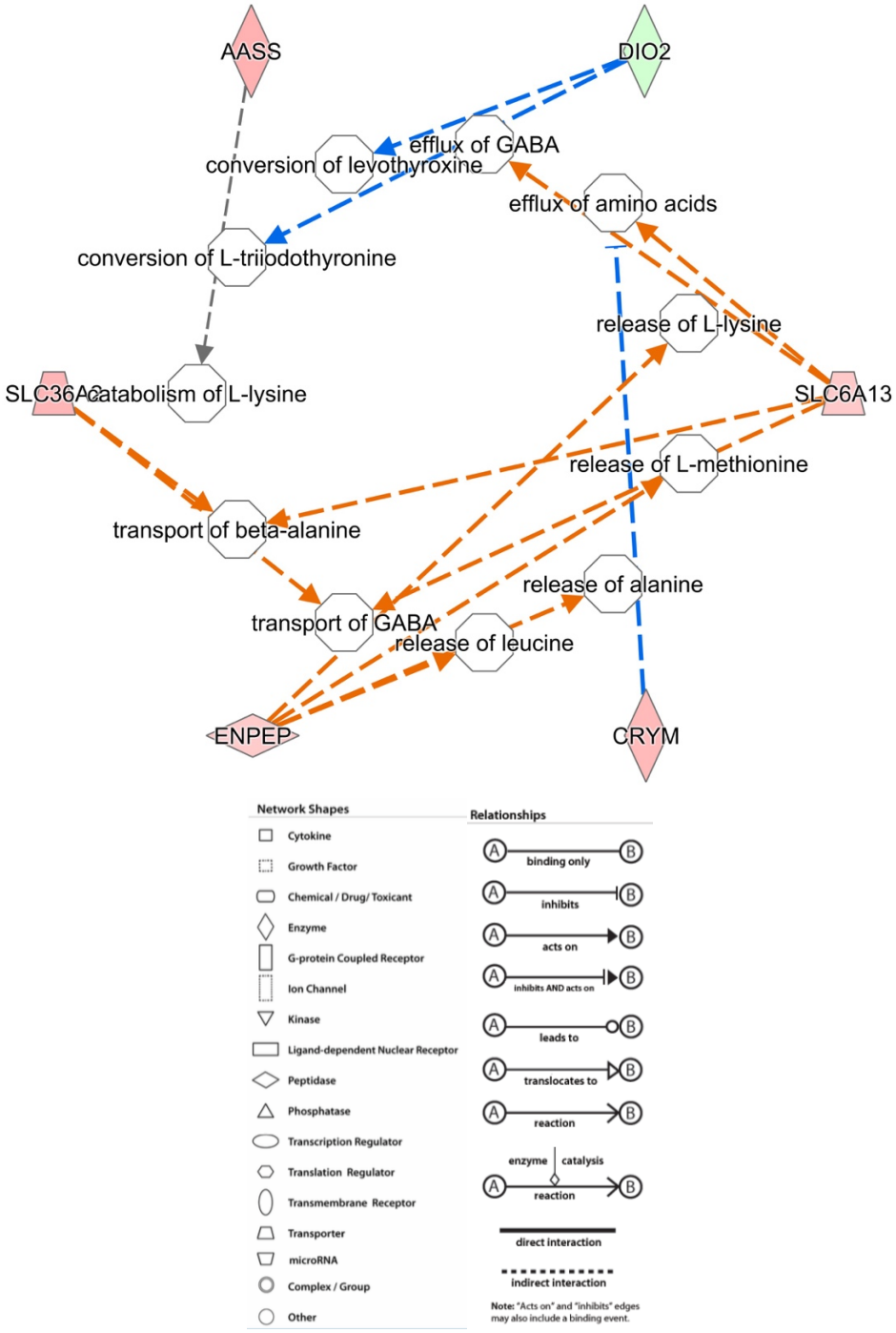

Figure 3.13 Amino acid metabolism pathway affected by metformin treatment

This figure shows the genes that were affected by the metformin treatment (outside) and that are related to Amino acid metabolism (white figures). In green are the genes that had a decreased expression with the metformin treatment and in red are the ones with an increased expression with the treatment. All the interactions are indirect. Blue lines indicate that the interaction produces an inhibition in the downstream node and oranges lines indicate an activation in the downstream node. Grey line indicates that the interaction could not be calculated. (n: control and control metformin: 4 placentas each).

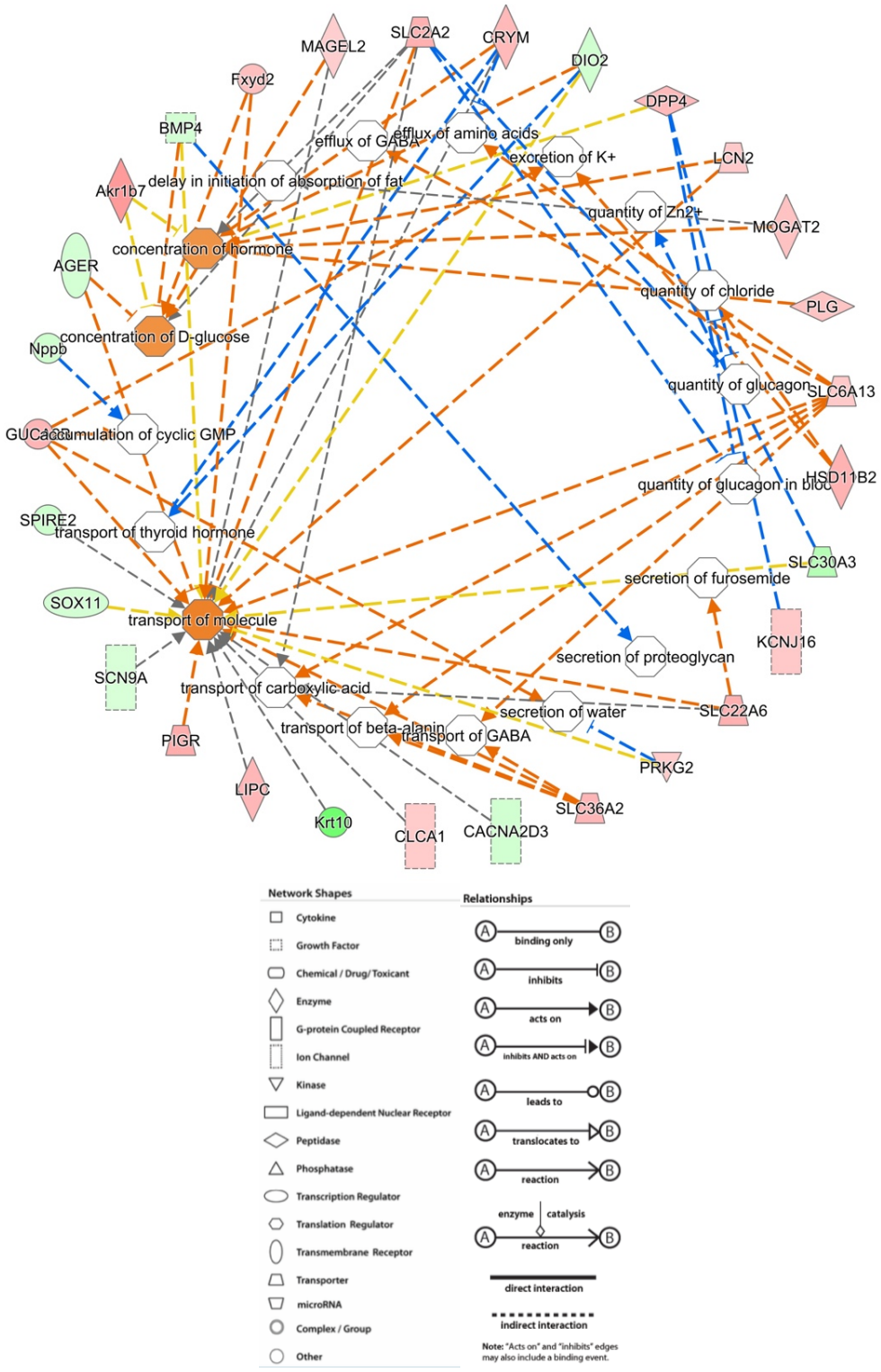

Figure 3.14 Molecular transport pathway affected by metformin treatment

This figure shows the genes that were affected by the metformin treatment (outside) and that are related to molecular transport (white figures). In green are the genes that had a decreased expression with the metformin treatment and in red are the ones with an increased expression with the treatment. All the interactions are indirect. Blue lines indicate that the interaction produces an inhibition in the downstream node and oranges lines indicate an activation in the downstream node. Yellow lines indicate that the findings of the analysis are inconsistent with the state of the downstream node. Grey line indicates that the interaction could not be calculated. (n: control and control metformin: 4 placentas each).

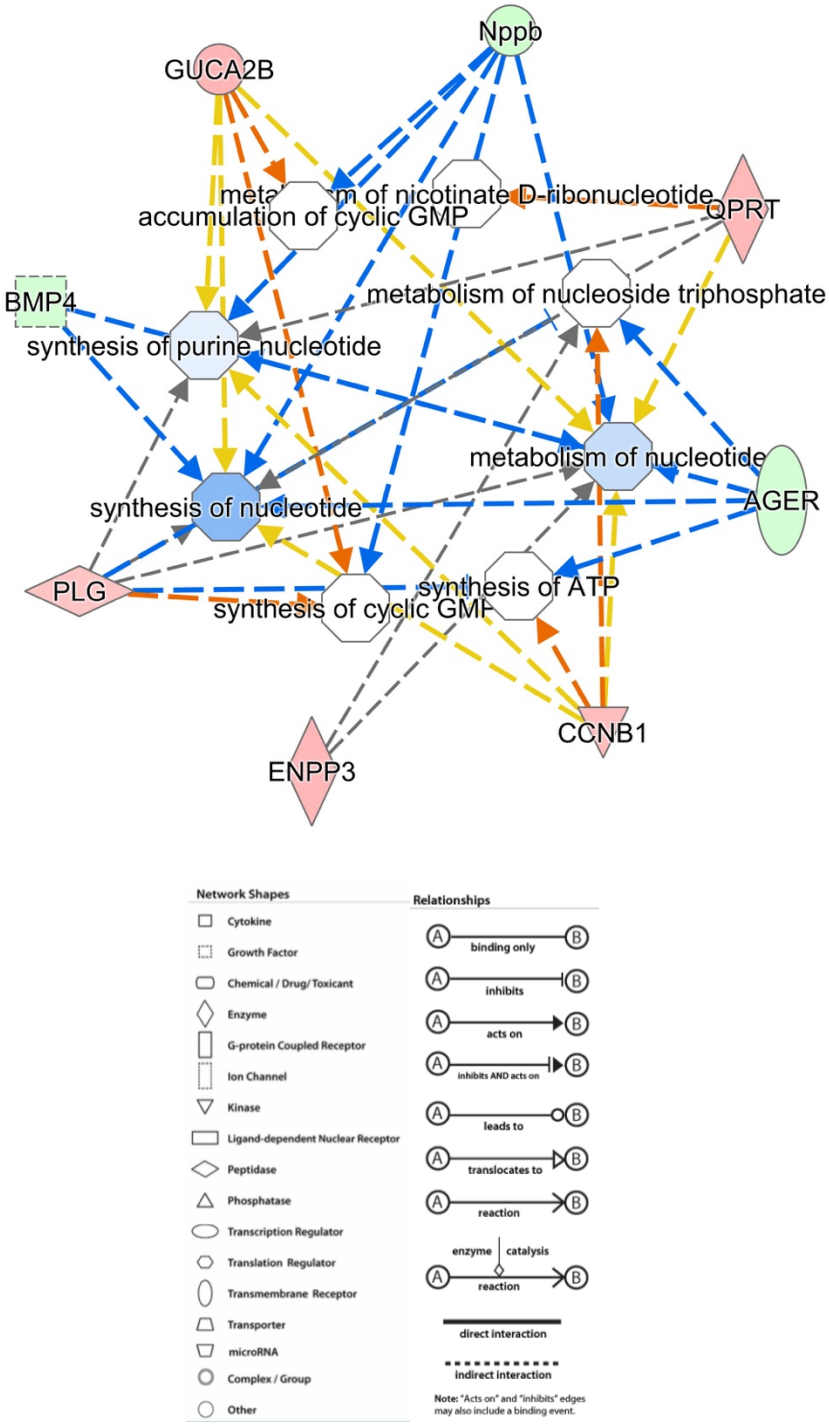

Figure 3.15 Nucleic acid metabolism pathway affected by metformin treatment

This figure shows the genes that were affected by the metformin treatment (outside) and that are related to Nucleic acid metabolism (white figures). In green are the genes that had a decreased expression with the metformin treatment and in red are the ones with an increased expression with the treatment. all the interactions are indirect. Blue lines indicate that the interaction produces an inhibition in the downstream node and oranges lines indicate an activation in the downstream node. Yellow lines indicate that the findings of the analysis are inconsistent with the state of the downstream node. Grey line indicates that the interaction could not be calculated. (n: control and control metformin: 4 placentas each).

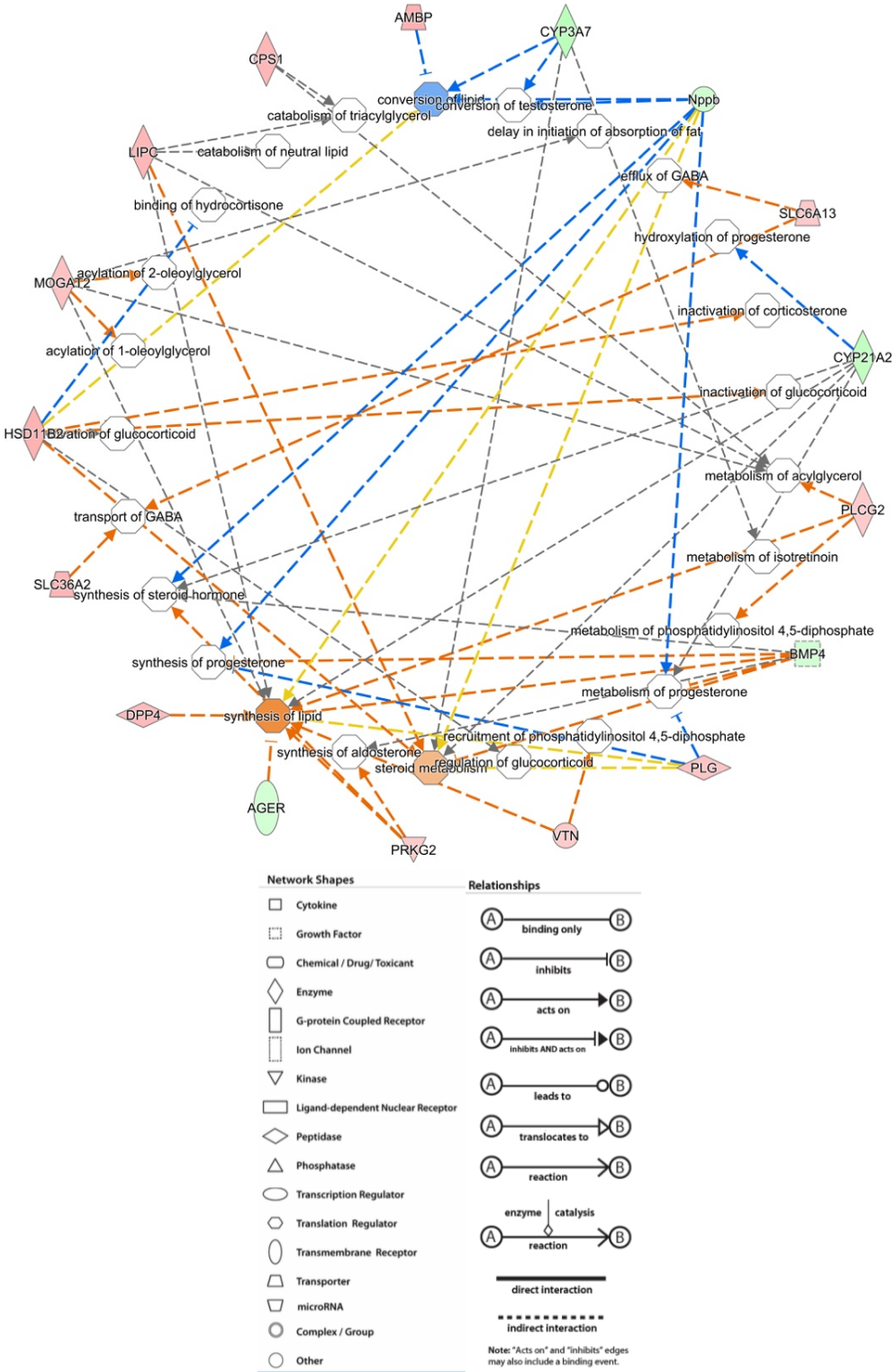

Figure 3.16 Lipid metabolism pathway affected by metformin treatment

This figure shows the genes that were affected by the metformin treatment (outside) and that are related to Lipid metabolism (white figures). In green are the genes that had a decreased expression with the metformin treatment and in red are the ones with an increased expression with the treatment. all the interactions are indirect. Blue lines indicate that the interaction produces an inhibition in the downstream node and oranges lines indicates an activation in the downstream node. Yellow lines indicate that the findings of the analysis are inconsistent with the state of the downstream node. Grey line indicates that the interaction could not be calculated. (n: control and control metformin: 4 placentas each).

3.4.3.2 Comparison of qPCR gene expression and RNA sequencing data

Table 3.8 shows a comparison between the RNA sequencing analysis and the qPCR gene expression. In the table, the means of metformin group minus means of the control group were calculated. The analysis using qPCR showed *Clock, Per2, Glut3, Tat1* and *Lat1* mRNA expression were reduced by the metformin treatment. *Lpl* and *Fatp2* were reduced with a borderline p value. In the RNA sequencing analysis only *Lpl* and *Fatp2* were reduced by the metformin treatment.

Table 3.8 Comparison of RNA sequencing analysis and qPCR gene expression

Gene	RNA seq analysis		qPCR gene expression	
	2FC	unadjusted p-value	Mean difference	p-value
Clock	-0.89	0.484	**-1.23**	**0.004**
Bmal	-1.05	0.642	0.01	0.958
Per2	-0.80	0.124	**-3.01**	**0.001**
Cry2	-0.87	0.19	0.12	0.563
Insig1	-0.99	0.898	-0.20	0.610
Fto	-1.01	0.916	0.00	0.997
Sirt1	-1.04	*0.74*	*-0.93*	*0.082*
Sirt3	-1.00	0.994	0.12	0.625
Glut1 (Slc2a1)	-0.81	0.102	-0.06	0.771
Glut3 (Slc2a3)	-0.98	0.789	**-0.48**	**0.034**
Tat1 (Slc26a8)	-1.05	0.806	**-2.58**	**0.008**
Lpl	**-0.64**	**$5x10^{-5}$**	*-0.32*	*0.065*
Fatp2 (Slc27a2)	**-1.32**	**0.04**	*-0.39*	*0.067*

2FC: 2 fold change of expression.

3.5 DISCUSSION

This study shows that exposure to high fat diet or metformin treatment had different effects on placental gene expression. This suggests that the placental response to metformin or high fat diet is controlled by a different mechanism. Furthermore, it showed that the prenatal exposure to metformin modifies some, but not all, of the effects of the maternal high fat diet suggesting that metformin effects could be directly in the placenta but also indirectly modifying maternal signals. This study shows that exposure to a high fat diet and a metformin treatment affected placental gene expression in a different way suggesting that the responses to metformin and high fat diet are sensed by distinct mechanisms in the placenta.

High fat diet reduced the expression of amino acid and glucose transporter genes suggesting that reduced nutrient transfer may explain the observed fetal growth restriction. High fat diet also decreased the expression of *Insig1* and glucose transporters in the mouse placenta. Insig1 is an insulin-induced gene that inhibited cholesterol synthesis. *Insig1* reduction in the placentas exposed to the high fat diet could indicate an alteration in the insulin signalling mechanism. This might indicate a reduction in the maternal insulin levels or the presence of insulin resistance, however, insulin levels were not measured in this study. A glucose tolerance test was carried out in the mothers confirming a reduction in insulin sensitivity in them. It is possible that the glucose tolerance state induced by the high fat diet during the pregnancy was affecting the placenta as well and producing the observed reduction in the nutrients transporters expression (Figure 3.17).

Previously, studies using the same model as the one used in this study, showed that prenatal high fat diet exposure contributes to the development of steatohepatitis by altering mitochondrial function in liver [214], and that the development of non-alcoholic fatty liver disease (NAFLD) in adulthood could be increase when it was a prenatal exposure to high fat diet. The development of NAFLD in this mouse was associated with alteration in mitochondrial function, sirtuins and clock genes levels [221]. Effects of

high fat diet on the mouse placenta are not consistent, with other studies showing an increase in amino acid transporters levels and increased in fetal weight [32,222]. Also in rats, a high fat diet during pregnancy has been shown to activate mTORC1 and reduced the activation of AMPK with a reduction in the protein levels of *Snat2* but without modifying protein levels of other amino acid or fatty acid transporters in the placenta [146]. Possibly the differences in the placental function that has been reported between in studies can be explained by the fat contents in the high fat diet. While this study is duplicating the levels of fat in the diet when compared with the control, the others studies are triplicating the fat content in the diet. This could mean that the effects of the high fat diet are doses-dependent and a higher exposure is necessary in order to produce fetal overweight.

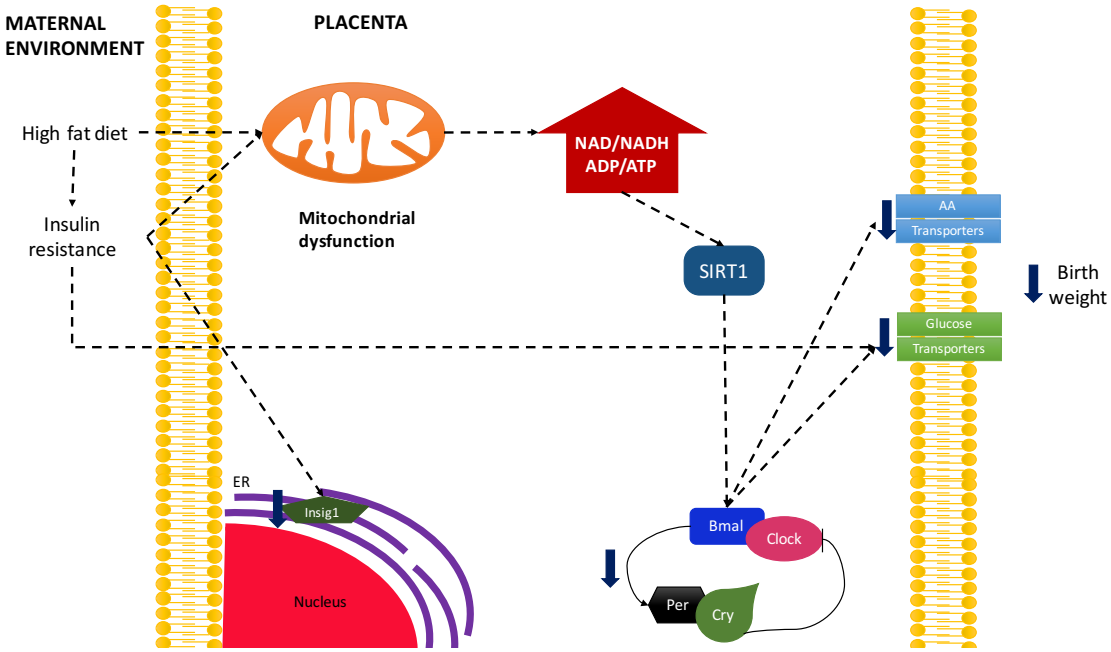

Figure 3.17 Proposed placental response to a high fat diet in a mouse model

The diagram is showing a potential mechanism for which the high fat diet is decreasing the nutrient transport levels in the placenta. Possibly the exposure to a HF diet produced insulin resistance in the mother, alteration in mitochondrial function and unbalance in the energy levels in the placenta. ER (endoplasmic reticulum).

Metformin's effects in the placenta were generally independent of the high fat diet effects. Metformin modified the gene expression of *Per2* and *Clock* that might indicate that metformin is acting by modifying the circadian metabolism in the cells. Metformin

also reduced the expression of genes related to lipid and glucose metabolism and transport. RNA sequencing analysis of the metformin exposed placentas showed that metformin affected pathway related with molecular transport, nutrient metabolism and vascular function suggesting that metformin could be affecting placental function in different ways. It is possible that metformin is modifying hormonal synthesis and transport in the placenta by its effect on lipid metabolism and molecular transport. Metformin could also be affecting placental nutrient transport by two different mechanisms affecting molecular transport but also vascular function. Metformin affected the expression of two of the clock genes that could suggest a modification in the circadian expression of these genes. This is supported by a study showing that metformin has been found to affect clock genes expression in mouse liver and muscle [216]. The possibility that metformin is acting by modification of the cellular circadian rhythms requires timeline experiments that prove a change in the circadian expression of the clock genes.

In humans, pregnancies complicated with diabetes have alterations in placental amino acid transport with a general increase in the transporter activity [124]. Metformin treatment in this study showed that metformin interacts with the high fat diet increasing the gene expression of amino acid transporter *Lat1.* It is possible that metformin is able to modify the effects of an insulin-resistant environment in the placenta. Metformin has been used as a common treatment for gestational diabetes but its effects on placental function are still being determined; this study, therefore, contributes to the understanding of the mechanism that is affected by this medication.

The RNA sequencing analysis gives a more global picture of the effects of the metformin exposure on the placental transcriptome. Effects on pathways such as the Molecular transport and Metabolism of Lipid, Amino acid and Nucleic acids in the placenta indicates that the metformin effects are more complex than just an improvement in glucose metabolism and insulin sensitivity. Prenatal metformin exposure in mice followed by a high fat diet during the adulthood has been shown to produce modification in metabolic pathways in the liver, indicating that metformin

might have programming effects that can be observed later in life [217]. In this study the exposure to metformin in a normal pregnancy showed modifications of metabolic pathways in the placenta. Molecular transport was affected by metformin exposure and not just genes of nutrients transporters were modified but also genes of transporters of transport waste products, ions among others were affected. This is consistent with one of the placenta's more important functions being the transfer of nutrients and other substances between the mother and the fetus. It is therefore important to the determine if the overall effect of metformin can affect fetal development due to a modification in the transport of substances such as hormones or nutrients, more studies are necessary in order to answer this question.

This study helps to understand how placental function can be affected by the exposure to a high fat diet or a metformin treatment during gestation (Figure 3.18). It showed that these interventions have an independent effect on the placental gene expression. It was also shown that metformin could be affecting placental function in different ways but it is still not clear how it could be affecting fetal development. More studies are necessary in order to determine how whether metformin effects on the placenta are direct or indirect and the mechanism behind the modifications produced by the interventions.

3.5.1 Limitations

The limitations of this study include the low numbers of the control samples and the fact that the samples were not independent because some belong to the same litter. The use of a mixed model that includes the litter as a random factor and the covariance added by the litter addresses the independence issue. Another limitation of this study is that it is not possible to determine if the interventions have an indirect effect (affecting maternal signals) or a direct effect (affecting placental signalling). An experiment that directly exposes the placenta to the interventions will be necessary to determine the mechanism behind the diet and the metformin effects.

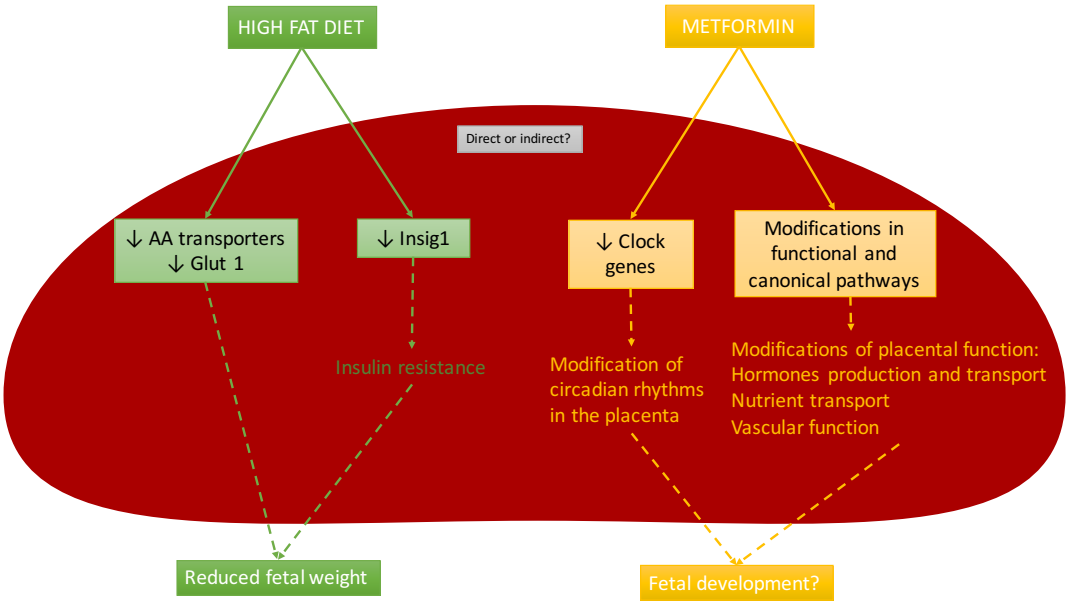

Figure 3.18 Overall effects of high fat diet and metformin treatment on the mouse placenta

High fat diet and metformin exposure acted independently over placental function. Green boxes show the main effects of the high fat diet in the placenta yellow boxes show the main effects of the metformin treatment. Solid lines show the findings in this study, dotted lines show suggested mechanisms. (AA: amino acid, Glut1: glucose transporter 1).

Validation of the RNA sequencing data was not carried out due to time limitations. To validate the RNA sequencing the most highly changed genes should be validated by qPCR. A comparison was made between RNA sequencing and PCR for the genes that had previously been measured in this chapter but none of these were genes that were shown to be highly changed by RNA sequencing.

The findings in this chapter are restricted to gene expression, which shows that the interventions have an effect in the tissue. Studies of protein levels and function are necessary to determine the extent of the treatments effects. This study was able to demonstrate that exposure to a high fat diet and metformin treatment during the pregnancy have independent effects on placental gene expression. It also suggests possible mechanisms of how these interventions are acting. Further studies are necessary to a better understanding of the pathways involve in this process.

3.6 CONCLUSION

Maternal metformin treatment and high fat diet affect the expression of placental amino acid, glucose and fatty acid transporters, which can lead to an altered placental function. The effects of the interventions are independent indicating different sensing mechanisms are involved in the placental response to these interventions. Maternal metformin treatment was demonstrated to have widespread effects on pathways of gene expression in the mouse placenta. These included changes in the transport of molecules, tissue remodelling and metabolism function. It is important to determine if the effects of metformin in the placenta are a direct effect of the drug on the tissue or are an indirect effect of the drug on the mother that produces a response that affects placental function.

CHAPTER 4 DIRECT EFFECT OF METFORMIN EXPOSURE ON GENE EXPRESSION

4.1 INTRODUCTION

The previous chapter showed that maternal metformin exposure affected mouse placental gene expression. Metformin affected pathways involved in cellular function such as transport and metabolism in placenta. Metformin exposure had different effects on placental gene expression compared with the effect of the high fat diet. From the mouse studies we cannot tell whether the effects of metformin were due to a direct effect of metformin on the placenta or if they were due to an effect of metformin on the mother that was in turn sensed by the placenta. The aim of this chapter was to determine whether direct exposure to metformin in mouse trophoblast stem cells has similar effects to those observed in the placentas of metformin treated mice.

The use of metformin as an antidiabetic drug has increased around the world [223]. After it was proved that metformin was safe to use during pregnancy [224], metformin has become a common treatment for gestational diabetes, and for pregnant women that already have type 2 diabetes [225]. Metformin use in pregnancy is effective in decreasing the blood glucose levels of the mother [226-228] and different studies have shown that does not have negative neonatal outcomes [226-228].

Metformin is able to cross the placenta but the exact mechanism is not well understood. *Ex-vivo* studies have shown that metformin is transferred through the placenta in both directions with a higher fetal-to-maternal transfer [229]. Metformin must be transported across cell membranes in order to enter the cell and have its effects. Organic cation transporters (OCT), such as OCT1, are able to transport metformin both into and out of cells by exchange [230], while ABC transporters are able to mediate active metformin efflux drug efflux [229,231]. ABC transporters are involved in the metformin efflux from the placenta to the mother [232].

Metformin is believed to have its effects via activation of AMP-activated protein kinase (AMPK) and this has been demonstrated in muscle from humans [233]. Metformin

reduces lipogenesis and increase fatty acid oxidation in rat hepatocytes also in isolated rat muscle, metformin stimulated glucose uptake also by AMPK activation [234] (Figure 4.1). Another study showed that metformin's effects on AMPK were indirectly through reduction of cellular energy metabolism in the mitochondria that produces an increase in ADP:ATP ratio and as a result the activation of AMPK through phosphorylation [235]. Metformin's effects are best understood in the liver where metformin is able to reduce gluconeogenesis and thus fasting plasma glucose levels in type 2 diabetes [236]. Metformin also reduces the lipogenesis by reducing the expression of lipogenic enzymes [234].

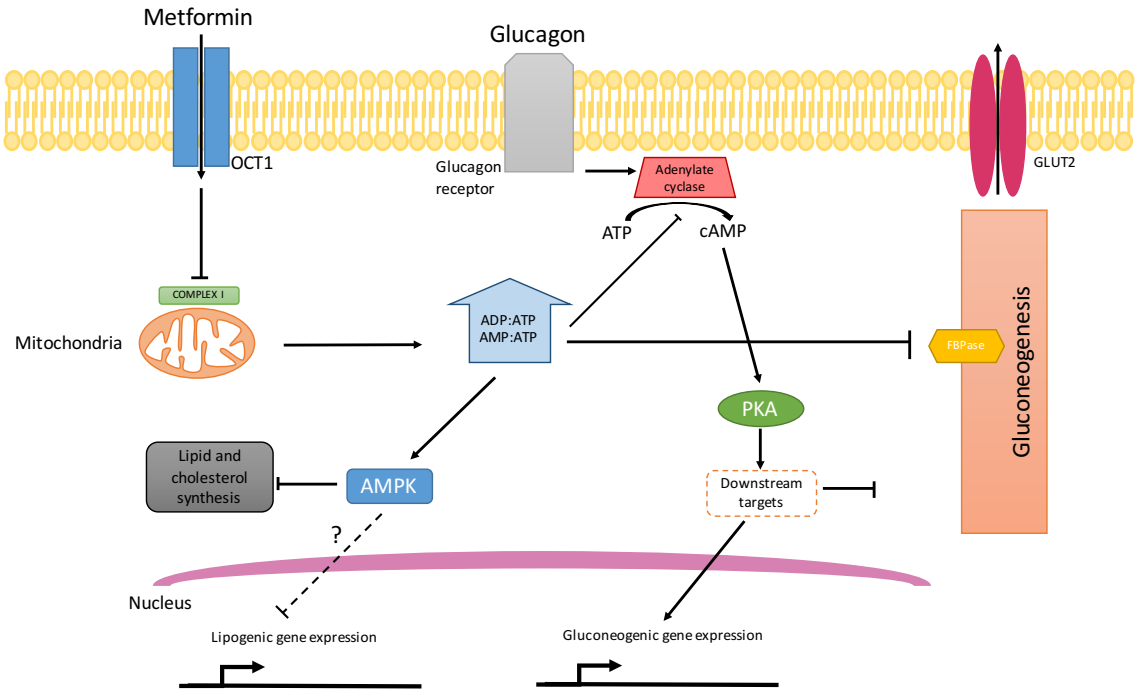

Figure 4.1 Diagram of the metformin effects in glucose and lipid metabolism in liver

Metformin is transported into the cell by OCT1, and its main effect is to inhibit Complex I in the mitochondrial respiratory chain by an unknown mechanism. The reduction in the mitochondrial respiration decreased the energy available in the cells increasing the ADP:ATP and AMP:ATP ratios. Reduction in cell energy activates AMP-activated kinase (AMPK) that inhibit lipid and cholesterol synthesis and might inhibit the expression of lipogenic genes. The decreased in ATP also inhibited the gluconeogenesis directly and the increased in AMP also has been proposed to inhibit the adenylate cyclase and its downstream effect over protein kinase A (PKA) that can also decrease the gluconeogenic genes expression. Modified from [223].

The direct effects of metformin on the placenta are still unclear. The results of the previous chapter suggest metformin does affect the placenta. However, it is not clear whether metformin is acting indirectly modifying the maternal metabolism and signalling and therefore affecting the placenta or is acting directly on placental function affecting the placental signalling pathways by modifying energy levels inside the placenta. Also is possible that metformin is acting directly on the fetus causing modifications in fetal metabolism that could be sensed by the placenta. This study aimed to determine if the effects of metformin observed in the mouse placenta could also be observed in mouse trophoblast culture. If this was the case it would suggest that the effects that I observed in vivo were direct effects of metformin on the mouse placenta.

4.2 AIMS

The initial aims of this chapter were to:

1. Determine the effects of chronic metformin exposure on the expression of potential sensors genes in the mouse trophoblast stem cells
2. Determine the effects of metformin chronic exposure on the expression of genes related to placental function in the mouse trophoblast stem cells

However, after the stem cells became unavailable due to persistent infection in the supplying laboratory it was necessary to focus on HEK 293 cell line.

4.3 METHODS

4.3.1 Cell culture of mouse embryonic fibroblast, trophoblast stem cells and human embryonic cells 293

Mouse embryonic fibroblast (MEF) and trophoblast stem cells (TS) were donated by Dr. Neil Smyth. Human embryonic kidney cells (HEK 293) were donated by Dr. Matt Darley. Cell culture were performed as described in section 2.3. Media and reagents used as described in Table 2.1 and Table 2.2.

4.3.1.1 Mouse embryonic fibroblast cells culture and conditioned medium production

MEF were cultured beforehand in order to obtain a stock of radiated MEF that can act as feeder bed for the TS or to be used to produce conditioned medium. Following a brief description of the production of the radiated MEF stocks and the conditioned medium as described in sections 2.3.2.1 and 2.3.2.2.

MEF were cultured in Dulbecco's Modified Eagle Medium and Ham's F12 (DMEM), containing 10% of FBS, penicillin (100 U/ml) and streptomycin (100 mg/ml) and 10 mM of l-glutamine. All medium and reagents were pre-warmed at 37°C in a water bath before any procedure. Cells were thawed and centrifuged with cell culture media, supernatant was discarded. Cell pellet was re-suspended in DMEM and split in two 1.75 cell culture flasks, with 20 ml of DMEM in each flask. Cells were incubated at controlled conditions (37°C and 5% CO_2 atmosphere). Media was changed every one or two days in order to provide enough nutrients to the cells.

MEF were grown until they reached around 90% confluency (approximately two weeks). Cell media was removed and cells were washed with PBS and detached using 0.05% trypsin/0.2 mM EDTA for 3 min at 37°C. DMEM was added to the mixture and the suspension for the flasks was collected in a 50 ml falcon tube and centrifuged, supernatant was discarded and cell were re-suspended in DMEM and split in eight 1.75 cell cultured flask. Culture process was repeated until 16 flasks of MEF were obtained. After, all the cells were harvested re-suspended in 100 ml of DMEM into two 50 ml

falcon tube. MEF were radiated using a Gammacell 1000 irradiator for 23.6 min at 50G. Radiated cells were centrifuged, re-suspended in 16 ml of freezing medium (Table 2.2) and stored as 1 ml aliquots each, at -80°C until they were needed again.

Condition medium stocks were prepared as described in section 2.3.2.2 after the radiated MEF were obtained. Briefly, 1 ml of radiated MEF were quickly thawed at 37°C and transfer to a 50 ml with 10 ml DMEM media centrifuged and re-suspended in 10 ml of trophoblast stem cells medium (TS medium) that was prepared as described in Table 2.2 (RPMI medium containing 20% of FBS, 100 U/ml of penicillin, 100 mg/ml of streptomycin, 20 mM of l-Glutamine, 1 mM of β-mercaptoethanol and 10 mM of sodium pyruvate). Cells were transferred to a 0.75 cm^2 cell culture flask and incubated at 37° and 5% CO_2 atmosphere. Medium was collected from the culture every 24 h and replaced with fresh TS medium. This process was repeated for three days. Collected medium was stored at -20°C. At the end of the three days cells were discarded and three batches of collected medium were combined, centrifuged for 20 min, cells debris were removed and then the conditioned medias was filtered using a 0.45 μM filter and stored at -20°C in 10 ml aliquots. Aliquots were thawed when necessary and stored at 4°C while they were used. Stocks of conditioned medium were not re-frozen.

4.3.1.2 Trophoblast stem cells culture

TS cells were cultured as described in section 2.3.2.3. All reagents and mediums were warmed at 37°C in a water bath. A vial of radiated MEF was thawed the day before the TS culture and plated in a six well plate (approximately 5 x 10^4 cells per dish). MEF were cultured in TS medium + 1 X of fibroblast growth factor 4 (FGF4) and heparin (TS + F4H) (Table 2.2). The day of the culture a vial of TS cells was thawed and the cells were centrifuged in 10 ml of pre-warmed TS medium. Supernatant was discarded and cells were re-suspended in 12 ml of TS + F4H medium. 2 ml of the suspension were added to the already plated radiated MEF and incubated at 37°C at 5% CO_2 atmosphere. TS cells growth was checked daily and cell medium was replaced every day. When the TS cells were 50% confluent they were harvested and transferred to a cell culture plate with conditioned medium + 1X of FGF4 and heparin.

4.3.1.3 Human embryonic kidney cells culture

HEK 293 cell media was prepared as follows, cultured in Dulbecco's modified Eagle's medium (DMEM, Sigma, United Kingdom) containing 10% of FBS, penicillin (100 U/ml) and streptomycin (100 mg/ml) (Sigma, UK) and 2 mM of l-glutamine (Lonza, UK) (Table 2.2). Cells were cultured as described in section 2.3.3. Briefly, all reagents were pre-warmed at 37°C before the experiment. Cells were thawed when necessary, centrifuged with HEK 293 cell culture medium and the supernant was discarded. The cell pellet was re-suspended in HEK 293 cell culture media and incubated at 37°C in 5% CO2 atmosphere. Medium was changed when necessary and cells were used for experiments when they were ≈80% confluent. Cell media was removed and cells were washed with PBS and detached using 0.05% trypsin/0.2 mM EDTA for 3 min at 37°C. HEK 293 cell media was added to the mixture and the suspension for the flask was collected in a 50 ml falcon tube and centrifuged, supernatant was discarded and cell were re-suspended in K=HEK 293 cell media and counted as described in section 2.3.1.2. All the cells for these experiments were used before passage 10.

4.3.2 Metformin exposure experiment

The metformin exposure experiment was performed in HEK 293 cells as described in section 2.3.5. A 100 mM metformin stock solution was prepared in ultrapure water, filtered and stored at -20°C until its use. Briefly, 100 mM metformin solution was used for this experiment. Reagents and medium were pre-warmed at 37°C in a water bath. 25 X 10^4 cells were plated per well in a 6 well (34.8 mm) cell culture plate. HEK 293 cell media and metformin were added to the cells with metformin at a final concentration of 20 μM per well. In each experiment 3 wells were incubated with metformin and 3 wells with ultrapure water (same that was used to diluted the metformin). The experiment was repeated three times. Concentration of metformin used in this study were decided having in account that in pregnant women metformin levels is plasma are between 7.1 to 11.9 μM [225] and in the mouse model used in the previous chapter, metformin plasma levels in the pregnant mouse were between 9.8 to 17.7 μM and in the amniotic liquid were between 7.3 to 7.8 μM (Personal communication with Dr. Hugh Thomas).

Cells were incubated with metformin for 48 h. After, the medium was removed and 1 ml of RNazol was added to each well, cells were scrapped and the mixture was frozen at -80°C until RNA was extracted.

4.3.3 RNA extraction, reverse transcription and quantitative PCR

Total RNA was extracted from the samples using RNAzol according to the manufactures instructions and as described in section 2.4.1.1. RNA quality and quantity were established using a NanoDrop® 1000 spectrophotometer and gel electrophoresis as described in sections 2.5.1 and 2.5.2 respectively.

Synthesis of cDNA was performed using Promega reagents as described in section 2.6.1. Briefly, 200 ng of sample were mixed with 0.5 µg of random primers to a final volume of 15 µl. The samples were heated at 70°C for 5 min on a Veriti® thermal cycler (Applied Biosystems). After, 50 nmol of triphosphate nucleotides mixture, 25 units of Recombinant RNasin® Ribonuclease Inhibitor, 200 units of M-MLV-RT, 5X M-MLV-RT buffer and water were added to the reaction mixture to a final volume of 25 µl. The mixture was heated at 37°C for 60 min and then 75°C for 10 min. The samples were mixed, centrifuged and diluted to 1:25 with RNA-free water. All the samples and NEC were reverse transcripted in one bach to reduce variation.

Gene expression levels were measured using qPCR according to the methodology described in section 2.6.2. Reactions were performed in a 384 wells plate using a LightCycler® 480 real time PCR system (Roche). In Table 4.1 and Table 4.2 are the sequences of the primers used in this study. Samples, standard curve, controls, NEC and NTC were added in triplicate as follow: 3 ng of cDNA were added to a mixture containing 1 µM of forward and reverse primers and probe and 1X master mix (LightCycler® 480 probes master mix, 2X) to give a final volume of 10 µl.

FTO, TXNIP, LPL, *SIRT1, SIRT3*, amino acid transporters (*SNAT2, TAT1,* and *LAT1*), glucose transporters (*GLUT1* and *GLUT3*) and fatty acid transport protein 2 (*FATP2*) primers and probes were designed using ProbeFinder® version 2.49 (Roche). Gene expression was measured using Universal ProbeLibrary® probes and protocol. The PCR

run protocol was: 1 cycle at 95°C for 5 min, then 45 cycles (95°C for 10 s, 60°C for 30 sec and 72°C for 1 s). Data collection was made at 72°C step, as described in Table 2.3.

Expression of *CLOCK*, *BMAL*, *PER2* and *CRY2* was measured using TaqMan® probes and protocol (Table 2.3). The PCR run protocol was: 1 cycle at 95°C for 10 min, then 40 cycles (95°C for 15 sec and 60°C for 60 s). Data collection was made at 60°C step.

Expression of reference genes *SDHA*, *ATP5B* and *GADPH* was measured using PerfectProbe® probes and protocol (Table 2.3). The PCR run protocol was: 1 cycle at 95°C for 10 min, then 50 cycles (95°C for 15 sec, 50°C for 30 sec and 72°C for 15 sec). Data collection was made at the 72°C step.

Cp values were collected using the second derivate method as described in section 2.6.2.1 and arbitrary RNA concentration were calculated using the standard curve method as described in section 2.6.2.2. Relative gene expression levels were calculated as a ratio between the gene of interest and the geometric mean of the three references genes (*SDHA, ATP5B* and *GADPH*).

4.3.4 Selection of reference genes for HEK 293 cells

The most stable reference genes were selected for the HEK 293 cell line using the geNorm^{TM} reference selection kit (Primerdesign, UK), following the manufacturer instructions and as described in section 2.6.3. The expression of 12 target genes was measured in 16 samples (8 control samples and 8 treatment samples), NEC and NTC. 3.2 ng of cDNA, 1 µM of each forward, reverse primers and 2X master mix (LightCycler® 480 probes master mix, Roche, UK) were added to each well for a final volume of 10 µl. All samples were measured in triplicates. The PCR run protocol was: 1 cycle at 95°C for 10 min, then 50 cycles (95°C for 15 sec, 50°C for 30 sec and 72°C for 15 sec). Data collection was made at the 72°C step. using the run protocol for PerfectProbe® as described in Table 2.3. Cp values were collected using the second derivate method as described in section 2.6.2.1. The results were analysed using qbase^{PLUS} data analysis software (Biogazelle, UK). The information obtained was the average expression stability value (M) of the reference genes that were evaluated,

with a lower M value indicating a higher stability. The GM is used to determine relative gene expression and is calculated using the most stable reference genes. In order to establish how many references genes are necessary a V score is calculated by the software. The V score indicates how the GM changes when another gene is included in the calculation. V score of 0.15 or below indicated that the additional gene had no significant contribution to the GM

Table 4.1 Primers and probes used for potential sensor genes expression

Gene	Gene bank accession number	Primers sequence (5'- 3')	UPL number
FTO	NM_001080432.2	F: CACAACCTCGGTTTAGTTCCA R: AAATATAATCCAAGGTTCCTGTTGAG	53
TXNIP	NM_006472.3	F: AACATCCCTGATACCCCAGA R: TCTCCAATCGGTGATCTTCA	52
SIRT1	NM_012238.4 NM_001142498.1	F: AAATGCTGGCCTAATAGAGTGG R: TGGCAAAAACAGATACTGATTACC	68
SIRT3	NM_012239.5 NM_001017524.2	F: CTTGCTGCATGTGGTTGATT R: CGGTCAAGCTGGCAAAAG	10
CLOCK	NM_004898.3 NM_001267843.1	F: TCACACGGCCGTCTCAGA R: TGGGTGGAGTGCTCGTATCC P: CTTCCTCAACACCAACCAAGATCCCG	-
BMAL	NM_0012286036.1 NM_178427.2 NM_001197325.1 NM_001668.3	F: GGTCCACTGCACAGGCTACA R: TCATCATCTGGGAGGGAAACA P: CAAGGCCTGGCCCCCAGCA	-
CRY2	NM_001127457.2 NM-021117.3	F: GGACAGGATCATTGAGCTGAATG R: TCCATGCGGCTGATGATG P: CAGAAGCCACCCCTTACATACAAGCGC	-
PER2	NM_022817.2	F: TGATGGCAAAATCTGAACACAAC R: CTTTGTGTGTGTCCACTTTCGAA P: CATCTACAAGTGGCTGCAGTAGCGACCA	-

F: Forward primer, R: Reverse primer, P: probe. UPL: Universal probe library.

Table 4.2 Primers and probes used for transport and metabolism related sensor genes expression

Gene	Gene bank accession number	Primers sequence (5'- 3')	UPL number
LPL	NM_00237.2	F: GTGGCCGAGAGTGAGAACA R: GGAAGGAGTAGGTCTTATTTGTGG	13
FATP2 (SLC27A2)	NM_003645.3	F: CATGGCGTGCCTCAATTAC R: TTCGACAGCTGCTTGTAGTTCT	38
GLUT1 (SLC2A1)	NM_006516.2	F: TCTGGCATCAACGCTGTC R: GAGCCAATGGTGGCATACA	66
GLUT3 (SLC2A3)	NM_006931.2	F: GGGCATCGTTGTTGGAAT R: GCTCTTCAGACCCAAGGATG	49
LAT1 (SLC7A5)	NM_003486.5	F: GTGGAAAAACAAGCCAAGT R: GCATGAGCTTCTGACACAGG	25
TAT1 (SLC16A10)	NM_018593.4	F: GGTGTGAAGAAGGTTTATCTACAGG R: AGGGCCCCAAAGATGCTA	6
SNAT2 (SLC38A2)	NM_018976.3	F: CCTATGAAATCTGTACAAAAGATTGG R: TTGTGTACCCAATCCAAAACAA	9

F: Forward primer, R: Reverse primer, P: probe. UPL: Universal probe library.

4.3.5 Statistical analysis

A Mixed model was used to determine the effects of the metformin exposure on the HEK 293 cells gene expression. In this model treatment was used as a fixed factor and experiment number was sued as a random factor. Using this model allowed to determine the effects of the metformin treatment excluding the variation between experiments. A p-value ≤ 0.05 was considered significant.

4.4 RESULTS

4.4.1 Mouse trophoblast stem cell culture

Trophoblast stem cell culture had not previously been established in the placenta laboratory and the method needed to be established and optimised. Initially MEF cells did not grow as well and the protocol was modified increasing the amount of time the cells were incubated and changing half of the media volume every day. Using the new protocol, the MEF started to grow. As established in the protocol they were passaged twice and then collected for radiation. However, the irradiated cells did not survive the freezing process. Figure 4.2 shows the radiated MEF (rMEF) cultured right after the radiation and the radiated MEF cultured after the freezing process.

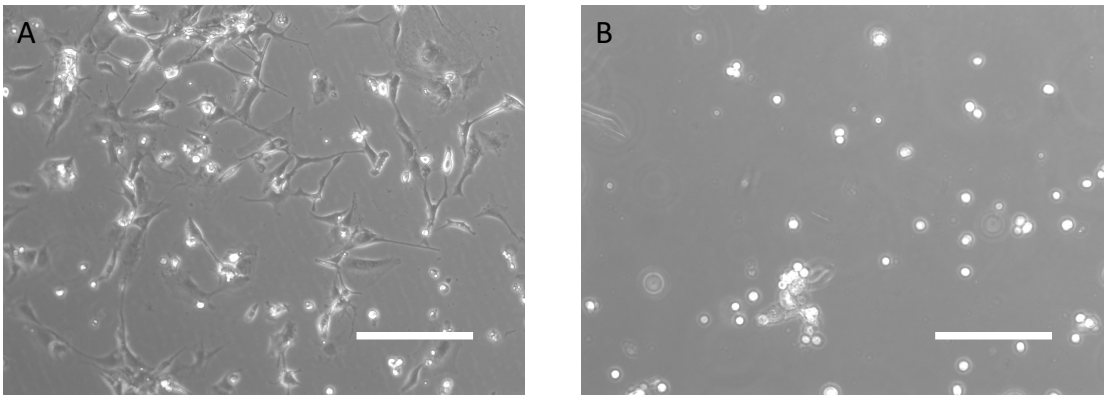

Figure 4.2 Radiated mouse embryonic fibroblast culture

Radiated mouse embryonic fibroblast (rMEF) did not survive the freezing process. A. shows rMEF that were cultured immediately after the irradiation was performed. B. shows rMEF that were irradiated and then frozen down before being cultured. Scale bar 100 μm.

Problems with the cultured of MEF and the production of rMEF were solved by ensuring that the MEF were 90% confluent or more before each passage. This increased the time of incubation days between passages and assure that the MEF survived the irradiation process. Stocks of conditioned medium and rMEF were produced and culture of the trophoblast stem cells (TS) started. The culture of the TS was initially successful while in the presence of MEF (Figure 4.3) but the TS cells did not adapt well when they were moved to the conditioned media culture (Figure 4.3).

At that point the laboratory that provided the TS cells developed a contamination problem with their cell culture and the cells were no longer available. It was decided to do the experiment with HEK 293 cells, an epithelial cell line that was established in the laboratory and which had been shown to have more similar patterns of gene expression to the placenta than the BeWo cell line (Personal communication Claire Simmer and Jane Cleal).

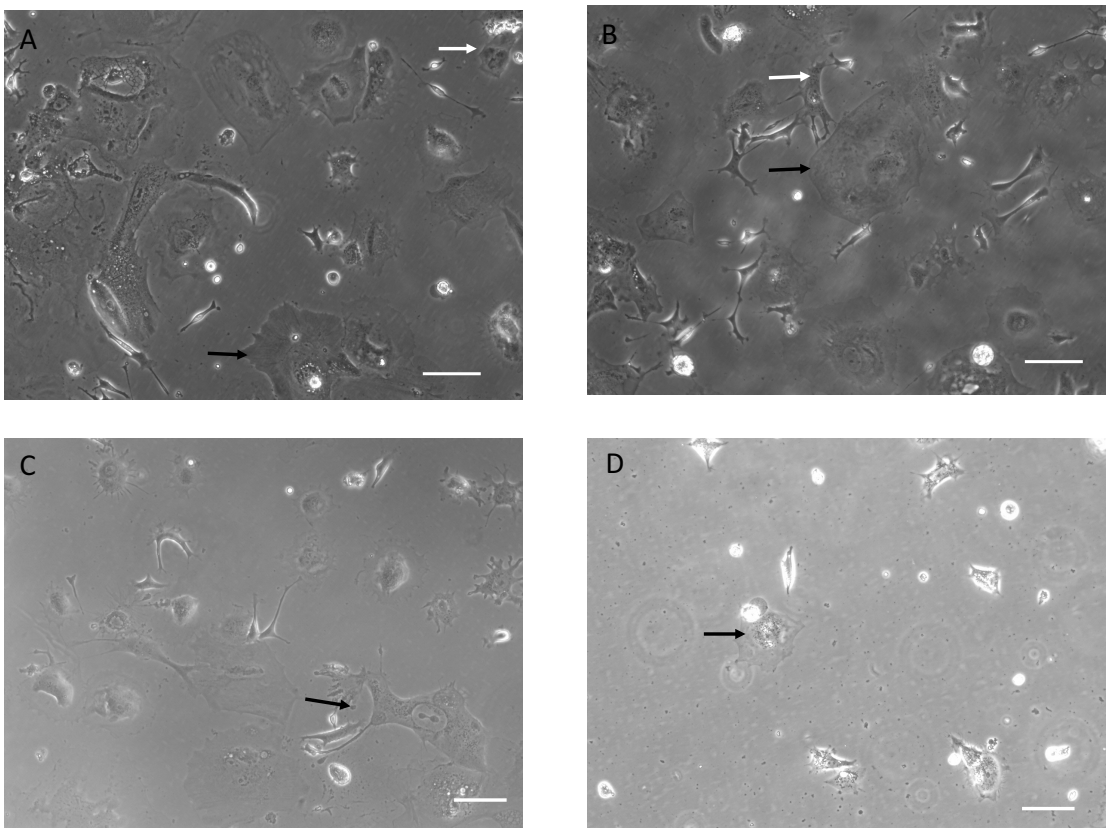

Figure 4.3 Trophoblast stem cells in culture

Trophoblast stem cells (black arrows) were cultured initially in a bed of rMEF (white arrows) (Figure A and B) but they did not survive when they were cultured with conditioned medium alone (figure C and D). Scale bar 100 μm.

4.4.2 Selection of references genes for HEK 293 cell line

The analysis of the geNorm results showed that the references genes: *ATP5B*, *SDHA*, *GADPH* and *ACTB* had a M value under 0.5 that meant that they had the higher stability in the cell line (Figure 4.4). The optimal number of reference genes necessary to normalize gene expression was also determined (Figure 4.5). It was found that 3 references genes were necessary for optimization of gene expression measurements

using HEK 293 cell line. It was decided then that gene expression of HEK 293 cells was going to be calculated as a ratio of the geometric mean of *GADPH*, *SDHA* and *ATP5B*.

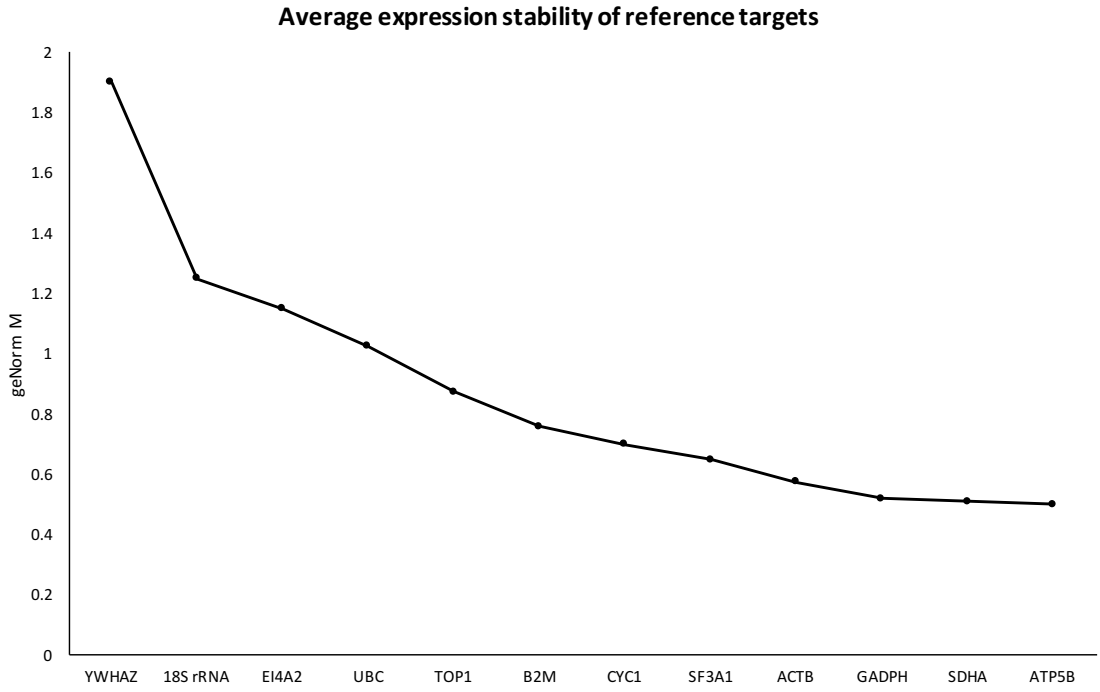

Figure 4.4 Average expression stability of 12 reference genes in the HEK 293 cell line

Average expression stability of reference genes was analysed using geNorm. M value showed the average expression stability of all the genes. Lower values indicated higher stability. N = 16 samples (8 controls, 8 experimental). 12 references genes were evaluated.

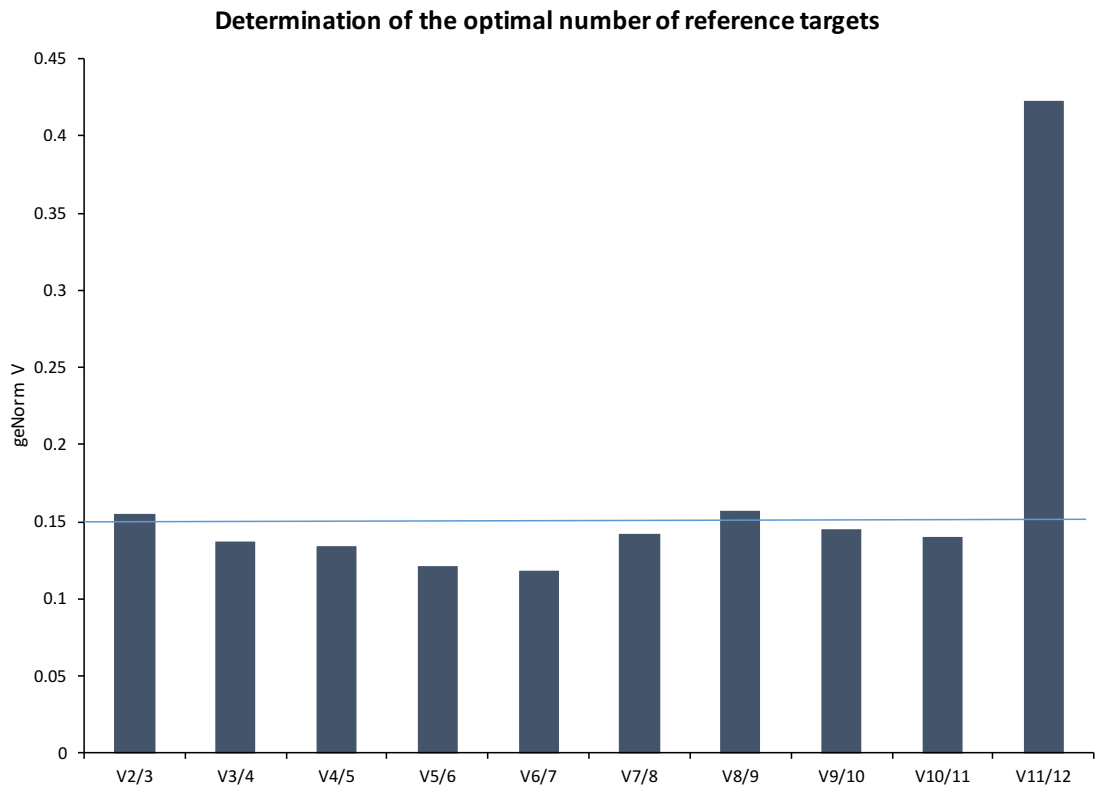

Figure 4.5 Optimal number of references genes for HEK 293 cell line

Optimal number of reference targets was determined by geNorm. V value calculated the different normalization factor when using different numbers of references genes. Number of genes is selected between the V values that are under 0.15. N = 16 samples (8 controls, 8 experimental).

4.4.3 Effect of metformin in HEK 293 gene expression

4.4.3.1 Potential sensor genes

Metformin decreased the expression of most of the potential sensors genes that were measured in this experiment in HEK cells. This included two of the clock genes *BMAL* (p = 0.042) and *CRY2* (p = 0.049) and *TXNIP* (p = 0.015), *FTO* (p = 0.021), *SIRT1* (p = 0.034) and *SIRT3* (p= 0.031). There was a trend for decreased *PER2* expression (p = 0.051)

while *CLOCK* expression was not affected by metformin (Figure 4.6 and Table 4.3).

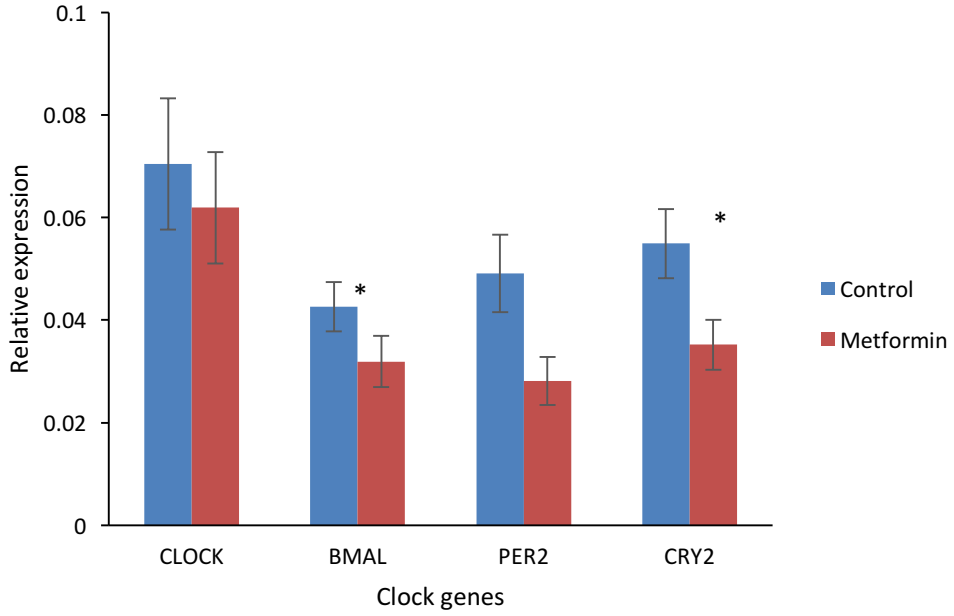

Figure 4.6 Effects of metformin on clock gene expression

*Metformin exposure reduced the expression of BMAL (*p = 0.042) and CRY2 (*p = 0.049) in HEK 293 cells. PER2 (p = 0.051) and CLOCK (p = 0.511) were not affected by metformin. Values are means ± SEM. (n: 3 experiments each with 3 control and 3 metfomin exposed wells).*

Table 4.3 Effects of metformin on potential nutrient sensors gene expression

Gene (mean ± SEM)	Control	Metformin	p-value
TXNIP	0.05 ± 0.01	0.04 ± 0.01	**0.015**
FTO	0.03 ± 0.01	0.02 ± 0.01	**0.021**
SIRT1	0.03 ± 0.02	0.02 ± 0.01	**0.034**
SIRT3	0.04 ± 0.01	0.02 ± 0.01	**0.031**

4.4.3.2 Metabolic and nutrient transport genes in HEK 293 cells

Metformin reduced the expression of *GLUT1* (p = 0.030) in HEK but it did not have an effect in the expression of *GLUT3, FATP, LPL, SNAT2, TAT1, LAT1*, Figure 4.7 and Table 4.4).

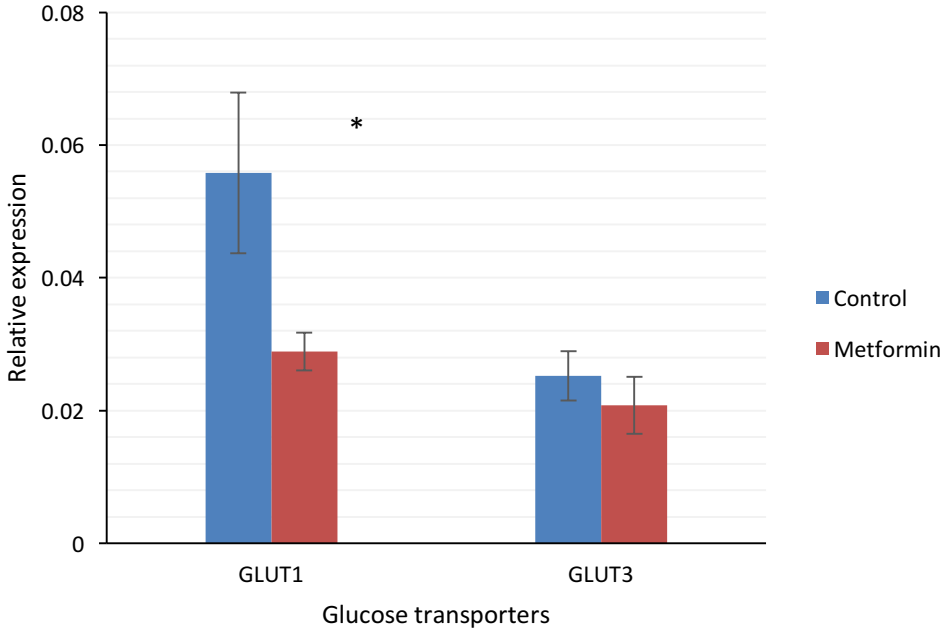

Figure 4.7 Effects of metformin on glucose transporter expression

*Metformin exposure reduced the expression of GLUT1 (*p = 0.030) but did not affect the expression of GLUT3 (p = 0.427) in HEK 293. Values are means ± SEM. (n: 3 experiments each with 3 control and 3 metfomin exposed wells).*

Table 4.4 Effects of metformin on nutrient transporter gene expression

Gene (mean ± SEM)	Control	Metformin	p-value
LPL	0.07 ± 0.03	0.06 ± 0.02	0.119
FATP2	0.03 ± 0.01	0.02 ± 0.01	0.142
SNAT2	0.03 ± 0.01	0.02 ± 0.01	0.135
LAT1	0.04 ± 0.01	0.03 ± 0.02	0.101
TAT1	0.05 ± 0.02	0.03 ± 0.02	**0.039**

4.5 DISCUSSION

Due to technical problems, the primary aim of this chapter, to determine if metformin had the same effect on mouse trophoblast as it did on the placenta *in vivo,* was not able to be achieved. As a result, experiments in this chapter were performed in HEK 293 cells. HEK 293 cells are a transporting epithelial, as the trophoblast, and have been shown to have a more similar gene expression pattern to human trophoblast than the placental cell line BeWO choriocarcinoma cells [188].

This study showed that an *in vitro* chronical exposure of HEK 293 cells to metformin has a direct effect on gene expression, decreasing the expression of many of the putative sensing genes. Metformin affected the gene expression of the circadian clock genes and *GLUT1* as it was found in the previous chapter. This could indicate that metformin has a direct effect on the clock genes and glucose transport.

Metformin also reduced the gene expression of sirtuins and *FTO* in the HEK 293 cells suggesting that these genes could be involved in the metformin sensing mechanism. Gene expression of sirtuins and *FTO* was not modified by metformin exposure in the mouse placenta. This might indicate that during pregnancy metformin has a direct effect on the placenta tissue and it also has an indirect effect over the maternal metabolism that possibly modifies some of the direct effects of metformin (Figure 4.8). Since HEK 293 cells are a suitable epithelial model and they have been tested to be used as a placenta model for nutrient transport function, the modifications in the sensing genes that were found in this study need to be evaluated with more suitable model for placenta. Nevertheless, the result in this study help to understand the direct effect of metformin in the cells.

Alterations of the circadian rhythm affects cell metabolism, but in this study, clock genes were measured at one point and in cells which may not have synchronous clock gene expression. As such this will indicate that there is a change in clock gene expression in the cells, however, it is difficult to interpret and does not show a modification in the circadian cycle. In cell culture, expression of clock genes can be

synchronised using serum shock [237,238]. However, when we attempted this approach in our laboratory, it did not appear to synchronise the expression of clock genes. Previously, it has been described how metformin affects the circadian clock in mouse muscle and liver affecting the overall metabolic process of this tissues [216]. Modification in the circadian clock genes and in the sirtuins due to a fetal exposure to a high fat diet have been described as a potential mechanism of the development of non-alcoholic steatohepatitis [221].

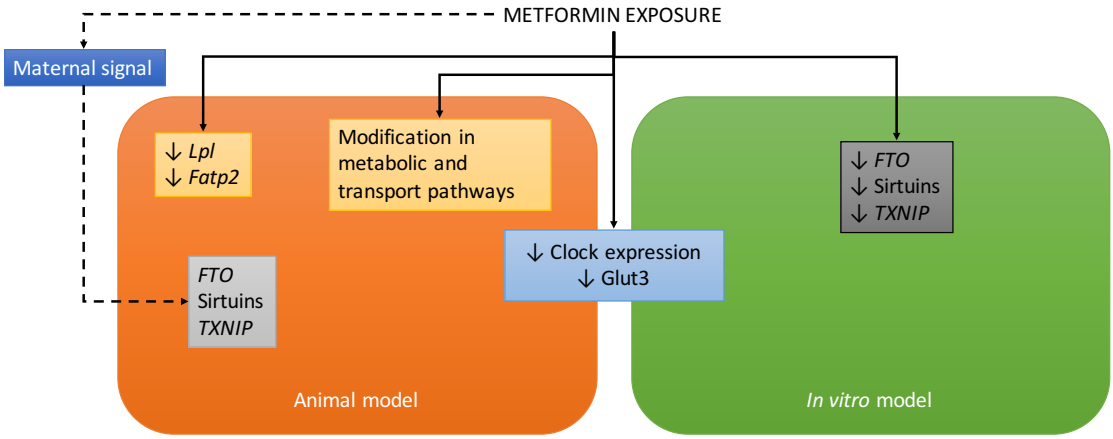

Figure 4.8 Metformin effects in the animal and the *in vitro* model

Metformin exposure has direct (continue lines) and indirect (discontinue lines) effect over cell function. The blue box shows the metformin modifications that were similar in both models, yellow boxes show the modifications in the animal model and black box shows the modification in the in vitro model.

Metformin's effects on sirtuin and *FTO* gene expression can be considered as a possible mechanism of metformin action. Sirtuin genes codified for histone deacetylases and the *FTO* gene codifies for a RNA demethylase. Both genes are involved in the control of gene expression and both of them were reduced by metformin. Sirtuins have been reported to be involved in the control of cell metabolism [169]. SIRT1 is also recognise as an energy sensor since it responds to the NAD/NADH levels [170] and hepatic activity of SIRT1 is supressed in mice with low birth weight [239]. On the other hand, FTO has also been involved as a possible nutrient sensor in the cells [153]. It is possible that metformin is affecting the expression of potential nutrient sensors in the placenta as a mechanism of affecting placental function.

The metformin effects on the gene expression in the *in vitro* model was different to the one found in the mouse placenta, indicating that metformin could be acting both, directly and indirectly over the placenta. The previous chapter showed that metformin affected genes that are part of important pathways involved in cell function but some of the findings were different to the ones in the *in vitro* model. It is possible that the sensing mechanism of metformin in the placenta is different to the one of the HEK 293 cells explaining the different results. It is also possible that the placental modifications of the sensing genes were occurring at the protein levels. Since in these study the effects were evaluated at the gene expression level other changes in cellular pathway could have been missed. Others studies are necessary in order to determine if these genes are acting as sensors in the cells and its importance in the context of placental function and fetal development.

4.5.1 Limitations

A major limitation of this study was that the trophoblast stem cells line was not available due to a contamination in the laboratory that provided this cells. While HEK 293 cells are not a placenta model they have been shown to have more similarities with the placental gene expression than other placenta cell lines such as BeWo. Other placental lines are available but these are derived from extravillous trophoblast cancer cell lines. Because of the unsuitability of these cells and time constraints it was decided to use HEK 293 cells. Another limitation of the study is that the HEK 293 cells are a human cell line making difficult to extrapolate the results between the two models. Nevertheless, the study is able to show similar respond in both models such as the reduction in the clock genes and the *GLUT3*. Experiments in the original cell line that was proposed for this study will help to support the findings of this research.

Another limitation was the target gene approach, which limited the amount of genes that are analysed. For future studies is might be better to use the RNA sequencing as an initial tool that with allow a broader analysis and then decide the target genes based on those results. This approach can be also combined with the knock down of the selected genes in the cells while they are being exposed to metformin. This could

help to understand the involvement of the sensing pathways in metformin effects in the cells.

In the future, establishing a more appropriate placenta cell culture model (TS cells or primary cell culture), is a possibility to help to determine the extent of metformin effects in the placenta. Other approaches such a proteomics analysis of samples previously exposed to metformin could help to answer the question. For example, obtaining human placentas from pregnancies where the mother was treated with metformin in order to determine the effect of this exposure in their function can also be a different approach in order to address this study question.

4.6 CONCLUSION

The technical difficulties encountered in this study mean that it is difficult to draw conclusions relating to the original hypothesis. However, metformin was shown to affect some of the same genes in HEK 293 cells as were affected in the mouse placenta and this is consistent with the idea that metformin is having direct effects on the placenta, assuming these pathways are conserved. Different approaches are necessary in order to determine the extent of metformin effect.

CHAPTER 5 HUMAN PLACENTAL *FTO* GENE EXPRESSION AND BIRTH WEIGHT

5.1 INTRODUCTION

Genetic variants in the fat mass and obesity-associated gene (*FTO*) have been shown to be strongly associated with increased BMI and the risk of developing obesity in both adults and children [152]. Genome-wide association studies have shown that a cluster of single nucleotide polymorphisms (SNPs) in the first intron of the *FTO* gene were highly associated with BMI and obesity in different adult populations [152,240-244]. Placental *FTO* gene expression has been correlated with birth weight [157]. Furthermore, FTO mRNA and protein levels are affected by amino acid availability and it is possible that *FTO* could be acting as a sensor in the placenta [153,154]. The protein that is encoded by *FTO* is an RNA demethylase which may regulate gene expression in the placenta. If it is acting as a nutrient sensor it could potentially regulate gene expression in response to nutrient availability. The aim of this chapter is to determine whether *FTO* gene expression in the placenta is correlated with fetal growth in other human cohorts and with amino acid nutrient transport gene expression in placenta.

Fto homozygous knock out (-/-) mice have increased food intake and oxygen consumption compared with normal mice when corrected for lean mass. In *Fto* heterozygous knock out (+/-) mice, a resistance to high fat diet-induced obesity has been shown [245]. The lack of the *Fto* gene in mice caused postnatal growth retardation and a reduction in adipose tissue. The reduction in body composition in these mice might be caused by an increase in energy expenditure [246]. Another study has shown that overexpression of the *Fto* gene in mice produced increased body weight, fat mass and impaired glucose tolerance in a dose-dependent manner. In these mice, overexpression of *Fto* increased food intake and altered energy expenditure [247]. All these data suggest that *Fto* is involved in the homoeostasis of energy expenditure in mice.

The biological functions of the FTO protein are not well described. The FTO protein is part of the Fe^{2+} and 2-oxoglutarate dependent dioxygenases family. These enzymes are involved in cellular processes such as DNA repair, fatty acid metabolism and post-translational modifications [245]. FTO is able to catalyse the demethylation of 3-

methyltimine and 3-methyluridine that are incorporated into single strand DNA or RNA. N6-methyladenosine (m^6A) is a major substrate for FTO and as m^6A is one of the most commonly modified nucleosides found in RNA it is possible that FTO is affecting the processing of pre-mRNA or other nuclear RNAs [155].

5.1.1 *FTO* and fetal growth

FTO gene expression in human placenta has been associated with increased birth weight and length [157,248]. *FTO* gene expression in the human placenta has also been associated with maternal parity and placental weight. Primiparous pregnancies with smaller placentas expressed more *FTO* per tissue weight and in non-primiparous pregnancies larger placentas expressed more *FTO* per tissue weight [157]. Infants from non-primiparous women showed increased weight and fetal to placental weight ratio, higher cord *IGF-1* levels, and higher *FTO* mRNA expression [157].

In new born babies, the presence of the obesity-related SNPs was not reported to be associated with birth weight, however, it was associated with weight gain and abdominal fat mass at two weeks of age [249]. This could indicate that *FTO* might be acting as a sensor of maternal nutrient status during pregnancy and modifying placental function, while the obesity-related SNP might have an effect on weight gain in postnatal life. In sheep exposed to a nutrient restricted diet (50% of intake) during pregnancy, it has been shown that placental *FTO* expression was not affected by maternal diet. However, they found a positive correlation between placental *FTO* mRNA expression and fetal weight at 110 days gestation [158] again suggesting a role of *FTO* in placental function.

5.1.2 *FTO* genotype and *IRX3*

The obesity-related SNPs in *FTO* have been shown to act as long-range *cis*-regulatory elements and affect the expression of Iroquois homebox 3 (*IRX3)* gene expression [250]. This study showed an association between the obesity-associated SNPs and the promoter region of *IRX3*. This interaction indicated that the obesity-associated polymorphism of the *FTO* gene may actually act via the regulation of *IRX3* and is

mediating functional interactions with *IRX3* in human, mouse and zebrafish genomes. Additionally, they found an increase in *IRX3* expression in human cerebellum associated with 11 SNPs that are related to the increase in body weight. A knock out mouse model for *IRX3* has shown a decrease in body weight compared with the wild type and a decrease in weight gain and adipose tissue even when exposed to high fat diet [250]. These findings raise the possibility that the functional link between *FTO* and obesity is through the control of *IRX3* expression rather than the expression of the *FTO* gene itself [250].

The finding of *IRX3* interactions with the SNPs in *FTO* raises questions about *FTO* function and the involvement of *IRX3* in energy homoeostasis. It appears that *IRX3* is the gene that is involved in the increase of weight associated with the SNPs in *FTO.* However, the association of *IRX3* with weight gain does not explain the relationship between knock down of *FTO* and energy homoeostasis alterations in the cells nor the association between placental *FTO* gene expression and birth weight. Since *FTO* is affected by nutrient availability it is possible that its function in fetal development is through placental function as a nutrient sensor. In this chapter, whether placental *FTO* mRNA expression is associated with birth weight, fetal growth, and childhood growth will be determined. Also, the relationship between placental *FTO* expression and the expression of other genes related to placental function will be evaluated and finally the effect of maternal environment on placental *FTO* expression will be determined.

5.2 AIMS

1. To determine whether the association between placental *FTO* gene expression with birth weight can be replicated in Southampton cohorts.
2. To determine whether placental *FTO* gene expression is different between babies that were small for the gestational age (SGA) compared with children that were normal for the gestational age.
3. To determine whether *FTO* gene expression is correlated with the expression of other genes in the placenta.
4. To determine whether the effects of placental *FTO* expression on fetal growth are related to placental *IRX3* gene expression.

5.3 METHODS

5.3.1 Human placenta sample selection and RNA extraction

Samples collected in the three human cohorts (section 2.1) were used for this study. To study the gene expression of *FTO* across the normal range of birth weights 99 placental samples from the Southampton Women's Survey (SWS) were selected according to the availability of neonatal data and European ethnicity [248]. In addition, 72 placental samples were available from the MAVIDOS cohort in which 32 had been treated with vitamin D and 38 with a placebo during the pregnancy (in 2 samples the information was unknown). To study whether FTO gene expression was affected in SGA pregnancies 80 placental samples were selected from a Cardiff cohort. This included 40 samples from SGA infants (children with custom birth centile below 10th, determined as described in 2.1.4.2) and 40 control samples that were matched for gestational and maternal age.

Total RNA was extracted from the SWS samples by Dr. Jane Cleal and from the MAVIDOS cohort by Dr. Claire Simner. RNA was extracted from samples from both cohorts using the miRNeasy® kit (Qiagen) following the manufacturer instructions and the methodology described in section 2.4.1.2. Total RNA from the samples from the Cardiff cohort was extracted by Dr. Anna Janssen using the Sigma GenElute Mammalian Total RNA Miniprep Kit (Sigma-Aldrich, Dorset, UK) according to the manufacturer's instructions, following the protocol with DNase treatment. Sample quality and concentration of RNA were assessed by gel electrophoresis and using a NanoDrop® as described in sections 2.5.1 and 2.5.2.

5.3.2 Quantitative RT-PCR in SWS and MAVIDOS cohorts

Synthesis of cDNA was performed using Promega reagents as described in section 2.6.1. Briefly, 200 ng of sample were mixed with 0.5 µg of random primers to a final volume of 15 µl. The samples were heated at 70°C for 5 min on a Veriti® thermal cycler (Applied Biosystems). After, 50 nmol of triphosphate nucleotides mixture, 25 units of Recombinant RNasin® Ribonuclease Inhibitor, 200 units of M-MLV-RT, 5X M-MLV-RT

buffer and water were added to the reaction mixture to a final volume of 25 µl. The mixture was heated at 37°C for 60 min and then 75°C for 10 min. The samples were mixed, centrifuged and diluted to 1:25 with RNA-free water. All the samples and NEC were reverse transcripted in one batch to reduce variation.

Placental gene expression for the SWS and MAVIDOS cohort was measured at University of Southampton as described in section 2.6.2. Primers and probes for *FTO* and placental function-related genes were designed using ProbeFinder® version 2.49. Reference genes and *VDR* expression were measured using PerfectProbe® probes and protocol and *FTO* and placental function related gene expression was measured using Universal ProbeLibrary® probes and protocol. Primer sequences are listed in Table 5.1 and Table 5.2.

Reactions were performed in a 384 well plate using a LightCycler® 480 real time PCR system (Roche). Samples, standard curve, controls, NEC and NTC were added in triplicate as follow: 3 ng of cDNA (or equivalent volume of water for NTC) were added to a mixture containing 1 µM of forward and reverse primers, probe and 1X master mix (LightCycler® 480 probes master mix, 2X) for a final volume of 10 µl. Run protocol for Universal ProbeLibrary® probes was: 1 cycle at 95°C for 5 min, then 45 cycles (95°C for 10 sec, 60°C for 30 sec and 72°C for 1 sec). Data collection was made at the 72°C step, as described in Table 2.3. Run protocol for PerfectProbe® probes was: 1 cycle at 95°C for 10 min, then 50 cycles (95°C for 15 sec, 50°C for 30 sec and 72°C for 15 sec). Data collection was made at the 72°C step, as described in Table 2.3.

Cp values were generated using the second derivative method and gene expression values were calculated using a standard curve as described in section 2.6.2.1 and arbitrary RNA concentration were calculated using the standard curve method as described in section 2.6.2.2. *UBC*, *TOP1,* and *YWHAZ* were measured as reference genes and a ratio between the gene of interest and the geometric mean of the three reference genes was used for the analysis. Researchers from the placenta group in Southampton had previously measured placental function-related gene and reference gene expression in the placental samples of the MAVIDOS and SWS cohorts.

5.3.3 Quantitative RT-PCR in Cardiff Cohort

Synthesis of cDNA was performed using Promega reagents as described in section 2.6.1. Briefly, 200 ng of sample were mixed with 0.5 µg of random primers to a final volume of 15 µl. The samples were heated at 70°C for 5 min on a Veriti® thermal cycler (Applied Biosystems). After, 50 nmol of triphosphate nucleotides mixture, 25 units of Recombinant RNasin® Ribonuclease Inhibitor, 200 units of M-MLV-RT, 5X M-MLV-RT buffer and water were added to the reaction mixture to a final volume of 25 µl. The mixture was heated at 37°C for 60 min and then 75°C for 10 min. The samples were mixed, centrifuged and diluted to 1:25 with RNA-free water. All the samples and NEC were reverse transcripted in one batch to reduce variation.

Placental gene expression of *FTO*, *YWHAZ* and y^{+}*LAT2* was measured in the Cardiff cohort at the University of Cardiff. Information about primers and probe sequences are in Table 5.1 and Table 5.2. Quantitative PCR was carried out as described in section 2.6.2, however, the machine available for the measures was a Chromo4 Continuous Fluorescence Detector mounted on a PTC 200 Thermocycler (MJ Research) that used 96 well plates; the samples needed to be plated differently in order to obtain the triplicates per sample. The samples, NTC and NEC were plated individually with a standard curve in duplicate in each plate and three plates were made for each gene. Samples were pipetted into the plates at the same time. Plates were frozen at -20°C until the master mix was added. The master mix for the three plates was prepared in a single tube and added to the first plate, the extra master mix was kept at 4°C until the next plate needed to be prepared. Each plate was gently mixed and centrifuged and the run protocol was set according to the primers and probes that were used (Table 2.3). Ct values were calculated using the threshold method as described in section 2.6.2.1. Standard curve results were used to determine intra and inter variation between runs. Samples relative concentration per plate was calculated using the standard curve method as described in section 2.6.2.2. In order to correct the variation between plates the relative concentration of the samples per plate was averaged, then the average concentration of plates 2 and 3 was divided by the average concentration of plate 1. A ratio for each plate was produced and used to adjust each plate (dividing the samples relative concentration per the ratio per plate). The adjusted relative

concentration was then averaged per sample and that was the value used as relative concentration per gene. *FTO* and *y^+LAT2 mRNA* expression were expressed as the relative concentration of the reference gene *YWHAZ*.

5.3.4 Quantification of miRNA in the SWS samples

As part of an exploratory study, levels of the miRNAs Hsa-miR-143 and hsa-27a3p were measured in the SWS cohort by Dr. Jane Cleal. The quantification of miRNA was performed using miScript II RT® (Qiagen, UK) and miScript SYBR green PCR® (Qiagen, UK). All the miRNAs were quantified following the manufacturer instructions and as described in section 2.7. Briefly, first the miRNA was converted to cDNA using miScript II RT®, 200 ng of total RNA were mixed with 5X miScript HiSpec buffer, 10X miScript nucleics mix, miScript reverse transcriptase mix and ultra-purified water, then the mixture was heated in a Veriti thermal cycler (Applied Biosystems) at 37°C for 60 min and then at 95°C for 10 min. Samples were mixed, centrifuged and diluted 1:10 before storage at -20°C.

After the cDNA was produced, the quantification of specific miRNA was performed using a LightCycler® 480 real time PCR system (Roche) and miScript SYBR green PCR master mix. ≈2 ng of diluted cDNA were added to QuantiTect SYBR green PCR master mix with miScript Universal primer and the specific miScript primer assay (Table 5.3). The run protocol was: 1 cycle (15 min at 95°C), and 45 cycles (15 sec at 94°C, 30 sec at 55C and 30 sec at 70°C) data was set to be collected per cycle at 70°C step. All the samples were measured in triplicates together with no template controls. Cp values were calculated using the second derivative method (section 2.6.2.1). *SNOD61* (small nucleolar RNA) was measured as the reference gene. MiRNA quantification was made using a standard curve as described in section 2.6.2.2.

Table 5.1 Primers and probes for genes related to placental function

Gene	Gene bank accession number	Primers sequence (5'- 3')	UPL number
FTO	NM_001080432.2	F: CACAACCTCGGTTTAGTTCCA R: AAATATAATCCAAGGTTCCTGTTGAG	53
Cubilin	NM_001081	F: GGACAATGTCAGAATAGCTTCGT R: CAGTGGCTAGCAGGGCTTT	10
Megalin	NM_004525.2	F: TTGTTTTGATGCCTCTGATGA R: AGCTAGGCATGTTCGCTCAG	34
RXRα	NM_001291920.1 NM_001291921.1 NM_002957.5	F: ACATGCAGATGGACAAGACG R: TCGAGAGCCCCTTGGAGT	26
VDR	NM_001017535.1 NM_001017536.1 NM_000376.2	F: GACGCCCACCATAAGACCTA R: CCACCATCATTCACACGAACT	N.A.
PMCA1 (ATP2B1)	NM_001001323.1 NM_001682.2	F: CCATAGTATCATTGGGCCTTTC R: CTTCTTCCTCCCCAACAGAA	75
PMCA4 (ATP2B4)	NM_001001396.2 NM_001684.4	F: GCACACCCTGGTGAAAGG R: AGAGCAGGCCCGTCATTT	9
NCX1 (SLC8A1)	NM_001112800.1 NM_001112801.1 NM_001112802.1 NM_001252624.1 NM_021097.2	F: GCCCTTGTGGTTGGGACT R: CCACATTCATCGTCGTCATC	78
DNMT1	NM_001130823.1 NM_001379.2	F: CGATGTGGCGTCTGTGAG R: TGTCCTTGCAGGCTTTACATT	66
TXNIP	NM_006472.3	F: AACATCCCTGATACCCCAGA R: TCTCCAATCGGTGATCTTCA	52
PTHrP	NM_002820.2 NM_198964.1 NM_198965.1 NM_198966.1	F: CTCGGTGGAGGGTCTCAG R: TGGATGGACTTCCCCTTGT	25

F: Forward primer, R: reverse primer. N.A: No aplicable. UPL: Universal probe library

Table 5.2 Primers and probes for amino acid transporter expression

Gene	Gene bank accession number	Primers sequence (5'- 3')	UPL number
LAT1 (SLC7A5)	NM_003486.5	F: GTGGAAAAACAAGCCAAGT R: GCATGAGCTTCTGACACAGG	25
LAT2 (SLC7A8)	NM_182728.1 NM_012244.2	F: TTGCCAATGTCGCTTATGTC R: GGAGCTTCTCTCCAAAAGTCAC	17
LAT3 (SLC43A1)	NM_003627.5 NM_001198810.1	F: GCCCTCATGATTGGCTCTTA R: CCGGCATCGTAGATCAGC	29
LAT4 (SLC43A2)	NM_001284498.1 NM_152346.2	F: ACAAGTATGGCCCGAGGAA R: GCAATCAGCAAGCAGGAAA	3
ASCT1 (SLC1A4)	NM_003038.2	F: TTTGCGACAGCATTTGCTAC R: GCACTTCATCATAGAGGGAAGG	78
ASCT2 (SLC1A5)	NM_005628.2 NM_001145144.1 NM_001145145.1	F: GAGGAATATCACCGGAACCA R: AGGATGTTCATCCCCTCCA	43
y^+LAT1 (SLC7A7)	NM_001126105.1 NM_001126106.1 NM_003982.3	F: ACACTGCCGTGAGAACCTG R: AGGAGAGGAAACCCTTCACC	72
y^+LAT2 (SLC7A6)	NM_001076785.1 NM_003983.4	F: GCTGTGATCCCCCATACCT R: GGCACAGTTCACAAATGTCAG	66
4F2HC (SLC3A2)	NM_001012661.1 NM_001012662.1 NM_002394.4 NM_001012663.1 NM_001012664.1 NM_001013251.1	F: TGGTTCTCCACTCAGGTTGA R: CAGCCAAAACTCCAGAGCAT	49
EAAT2 (SLC1A2)	NM_004171.3	F: AAAATGCTCATTCTCCCTCTAATC R: GCCACTAGCCTTAGCATCCA	78
EAAT3 (SLC1A1)	NM_030674.3 NM_001077484.1	F: AGTTGAATGACCTGGACTTGG R: GCAGATGTGGCCGTGATAC	9
SNAT1 (SLC38A1)	NM_030674.3 NM_001077484.1	F: ATTTTGGGACTCGCCTTTG R: AGCAATGTCACTGAAGTCAAAAGT	47
SNAT4 (SLC38A4)	NM_018018.4 NM_001143824.1	F: TGTTCTGGTCATCCTTGTGC R: AAAACTGCTGGAAGAATAAAAATCAG	29
TAT1 (SLC16A10)	NM_018593.4	F: GGTGTGAAGAAGGTTTATCTACAGG R: AGGGCCCCAAAGATGCTA	6

F: Forward primer, R: reverse primer. UPL: Universal probe library

Table 5.3 Human miRNA primer sequences

miRNA	miRBaseID	Primer sequence
Hsa-miR-27a-3p	MIMAT0000084	5'UUCACAGUGGCUAAGUUCCGC
Hsa-miR-23a-3p	MIMAT0000078	5'AUCACAUUGCCAGGGAUUUCC
Hsa-miR-221-3p	MIMAT0000278	5'AGCUACAUUGUCUGCUGGGUUUC
Hsa-miR-143-3p	MIMAT0000435	5'UGAGAUGAAGCACUGUAGCUC

5.3.5 Fetal, neonatal, childhood and maternal measurements

5.3.5.1 SWS cohort

Before pregnancy and at 11 and 34 weeks of pregnancy, trained research nurses took maternal body size measurements as described in section 2.1.2.1. Height and weight were record and four skinfold thicknesses (triceps, biceps, subscapular and suprailiac) were measured in triplicate to the nearest 0.1 mm on the non-dominant side using Harpenden skinfold callipers. Mid upper arm circumference was also measured using a tape measure. Body mass index was calculated using the formula: weight/height^2 (Units: kg/m^2). Fat mass was estimated from skinfold thickness measurements using the method of Durnin & Womersley [190]. Arm muscle area was derived using a formula ((mid arm circumference – π x triceps skinfold thickness)^2/4π) - 6.5).

Fetal size and children anthropometric measures were included in the analysis when available. Following the time when the measures were taken is the number of samples that have the information for this study. Fetal, neonatal and child measures were done as described in section 2.1.2.3). Fetal size was measured at 11 (n = 66), 19 (n = 91) and 34 weeks (n = 98) of gestation by a research sonographer. Head circumference (HC), abdominal circumference (AC), femur length (FL) and crown-to-rump length (CRL) were measured using a high-resolution ultrasound system (Acuson 128 XP, Aspen and Sequoia).

Shortly after delivery, research midwives recorded neonatal anthropometric measures (birth weight, HC, AC, mid-upper arm circumference and CRL). Within 2 weeks of birth, a subset of infants had body composition measurements made using dual X-ray

absorptiometry (DXA) with a Lunar DPX-L machine. Fat mass, fat-free mass and bone indices (bone area, bone mass content and bone mass density) were calculated from the whole-body scan by using paediatric small scan mode, v 4.7c (paediatric software). Children were followed up at 4 (n = 42) and 6 (n = 44) years of age anthropometric measures were repeated. Height was measured using a Leicester height measurer and weight was measured using Seca calibrated digital scales. Whole body composition DXA was measured using a Hologic Discovery Instrument and paediatric scan mode software. Anthropometric data collection was carried out by the SWS Study Group [191].

Plasma phospholipid fatty acids were measured using gas chromatography in SWS plasma samples by Dr. Charlene Sibbons at 11 (early pregnancy) and 34 (late pregnancy) weeks of pregnancy as described in section 2.1.2.2. Briefly, Fatty acid were analysed in plasma phosphatidylcholine (PC), in order to do that and initially lipid extraction was made using chloroform:methanol (2:1 vol/vol) and butylated hydroxytoluene (50 mg/L) as an antioxidant. Afterwards, plasma lipid fractions were separated and isolated by solid phase extraction on aminopropylsilica cartridges. Cholesterol esters and triacylglycerols were first eluted with chloroform, then PC, the major plasma phospholipid, was eluted with chloroform:methanol (60:40, vol/vol). The PC fraction was dried under nitrogen and dissolved in toluene. Fatty acid methyl esters (FAME) were formed by incubation with methanol containing 2% (vol/vol) H_2SO_4 at 50°C for 2 h. After allowing the tubes to cool, samples were neutralised with a solution of 0.25 M $KHCO_3$ and 0.5 M K_2CO_3. FAME were extracted into hexane, dried down, dissolved in a small volume of hexane, and separated by gas chromatography. Gas chromatography was performed on a Hewlett-Packard 6890 gas chromatograph fitted with a BPX-70 column (30 m x 0.22 mm x 0.25 μm). The inlet temperature was 300°C. Oven temperature was initially 115°C and this was maintained for 2 min post-injection. Then the oven temperature was programmed to increase to 200°C at the rate of 10°C/min, to hold at 200°C for 16 min, and then to increase to 240°C at the rate of 60°C/min and then to hold at 240°C for 2 min. Total run time was just over 29 min. Helium was used as the carrier gas. FAME were detected by a flame ionisation detector held at a temperature of 300°C. The instrument was controlled by and data collected using HPChemStation (Hewlett Packard, Waldbronn, Germany). FAME were

identified by comparison of retention times with those of authentic standards run previously.

FTO obesity-related SNPs r9939609 and rs142085 were measured in DNA extracted from SWS cord blood (n = 99). Genotyping was performed by Kbiosciences (Hoddesdon, Herts, UK) using a custom SNP panel. SNP information was provided by Dr. Shelia Barton [248].

5.3.5.2 MAVIDOS cohort

Neonatal anthropometry, including birth weight, crown-to-heel length, subscapular and triceps skinfold thicknesses, mid-upper arm, and head and abdominal circumference were measured by the researcher nurses as described in section 2.1.3. Neonatal anthropometry was measured and neonatal DXA was carried out using a Hologic Discovery Instrument for fat mass, lean mass and bone index.

5.3.5.3 Cardiff cohort

Obstetric covariants such as parity, previous stillbirths, low weight birth or macrosomic pregnancies and information about the current pregnancy such as maternal smoking, alcohol consumption and drug use before pregnancy, were collected from the participant's medical record as described in section 2.1.4.1. Neonatal measures (birth weight, head circumference, Apgar) were recorded as described in section 2.1.4.2. Custom birth weight centiles were calculated based on maternal height, weight, parity and ethnicity as well as infant birth weight, gestational age and gender using the GROW bulk centile calculator (UK), version 6.7.5. Infants with custom birth weight below the 10th percentile were considered SGA.

5.3.6 qPCR measurement of placental *IRX3* mRNA expression

IRX3 primers and probes for qPCR were designed using ProbeFinder® version 2.49 (Table 5.4 - *IRX3*, gene bank accession number NM_024336.2). The validation of *IRX3* mRNA expression was made using three human placental samples and a human lung sample. Synthesis of cDNA was performed as described in section 2.6.1. Placental and

pulmonary gene expression was measured as described in section 2.6.2. The protocol used was Universal ProbeLibrary® protocol. Reactions were performed in triplicate in a 384 well plate using a LightCycler® 480 real time PCR system (Roche). Samples, NEC and NTC were added as follow: 3 ng of cDNA (or equivalent volume of water for NTC) were added to a mixture containing 1 μM of forward and reverse primers, probe and 1X master mix (LightCycler® 480 probes master mix, 2X) for a final volume of 10 μl. Run protocol for Universal ProbeLibrary® probes was: 1 cycle at 95°C for 5 min, then 45 cycles (95°C for 10 sec, 60°C for 30 sec and 72°C for 1 sec). Data collection was made at the 72°C step, as described in Table 2.3.

In order to confirm that the qRT-PCR assays were working a second qPCR experiment was carried out using a lung sample of a higher RNA concentration in the RT-PCR reaction (0.2 μg/μl), the cDNA was synthesised as described in section 2.6.1. The cDNA obtained from this process was then diluted four times in order to check the linearity of the assay and a qRT-PCR was performed as described above.

Due to a low signal in the qPCR measurement of *IRX3* in placental samples, a non-quantitative PCR was carried out using one placental sample and another tissue where *IRX3* had been reported to be expressed [250] (brain or liver according to availability) as the control. Briefly, 200 μg of cDNA (placenta or lung), 1 μM of forward and reverse primers, RNase-free water and master mix were added to an tube for a final volume of 25 μl. The run protocol was: 1 cycle of 94°C per 3 min; 40 cycles of 94°C per 3 sec, X per 30 sec and 70°C per 30 sec; 1 cycle of 72°C per 7 min and then 4°C continuous. The X (annealing temperature) was set according to the average melting temperature per set of primers (Table 5.4). The expression of *IRX3* mRNA was confirmed in terms of the size and presence of a PCR product as determined using agarose gel electrophoresis and visualisation under UV light.

Table 5.4 *IRX3* primers sequences

Set number	Primers sequence, 5'-/3'	UPL number	Melting temperature	Product size (bp)
1	F: CTCTCCCTGCTGGGCTCT	70, 62	67	129
	R: CAAGGCACTACAGCGATCTG		55	
2	F: AAAAGTTACTCAAGACAGCTTTCCA	57	36	92
	R: GGATGAGGAGAGAGCCGATA		55	
3	F: CGTGCTCTCGTCCGTGTA	4	61	144
	R: GGGCTGTCCTTCAGCTCATA		55	

F: Forward primer, R: reverse primer

5.3.7 Statistical analysis

Statistical analysis, such as normality test, correlations, and linear regressions were calculated using SPSS V 22.0 (IBM, Portsmouth UK). Normal distribution was determined for all the variables using skewness statistics and histograms. Variables were logarithmic transformed when necessary and the distribution was assessed again. For all statistical test, a p-value ≤ 0.05 was considered significant.

5.3.7.1 SWS cohort

Due to data confidentially issues, Dr. Jane Cleal and Dr. Sheila Barton performed analysis of the data in the SWS cohort. Summary data are presented as mean (SD) or median (interquartile range) depending on whether the data were normally distributed. An adjustment was made for fetal sex as gene expression was higher in placentas from male fetuses than in placentas from female foetuses [202] in the correlation analysis between mRNA placental expression and maternal anthropometric measures. Pearson's correlation coefficient was used to determine partial correlation adjusted for sex and gestational age between placental mRNA levels and fetal and neonatal measures. Neonatal measures were also adjusted by mode of delivery.

Dr. Sheila Barton performed the genotype analysis of *FTO* expression *vs FTO* obesity-related SNPs rs9939609 or rs142085.

5.3.7.2 MAVIDOS cohort

The analysis of the Mavidos placental gene expression and anthropometric measures was performed by S. D'Angelo (MRC, LEU, Southampton) due to confidentially issues. The association between placental *FTO* expression and birth weight or head circumference was determined using a linear regression with the analysis adjusted for sex and gestational age. Person's correlation coefficient was used to determine associations between placental *FTO* gene expression and placental function-related gene expression.

5.3.7.3 Cardiff cohort

The distribution of the data was analysed for normality and when necessary the gene expression was logarithmically transformed. Summary data are presented as mean (SD) or median (interquartile range) depending on whether the data were normally distributed. A t-test was used to determine the differences between the control group and the SGA group in the variables of interest. Pearson's correlation coefficient was calculated to determine the correlation between expression of placental genes and between placental gene expression and custom centile birth weight. Partial correlation was used to determine the correlation between neonatal head circumference and placental gene expression adjusted for sex and gestational age. All the correlations were determined for the complete cohort and for each group (SGA and control).

5.4 RESULTS

5.4.1 SWS cohort

5.4.1.1 FTO gene expression and fetal, neonatal and childhood growth

Placental *FTO* mRNA expression was positively correlated with birth weight (Figure 5.1), head circumference and neonatal fat mass but not with other measures of neonatal anthropometry and body composition (Table 5.5).

There was a positive correlation between placental *FTO* gene expression and several fetal measures during the pregnancy (Table 5.6). Placental *FTO* mRNA expression was correlated with fetal AC, crown to heel length and biparietal diameter (BPD) at 11 weeks of pregnancy; the BPD correlation with placental *FTO* expression was also found at 19 weeks of pregnancy. At 34 weeks of pregnancy, placental *FTO* expression was correlated with AC, head circumference, and BPD. No other significant correlations were found between *FTO* expression and fetal growth (Table 5.6).

Placental *FTO* gene expression was not correlated with any body composition measures in the children at 4 or 6 years of age (Table 5.7).

5.4.1.2 Placental FTO gene expression and FTO genotype of children from the SWS cohort

Placental *FTO* mRNA expression was not affected by the presence of the risk alleles in two of the main obesity-related SNPs (Figure 5.2).

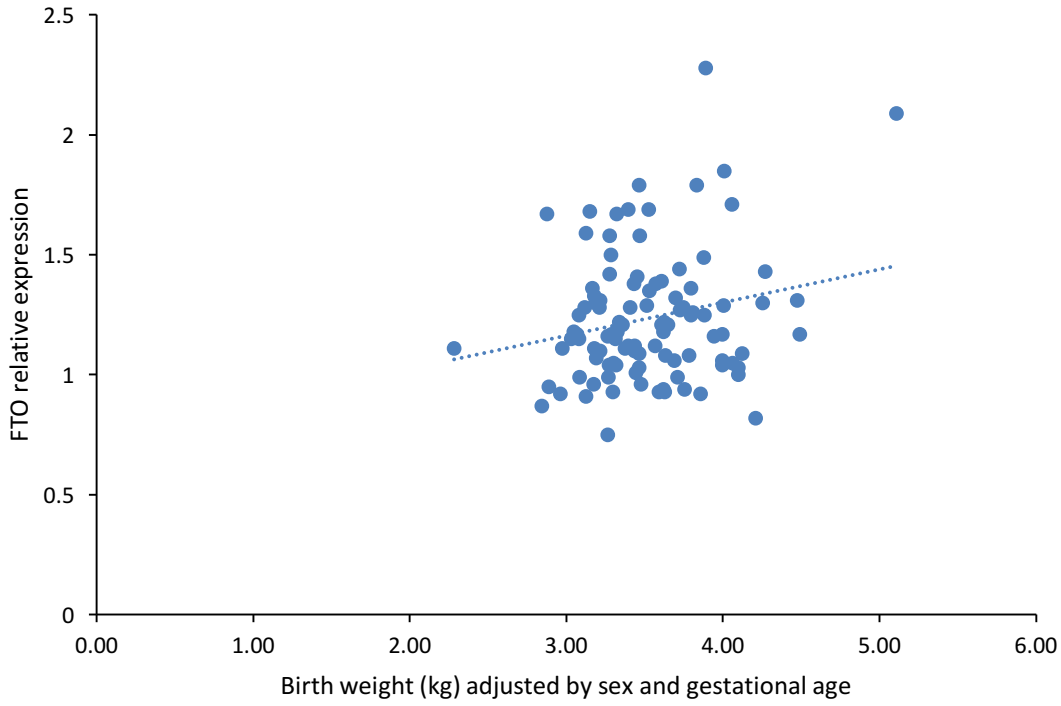

Figure 5.1 Correlation between placental *FTO* mRNA expression and birth weight in the SWS cohort

Term placental FTO gene expression was positively associated with birth weight adjusted for sex and gestational age. (r = 0.204, n = 99, p = 0.046).

Table 5.5 Correlation between placental *FTO* gene expression and postnatal measures in the SWS cohort

Neonatal Variables (n = 99)	r	p*	n
Birth weight (g)	**0.204**	**0.046**	99
Head circumference (cm)	**0.276**	**0.006**	99
Abdominal circumference (cm)	0.165	0.107	99
Crown-heel length (cm)	0.152	0.139	94
Bone mineral content (BMC) (g)	0.145	0.154	96
Neonatal lean mass (g)	0.113	0.268	96
Neonatal fat mass (g)	**0.290**	**0.004**	96

Data was adjusted for sex, gestational age and mode of delivery. *In bold $p \leq 0.05$

Table 5.6 Correlation between placental *FTO* gene expression and fetal growth at 11, 19 and 34 weeks of pregnancy in the SWS cohort

Fetal scan	11 weeks			19 weeks			34 weeks		
Royston (z-score)	r	p*	n	r	p*	n	r	p*	n
Abdominal circumference	**0.345**	**0.023**	44	0.179	0.091	**91**	**0.242**	**0.017**	**98**
Crown to heel length	**0.289**	**0.020**	66	N.A	N.A		N.A	N.A	
Head circumference	0.205	0.172	47	0.180	0.090	91	**0.324**	**0.001**	98
Femur length	N.A	N.A		0.082	0.546	55	0.038	0.776	56
Biparietal diameter	**0.359**	**0.014**	47	**0.212**	**0.045**	91	**0.241**	**0.018**	97

Data were adjusted for sex. N.A. Not available. *In bold $p \leq 0.05$

Table 5.7 Correlation between placental *FTO* gene expression and body size at 4 and 6 years of age in the SWS cohort

Child Variables	4 years (n = 42)		6 years (n = 44)	
	r	p	r	p
Weight (g)	0.125	0.369	0.031	0.829
Total fat mass (kg)	0.064	0.678	-0.036	0.810
Total lean mass (kg)	0.178	0.247	0.067	0.660

Data was adjusted for sex.

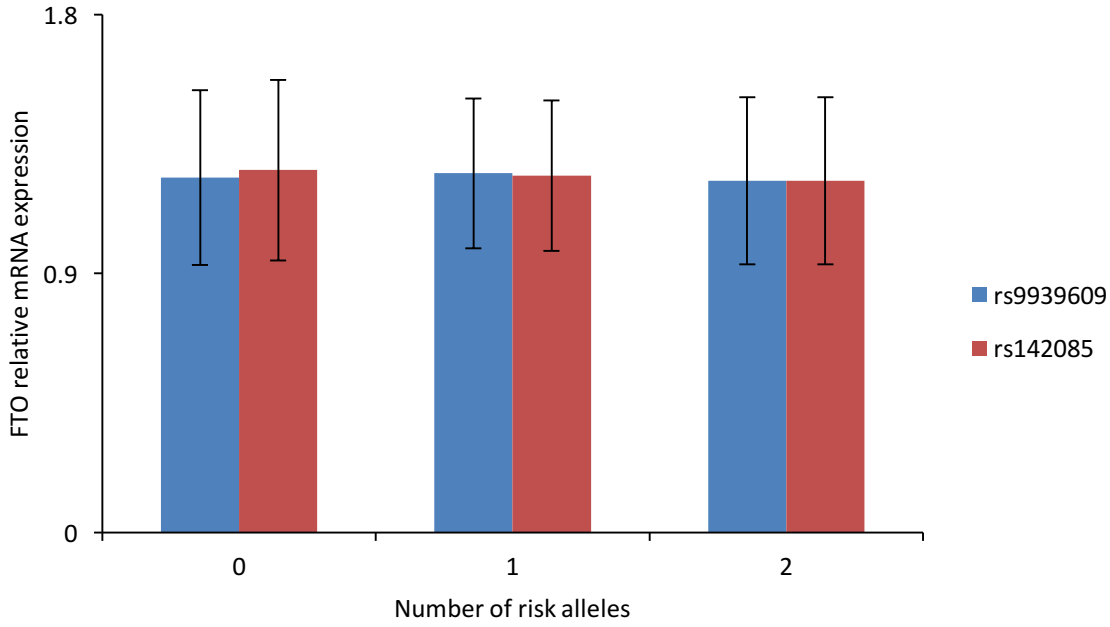

Figure 5.2 Obesity-related SNP effect on placental *FTO* expression in the SWS cohort

Term placental FTO gene expression is not affected by the presence of the obesity-associated SNPs in FTO (ANOVA, p = 0.14). rs9939609 and rs142085: main obesity-associated SNPs in FTO, (n: 99).

5.4.1.3 Correlations between the placental expression of FTO and genes related to placental function and specific miRNA expression in the SWS cohort

There was a positive correlation between placental mRNA levels of *FTO* and the amino acid transporters *ASCT2*, *EAAT2*, and *y^+LAT2*. No other correlations were found between placental *FTO* mRNA levels and the other amino acid transporters studied (Table 5.8).

FTO expression was negatively correlated with the expression of Vitamin D receptor (*VDR*) and retinoid X receptor alpha (*RXRα*), no correlation was found between *FTO* and *Cubilin*, *Megalin, DNMT1* and *PMCA1* (Table 5.9).

Placental *FTO* mRNA expression was negatively correlated with the placental expression of hsa-miR-27a-3p (Figure 5.3), but not with the expression of hsa-miR-143-3p (r = 0.01, p = 0.9). Expression of hsa-miR-27p-3p was also correlated with the placental expression of *EAAT2, LAT2* and *4F2HC* in the SWS cohort (Table 5.10).

5.4.1.4 Placental FTO gene expression and maternal body size and plasma phospholipid fatty acid in the SWS

There was no correlation between maternal body size and placental *FTO* gene expression (Table 5.11).

Higher placental *FTO* expression was associated with lower maternal 11-weeks plasma phospholipid concentrations of Eicosadienoic acid (20:2n-6), Dihomo-g-linolenic acid (20:3n-6), Eicosatetraenoic acid (20:4n-3) and Nervonic acid (24:1n-9), and with higher maternal 32-weeks plasma concentrations of Docosapentaenoic acid (22:5n-3) and Docosahexaenoic acid (22:6n-3). No other correlations were found between *FTO* gene expression and maternal plasma phospholipid fatty acid (Table 5.12).

Table 5.8 Correlation between *FTO* and amino acid transporter gene expression in placenta in the SWS cohort

Amino acid transporter	r	p*	n
TAT1	0.187	0.060	102
LAT1	0.170	0.087	102
LAT2	-0.025	0.804	101
LAT3	0.120	0.229	102
LAT4	-0.001	0.989	102
y^+LAT1	0.120	0.231	102
y^+LAT2	**0.37**	**0.002**	**99**
SNAT1	0.029	0.773	102
SNAT2	0.178	0.073	102
SNAT4	0.136	0.171	102
ASCT1	0.009	0.929	102
ASCT2	**0.286**	**0.004**	**99**
4F2HC	-0.029	0.769	102
EAAT2	**0.22**	**0.027**	**99**
EAAT3	0.065	0.515	102

Data was adjusted for sex and gestational age. *In bold $p \leq 0.05$

Table 5.9 Correlations between *FTO* and placental function-related gene expression in the SWS cohort

Gene	r	p*	n
Cubilin	0.030	0.767	100
DNMT1	0.073	0.471	100
VDR	**-0.291**	**0.003**	100
Megalin	0.137	0.176	100
RXRα	**-0.199**	**0.048**	100
PMCA1	0.191	0.057	100

DNMT1: DNA (cytosine-5-) methyltransferase 1, VDR: Vitamin D (1,25 dihydroxy vitamin D3) receptor, RXRα: retinoid X receptor alpha and PMCA1: ATPase plasma membrane Ca2+ transporting 1. *In bold $p \leq 0.05$

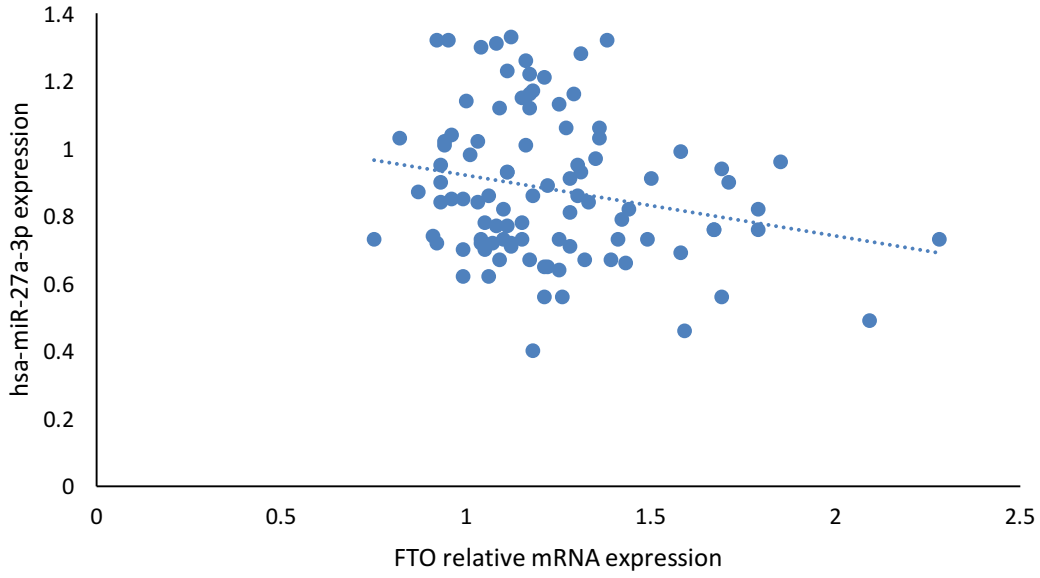

Figure 5.3 Correlation between FTO mRNA expression and hsa-miR-27a-3p in SWS placentas

Term placental FTO mRNA expression was correlated with placental hsa-miR-27a-3p expression (r = -0.21, p = 0.036) in the SWS cohort, (n: 99).

Table 5.10 Correlation between amino acid transporter gene expression and hsa-miR-27a-3p in SWS placentas

Amino acid transporters	r	p*
SNAT1	0.013	0.899
SNAT2	-0.006	0.953
SNAT4	-0.106	0.295
ASCT1	-0.162	0.108
ASCT2	-0.016	0.874
y^+LAT1	0.054	0.594
y^+LAT2	-0.134	0.185
EAAT2	**-0.23**	**0.019**
EAAT3	0.003	0.980
LAT1	0.154	0.126
LAT2	**0.366**	**<0.001**
LAT3	-0.069	0.494
LAT4	0.157	0.120
4F2HC	**0.312**	**0.002**
TAT1	-0.172	0.87

*In bold $p \leq 0.05$

Table 5.11 Correlation between placental *FTO* gene expression and maternal body size measures before pregnancy in the SWS cohort

Maternal body size measures (n = 99)	Initial visit	
	r	p
Log BMI	-0.121	0.230
Log Sum of skinfolds (mm)	-0.027	0.793
Log fat mass (Kg)	-0.061	0.545
Log ratio of subscapular/triceps	-0.167	0.98
Log mid-upper arm circumference (cm)	-0.063	0.533
Log arm muscle area	-0.138	0.170

BMI: Body mass index

Table 5.12 Correlations between placental *FTO* gene expression and maternal plasma phospholipid fatty acid concentration during early (11 weeks) and late (32 weeks) pregnancy in the SWS cohort

Fatty acid (ug/ml)	Early pregnancy (11 weeks) (n = 41)		Late pregnancy (32 weeks) (n = 90)	
	r	p*	r	p*
Fatty acid: 14:0 (myristic acid)	-0.175	0.273	0.031	0.774
Fatty acid: 16:0 (palmitic acid)	-0.231	0.147	-0.008	0.941
Fatty acid: 16:1n-7 (palmitoleic acid)	-0.272	0.085	-0.059	0.578
Fatty acid: 18:0 (stearic acid)	-0.236	0.138	0.057	0.593
Fatty acid: 18:1n-9 (oleic acid)	-0.230	0.148	-0.033	0.757
Fatty acid: 18:1n-7 (cis-vaccenic acid)	-0.127	0.429	0.017	0.870
Fatty acid: 18:2n-6 (linoleic acid)	-0.203	0.203	-0.047	0.658
Fatty acid: 18:3n-6 (gamma linolenic acid)	-0.189	0.237	0.040	0.711
Fatty acid: 18:3n-3 (alpha linolenic acid)	-0.167	0.295	-0.025	0.815
Fatty acid: 20:0 (arachidic acid)	-0.223	0.167	0.057	0.591
Fatty acid: 20:1n-9 (eicosenoic acid)	-0.247	0.119	0.043	0.688
Fatty acid: 20:2n-6 (eicosadienoic acid)	**-0.310**	**0.049**	0.009	0.931
Fatty acid: 20:3n-6 (dihomo-γ-linolenic acid)	**-0.355**	**0.023**	-0.093	0.382
Fatty acid: 20:4n-6 (arachidonic acid)	-0.169	0.292	0.056	0.597
Fatty acid: 22:0 (behenic acid)	-0.162	0.311	-0.026	0.808
Fatty acid: 20:4n-3 (eicosatetraenoic acid)	**-0.338**	**0.033**	-0.031	0.773
Fatty acid: 20:5n-3 (eicosapentaenoic acid)	-0.033	0.836	0.165	0.120
Fatty acid: 22:4n-6 (adrenic acid)	-0.260	0.101	-0.004	0.972
Fatty acid: 22:5n-6 (osbond acid)	-0.173	0.279	0.071	0.509
Fatty acid: 24:1n-9 (nervonic acid)	**-0.314**	**0.045**	0.054	0.612
Fatty acid: 22:5n-3 (docosapentaenoic acid)	-0.028	0.863	**0.265**	**0.012**
Fatty acid: 22:6n-3 (docosahexaenoic acid)	0.039	0.810	**0.255**	**0.015**
Fatty acid: Total	-0.244	0.124	0.008	0.941

Data was adjusted for sex. *In bold $p \leq 0.05$

5.4.2 MAVIDOS cohort

5.4.2.1 Placental FTO gene expression and neonatal measures

Linear regression model using birth weight or head circumference as independent variable and placental FTO mRNA expression as dependent variable showed that birth weight and head circumference were not correlated with placental *FTO* mRNA expression in the MAVIDOS cohort (Table 5.13).

5.4.2.2 FTO placental expression and placental function related genes expression in MAVIDOS cohort

Placental *FTO* mRNA expression was positively correlated with the mRNA expression of several amino acid transporters: y^+*LAT2, ASCT2, LAT1, LAT3, LAT4* and *SNAT1* (Table 5.14).

Placental *FTO* expression was also correlated with the expression of placental function related genes such as: genes related with vitamin D metabolism: cubilin, megalin and *RXR*α, calcium transporters: NCX1, PMCA1 and PMCA4, DNA methyltransferase 1 (DNMT1) and genes involved in the metabolism of thioredoxin (*TXNIP*), (Table 5.15).

Table 5.13 Linear regression model between birth weight or head circumference and placental *FTO* mRNA expression in the MAVIDOS cohort

	β (95% IC)	p-value
Birth weight	-135.1 (-636.7 – 366.4)	0.593
Head circumference	0.12 (-1.07 – 1.31)	0.840

Data was adjusted for sex and gestational age

Table 5.14 Correlations between *FTO* and amino acid transporter gene expression in placentas from the MAVIDOS cohort

Amino acid transporters (n = 74)	r	p*
ASCT1	0.144	0.226
y$^+$LAT2	**0.355**	**0.002**
ASCT2	**0.397**	**0.001**
LAT1	**0.240**	**0.043**
LAT3	**0.466**	**<0.001**
LAT4	**0.314**	**0.007**
SNAT1	**0.389**	**0.001**
TAT1	0.218	0.066

*In bold $p \leq 0.05$

Table 5.15 Correlations between *FTO* and function related gene expression in placentas from the MAVIDOS cohort

Gene (n = 74)	r	p*
Cubilin	**0.297**	**0.011**
Megalin	**0.279**	**0.018**
RXRα	**0.346**	**0.003**
VDR	0.113	0.346
NCX1	**0.395**	**0.001**
PMCA1	**0.258**	**0.029**
PMCA4	**0.521**	**<0.001**
PTHrP	0.204	0.086
DNMT1	**0.386**	**0.001**
TXNIP	**0.521**	**<0.001**
VEGF	0.225	0.057

DNMT1: DNA (cytosine-5-) methyltransferase 1, VDR: Vitamin D (1,25 dihydroxyvitamin D3) receptor, RXRα: retinoid X receptor alpha and PMCA1: ATPase plasma membrane Ca2+ transporting 1, NCX1: Sodium-calcium exchanger protein 1, TXNIP: Thioredoxin interacting protein, VEGF: Vascular endothelial growth factor. *In bold $p \leq 0.05$

5.4.3 Cardiff cohort

There was no difference in the placental *FTO* or *y⁺LAT2* mRNA expression between the SGA group and the control group (Figure 5.4).

Placental FTO mRNA expression was not correlated to custom birth weight centile in the complete group or the control group but it was negatively correlated with custom birth weight in the SGA group (Table 5.16). This correlation might be due to the system that the groups were classified, with a smaller distribution of custom birth weight in the SGA group (Figure 5.5). Similar to the findings in the SWS cohort, *FTO* expression was correlated with y^+LAT2 expression, this correlation was found in both groups as well as the total cohort (Table 5.16 and Figure 5.6). No other correlations were found between *FTO* and the available neonatal measures.

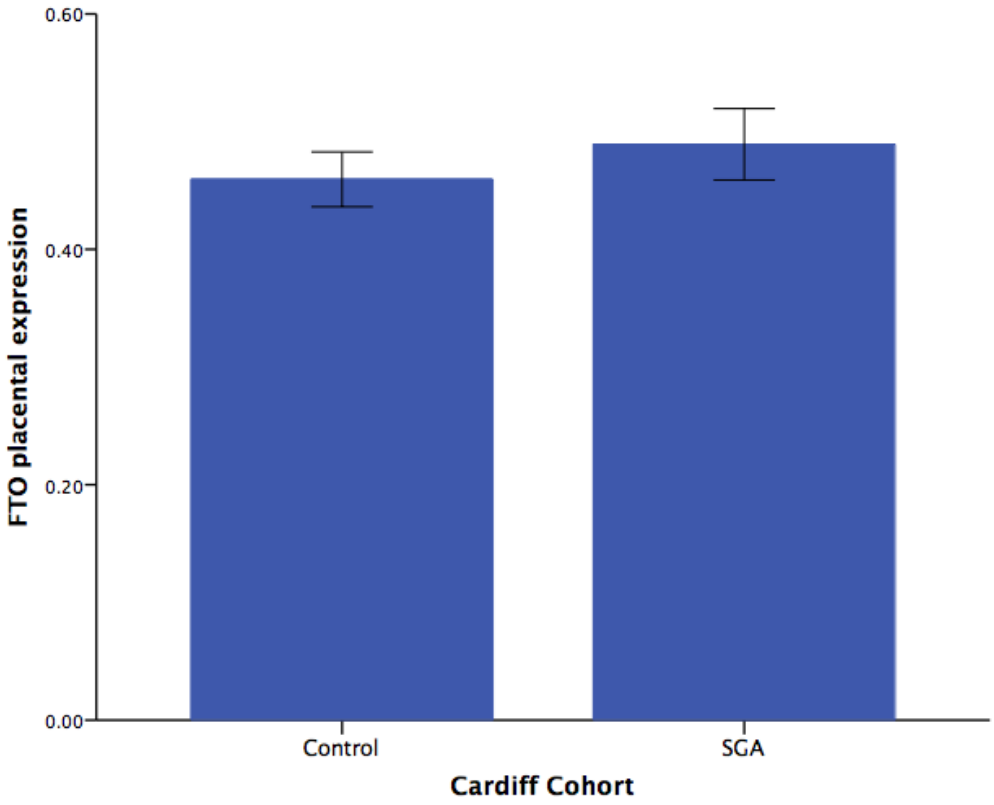

Figure 5.4 Placental *FTO* relative mRNA expression in the Cardiff cohort

Term placental FTO mRNA expression was not different between the control group and the SGA group. (t-test, p = 0.68, n: 40 controls and 40 SGA). SGA: Small for gestational age.

Table 5.16 Correlations between placental *FTO* expression and custom birth weight centile, head circumference and placental y^+LAT2 expression in the Cardiff cohort

Variable	CONTROL			SGA			TOTAL		
	r	p*	n	r	p*	n	r	p*	n
Custom birth weight centile	0.054	0.739	40	**-0.395**	**0.012**	40	-0.051	0.655	80
Head circumference*	0.220	0.303	22	-0.257	0.214	23	0.003	0.985	49
y^+LAT2 expression	**0.485**	**0.002**	**37**	**0.518**	**0.001**	**39**	**0.507**	**<0.0001**	**76**

*Adjusted for gestational age and sex. *In bold $p \leq 0.05$

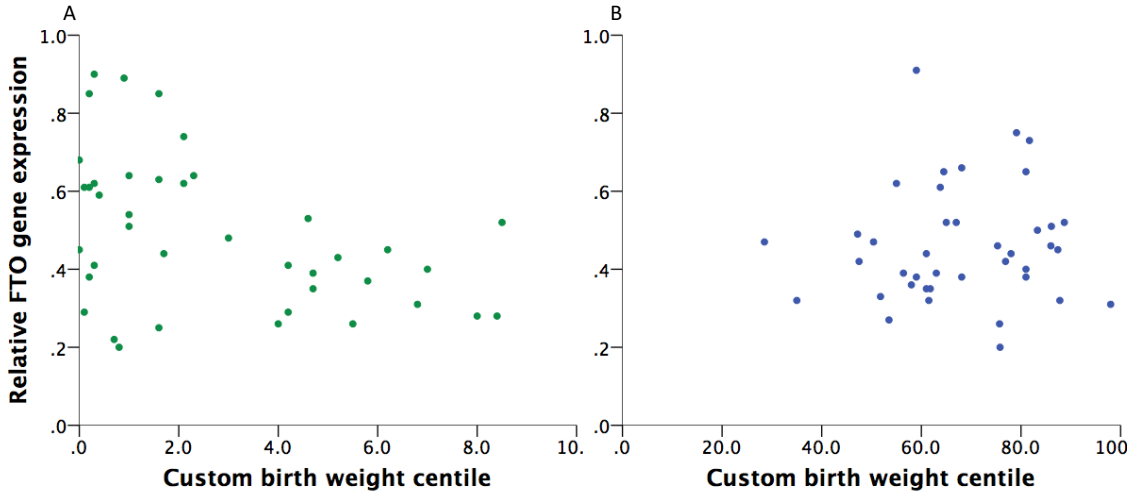

Figure 5.5 Correlation between placental FTO expression and custom birth weight centile in the Cardiff cohort

Term placental FTO expression was negatively correlated with custom birth weight centile in the SGA group (r = -0.395, p = 0.012 – A, n: 40 controls and 40 SGA). Placental FTO expression was not correlated with custom birth weight in the control group (B).

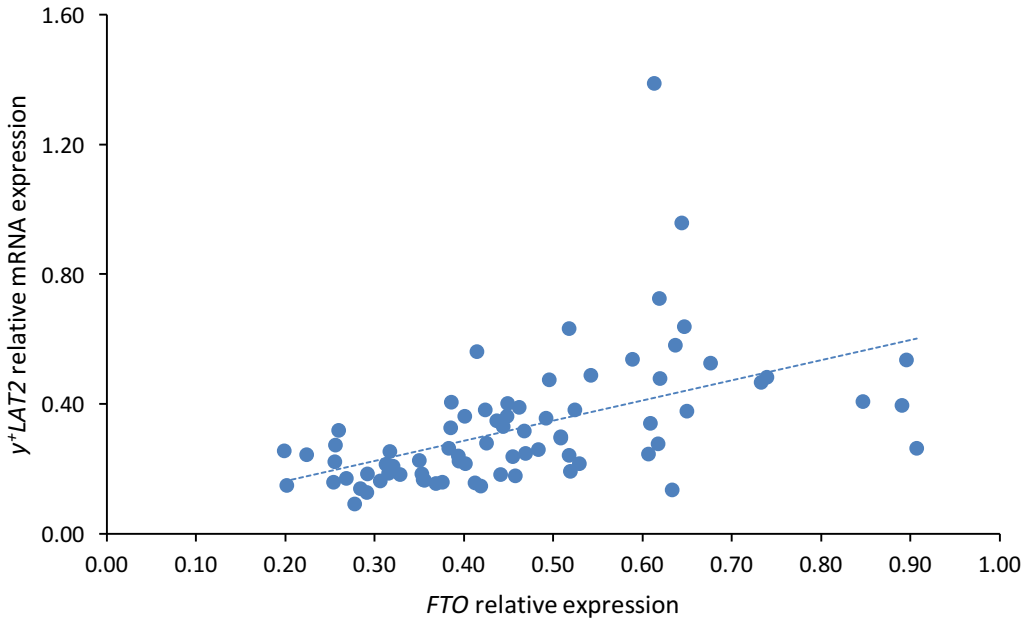

Figure 5.6 Correlation between placental FTO mRNA expression and y^+LAT2 mRNA expression in the Cardiff cohort

Term placental expression of FTO was correlated with the expression of y^+LAT2 in the Cardiff cohort (r = 0.51, $p \leq 0.001$, n = 76).

5.4.4 Summary of the findings from the human cohorts

Table 5.17 summarises the correlations between placental *FTO* gene expression and neonatal anthropometric measures and placental gene expression in the three cohorts. In the three cohorts *y^+LAT2* placental expression was positive correlated with *FTO* placental expression. In the MAVIDOS and in the SWS cohorts *FTO* placental expression was positive correlated with *ASCT2* and the correlation between *FTO* and *RXRα* was opposite between the two cohorts. Others genes were not significant or were not measured as it is showed in the table.

Table 5.17 Summary of main correlations between placental *FTO* expression, neonatal measures and placental gene expression in the three cohorts

Variable	SWS cohort		MAVIDOS cohort		Cardiff cohort	
	r	p	r	p	r	p
Neonatal measures						
Birth weight	0.204	0.046	N.S		N.S	
Head circumference	0.276	0.006	N.S		N.S	
Neonatal fat mass	0.290	0.004	N.M		N.M	
Placental gene expression						
Y^+LAT2	0.37	0.002	0.355	0.002	0.507	<0.001
ASCT2	0.286	0.004	0.397	0.001	N.M	
EAAT2	0.22	0.027	N.M		N.M	
LAT1	N.S		0.240	0.043	N.M	
LAT3	N.S		0.466	<0.001	N.M	
LAT4	N.S		0.314	0.007	N.M	
SNAT1	N.S		0.389	0.001	N.M	
VDR	-0.291	0.003	N.S		N.M	
RXRα	-0.199	0.048	0.346	0.003	N.M	
Cubilin	N.S		0.297	0.011	N.M	
Megalin	N.S		0.279	0.018	N.M	
NCX1	N.M		0.395	0.001	N.M	
PMCA1	N.S		0.258	0.029	N.M	
PMCA4	N.M		0.521	<0.001	N.M	
DNMT1	N.S		0.386	0.001	N.M	
TXNIP	N.M		0.521	<0.001	N.M	
Hsa-miR-27a-3p	-0.21	0.036	N.S		N.M	

N.S: No significant, N.M: No measured

DNMT1: DNA (cytosine-5-) methyltransferase 1, VDR: Vitamin D (1,25 dihydroxy vitamin D3) receptor, RXRα: retinoid X receptor alpha and PMCA: ATPase plasma membrane Ca2+ transporting, NCX1: Sodium-calcium exchanger protein 1, TXNIP: Thioredoxin interacting protein, VEGF: Vascular endothelial growth factor.

5.4.5 *IRX3* expression in the placenta

The *IRX3* qPCR assay was not able to quantify *IRX3* expression in the placenta since its expression in this tissue was below the linear range of the standard curve. PCR was performed and showed that *IRX3* was expressed in placenta (Figure 5.7), but the expression is below what qRT-PCR is able to meaningfully quantify. The standard curve of the qRT-PCR using the lung sample at a higher concentration shows that the assay was working appropriately (Figure 5.8).

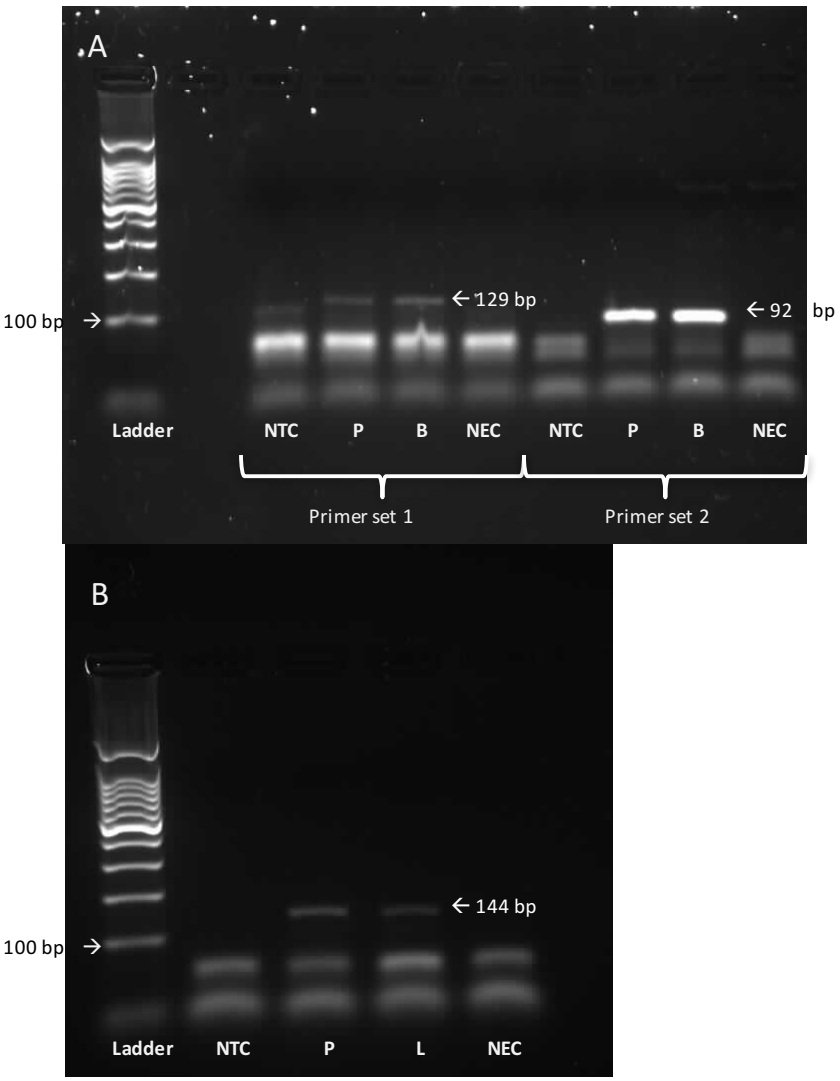

Figure 5.7 Electrophoresis of *IRX3* PCR products

A: Primers set 1 and 2 (expected band size: 129 and 92 bp respectively). B: Primers set 3, expected band size: 144 bp. NTC: No template control, P: Term placenta, B: Brain, NEC: No enzyme control, L: Liver. DNA Ladder 1Kb.

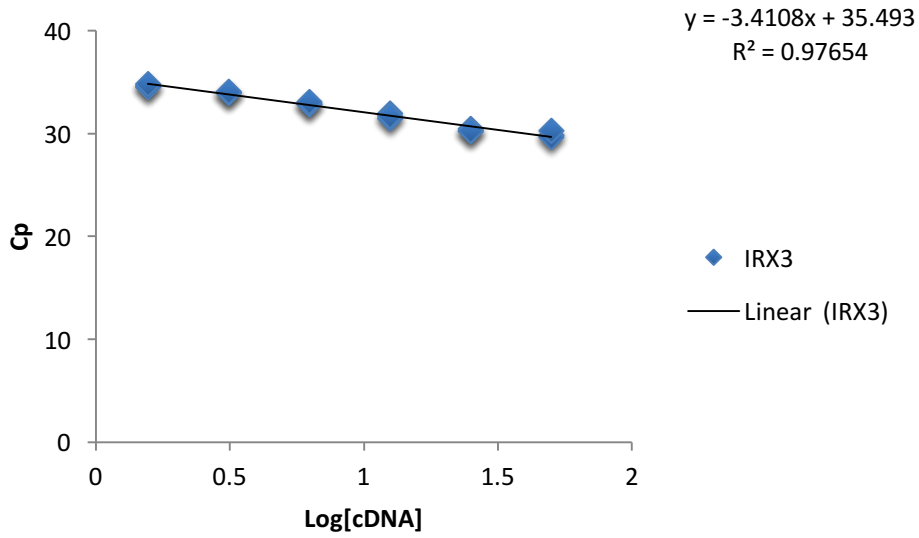

Figure 5.8 Standard curve of *IRX3* in quantitative RT-PCR amplification

Quantitative RT-PCR of IRX3 using a lung sample to determine assay functionality. Efficiency: 0.96.

5.5 DISCUSSION

The primary aim of this study was to determine the association between placental *FTO* expression, fetal development and birth weight in humans. In the SWS cohort a positive correlation between placental expression of *FTO* with birth weight and fetal anthropometric measures was shown, consistent with a previous report in the literature. However, no association was observed in the smaller MAVIDOS cohort (which was complicated by vitamin D treatment) or between AGA and SGA babies. *FTO* expression was correlated with the expression of specific genes and miRNAs in the placenta suggesting a possible mechanism of *FTO* action via regulation of gene expression.

The association between *FTO* and birth weight in the SWS was consistent with a previous study, where placental expression of *FTO* was associated with fetal weight and length [157]. Furthermore, this study demonstrated a correlation between placental *FTO* expression and other neonatal and fetal growth measures [248]. While *FTO* was associated with fetal growth, head circumference and neonatal fat mass in the SWS there was no association between placental *FTO* expression and childhood growth.

When these relationships were explored in the MAVIDOS study the association with birth weight or the other neonatal measures could not be replicated. The MAVIDOS study which, like the SWS represents the normal range of birth weight, was smaller than the SWS and interpretation of this result is complicated because half of the group was treated with vitamin D. However, the fact that there was not an association in the MAVIDOS cohort suggests that larger studies are required to address this issue.

The SWS cohort found an association with neonatal anthropometric measures but, it also found stronger associations with specific aspects of fetal growth. Unfortunately, fetal measures were not collected in the MAVIDOS or Cardiff cohorts and the association between head circumference and placental *FTO* expression in the SWS cohort could not be replicated in the other two cohorts, so these observations could not be confirmed. If *FTO* gene expression was primarily associated with changes in

specific growth parameters, then the effect on overall fetal weight may be more difficult to observe. In any future larger study, it would be important to measure fetal growth parameters additional to the neonatal anthropometric measures. But, from the results from SWS, it is possible to suggest that *FTO* is affecting placental function and therefore fetal development.

The Cardiff cohort explored the possibility that *FTO* placental expression was altered between babies with altered growth (SGA) when they were compared with the control group. Differences in *FTO* gene expression were not found in this cohort. The failure to observe a difference in SGA babies may suggest that *FTO* expression is not itself a cause of fetal growth restriction. It may be that *FTO* is associated with fetal growth but that other factors, not sensed by or mediated through *FTO*, caused fetal growth restriction in these babies. Alternatively, the study may have been underpowered to see an effect of *FTO*. As with the MAVIDOS study in a future larger study would be important to measure others specific fetal growth parameters such as abdominal circumference to see if *FTO* is having specific effects on fetal growth.

This study was able to show a correlation between placental *FTO* gene expression and expression of specific amino acid transporters in the placenta in three different cohorts. Additionally, in the SWS cohort and in the MAVIDOS cohort *FTO* expression was correlated with the expression of genes involved in vitamin D metabolism and calcium transport. Placental FTO expression was also found to be correlated with the levels of hsa-miR-27a-3p. This suggested another possibility of how *FTO* could be affecting placenta function (Figure 5.9). The FTO product is a RNA demethylase [218,251] and RNA methylation is one of the most frequent posttranscriptional modifications found in RNA molecules [156]. In HEK 293 cells, up or down regulation of FTO affected the transcriptome [218]. FTO was also reported to have an intranuclear location raising the possibility that FTO is involved in the posttranscriptional processing of mRNA or miRNA. Here, we found that *FTO* expression was correlated with the expression levels of nutrient transporters and with genes involved in placental function. This together with the finding of *FTO* being associated with miRNA levels raise the possibility that

FTO might influence fetal development by regulating gene expression in placenta (Figure 5.9).

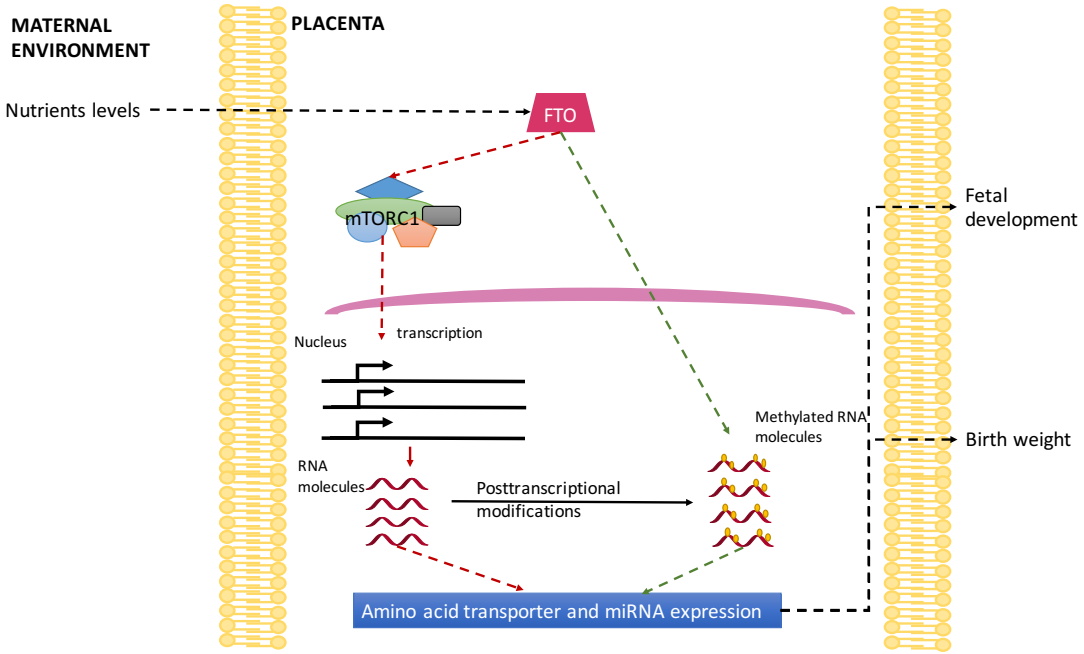

Figure 5.9 Possible mechanism of FTO involvement in placental function

FTO has been reported as a nutrient sensor in vitro experiments [154]. Red arrows showed how it has been proposed that when FTO is affected by nutrient levels it can affect mTORC1 and therefore affect transcription in the cells. This study proposed that FTO can also be acting directly (green arrows) by mediating posttranscriptional modification to the RNA molecules affecting their stability and therefore affecting their levels.

FTO has been reported to be involved in cellular nutrient sensing, in particular in the response to amino acid levels. *In vitro* experiments in HEK 293 cells showed that *FTO* expression is reduced when there is a reduction in the glucose or amino acid levels and that the *FTO* response to the nutrient deprivation is reversed when the nutrients are added back. Additionally, *FTO* expression was affected by plasma essential amino acid levels [154]. The involvement of *FTO* as an amino acid sensor has been studied in mouse embryonic fibroblast and human kidney embryonic cells. These have shown that a *FTO* knock out produced an alteration in the normal activation of the mechanistic target of rapamycin complex 1 (mTORC1) in response to amino acid deprivation and also producing a reduction in translation and cell growth in MEF [153]. This mechanism could

explain the association found in this study between *FTO* expression levels, amino acid transporters levels and fetal development and birth weight as showed in Figure 5.9.

The fact that placental *FTO* expression is associated with maternal plasma lipid levels, a measure of maternal nutritional status, in the SWS cohort reinforces the possibility that *FTO* is acting as a nutrient sensor but, this needs to be investigated further. In chapter 3 no changes in mouse placental *FTO* gene expression were observed in response to a highly palatable/high fat diet. This suggests in mouse placenta *FTO* gene expression is not responding to higher lipids levels or glucose. In humans, glucose transporters expression in the placenta is not regulated by glucose at the end of the pregnancy [252]. However, we do not know if amino acid levels were changed in the maternal plasma from these pregnancies.

5.5.1 *FTO* obesity-related SNPs, *IRX3* expression, and *FTO* expression

This study also showed that placental *FTO* expression was not associated with the obesity-associated SNPs within the gene. The fact that *FTO* expression was not affected by the presence of the risk alleles in the SNPs in the SWS cohort [248] is consistent with the recent finding proving that the SNPs within *FTO* actually are regulating the expression of IRX3 instead of the expression of *FTO* [250]. However, it was not possible to measure IRX3 expression in term human placenta due to its low levels of expression in this tissue. It is therefore difficult to confirm that IRX3 gene expression is also related with fetal or childhood growth. In previous studies that have been focused on the obesity-related *FTO* SNPs and child development, the association between them has not been completely clear. In a cohort of children, there were no associations between the obesity-related SNPs in *FTO* and birth weight. However, in this cohort, they found an association between *FTO* and weight gain in the first 2 weeks of life and with total, truncal and abdominal fat at 2 weeks age [249]. In another study, no association was found between the *FTO* obesity-related SNP and energy expenditure but an increased energy intake associated to *FTO* SNPs was described independently of body weight [253]. The potential role of IRX3 in the regulation of placental function still needs to be established.

The findings in this study raise questions about *FTO* function and its possible association with fetal development, placental gene expression and maternal environment. However, further investigation is necessary to confirm its importance for fetal growth and its function within the cell. It is also important to try to determine whether *IRX3* is also involved in this process as a genetic factor that can affect fetal development.

5.5.2 Limitations and future work

The main limitation of this study was sample size and this may explain the inconsistent findings compared to placental *FTO* expression previously measured in another human cohort. A retrospective sample size calculation within the data of this study, showed that 186 samples were necessary in order to obtain a correlation between placental *FTO* expression and birth weight (with 80% power and p = 0.05). 107 samples were necessary in order to obtain a 10% different in the placental expression of *FTO* between two groups with equal number of participants (with 80% power and p = 0.05) [207]. The sample size in this study was determined by the number of samples available but bigger studies are necessary in order to confirm these findings.

Another limitation was that the growth data collected for the different cohorts was not the same. With the SWS cohort having fetal growth data and follow-up data on the children while the MAVIDOS and Cardiff cohorts did not have fetal growth and childhood measures which meant that we could not confirm some observations in all studies and made it difficult to compare the cohorts.

Additionally, all target genes could not be measured in all cohorts, in particular, due to technical difficulties in Cardiff where we were only able to measure *FTO* and y^+*LAT2*. Therefore, the correlations that were found were not validated in all three cohorts. If time and resources were available, it would be interesting to validate the association between FTO and genes related to vitamin D metabolism and miRNA expression in all three cohorts. However, the correlations between placental FTO expression and the amino acid transporter expression was reproducible in the three cohorts.

As discussed above we could not measure IXR3 in the placenta and we were not able to confirm whether placental *IRX3* expression was correlated with birth weight of fetal measures as *FTO* was. In a future study, *FTO* could be knocked down in primary trophoblast culture to study whether it was associated with *IRX3* expression. Also, protein levels of *IRX3* could be measured in order to determine whether *IRX3* has an effect on the placenta function and at which levels this effect is happening.

A potential limitation of the Cardiff study was that the SGA babies may have been small but not growth restricted. We used individualised birth weight centiles which should help identify poorly growing babies compared to simply using standard growth charts but a proportion of the SGA babies may have been normally grown. In a future study serial ultrasound could be used to identify babies who fall off their growth trajectory and are more likely to be growth restricted.

Additional studies are necessary in order to access the importance of the findings in this study. The possibility of measuring *FTO* mRNA in other human cohorts with different maternal status (gestational diabetes) could help to understand whether *FTO* is involved in the nutrient sensing mechanism of the placenta. Also *in vitro* experiments are necessary in order to determine the effects of FTO function in cellular pathways.

5.6 CONCLUSION

The relationships found in this study, suggest how FTO could be involved in the regulation of RNA levels in the human placenta and how this could affect fetal development and birth weight. Multiple molecules could be involved in the placental sensing of maternal environment and FTO could be affecting the placental transcriptome and the miRNA levels. Other studies are necessary in order to determine the importance of FTO in the placental function and possibly in the pregnancy and fetal development.

CHAPTER

6 THE FAT MASS AND OBESITY ASSOCIATED GENE EFFECTS ON miRNA EXPRESSION

6.1 INTRODUCTION

In chapter 5, human placental mRNA expression of *FTO* was associated with birth weight and fetal growth parameters [248]. However, the mechanism of action of *FTO* remains to be established. As the data in chapter 5 showed associations between *FTO* and expression of placental mRNA and miRNA the aim of this chapter is to determine whether *FTO* knock down is affecting the expression of different RNAs, specially miRNA expression and indirectly affecting cell functional pathways.

The *FTO* protein product is a RNA demethylase, specifically, the FTO enzyme has an oxidative demethylation activity in N^6-methyladenosine (m^6A) residues in RNA *in vitro* [155]. RNA methylation is one of the most common RNA modifications. The most prevalent RNA methylation is m^6A that is present in almost all types of RNAs and is the most common modification in messenger RNAs (mRNA) and long non-coding RNAs (lncRNA) [254-256]. Additionally, M^6A modification has been reported to be present in primary miRNAs (pri-miRNA) regions as a necessary modification for the pri-miRNAs being processed to pre and mature miRNAs [257]. Transcriptome-wide mapping studies have shown that m^6A could act as a marker to determine the destiny of the RNA molecules since the presence of m^6A is recognise by specific binding proteins [156,254,258,259]. M^6A has also been involved in the recognition of mRNA and lncRNA by selectively binding proteins that can affect their translation status and/or stability [156]. Despite the information that has been gathered about m^6A enrolment in the dynamics of the RNA molecules, it is still necessary to determine the importance of the enzymes involved in the methylation and demethylation of RNA molecules.

There are a few studies investigating the relationship between *FTO* and RNA processing. In a mouse 3T3-L1 pre-adipocyte cell line it was shown that the knock down of *FTO* increased the total m^6A levels in the cells while reducing their ability to differentiated. It also showed that exonic splice sites were enriched with m^6A with this modification being recognised by the splicing proteins. They showed how the modified levels of m^6A after the *FTO* knock down altered the splicing of mRNA molecules including adipogenesis-related factor [255]. In a different study, it was shown that *FTO*

knock down affects genes that are involved in mitotic clonal expansion of mouse adipocytes [260]. In HEK 293 cell line it has been shown that *FTO* knock down affects the transcription levels of genes involved in the response to starvation [218]. *FTO* knock down also appeared to affect levels of specific miRNAs in HEK 293 cells [261]. In this chapter the hypothesis that *FTO* is affecting cellular function by modifying the methylation of different RNA molecules will be tested.

6.2 AIMS

1. To determine whether *FTO* knock down affects miRNA expression levels in HEK 293 cells and identify the cellular pathways these may regulate.
2. To determine predicted targets of the miRNAs identified in the *FTO* knock down cells and their associated pathways.
3. To explore the potential relationship between *FTO* and long non-coding RNA.

6.3 METHODS

6.3.1 Human embryonic kidney cells culture

HEK 293 cells were kindly donated by Dr. Matt Darley. HEK 293 were cultured in HEK 293 cell culture media: Dulbecco's modified Eagle's medium (DMEM, Sigma, United Kingdom) containing 10% of fetal bovine serum (Sigma, UK), penicillin (100 U/ml) and streptomycin (100 mg/ml) (Sigma, UK) and 2 mM of l-glutamine (Lonza, UK). Cells were cultured as described in section 2.3.1 and 2.3.3. Briefly, all reagents were pre-warmed at 37°C before the experiment. Cells were thawed when necessary, centrifuged with HEK 293 cell culture medium and the supernatant was discarded. The cell pellet was re-suspended in cell culture media and incubated in 0.75 cm^2 cell culture flasks at 37°C in 5% CO_2 atmosphere. The medium was changed when necessary and when cells reached ≈80% confluency they were split using trypsin (Section 2.3.1.2).

6.3.2 Human embryonic kidney cells siRNA experiments

When the cells became 80% confluent cell counting was carried out in order to determine the approximate amount of cells to add the 24-well plates for the experiment. Cells were counted as described in section 2.3.1.2. All the cells for these experiments were used before passage 10. FTO mRNA expression was knocked down in HEK 293 cells using siRNA inhibition. The transfection was performed using Lipofectamine™ RNAiMAX (Ambion-Life technologies, UK) reagents and the following siRNAs: a positive control (PC; siRNA that knock down the expression of *GADPH*), a negative control (NC; scrambled siRNA that does not target any gene) and 2 siRNAs for the target gene (Ambion-life technologies; Table 6.1). Initial experiments were performed using the reverse protocol (section 2.3.4), which is when the siRNA and the transfection reagent are added to the cells the same day they are plated.

6.3.2.1 Optimization of FTO knock down experiments

Initial experiments were performed using the reverse protocol provided by the manufacturer and an optimisation of the method was performed to determine the most reliable conditions in our lab. The protocol was tested in order to determine the concentration of siRNA, time of incubation and amount of cells that were necessary in

order to obtain a knock down of the gene expression up to 90% for the positive control and up to 70% for the *FTO* gene. Also, the two siRNA provided by the company were tested in order to determine which one induced the greatest reduction of *FTO* expression in the cells. Table 6.2 describe the conditions that were evaluated during the optimization.

Table 6.1 siRNAs information and sequences

siRNA	Knock down gene	Sequence
Silencer® Select *GADPH* positive control	*GADPH*	-
Silencer ® select negative control No. 2	none	-
siRNA 1	*FTO*	Sense: CAUCCUCAUUGGUAAUCCAtt Antisense: UGGAUUACCAAUGAGGAUtt
siRNA 2	*FTO*	Sense: CAUUACCUGCUGAUCAGAAtt Antisense: UUCUGAUCAGCAGGUAAUGtt

Three optimization experiments were performed as follow All the siRNAs (PC, NC, and target siRNA1 and siRNA2) were diluted to a 100 μM stock solution that was aliquoted and stored at -20°C until they were used. On the day of the experiment a 10 μM working solution of each siRNA was prepared. A solution containing DMEM media without FBS or antibiotics and each siRNA at the different concentration described in Table 6.2 was mixed with the Lipofectamine® RNAiMAX reagent (1 μl of reagent in a final volume of 600 μl). The mixture was left for 20 min at RT to allow the formation of the siRNA oligomer-lipofectamine® RNAiMAX complexes.

HEK 293 cells were harvested and counted as described in section 2.3.1.2. The experiment was plated as follow: in a 24-well cell culture plate 102 μl of the oligomer-lipofectamine®RNAiMAX media mixture was added to each well. Then 5 x 10^4 cells were added per well and DMEM media without FBS or antibiotic was added to make a final volume of 600 μl. All the siRNAs were plated in duplicate as shown in Figure 6.1. A

mock control (MC - cells exposed to the transfection reagent but without any siRNA) and untransfected cells control (UTC) were included with each experiment.

Table 6.2 Conditions evaluated during optimization of knock down experiments

Variable	Conditions evaluated
siRNA concentrations	10 nM, 20 nM and 50 nM
siRNA effectivity	siRNA1 and siRNA2 capacity to knock down *FTO* gene expression

When the most suitable conditions were established. Five experiments were performed using the optimized protocol as follows. Previously cultured HEK 293 cells were harvested and counted as described above. PC, NC, siRNA1 were mixed with the Lipofectamine® RNAiMAx regent and DMEM without FBS or antibiotics in order to form the complexes (final concentration 50 nM). Experiments were plated in duplicate. Media containing the oligomer-Lipofectamine® RNAiMAX was added to each well, then 5 x 10^4 cells were added per well and the DMEM media without FBS or antibiotics was added to complete a final volume of 600 µl. MC and UTC controls were included in these experiments as well.

Cells were incubated at 37°C in a 5% CO_2 atmosphere for 48 h. 500 µl of RNAzol (Sigma, UK) were added to the wells after the media was removed. Cells were harvested within the RNAzol and kept at -80°C until the RNA extraction was performed.

6.3.3 RNA extraction, reverse transcription and quantitative PCR

After each experiment, total RNA (including both mRNA and miRNA) was extracted from the samples using RNAzol according to the manufacturer's instructions as described in section 2.4.1.1. RNA quality and quantity were established using a NanoDrop® 1000 spectrophotometer and gel electrophoresis as described in sections 2.5.1 and 2.5.2 respectively.

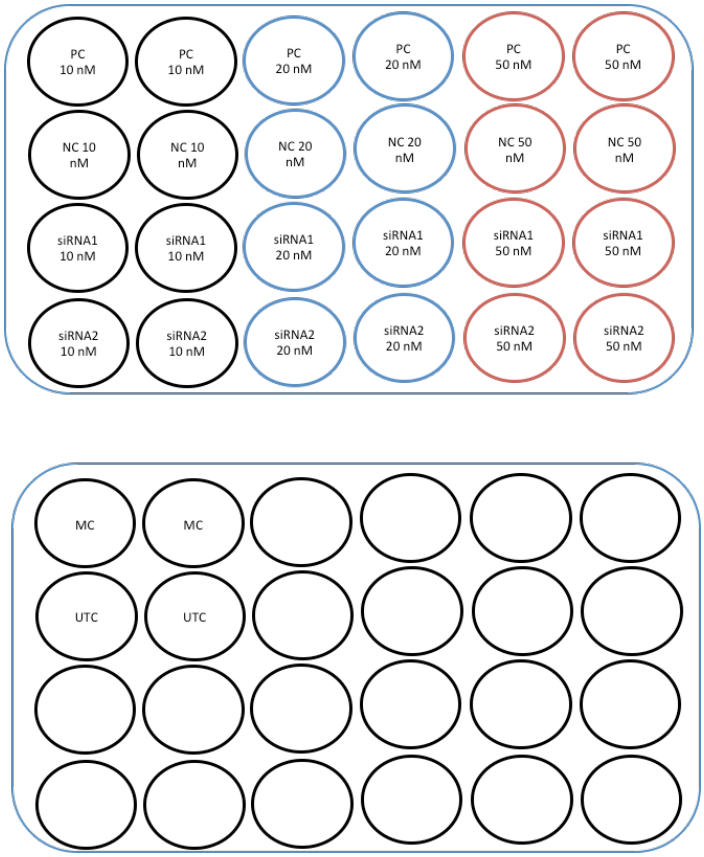

Figure 6.1 siRNA knock down optimization experiment

Sample distribution in two 24-well cell culture plate. PC: positive control, NC: negative control, siRNA1, and siRNA2: siRNA designed to knock down the expression of fat mass and obesity associated (FTO) gene. Experiments were performed in duplicate MC: mock control, UTC: untransfected cells.

Synthesis of cDNA was performed using Promega reagents as described in section 2.6.1. Briefly, 200 ng of sample were mixed with 0.5 µg of random primers to a final volume of 15 µl. The samples were heated at 70°C for 5 min on a Veriti® thermal cycler (Applied Biosystems). After, 50 nmol of triphosphate nucleotides mixture, 25 units of Recombinant RNasin® Ribonuclease Inhibitor, 200 units of M-MLV-RT, 5X M-MLV-RT buffer and water were added to the reaction mixture to a final volume of 25 µl. The mixture was heated at 37°C for 60 min and then 75°C for 10 min. The samples were mixed, centrifuged and diluted to 1:25 with RNA-free water. All the samples and NEC were reverse transcripted in one batch to reduce variation.

Gene expression levels were measured using qPCR according to the methodology described in section 2.6.2. Reactions were performed in a 384 wells plate using a LightCycler® 480 real time PCR system (Roche). Samples, standard curve, controls, NEC and NTC were added in triplicate as follow: 3 ng of cDNA were added to a mixture containing 1 μM of forward and reverse primers and probe and 1X master mix (LightCycler® 480 probes master mix, 2X) to give a final volume of 10 μl.

Gene expression was measured using Universal ProbeLibrary® probes and protocol. Run protocol was: 1 cycle at 95°C for 5 min, then 45 cycles (95°C for 10 s, 60°C for 30 sec and 72°C for 1 s). Data collection was made at 72°C step, as described in Table 2.3.

Expression of reference genes *SDHA*, *ATP5B* and *GADPH* was measured using PerfectProbe® probes and protocol (Table 2.3). Run protocol was: 1 cycle at 95°C for 10 min, then 50 cycles (95°C for 15 sec, 50°C for 30 sec and 72°C for 15 sec). Data collection was made at the 72°C step. Primers sequences are listed in Table 6.3.

Cp values were collected using the second derivate method as described in section 2.6.2.1 and arbitrary RNA concentration were calculated using the standard curve method as described in section 2.6.2.2. Relative gene expression levels were calculated as a ratio between the gene of interest and the geometric mean of the three references genes (*SDHA, ATP5B* and *GADPH*).

6.3.3.1 Determination of knock down efficiency

It was necessary to determine the efficiency of *FTO* knock down in each experiment. Initially, mRNA expression of *GADPH (PC)*, *FTO,* and *YWHAZ* or *ATP5B* was measured in all the samples. The level of knock down for all the experimental conditions was determined by calculating a ratio between the expression of the gene of interest (i.e. *GADPH* or *FTO*) divided by the expression of the gene of interest in the NC. Efficiency was calculated as the level of knock down of the *FTO* gene for each siRNA.

Experiments where *FTO* expression was reduced by at least 60% and the PC expression was reduced by at least 80% were accepted as satisfactory and used for the following

measures. The ratios between the gene of interested and the other controls were also calculated and used as an internal quality control. The ratios of the gene of interest expression when compare with any of the controls (NC, MC, and UTC) should be under 10%.

Table 6.3 Primers and probes used for quantification of *FTO, PLAC1* (lncRNA) and amino acid transporter expression

Gene	Gene bank accession number	Primer sequence (5' – 3')	UPL number
FTO	NM_001080432.2	F: CACAACCTCGGTTTAGTTCCA R: AAATATAATCCAAGGTTCCTGTTGAG	53
ASCT2 (SLC1A5)	NM_005628.2 NM_001145144.1 NM_001145145.1	F: GAGGAATATCACCGGAACCA R: AGGATGTTCATCCCCTCCA	43
y^+LAT2 (SLC7A6)	NM_001076785.1 NM_003983.4	F: GCTGTGATCCCCCATACCT R: GGCACAGTTCACAAATGTCAG	66
TAT1 (SLC16A10)	NM_018593.4	F: GGTGTGAAGAAGGTTTATCTACAGG R: AGGGCCCCAAAGATGCTA	6
PLAC1 (TINCR)		F: AGCTCCCCAGACCACTCC R: CTGCACCATCCACTAGTAGCC	13

F: Forward, R: Reverse. UPL: Universal probe library.

6.3.4 Quantification and validation of miRNA

6.3.4.1 Quantification of miRNA using a SYBR green-based method

Table 6.4 contains the information about the miRNAs quantified in this study. The quantification of miRNA was performed using miScript II RT® (Qiagen, UK) and miScript SYBR green PCR® (Qiagen, UK). Hsa-miR-23a-3p, Hsa-miR-27a-3p, and Hsa-miR-221-3p were quantified in the HEK 293 cell NC and *FTO* knock down samples. All the miRNAs were quantified following the manufacturer instructions and as described in section 2.7. Briefly, the miRNAs were converted to cDNA using miScript II RT®, with 200 ng of total RNA mixed with 5X miScript HiSpec buffer, 10X miScript nucleics mix, miScript reverse transcriptase mix and ultra purified water. Then the mixture was heated in a

Veriti thermal cycler (Applied Biosystems) at 37°C for 60 min and then at 95°C for 10 min. Samples were mixed, centrifuged and diluted 1:10 before storage at -20°C.

After the cDNA was produced, the quantification of specific miRNA was performed using a LightCycler® 480 real time PCR system (Roche) and miScript SYBR green PCR master mix. Diluted cDNA (≈2 ng) was added to QuantiTect SYBR green PCR master mix with miScript Universal primer and the specific miScript primer assay (Table 6.4). The run protocol was: 1 cycle (15 min at 95°C), and 45 cycles (15 sec at 94°C, 30 sec at 55C and 30 sec at 70°C) data was set to be collected per cycle at 70°C step. All the samples were measured in triplicates together with NTC. Cp values were calculated using the second derivative method (section 2.6.2.1). MiRNA expression levels were quantified using the deltaCT method as described in section 2.6.2.2. *SNOD61* (small nucleolar RNA) was measured as the reference gene and MiRNA expression was normalised to its expression.

Table 6.4 Human miRNA primer sequences

MicroRNA	miRBaseID	sequence
Hsa-miR-27a-3p	MIMAT0000084	5'UUCACAGUGGCUAAGUUCCGC
Hsa-miR-23a-3p	MIMAT0000078	5'AUCACAUUGCCAGGGAUUUCC
Hsa-miR-221-3p	MIMAT0000278	5'AGCUACAUUGUCUGCUGGGUUUC
Hsa-miR-143-3p	MIMAT0000435	5'UGAGAUGAAGCACUGUAGCUC

6.3.5 Sequencing of miRNA

6.3.5.1 Assessing RNA quality and sample selection

Samples with a RNA concentration ≥200 ng/µl (7 NC and 7 *FTO* knock down) were selected for the miRNA sequencing analysis. The quality of the samples was analysed using a Bioanalyser 2100 (Agilent, UK) as described in section 2.5.3. Briefly, the samples were loaded in a chip that separated and dyed the RNA molecules that form a complex that is detected by laser-induced fluorescence. Data are transformed into gel-like images and electropherograms (Figure 2.4). This analysis determines the integrity

of the RNA (RNA integrity number – RIN) using the ribosomal RNA ratio (28S rRNA/18S rRNA) and the presence/absence of degradation products.

Four pairs of NC - *FTO* knock down samples (each pair from a different experiment) with RIN number ≥ 8.5 were selected for the miRNA sequencing.

6.3.5.2 Sequencing of miRNAs

The selected 8 total RNA samples were sent to Expression Analysis – Q^2 solutions (EA/Q^2 solutions – USA) for the miRNA sequencing and analysis. Samples were sequenced as described in section 2.9.2 and 2.9.3. First, the company prepared the cDNA libraries using Illumina's TruSeq Small RNA sample preparation kit (Figure 2.10). Samples were processed according to the manufacturer's instructions and quality of the final libraries was confirmed using the Agilent 2200 Tapestation (D1000 Screentape, Agilent). Libraries were then size-selected, resulting in a mean library size of ≈135 bp. The libraries were quantified by qPCR and normalized to 2 nM in preparation for sequencing.

In the sequencing, the libraries were bound to a flow cell that contained specific oligonucleotides. A cluster of individual oligonucleotides was created for each template by clonally amplifying each molecule up to 1000 fold. Paired-end sequencing was determined using sequencing-by-synthesis technology to a depth of 19 million reads. Information obtained was then used for the analysis.

6.3.5.3 Analysis of miRNA sequencing

The analysis was performed using a miRNA pipeline developed by EA/Q^2 Solutions as described in section 2.9.5. Briefly, the primary sequence was checked to ensure the data integrity. Clipping and trimming of the sequencing data were carried out which involved removing the adapters used during the preparation of the library from the sequencing data together with low-quality bases at the end of the reads. All remaining sequences that were at least 13 nucleotides in length were used in the following analysis. The next step was to collapse unique sequence reads and then align them to the reference library (miRBase.org – University of Manchester). The alignment was

performed using Bowtie version 0.12.9. miRNA counts were then normalized and log transformed across the samples. A principal component analysis (PCA) was performed in order to determine the miRNA that was different between the NC and *FTO* knock down groups.

6.3.5.4 Pathways analysis of miRNA sequencing

Further analysis was carried out on the miRNAs that were different between the NC and FTO knock down. Since this is an exploratory analysis, miRNAs that had an unadjusted p-value under 0.05 were used for this analysis. Pathway analysis was used to identify the gene expression pathways that were targets of the miRNAs whose expression was increased or decreased by the *FTO* knock down. DIANA miRPath version 3.0 a free online software was used to do this analysis [206]. The selected miRNAs were used for a multiple miRNA effects analysis. Tarbase v7.0 database was selected and both the predicted and validated targets for the selected miRNA were used in the analysis. Union genes and union pathways results were obtained.

6.3.6 Statistical analysis

Gene and miRNA expression and efficiency were calculated using Microsoft Excel 2011. Statistical analysis such as t-test, correlation, and mixed models were calculated using SPSS V 22.0. For all statistical tests, a p-value ≤ 0.05 was considered significant.

Differences in the gene or miRNA expression were determined using a mixed model. Generalized mixed models allow the inclusion of random and fixed factors to the linear predictor. The experimental condition was added as a fixed factor and the experiment number was added as a random factor.

6.4 RESULTS

6.4.1 Optimization of siRNA experiments

Figure 6.2 shows the optimization results using two different siRNAs to knock down *FTO* and three different concentrations of siRNA. From the results of the optimization experiments it was decided to use the siRNA1 at 50 nM concentration, since it showed the least variation and the highest knock down efficiency (70%). *FTO* expression was compared against the NC, MC, and UTC (Figure 6.2). *FTO* knock down was reduced consistently when compared with the MC and UTC, showing that the reagent on its own (MC) was not having an effect on gene expression and that the normal *FTO* expression (UTC) was being reduced by the siRNAs.

Once the optimal conditions were selected 5 further *FTO* knock down experiments were performed using siRNA 1 at a 50 nM concentration. Figure 6.3 shows average expression of *FTO* in the knock down samples and NC samples with the average efficiency of the experiments at around 65%. Figure 6.4 shows the PC results for the eight experiments performed, with an average efficiency of 75%.

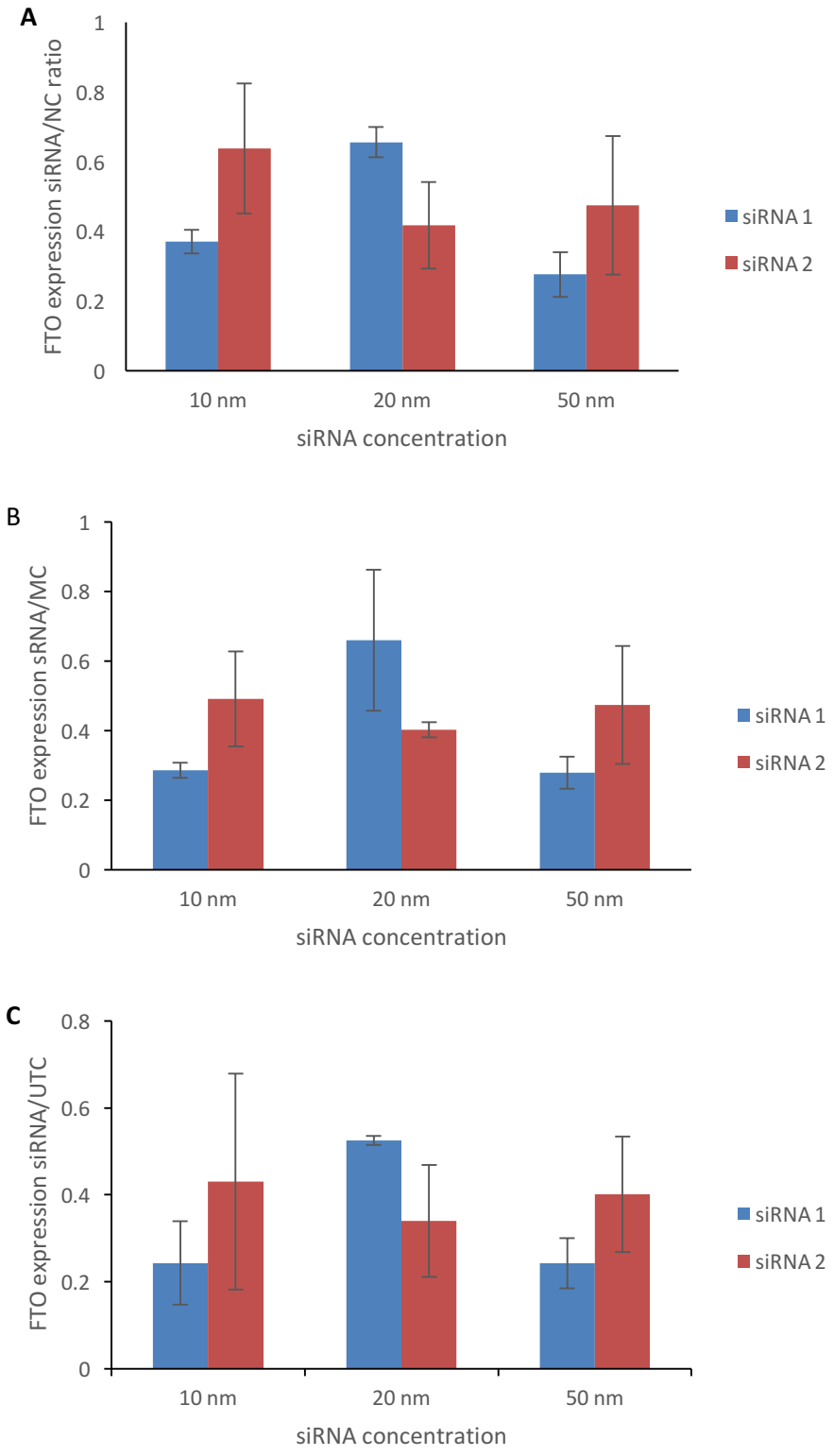

Figure 6.2 siRNA optimization experiments

siRNA experiments were optimized in order to determine the highest knock down efficiency. A. Ratio of FTO expression between experimental siRNA and negative control. B. Ratio of FTO expression between experimental siRNA and mock control (MC). C. Ratio of FTO expression between experimental siRNA and untransfected cells (UTC). siRNA concentration: amount of siRNA or negative control added to the experiment. Values are mean ± SEM. (n: 3 experiments each with 2 control and 2 siRNA exposed wells).

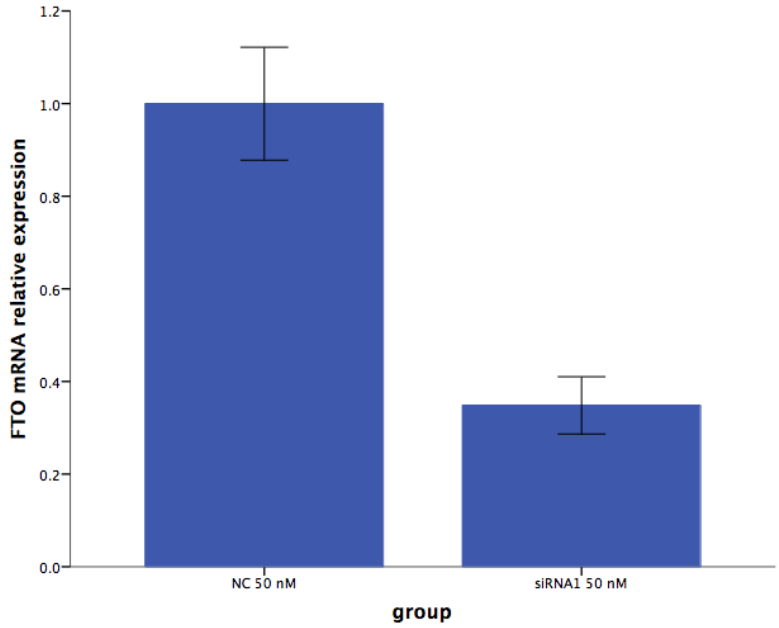

Figure 6.3 *FTO* relative mRNA expression between negative control and siRNA1

FTO relative mRNA expression when the negative control or the siRNA1 were added. NC: Negative control. 50 nM: concentration of siRNA or negative control added to the wells. N = 8 experiments. Values are means ± SEM. Relative expression was calculated as a ratio between the expression of the gene of interest and the geometrical mean of the reference genes (ATP5B, GADPH and SADH)

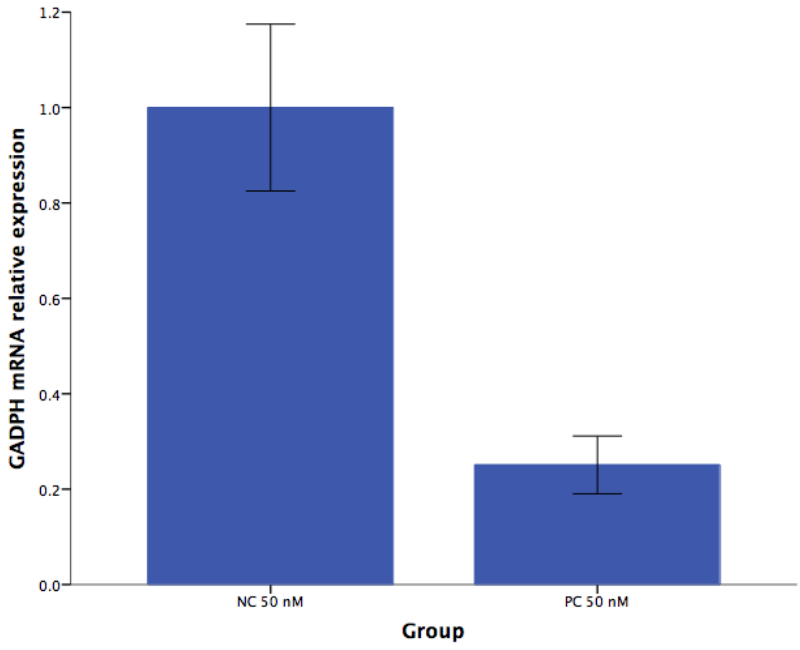

Figure 6.4 *GADPH* relative mRNA expression between negative control and positive control

GADPH relative mRNA expression when the negative control or the C were added. NC: Negative control, PC: positive control. 50 nM: concentration of positive or negative control added to the wells. N = 8 experiments. Values are means ± 1 SEM. Relative expression was calculated as a ratio between the expression of the gene of interest and the geometrical mean of the reference genes (ATP5B, GADPH and SADH)

6.4.2 Gene expression and miRNA expression following *FTO* knock down

TAT1 mRNA expression was increased in the *FTO* siRNA knock down group compared with the control group (Figure 6.5). y^{+}*LAT2* and *ASCT2* mRNA expression was not affected by the knock down of *FTO* (Table 6.5). Expression of the miRNAs hsa-miR-27a-3p, hsa-miR-221-3p and hsa-miR-23a-3p were not affected by the knock down of *FTO* (Table 6.5).

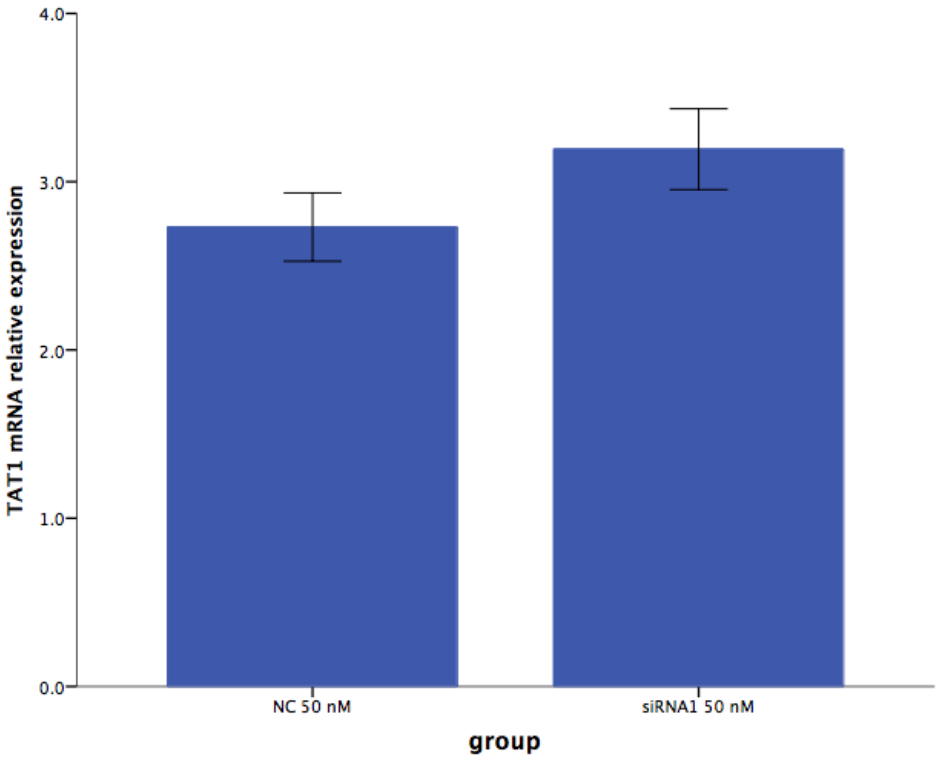

Figure 6.5 *TAT1* expression in the *FTO* knock down and in the negative control

TAT1 relative mRNA expression was increased in the FTO knock down samples compared with the negative controls (p = 0.029). N = 8 experiments. Data expressed as mean ± SEM. NC: Negative control.

Table 6.5 Differences between *FTO* knock down samples *vs* controls in the expression of lncRNA, mRNA and miRNA

Gene/miRNA	NC	n	siRNA 1	n	p
y^+LAT2	2.98 ± 0.31	15	2.74 ± 0.18	14	0.505
ASCT2	1.9 ± 0.18	6	1.80 ± 0.27	6	0.710
PLAC2 (lncRNA)	0.19 ± 0.05	15	0.12 ± 0.04	14	0.231
hsa-miR-27a-3p	2.16 ± 0.94	9	2.04 ± 0.84	8	0.123
hsa-miR-221-3p	0.81 ± 0.3	9	0.53 ± 0.18	9	0.248
hsa-miR-23a-3p	0.65 ± 0.12	9	0.82 ± 0.2	9	0.511

Values are mean ± SEM.NC: negative control.

6.4.3 Analysis of miRNA sequencing

451 miRNAs were detected by the miRNA sequencing in the HEK 293 cell line after the *FTO* knock down experiment. Two miRNAs, hsa-miR-935 and hsa-miR-25-5p were significantly different after accounting for multiple comparisons in the *FTO* knock down group compared to the controls and were used in the pathway analysis together with another 17 miRNA that had an unadjusted p-value under 0.05 (Table 6.6).

6.4.3.1 Pathway analysis of miRNA sequencing data

Figure 6.6 shows the heat map for the pathways that contain genes that are predicted targets of the miRNA that were increased in the *FTO* knock down group. The analysis shows that these miRNAs target genes that have been shown to change in cancer. They also target genes involved in extracellular matrix metabolism (Glycans degradation) and they also affected genes involved in fatty acid metabolism and in the mTOR pathway. Figure 6.7 shows the mTOR pathway and the 28 genes that have been experimentally shown to interact with two of the miRNA from this analysis (hsa-miR148-5b and hsa-miR-34a-5p).

Figure 6.8 shows the heat map for the pathways that contain genes that are predicted targets of the miRNA that were decreased in the *FTO* knock down group. The analysis shows that these miRNAs target genes related to cancer. The decreased miRNA from this analysis also affected fatty acid metabolism pathways as the increased miRNA,

interestingly the same genes were target by the increasing and the decreasing miRNA (Figure 6.9).

Table 6.6 List of miRNA that have an unadjusted p-value under 0.05 and were used in the pathway analysis

miRNA	miRBaseID	Unadjusted P-value	FDR	log2FC
hsa-miR-935	MIMAT0004978	**1.17×10^{-05}**	**0.005**	7.124
hsa-miR-25-5p	MIMAT0004498	**0.0002**	**0.04**	-1.151
hsa-miR-378a-3p	MIMAT0000732	0.004	0.558	-0.589
hsa-miR-31-5p	MIMAT0000089	0.01	0.666	-0.391
hsa-miR-34a-5p	MIMAT0000255	0.01	0.666	7.401
hsa-miR-1284	MIMAT0005941	0.01	0.666	-6.481
hsa-miR-424-5p	MIMAT0001341	0.01	0.666	-7.908
hsa-miR-3180-3p	MIMAT0015058	0.02	0.666	-7.591
hsa-miR-4745-5p	MIMAT0019878	0.02	0.666	7.595
hsa-miR-1275	MIMAT0005929	0.02	0.666	0.561
hsa-miR-26a-5p	MIMAT0000082	0.02	0.666	-0.350
hsa-miR-148b-5p	MIMAT0004699	0.02	0.666	7.379
hsa-miR-940	MIMAT0004983	0.02	0.666	-7.171
hsa-miR-128		0.03	0.666	0.319
hsa-miR-30c-5p	MIMAT0000244	0.03	0.666	-0.413
hsa-miR-424-3p	MIMAT0004749	0.04	0.666	-0.364
hsa-miR-1229		0.04	0.666	-6.8
hsa-miR-21-3p	MIMAT0004494	0.04	0.666	-4.81
hsa-miR-22-3p	MIMAT0000077	0.05	0.666	-0.232

FDR: False discovery rate estimate using a Benjamin-Hochberg correction to raw p-values. Log2FC: log 2 of the fold change (ratio of experiment to baseline).

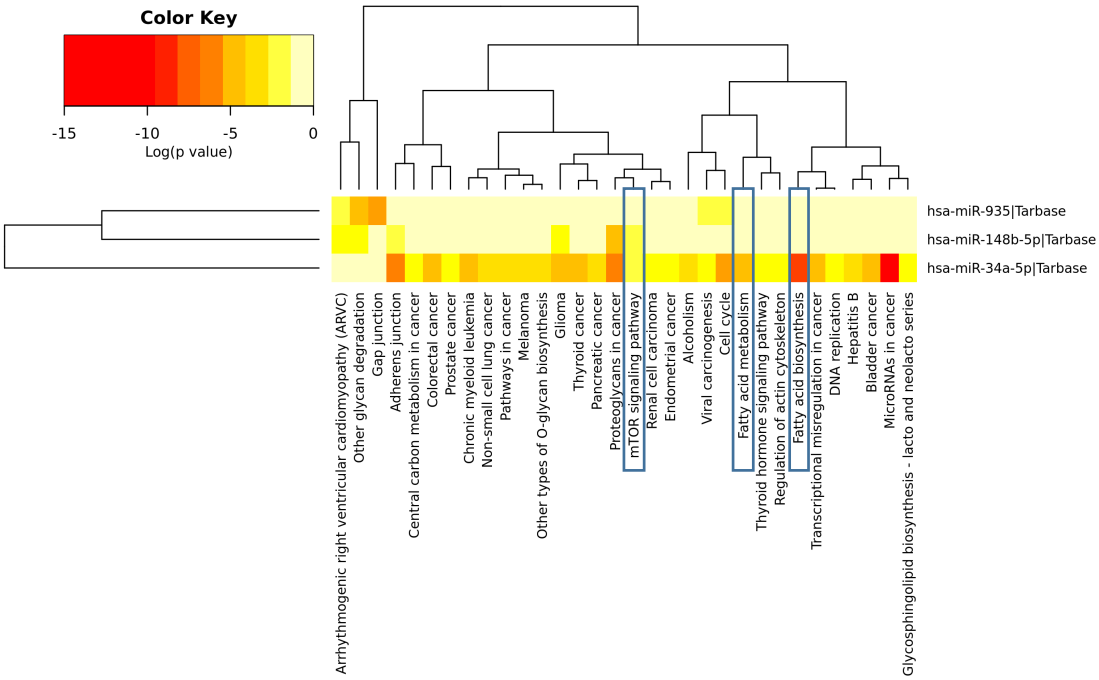

Figure 6.6 Heat map for the miRNAs that were increased in the miRNA sequencing analysis

Pathway analysis showed that the three miRNAs that were increased in the miRNA sequencing analysis target genes involved in fatty acid metabolism and mTOR signalling pathway (blue boxes).(n: 4 control and 4 siRNA1 exposed wells).

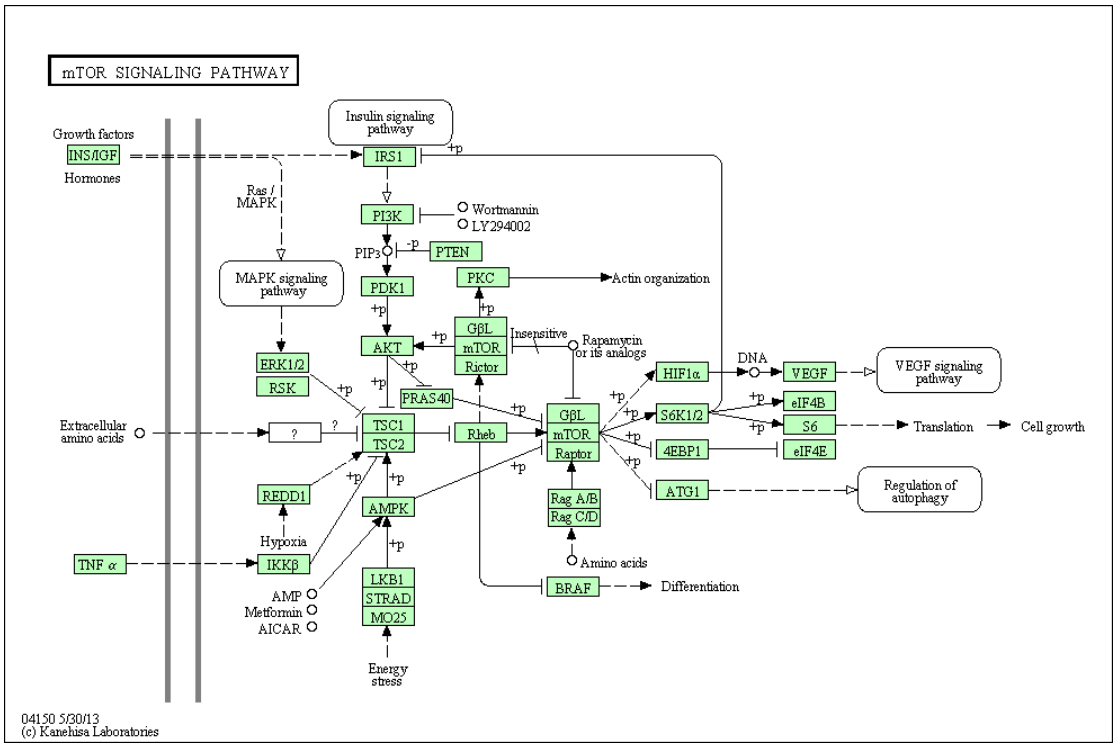

Figure 6.7 Targets of miRNAs in the mTOR signalling pathway

In green are the experimentally predicted target of hsa-miR-148b-5p and hsa-miR-34a-5p that are part of the mTOR signalling pathway, both miRNAs were increased after the knock down of FTO. Download from DIANA-miRPath v3.0 [206].

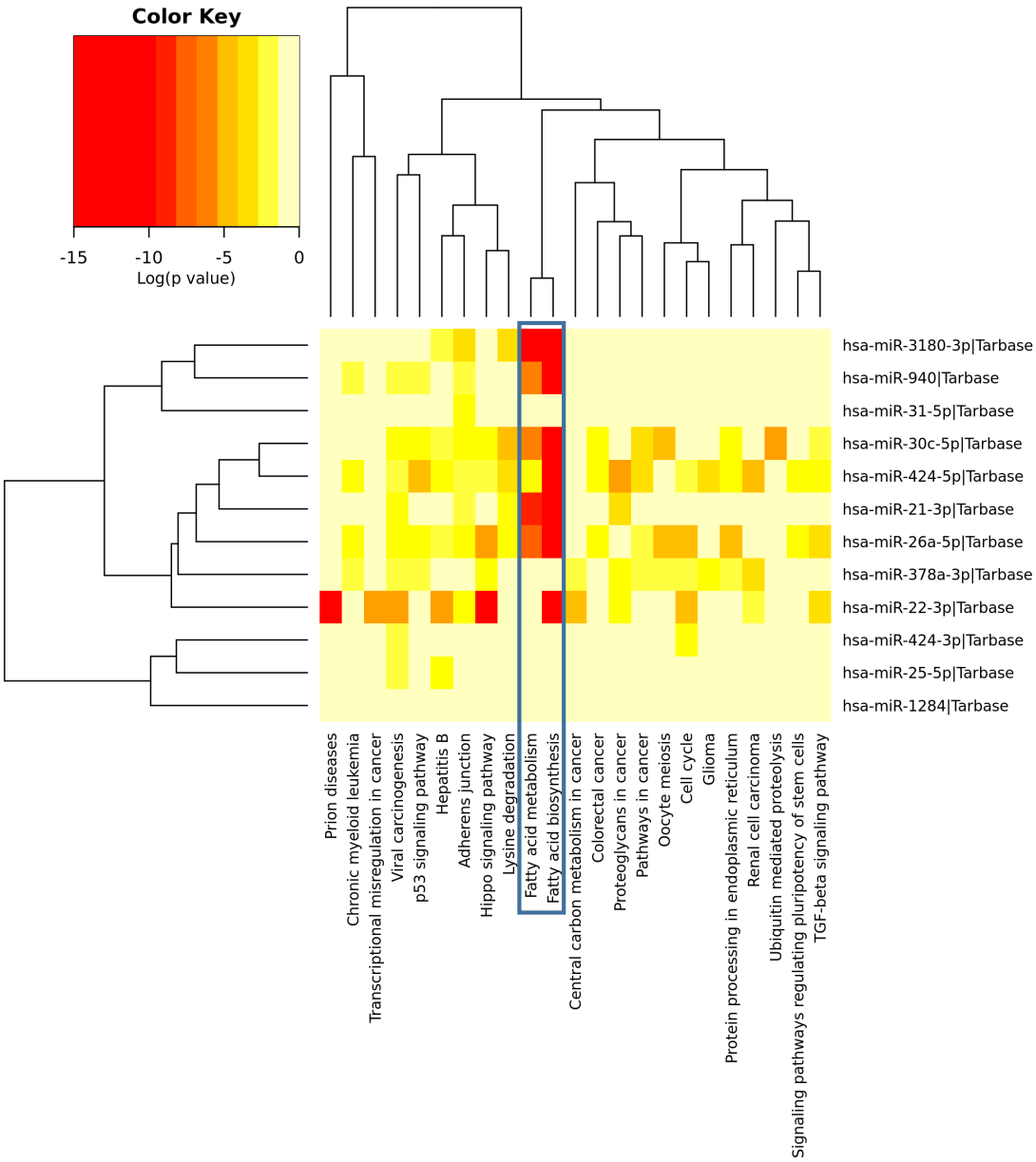

Figure 6.8 Heatmap for miRNAs that were decreased in the miRNA sequencing analysis

Pathway analysis showed that the twelve miRNAs that were decreased in the miRNA sequencing analysis target genes involved in fatty acid metabolism (blue boxes). (n: 4 control and 4 siRNA1 exposed wells).

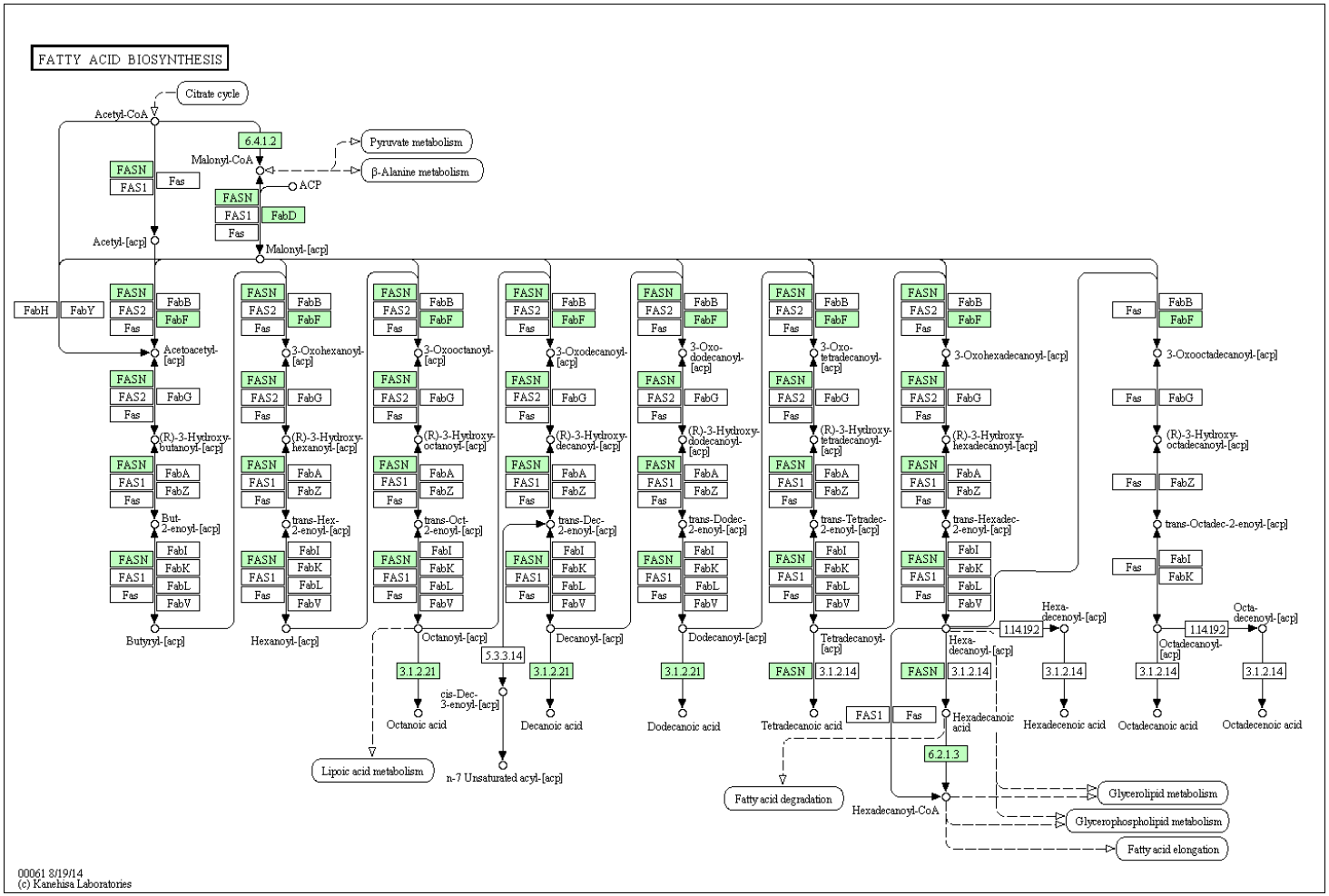

Figure 6.9 Targets of miRNA in the fatty acid biosynthesis pathway

In green is the experimentally predicted target from the miRNA pathway analysis. Download from DIANA-miRPath v3.0 [206].

6.5 DISCUSSION

In chapter 5, a correlation between placental *FTO* gene expression, amino acid transporters expression and miRNA expression was found, and a potential mechanism of how *FTO* could be acting in the placenta was proposed. The aim of this chapter was to determine if an *in vitro* knock down of *FTO* gene would affect the overall miRNA expression in the cells and the downstream targets of these miRNA. It was found that the knock down of *FTO* changed the expression of two miRNAs, but did not affect the overall miRNA expression in the cells. However, the exploratory analysis using the miRNAs whose expression was changed by the lack of *FTO* (using the unadjusted p-value), showed that these miRNAs targeted genes involved in fatty acid synthesis and degradation and mTOR signalling pathway. Additionally, it was found that *FTO* knock down increased the expression of the amino acid transporter *TAT1.* These findings suggest that the lack of *FTO* as a demethylase does not affect the total miRNA processing but it also does not rule out the possibility that *FTO* could be involved in regulation of gene expression in the cells.

6.5.1 *FTO* knock down and miRNA expression

In this study, it was proposed that the knock down of *FTO* could affect the overall expression of miRNA. Contrary to the hypothesis *FTO* knock down had a limited effect on miRNA expression so *FTO* is unlikely to be acting by a global effect into miRNA methylation-mediated processing. Data about the effects of methylation in miRNA is relatively new, Alarcon *et al,* proved that m^6A is present in the pri-miRNA regions and that when methyltransferase-like 3 (METTL3 – an enzyme that methylates RNA) is knock down or overexpressed, the levels of miRNA will be reduced or increased respectively [257]. That study also proposed that m^6A in pri-miRNAs was necessary for their processing to mature miRNAs. In this study, it was found that the knock down of *FTO* (RNA demethylase) did not affect the overall expression of miRNA. A possible explanation could be that the demethylation of pri-miRNAs is not as active as the methylation process. The lack of *FTO* may not be affecting the methylation levels of the pri-miRNAs and therefore not affecting the total miRNA levels in the cells (Figure 6.10). Another possibility is that the activity of *FTO* is greater than METTL3 activity,

therefore, a reduction in *FTO* levels did not produce an important reduction in the demethylation activity. In this study levels of methylated RNA or *FTO* activity was not measured but they could be evaluated in future studies.

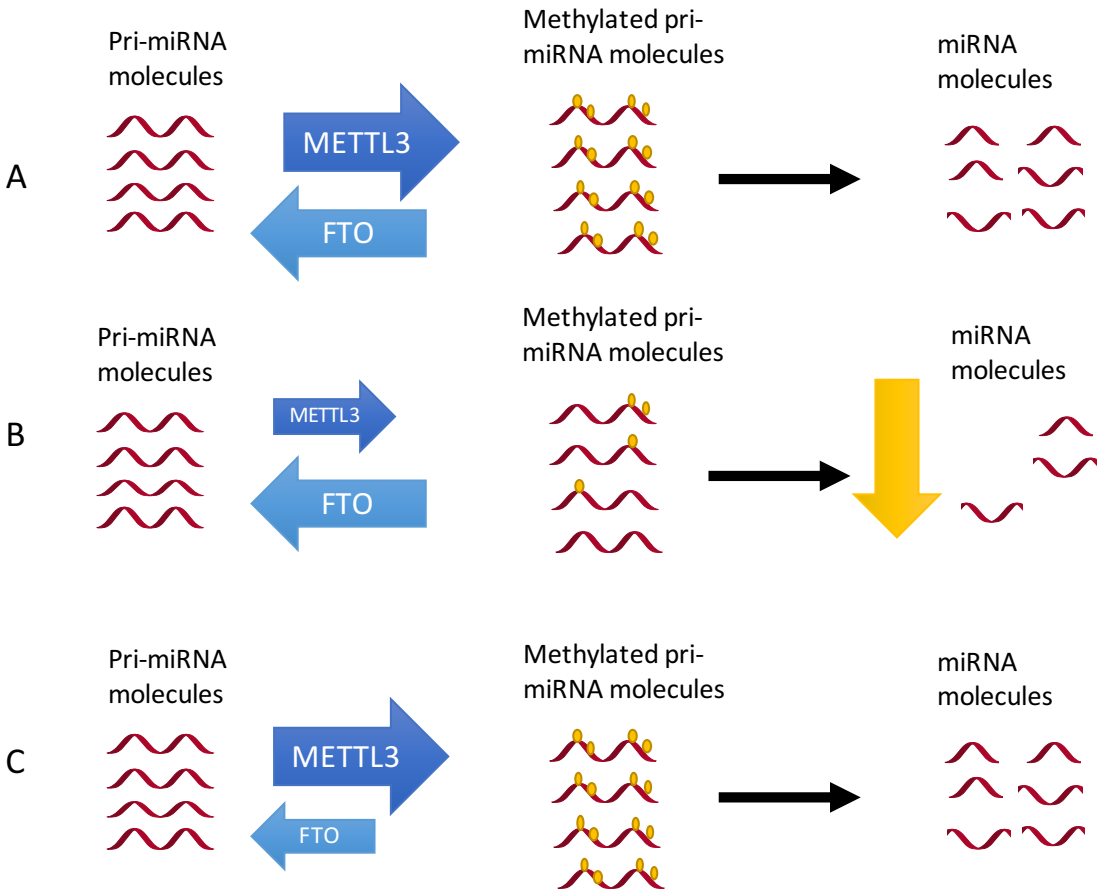

Figure 6.10 Effects of knock down of RNA methylases and demethylases

Methylation of pri-miRNAs has been proposed as a necessary step of these molecules. Figure A shows the process where the levels of miRNA in the cells are determined by the activity of methyltransferase like 3 (METTL3) and FTO (RNA demethylase). B. shows what happens when the METTL3 is knock down producing a reduction of miRNA levels. C. Shows this study found in this study that a knock down of FTO does not affect the miRNA levels.

Berulava *et al*, have recently reported the effects of the *FTO* knock down in miRNA levels in HEK 293 cells [261], they found that miRNA levels were modified after the knock down (51 miRNA with modified levels) but not in a consistent manner (42 increasing and 9 decreasing). This study also reported a higher number of total miRNA detected by the sequencing (876 *vs* 451 in this study). Possibly, the difference in the number of modified miRNA by the *FTO* knock down could be explained by the fact that this study detected less miRNA during the sequencing. The possibility that the miRNA in the

samples of this study were degraded is low, since the quality sample was tested before the sequence. Additionally, mature miRNA are stable molecules and no specific ribonucleases have been described for them so their concentration is stable when they are kept in the appropriate conditions [262]. Nevertheless, both studies found that the knock down of *FTO* did not affect the overall levels of miRNA but did affect miRNA levels suggesting that the demethylase activity could be involved in the processing of miRNA.

6.5.2 *FTO* knock down and pathway analysis

The other aim of this study was to determine the genes that were targets of the miRNA modified by the knock down of *FTO.* In the previous chapter, it was proposed that *FTO's* function as a RNA methylase could be involved in the placenta sensing mechanism. In this chapter, it was already discussed that *FTO* did not affect the overall expression of miRNA. However, the analysis of the targets of the modified miRNA showed that mTOR pathway and fatty acid metabolism were affected and also the expression of one amino acid transporter (*TAT1*) was increased in the knock down. It is possible that *FTO* is part of the sensing mechanism in the placenta by a different mechanism that the one proposed in chapter 5.

As it was mentioned in the previous chapter, *FTO* has been found to be necessary for mTOR activation and the lack of *FTO* produced a decreased in the downstream activation of mTOR targets [153]. In this chapter, it was shown that the reduction of *FTO* increased two miRNAs that affected genes in the mTOR signalling pathway. It is possible that *FTO* is acting by modifying miRNA expression and indirectly modifying mRNA expression. In this study, the levels of the target genes of the miRNA were not measured in the knock down samples in order to determine if the target genes were affected. The expression of these genes could be measured in order to determine if these targets were reduced by the knock down. Levels of amino acid transporters were measured in this study showing an increase in the gene expression of *TAT1* after the knock down of FTO. It is possible that *FTO* is involved in mTOR regulation and that the lack of *FTO* is affecting mTOR and amino acid transporter expression by modifying the levels of specific miRNA (Figure 6.11). Previously, it has been shown that a reduction in

essential amino acid levels also reduced *FTO* expression [154]. This could also be considered a potential sensing pathway. Studies, where the reduction of specific amino acids and *FTO* knock down, are combined and miRNA levels and mTORC target genes are measured could help to understand the relationship between *FTO* and nutrients sensing mechanism.

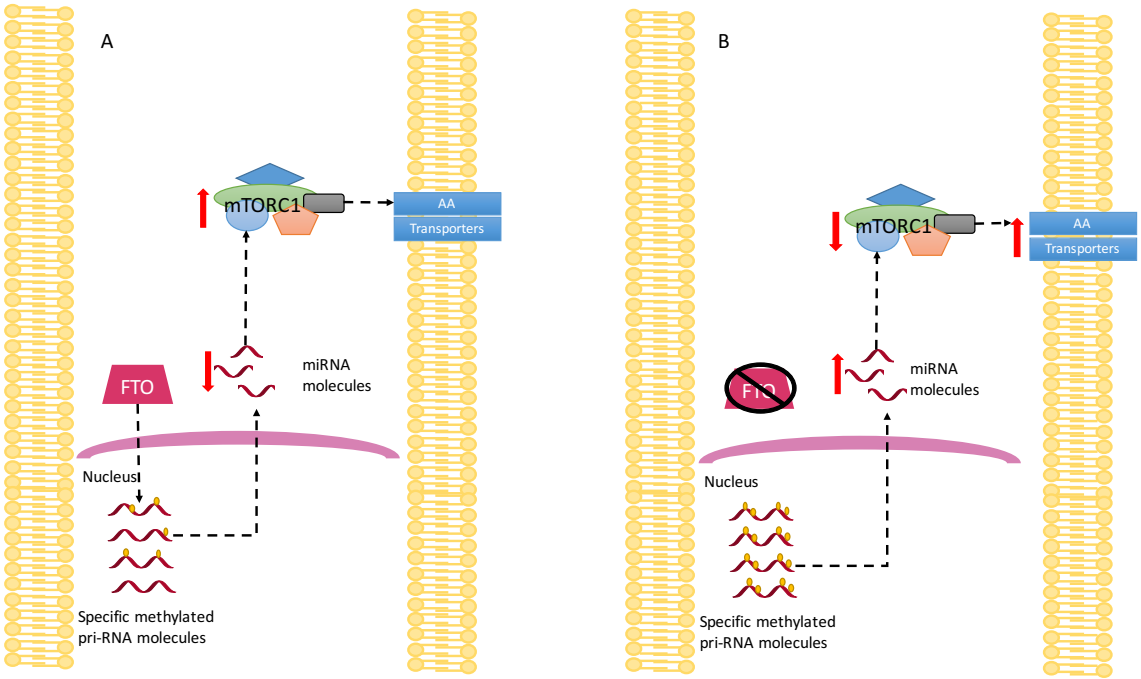

Figure 6.11 Proposed mechanism of *FTO* interaction with mTORC1

A. The figure shows the proposed interaction of FTO and mTORC1, where FTO demethylase modified specific pri-miRNA and reduced the expression of the miRNAs that act over genes involved in the mTOR signalling pathway. Figure B shows what happened in the cells when FTO was knocked down producing and increased in miRNAs that target mTOR genes and therefore produced a decreased in mTORC1 and an increase in amino acid transporter expression.

FTO knock down also showed that fatty acid metabolism could be affected indirectly by the modifications of miRNAs. This is interesting in the light of studies linking *FTO* to obesity and fat mass. *FTO* has been previously shown to be involved in adipogenesis. Zhao *et al*, showed that *FTO* expression affected m^6A levels during the adipogenesis process and also showed that mRNA splicing of specific genes in adipose tissue is regulated by *FTO* [255]. Merkestein *et al*, showed that in mouse embryonic fibroblast (MEF) after induction of adipogenesis, the proliferation of *FTO* knock out MEFs was reduced when compare with the wild type MEFs and MEFs overexpressing *FTO*

showed a greater proliferation after adipogenesis induction. They also showed that *FTO* overexpression promotes adipogenesis *in vivo* in a mice model [260]. In this study, a potential relationship between *FTO* and fatty acid synthesis was described indicating that the involvement of *FTO* in the function of adipose tissue could be at different levels. Modifications in metabolic pathways could be another potential mechanism of how *FTO* helps a tissue to respond to modifications in nutrient availability. It is possible, that the paper of *FTO* in weight gain is mainly over adipose tissue. *FTO* has been shown to be able to modified amount of pre-adipocytes and its maturation and in this study were showing a potential regulation of *FTO* in lipid synthesis and storage. Studies in adipocytes in order to determine the importance of *FTO* in fatty acid mobilization could help to understand this process.

In this study *PLAC2*, a lncRNA was measured to determine whether *FTO* methylation activity could be affecting the stability of RNA molecules in general. In a previous study, m^6A modification was found to interact with proteins that regulate RNA degradation (YTHDF2). They showed that *PLAC2* had an m^6A area that could be recognised by the protein and when this protein was knocked down *PLAC2* lifetime was increased [257]. In this chapter, *PLAC2* was not modified by the lack of FTO, which indicates that the demethylase activity probably is not affecting the stability of this molecule. However, it is necessary to measure more genes that have been reported to be affected by the RNA methylation levels and also determined whether they are being targeted by the degradation proteins decreasing their lifespan.

6.5.3 Limitations and future work

One of the limitations of this study is that the miRNAs were not validated due to a technical issue and the time available, also the targets of the miRNAs could not be measured due to the time available. In order to determine if the modifications via *FTO* have an important effect in the mTOR pathway or in fatty acid biosynthesis measures of these genes and/or their proteins will help to confirm what was proposed.

An additional limitation to this study is that the efficiency of the experiment was measured just at the mRNA levels so this study was not able to confirm that the knock

down of *FTO* was also at the protein levels. Since the knock down levels were 70%, a reduction in protein levels is expected but for the next studies a confirmation using western blot is necessary.

Furthermore, in this study the interaction between *FTO* knock down and nutrient restriction has not evaluated. Previous studies have shown that *FTO* is affected by nutrient levels, but an experiment to determine whether *FTO* absence modifies the respond to nutrients levels is necessary.

Studies using photoactivatable-ribonucleoside-enhanced crosslinking and immunoprecipitation could be used to determine the most common regions of interaction between *FTO* and RNA molecules and possibly determine if *FTO* recognises specific sequence as a demethylase.

It would also be interesting to do an RNA and miRNA sequencing analysis in the same samples at the same time in order to determine if the predicted targets of the miRNA are actually changing.

6.6 CONCLUSION

Reduced *FTO* gene expression did not affect the overall expression of miRNAs in HEK 293 cells. However, *FTO* has an effect on specific miRNA expression and potentially by the modification of these miRNAs could be affecting cellular function.

CHAPTER
7 GENERAL DISCUSSION

7.1 OVERVIEW

The broad aim of this thesis was to explore the mechanisms by which the placenta senses the maternal environment. In chapters 3 and 4, the placental response to a maternal high-fat diet and metformin treatment was investigated. In chapters 5 and 6, the role of FTO in the placenta and its potential role in the regulation of miRNA was investigated. Placental responses to maternal plasma nutrient levels have been focused on the mTOR signalling pathway and its involvement in the regulation of nutrient transport. In this study, evidence for alternative sensing pathways in the placenta were investigated. These alternative mechanisms included circadian rhythms, sirtuins and FTO, and could be involved in the control of placental function as they were modified in response to the maternal environment. This study provided some evidence for the role of these pathways, but more work is needed in order to demonstrate if they operate independently of mTOR. The studies did show that the placenta can respond differently to different stimuli suggesting that there are multiple sensing systems in operation.

It was proposed that modifications in the maternal environment, such as diet alterations or drug treatments would stimulate distinct cellular pathways and produce different effects on placental nutrient transport. The study in chapter 3 showed that maternal exposure to the drug metformin altered placental function independently of a high fat diet. This also showed that metformin is affecting placental function acting directly on the tissue and indirectly by affecting maternal signals to the placenta. Excessive consumption of fat and hypercaloric diets has increased in the population producing an increase in the prevalence of maternal obesity and gestational diabetes which has deleterious effects on the health of the baby. Use of drugs such as metformin during pregnancy to treat these conditions could however, modify placental function and potentially affect fetal development.

The potential involvement of FTO as a placental nutrient sensor was studied in chapters 5 and 6. We were able to show that placental mRNA expression of *FTO* was associated with fetal growth and baby's anthropometric measures. Association

between SNPs in *FTO* and BMI have been described in different populations, but it is still not clear whether FTO function is involved in fetal weight gain. In this study, it was proposed that FTO could be acting as a posttranscriptional regulator of miRNA production. It was found that the reduction of *FTO* gene expression did not affect the overall miRNA expression in cells but affected the expression of miRNA that targeted genes that are part of the mTOR signalling pathway and fat metabolism.

7.1.1 Placental sensing pathways

The overall aim of this study was to stablish how the placenta responds to modifications in the maternal environment. The placenta is able to adapt to changes in the maternal environment but the mechanisms behind this process are poorly understood [78]. However, nutrient-sensing pathways such as mTOR and AMPK have been strongly involved in the placental response to maternal modifications [143]. These pathways regulate metabolism in the cell, modifying the degradation, synthesis, import and export of nutrients in response to their availability. In the placenta, modifications in the transport of nutrients to the fetus become extremely important since they will determine fetal growth during the pregnancy but they will also influence adulthood health.

In the placenta, mTOR is able to respond to maternal signals such as hormone levels, nutrient supply (increase and decrease), and oxygen supply. The signals involved in how the nutrients are sensed by mTOR are not completely clear [138]. In this study, other molecules that could be involved in the sensing mechanism were investigated. It was shown that molecules such as clock genes are modified in the placenta after the exposure to a high fat diet or to an antidiabetic drug. It is difficult to determine if the modifications in the clock genes were independent of mTOR or other sensing pathways described in the placenta (Figure 7.1). A potential mechanism is that the high fat diet is producing a glucose intolerant state during the pregnancy that modifies the maternal hormone levels or the ability of the tissue to recognise them. This could produce mitochondrial dysfunction and energy reduction in the placenta, measured as the ratios of molecules such as ADP/ATP or NAD/NADH that would alter clock gene expression directly or indirectly. Modifications of clock genes due to a mitochondrial

dysfunction has been proposed as an explanation of the development of non-alcoholic steatohepatitis in mouse liver [214]. It was proposed that the exposure to high fat diet altered the cellular energy status and sirtuins sensed the modifications and inhibited clock gene expression as a result. In this study, sirtuin gene expression was not modified by the exposure to a high fat diet, which indicates that other molecules could be involved in the placenta response. Also, in this study metformin reduced clock gene expression. Metformin action in the cells involves the inhibition of complex I in the mitochondria and this action helps to increase glucose tolerance.

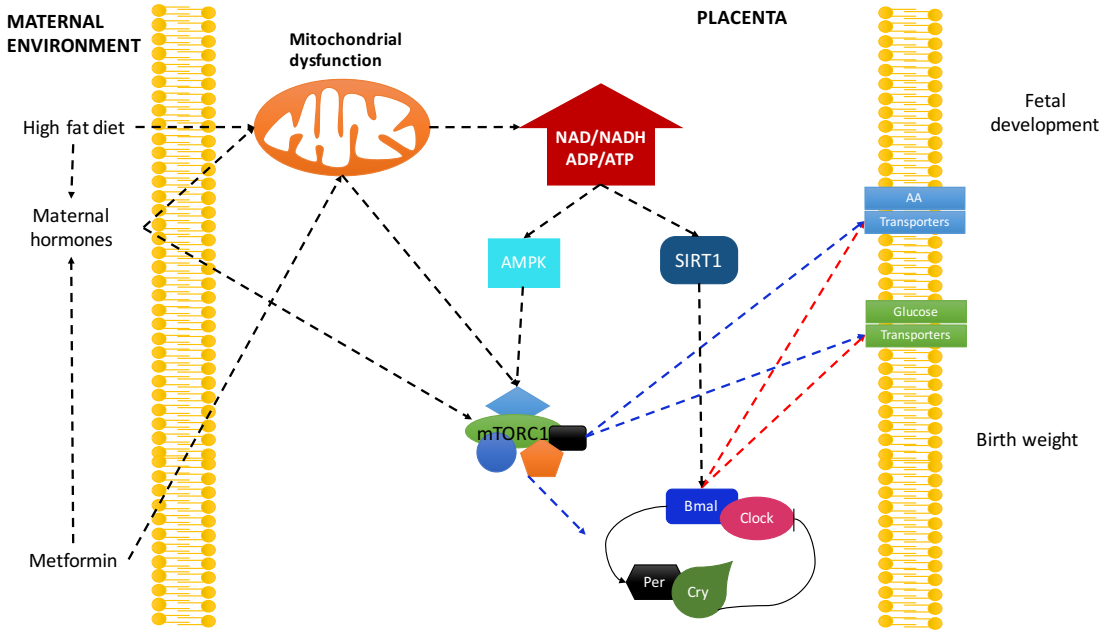

Figure 7.1 Placental response to specific modifications in maternal environment

Exposure to a high fat diet or metformin during normal pregnancy could produce modifications in maternal signals affecting mitochondrial function (black arrows). The placenta response to the modifications in energy status could be through mTOR (blue arrows) or AMPK-mTOR. These pathways could be responsible for both the nutrient transporter and clock gene modifications found in this study. Also, the altered energy status could act through sirtuins and modified clock gene expression and as a response, the clock genes could modify the expression of nutrient transporters in the placenta (red arrows).

This could be counterproductive in a normal pregnancy producing an altered energy status in the placenta and modifying the energy use and nutrient transport (Figure 7.1). This study was able to show that molecules such as clock genes and FTO could be

modified by the maternal environment but whether they are acting independently of mTOR needs to be studied.

An additional potential sensor that was suggested in this study was FTO, it was proposed that FTO could be acting as a sensor in the placenta by altering levels of specific miRNA that affected the mTOR signalling pathway and fatty acid metabolism. It was proposed that the mTOR signalling pathway function was reduced by the increased expression of miRNAs and modified amino acid transporter expression as a result. Understanding the molecular mechanism of placental adaptations to altered nutrient levels will require more research.

This study also investigated how the placenta responds to metformin exposure. It showed how exposure to metformin for more than half of the mouse pregnancy modified several functions related to placental function, development, and metabolism. This mouse model could be an example of the effects of metformin during a pregnancy that is complicated with type II diabetes or polycystic ovary syndrome; both are diseases that receive metformin treatment throughout pregnancy. Establishing the effects of a medicine in a tissue is a complex process that involves the knowledge of the pharmacokinetics of that drug. Metformin pharmacokinetics have previously been studied in pregnancy in humans [225], showing that maternal plasma metformin concentration and renal clearance change during the pregnancy. That study also showed that metformin concentration in cord blood at the end of the pregnancy is highly variable, however, the concentration of the drug was not measured in the placenta. In human pregnancy, metformin is used to treat gestational diabetes and type II diabetes, which could produce a placental response to the drug depending on the length of exposure (Figure 7.2). Hypothetically in normal pregnancy placental function is not altered and the placenta is working at its normal potential; when a complication occurs placental function will decrease accordingly. The treatment for a pregnancy complication will improve placental function to some extent but it is difficult to predict whether the treatment is able to return the placenta to its full "normal function".

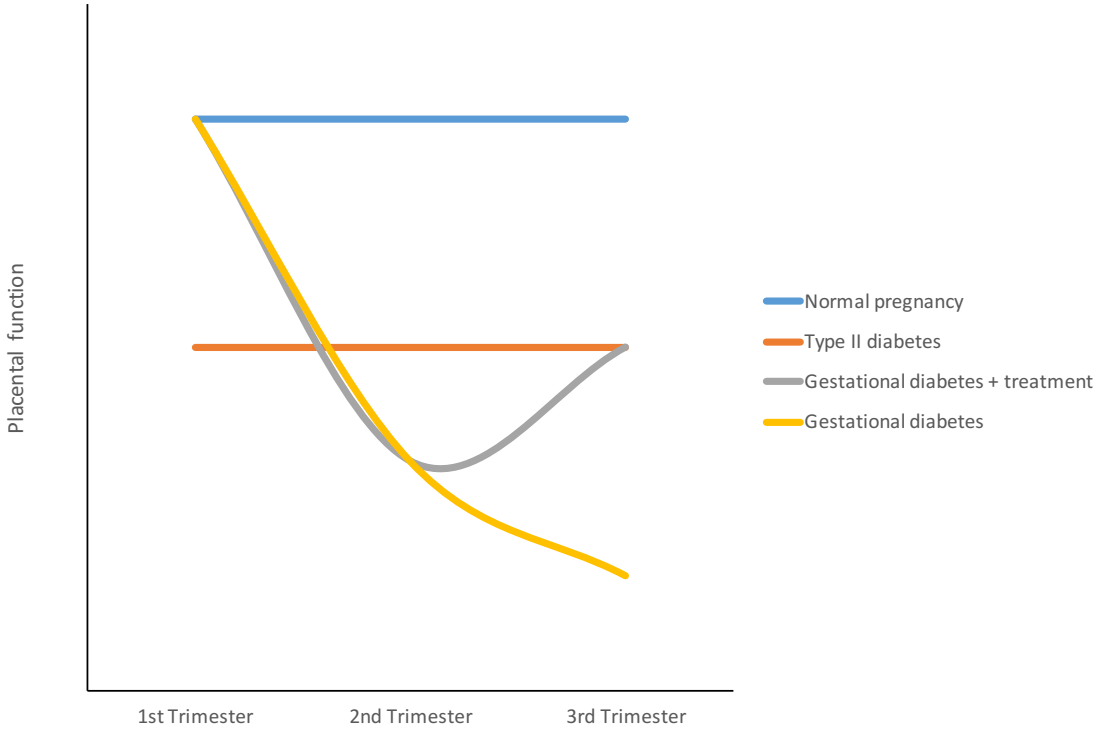

Figure 7.2 Placental function with diabetes during pregnancy

Hypothetically, in normal pregnancy, the placenta is working at its normal potential. Modifications in placental function due to a treatment are complex and depend on when the complication starts and when the treatment is provided. In a pregnancy complicated with controlled type II diabetes, placenta function will be reduced from the beginning of the pregnancy and the exposure to the drug will affect not just placental function but also placental development. In a pregnancy complicated with gestational diabetes, the placental function will be reduced as the pregnancy advances and it will continue if treatment is not provided. When treatment is provided placental function could be partially recovered and in this case, the drug will affect placenta function but its effect on placenta development would be less.

The prevalence of maternal obesity, type 2 diabetes and gestational diabetes have increased in the last decade in the United Kingdom and around the world. Gestational diabetes is developed in about 5% of pregnant women and oral hypoglycaemic agents such as metformin or glibenclamide are used to treat this condition, as they are considered safe to use during pregnancy [210-212]. The findings in this study show that metformin effects in the placental function are not directly modifying the effects of a obesity-induced diet and is possible that the use of metformin during or before pregnancy have additional effects in the placenta formation, metabolism and

potentially in fetal development. More studies are necessary in order to determine the effects of the oral hypoglycaemic during the pregnancy.

In all tissues, the ability to modify their function according to the nutrient availability is basically to assure survival when conditions are not favourable and to store energy when an excess is available. In the placenta, the response to these modifications will affect not only the tissue but also the fetus that depends on the placenta to obtain its nutrients. Regulation of nutrient transporter levels and activity has been one of the main focuses of the study of placenta sensing mechanisms. In this approach, it is assumed that nutrient transporter modifications will provide the necessary information about what is happening in the pregnancy. This approach without including placental metabolism assumes the placenta as a channel for the transit of molecules between the mother and the fetus. Recently, it has been shown that the amino acids in the placenta could exist as part of proteins and as free amino acids inside the tissue [98,263] and the rate of amino acid transfer depends on the metabolism of them inside the placenta. This study has shown how, not just metabolic pathways, but also pathways related with placental development could be altered by the chronic exposure to a drug. Study of placenta function needs to be treated as a whole, taking into consideration the complexity of the tissue. Placental adaptation to maternal conditions and its capacity to improve fetal supply even in adverse conditions has been studied to a great extent. Different animal models and both normal and altered human pregnancy show how the placenta will adapt its function and size to fulfil fetal necessities [119]. Studies on the placental adaptations following exposure to drugs are less available. In this study, it was shown how chronic exposure to an antidiabetic drug has effects on how the nutrients are used and transported in the tissue (essential adaptations of placental function). It also showed that drug exposure can have effects on other important functions of the placenta such as angiogenesis and hormones production. Figure 7.3, is a representation of the possible adaptations that the placental could undergo after a modification in the environment. Exposure to drugs such as metformin at different points during pregnancy (depending on the type of conditions that is being treated) will produce a placental adaptation that will involve the tissue to modify its function in order to accept the new conditions.

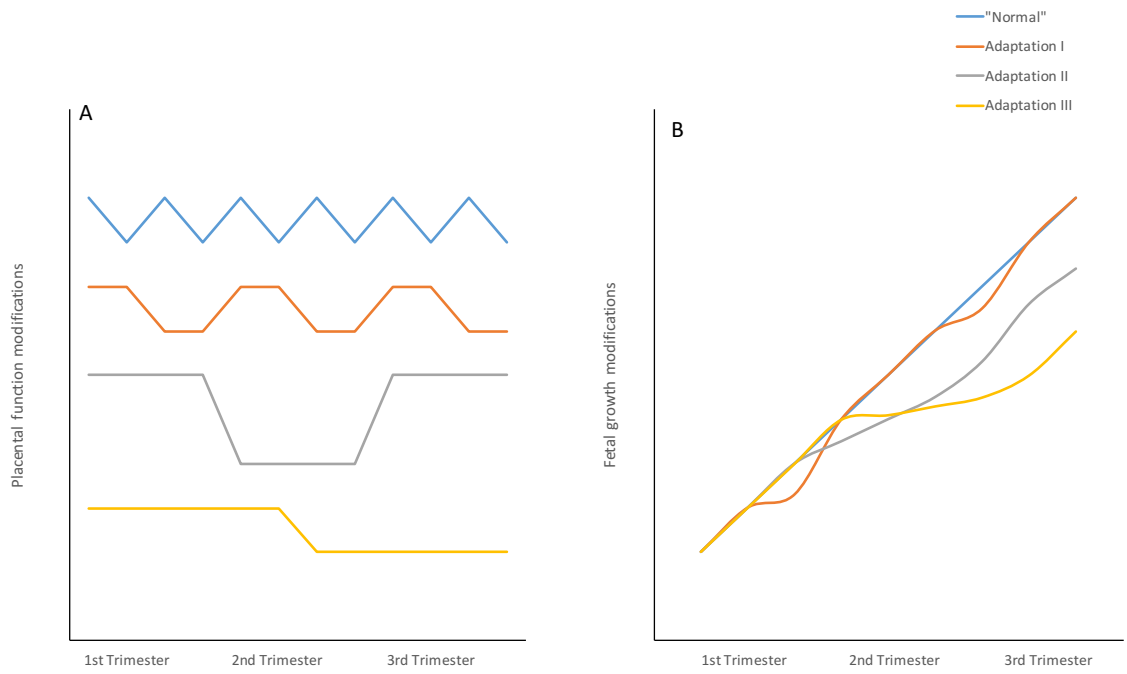

Figure 7.3 Proposed model of placental adaptations

The placental adaptations to the environment are a dynamic process during the pregnancy, the capacity of the placenta to adapt to different situation will produce modifications in the placental status during the pregnancy. The idea is that the "normal" placenta will be able to adapt to different stimuli in relatively short periods of time assuring nutrient supply to the fetus. Adaptation I and II, are proposed when the capacity of the placenta to adapt to new environments is reduced so it takes longer to be able to go back to its normal function. In this situations alterations in fetal growth could be observed during the pregnancy but not always observed at the end of it. And last is adaptation III where the placental response to the new environment is a modification in the function that will produce a "new" placenta status that will remain during the rest of the pregnancy. Figure A shows placental function adaptions and figure B shows fetal growth modifications.

7.2 LIMITATIONS

In this study, it was proposed that clock genes could be part of the placental sensing mechanism, and it found a reduction in the placental expression of them when exposed to an altered maternal environment. In order to determine if a modification in the circadian clock has occurred in a tissue samples need to be collected at specific time points. Time-point experiments are difficult to set up due to the amount of animals that are needed and the subsequent samples that need to be analysed. In this study, it was shown that clocks genes were differentially expressed however a time

point experiment is necessary in order to determine if the modification in maternal diet or drug exposure are producing a shift in the circadian clock in the placenta.

In this the study an additional limitation was the targeted gene approach adopted in most of the chapters. A targeted gene approach targeted genes selected as potential nutrient sensors, which reduced the extent of the findings. Selecting target genes helps to avoid excessive analysis without a specific target but can produce a limited picture of what is happening in a tissue without showing the whole process. In some experiments we were able to use RNA sequencing which allows an unbiased approach to identify genes changing in response to the stimuli. The advantage of RNA sequencing is that it identifies genes that might not have been expected to change. The disadvantage of such as sequencing is that it is not known if the genes changing are direct changes or downstream effects and it also produces a large amount of data which may obscure the primary changes. At the beginning, this study was focused on the selected genes but if a broader analysis could have been used it is possible that other target genes could have been identified as candidates.

This study was focused on the regulation of gene expression, however, regulation in the cell occurred at different levels. Mechanism such as modification in protein levels, allosteric modifications and covalent modifications such as phosphorylation are also an important part of placental adaptation and they were not included in this study. Broader approaches, such as proteomics analysis after affinity purification could be used it. In this method the protein to be analysed will be previously selected using beads that contain specific binding molecules for the protein of interest. An example of this is the affinity enrichment of kinases that use an ATP-analog in the solid matrix to capture the kinases present in a sample. Techniques such as cell permeable activity-based probes, can also be used in order to determine function in live cells. The probe can be added to the cell culture, in the experiment and it will bind the protein of interest. During proteomics analysis the probe will help to identified which proteins interact with it. In the study of RNA function and regulation, methods such as cross-linking immunoprecipitation and RNA sequencing analysis help to determine

interaction between proteins and RNA molecules. Using those techniques will help to increase the power of the findings in new studies.

Additionally, sample size is a limitation in this study. Samples in the human cohorts were selected by their availability, but a retrospective sample calculation showed that bigger numbers were necessary.

7.3 FUTURE WORK

One of the questions that this study raises is whether metformin exposure during human pregnancy will produce similar modifications in placental function as the ones that were found in mouse placenta. A possible approach to addressing this question is using human cohorts where normal pregnancy can be compared with pregnancy complicated with gestational diabetes or type two diabetes. This could allow the effects of metformin on the human pregnancy and on placenta function to be determined. It could also help to understand whether there is a difference between chronic metformin exposure (type two diabetic pregnancies) and short-term metformin exposure (gestational diabetes). Placenta collected from these cohorts could be used for placental perfusion experiments, in order to evaluate how metformin exposure alone and in the presence of different hormones affected nutrient transport in the placenta. Gene and protein expression could be measured to help to understand which molecules are responding to metformin.

A question that it is necessary to address is the consequences of using metformin when a metabolic condition is not present. Metformin is also used to help to reduce weight in overweight women that want to become pregnant and women with polycystic ovary syndrome [224,264]. A following cohort with women that used metformin to reduce weight before pregnancy can help to understand the effects of metformin when used in the absence of diabetes.

Additional studies in order to determine downstream effects of metformin in the placenta are also necessary. Studies in mouse, suggest that metformin exposure when

is not necessary for glucose control could have deleterious effect on the liver [265]. It is possible that the placental response to metformin is different to the liver response. A mouse model where after metformin exposure, mitochondrial function and AMPK activation is measured, could help to understand the mechanism of action of this drug in the placenta.

Also, a question that is necessary to address is the potential role of *IRX3* in weight gain during the pregnancy. *IRX3* has been proposed as the gene that is affected by the SNP in *FTO,* therefore, it is important to determine whether IRX3 is involved in the control of placental nutrient transport to the fetus. In this study, it was shown that *IRX3* was expressed in the term human placenta but in levels below the qRT-PCR detection capacity. An approach where the mRNA and protein levels of *IRX3* gene are measured in the placenta at different stages of the pregnancy could help to understand which could be the best time and form to measure this molecule. Additionally, *IRX3* is a transcription factor that has been involved in neural development and it has been shown to be expressed in the mouse placenta. This could allow the use of an *IRX3* knock out mouse model where the effects of the lack of this gene in placental development and function could be studied in more detail.

It is important to address the role of the methylation and demethylation of RNA molecules in tissue function. Methylation of RNA is one of the most common postranscriptional modifications. Understanding the involvement of this process in RNA transport, regulation and processing is one question that needs to be addressed. In this study, it was shown that knock down of the *FTO* gene did not modify the overall levels of miRNA in HEK 293 cells. However, other studies have shown that the knock down of methylase proteins did affect miRNA levels and lncRNA levels in HEK 293 cells. This raises the question as to whether there is a role of methylation and demethylation of RNA and the later destination of these molecules in the cells. A possible way to address this question is to knock down methylases and demethylases in cell culture and then measure modifications in the levels of mRNA, miRNA, and lncRNA. Also in the same experiment, a precipitation of methylated molecules could be done before the sequencing in order to compare how the population of the RNA

molecules was modified. Additionally, in the placenta, the importance of RNA methylation needs to be studied. Measures of methylated RNA molecules in term placenta could help to understand how important this process is and its potential involvement in placental function.

7.4 CONCLUSION

Placental function is controlled at different levels. Understanding the relationship between maternal and fetal signals and their importance in placental adaptation will help to improve the current understanding of pregnant physiology and to develop effective interventions to improve fetal and maternal health.

Appendices

Appendix A List of abstracts

1. **Does FTO control de amino acid transporter expression in human placenta?** *Mosquera M***,** Barton S, Holloway J, Inskip H, Godfrey K, Cleal JK Lewis RM and the SWS study group. (Faculty of Medicine research conference and Centre of trophoblast Research meeting 2014).

2. **The effect of maternal high fat diet and metformin during pregnancy on placental expression of amino acid transporter and circadian clock genes in the mouse.** *Mosquera M***,** Thomas H, Cleal JK, Cagampang FR, Lewis RM. (Physiological Society Meeting, 2014).

3. **Placental FTO gene expression is correlated with maternal fatty acid concentration in blood at early and late pregnancy.** *Mosquera M***,** Cleal JK, Barton SJ, Holloway JW, Sibons C Inskip HM, Calder PC, Cooper C, Godfrey KM[1], Lewis RM and the SWS study Group. (International Federation of Placental associations, 2014).

4. **The effect of maternal high fat diet and metformin during pregnancy on placental expression of amino acid transporter and circadian clock genes in the mouse.** *Mosquera M***.,** Thomas H., Cleal J.K., Cagampang F.R. and Lewis R.M. (Faculty of Medicine research conference 2015).

Appendix B Publication

Contents lists available at ScienceDirect

Placenta

journal homepage: www.elsevier.com/locate/placenta

Relation of *FTO* gene variants to fetal growth trajectories: Findings from the Southampton Women's survey

S.J. Barton [a, *], M. Mosquera [b, c], J.K. Cleal [b], A.S. Fuller [a], S.R. Crozier [a], C. Cooper [a, d], H.M. Inskip [a], J.W. Holloway [e], R.M. Lewis [b], K.M. Godfrey [a, f]

[a] MRC Lifecourse Epidemiology Unit, Faculty of Medicine, University of Southampton, Southampton SO16 6YD, UK
[b] Institute of Developmental Sciences, Faculty of Medicine, University of Southampton, Southampton SO16 6YD, UK
[c] Department of Physiological Sciences, Faculty of Health, University of Valle, Cali, Colombia
[d] NIHR Musculoskeletal Biomedical Research Unit, University of Oxford, Oxford, OX1 2JD, UK
[e] Human Genetics and Genomic Medicine, Human Development & Health, Faculty of Medicine, University of Southampton, Southampton SO16 6YD, UK
[f] NIHR Southampton Biomedical Research Centre, University of Southampton and University Hospital Southampton NHS Foundation Trust, Southampton, SO16 6YD, UK

ARTICLE INFO

Article history:
Received 27 July 2015
Received in revised form
17 December 2015
Accepted 21 December 2015

Keywords:
Fetal growth trajectories
FTO genotype
MC4R genotype
Placental amino acid transporter expression
Placental FTO expression

ABSTRACT

Introduction: Placental function is an important determinant of fetal growth, and fetal growth influences obesity risk in childhood and adult life. Here we investigated how FTO and MC4R gene variants linked with obesity relate to patterns of fetal growth and to placental FTO expression.
Methods: Southampton Women's Survey children (n = 1990) with measurements of fetal growth from 11 to 34 weeks gestation were genotyped for common gene variants in FTO (rs9939609, rs1421085) and MC4R (rs17782313). Linear mixed-effect models were used to analyse relations of gene variants with fetal growth.
Results: Fetuses with the rs9939609 A:A FTO genotype had faster biparietal diameter and head circumference growth velocities between 11 and 34 weeks gestation (by 0.012 (95% CI 0.005 to 0.019) and 0.008 (0.002–0.015) standard deviations per week, respectively) compared to fetuses with the T:T FTO genotype; abdominal circumference growth velocity did not differ between genotypes. FTO genotype was not associated with placental FTO expression, but higher placental FTO expression was independently associated with larger fetal size and higher placental ASCT2, EAAT2 and y + LAT2 amino acid transporter expression. Findings were similar for FTO rs1421085, and the MC4R gene variant was associated with the fetal growth velocity of head circumference.
Discussion: FTO gene variants are known to associate with obesity but this is the first time that the risk alleles and placental FTO expression have been linked with fetal growth trajectories. The lack of an association between FTO genotype and placental FTO expression adds to emerging evidence of complex biology underlying the association between FTO genotype and obesity.

1. Introduction

Obesity is a major public health problem as it increases the risk of coronary heart disease, stroke, metabolic syndrome, some cancers and a wide range of other diseases. Children who are obese are likely to continue to be obese when they become adults, highlighting the need for research into early determinants of obesity [1]. In order to develop effective interventions it is important to understand the genetic and environmental determinants of obesity. There is evidence suggesting critical windows during fetal and early postnatal life, within which altered development may predispose the individual to obesity in later life [2,3].

Genome wide association studies (GWAS) have been instrumental in the discovery of genes associated with obesity, including the fat mass and obesity-associated (*FTO*) gene [4]. A common variant in the *FTO* gene, rs9939609 has been identified that predisposes to type 2 diabetes through an effect on body mass index (BMI) [4–6]. *FTO* variants, including rs9939609 and rs1421085,

* Corresponding author. MRC Lifecourse Epidemiology Unit, University of Southampton, Southampton General Hospital, SO16 6YD, UK.
E-mail address: S.J.Barton@soton.ac.uk (S.J. Barton).

http://dx.doi.org/10.1016/j.placenta.2015.12.015

have been reported to be associated with BMI from age 5.5 years [4,7–11] and throughout adult life [4–6,12], although associations are less consistent in childhood. In addition, one study has shown that *FTO* genotype is associated with fat mass in the first 2 weeks of life [13].

Associations have also been observed between the genotype of a Single Nucleotide Polymorphism (SNP), rs17782313, near the *MC4R* gene [14,15] and adult obesity. This SNP is also associated with obesity in children [14,16,17] and one study reported an association with changes in BMI over the first two weeks of life [18]. *MC4R* genotype is thought to act through an influence on satiety and it is therefore interesting to investigate the effect of this SNP on the fetus where conventional appetite mechanisms cannot play a part.

FTO is an RNA demethylase and could act through regulation of mRNA stability [19]. However, no direct connection between obesity associated variants and *FTO* expression and function has been made. A recent study has demonstrated that obesity-associated non-coding variants in *FTO* affect the expression of the gene *IRX3* in humans, mice and zebrafish [20]. Obesity associated SNPs in *FTO* were found to be associated with the expression of *IRX3*, but not *FTO*, in the cerebellum of the human brain. *IRX3* is a homeobox gene involved in pattern formation in the early embryo and is expressed at much lower levels in later life [21]. This raises the possibility that the effects of *FTO* genotype on fetal growth and postnatal obesity may have originated through *IRX3* expression in embryonic life.

Recent research has shown that *FTO* plays a key role in the cellular sensing of amino acids and the regulation of cell growth and global mRNA translation through the mTORC1 pathway [22]. This could explain why carriers of the obesity predisposing SNPs in *FTO* not only consume more calories during test meals but also show an alteration in nutrient preference [23] and a higher dietary protein intake [24]. In utero, fetal growth is regulated by placental amino acid transporters as they control the supply of nutrients to the fetus. Thus *FTO* could potentially regulate fetal growth through a mechanism of altered placental amino acid transport.

The primary aim of this study was to investigate the association of obesity related SNPs (two *FTO* SNPs and one SNP near *MC4R*) with fetal growth throughout gestation in children of the Southampton Women's Survey (SWS) [25]. The secondary aim of this study was to investigate associations between *FTO* genotype, the expression of this gene in the placenta, a fetal tissue, and placental amino acid transporter expression.

2. Methods

Offspring of participants in the Southampton Women's Survey were studied [25]. Between 1998 and 2007, 3158 babies were born and data gathered on these babies both during the pregnancy via ultrasound scans and after the birth.

Gestational age of the SWS babies was determined using an algorithm based on last menstrual period, or where this was not available early ultrasound data. Using Acuson 128 XP, Aspen and Sequoia ultrasound machines calibrated to 1540 m/s; experienced research ultrasonographers used standardised anatomical landmarks to measure fetal head, abdominal circumference and biparietal diameter at 11, 19 and 34 weeks gestation.

The method of Royston [26] was used to calculate measures of fetal size, correcting for exact gestational age at measurement.

Maternal smoking during pregnancy was assessed by questionnaire in early and late pregnancy.

DNA was extracted from the cord blood of SWS babies by the salting out method and stored at −80 °C. 1990 children from the SWS cohort with DNA available were genotyped for the following polymorphisms: rs9939609 and rs1421085 located in the *FTO* gene on chromosome 16, and rs17782313 located near the *MC4R* gene on chromosome 18. Genotyping was performed by Kbiosciences (Hoddesdon, Herts, UK) using a custom SNP panel and an in-house calling algorithm. All three SNPs were found to be in HWE (chi squared p value $\geq$ 0.05); call rate was $\geq$ 97%; 5% duplicates were included with an error rate of 0%.

We analysed 99 SWS placentas based on availability of neonatal data and Caucasian ethnicity and collection within 30 min of delivery. Five villous tissue samples were selected using a stratified random sampling method and stored at −80 °C and powdered in a frozen tissue press. Total RNA was extracted from 30 mg tissue using the Rneasy fibrous tissue RNA isolation mini kit (Qiagen, UK) according to the manufacturer's instructions. The integrity of total RNA was confirmed by agarose gel electrophoresis. Total RNA (0.2 μg) was reverse transcribed with 0.5 μg random hexamer primer, 200 units M-MLV reverse transcriptase, 25 units recombinant RNasin ribonuclease inhibitor and 0.5 mM each of dATP, dCTP, dGTP and dTTP in a final reaction volume of 25 μl in 1 x MMLV reaction buffer (Promega, Wisconsin, USA). All 99 samples were produced in one batch to reduce variation.

Oligonucleotide probes and primers for *FTO* and the amino acid transporter genes were designed using the Roche (West Sussex, UK) ProbeFinder version 2.45 for human. Probes were supplied by Roche from the human universal probe library and primers were synthesised by Eurogentec (Seraing, Belgium). *FTO* (NM_001080432.2): Forward 5′- cacaacctcggtttagttcca -3′, Reverse 5′- aaatataatccaaggttcctgttgag -3′, probe #53. *ASCT2* (NM_005628.2): Forward 5′-gaggaatatcaccggaacca-3′, Reverse 5′-aggatgttcatcccctcca-3′, probe 43. *EAAT2* (NM_004171.3): Forward 5′-aaaatgctcattctccctctaatc-3′, Reverse 5′-gccactagccttagcatcca-3′, probe 78. *y⁺LAT2* (NM_001076785.1): Forward 5′-gctgtgatccccca-tacct-3′, Reverse 5′-ggcacagttcacaaatgtcag-3′, probe 66. Control genes were selected using the geNormTM human Housekeeping Gene Selection Kit (Primer Design Limited, Southampton, UK).

FTO and amino acid transporter mRNA expression levels were quantified by real-time reverse transcriptase PCR using a Roche LightCycler 480. For Roche universal probe library probes the cycle parameters were 95 °C for 5 min, followed by 45 cycles of 95 °C for 10 s, 60 °C for 30 s and 72 °C for 1 s. For primer design Perfect Probes (control genes) the cycle parameters were 95 °C for 10 min, followed by 40–50 cycles of 95 °C for 15 s, 50 °C for 30 s and 72 °C for 15 s. Intra-assay CV's for each gene were 5–8%. Each of the 99 samples was run on the same plate in triplicate. All mRNA levels are presented relative to the geometric mean of the three control genes, tyrosine 3-monooxygenase/tryptophan 5-monooxygenase activation protein, zeta polypeptide (YWHAZ), ubiquitin C (UBC) and topoisomerase (TOP1) [27].

2.1. Statistical analysis

Statistical procedures were performed in Stata version 12 (StataCorp, Texas, USA) and SPSS version 21 (IBM, Armonk, New York). Babies with congenital growth abnormalities and babies of mothers listed as having non-white ethnicity were excluded from analysis.

Anthropometric variables were checked for normality and then standardised to z-scores. For cross-sectional analysis genotypes were coded according to the additive model (0, 1 or 2 copies of the risk allele). The risk allele was considered to be A for *FTO* rs9939609, C for FTO rs1421085 and C for *MC4R* rs17782313. Univariate linear regressions were run with each genotype separately as predictor variable for each outcome (CRL, BPD, HC and AC), adjusting for sex, maternal smoking during pregnancy, pregnancy weight gain category (IOM (2009)) and pre-pregnancy maternal BMI. Results were expressed in SDs of change in outcome per unit increase in number of risk alleles.

Linear mixed-effect models [28] were used to conduct the longitudinal analyses. Intercept and gestational age were entered into the model as random effects and a genotype x gestational age interaction was also included to assess growth velocity in the measurements over time. Sex, maternal smoking, pregnancy weight gain category and pre-pregnancy maternal BMI were included as covariates. Genotype was included as a categorical covariate because exploratory analysis (see Fig. 1) indicated that this was more appropriate.

Partial correlations of *FTO* gene expression in the placenta and anthropometric variables, were calculated, controlling for sex. Neonatal variables were additionally adjusted for gestational age and mode of delivery (Caesarean or vaginal).

Bonferroni correction was applied to account for multiple testing for each of the main hypotheses tested.

3. Results

Analysis of fetal growth, was based on 1990 SWS singleton births with available fetal measurements and *FTO* or *MC4R* genotype or placental gene RNA data. Supplementary Figure 1 shows the numbers of SWS babies with available DNA and genotype. Table 1 shows summary statistics for the SWS cohort divided into groups according to whether genotype was available or not. There does not appear to be much difference between these groups.

The minor allele frequency for the *FTO* rs9939609 genotype in the SWS was A = 0.41, similar to the minor allele frequency quoted in HapMap [29] for Caucasians (CEU: A = 0.45).

3.1. Cross-sectional analysis

Table 2 shows there were a number of potentially significant associations at the 5% level between *FTO* and *MC4R* SNPs and fetal anthropometric measurements. While none of these associations remained significant at $p < 0.05$ after a strict Bonferroni correction, many of the fetal measures are correlated, so a Bonferroni correction is likely to be overly conservative. A retrospective power calculation indicated that to find a difference in means of fetal measure z-scores between genotype groups of 0.18, 1446 SWS children would be required to achieve a power of 90% at a 5% significance level.

Fig. 1 shows the means and 95% confidence intervals for biparietal diameter z-score at 11, 19 and 34 weeks for the *FTO* rs9939609 genotypes. At 11 weeks gestation, fetuses with the A:A genotype tended to have a lower biparietal diameter z-score than either the T:A genotype or the T:T genotype. At 19 weeks, biparietal diameter z-score was similar in the three genotypes. However, at 34 weeks gestation, fetuses with the A:A genotype had a higher biparietal diameter z-score than either of the other two genotypes. This implies a different fetal biparietal diameter growth trajectory in fetuses with the A:A genotype compared to the other two genotypes, with a smaller 11 week size followed by a faster growth velocity for the A:A genotype.

3.2. Linear mixed-effect models

Maternal weight gain category and sex were significantly associated with biparietal diameter, head circumference and abdominal circumference when included in linear mixed-effect models ($p < 0.0001$), with males having a larger measurement than females. Maternal smoking in pregnancy was associated with biparietal diameter and head circumference ($p \leq 0.05$), with the fetuses of mothers who did not smoke in pregnancy having a larger head size. Maternal smoking in pregnancy was not associated with

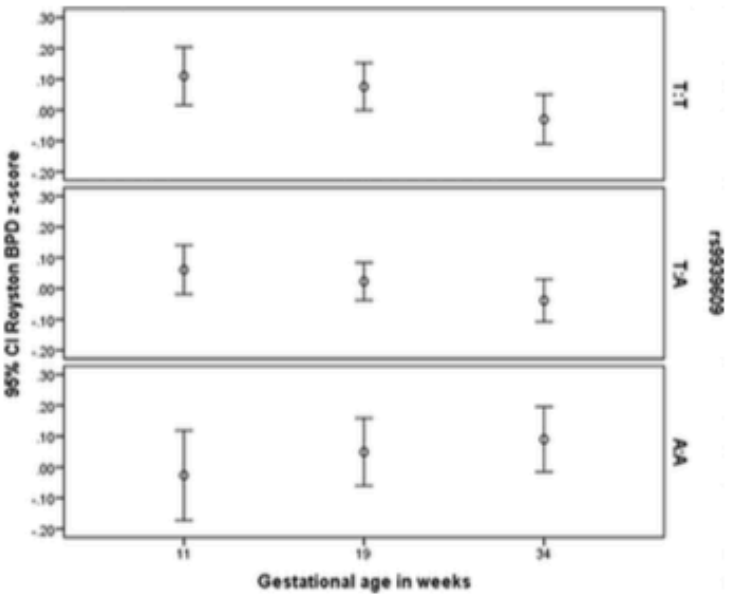

Fig. 1. The means and 95% CIs of Royston biparietal diameter z-score at all three available gestational ages for each rs9939609 genotype separately. For the T:T and T:A genotypes the biparietal diameter z-score decreases with increasing gestational age, however for the A:A genotype biparietal diameter z-score increases with gestational age. This shows that the biparietal diameter for the A:A genotype has a significantly different fetal growth trajectory, with fetal biparietal diameter growing faster than the T:T genotype. This was confirmed by linear mixed-effect modelling ($p = 0.0009$).

Table 1
Summary statistics for the Southampton Women's Survey Cohort, showing subgroups defined by availability of genotype

Variable	Genotype available			Genotype not available		
	N	Mean	Std. Dev.	N	Mean	Std. Dev.
11 week scan: Crown rump length (mm)	1593	53.48	9.07	808	53.32	8.88
11 week scan: Biparietal diameter (mm)	1247	18.72	2.59	609	18.66	2.52
19 week scan: Biparietal diameter (mm)	1912	45.5	2.54	961	45.75	2.49
34 week scan: Biparietal diameter (mm)	1869	86.98	3.6	896	87.09	3.51
11 week scan: Head circumference (mm)	1223	70.46	9.41	602	69.99	8.94
19 week scan: Head circumference (mm)	1912	168.43	8.53	960	168.79	8.53
34 week scan: Head circumference (mm)	1869	317.94	10.98	902	317.42	11.02
Birth: Head circumference (mm)	1955	350.33	13.47	848	348.74	14.87
11 week scan: Abdominal circumference (mm)	1152	55.99	7.91	555	55.96	7.42
19 week scan: Abdominal circumference (mm)	1902	146.46	8.95	960	146.97	8.75
34 week scan: Abdominal circumference (mm)	1958	307.87	15.42	940	307.22	15.02
Birth: Abdominal circumference (mm)	1953	318	20.18	846	315.22	21.86
Birth: Birthweight (g)	1976	3485.49	506.91	984	3373.68	623.77
Maternal pre-pregnancy BMI (kg/m2)	1964	25.35	4.77	999	25	4.78
Sex	1982	51.6% male		1008	52.5% male	
IOM maternal weight gain	1744	28.5% adequate		600	31.7% adequate	
maternal smoking	1944	16.9% yes		887	16.1% yes	
maternal pre-eclampsia	1982	2.8% yes		1008	3.3% yes	
maternal gestational diabetes	1982	1.1% yes		1008	1.0% yes	
SGA (WHO UK z-score)	1976	7.5% yes		984	8.8% yes	

Table 2
Regression results for cross-sectional analysis of fetal measurements, controlling for sex, maternal smoking during pregnancy, gestational weight gain and maternal BMI. Beta values represent change in fetal measure per risk allele, p values are uncorrected.

Variable	FTO rs9939609			FTO rs1421085			MC4R rs17782313		
	beta	se	p value	beta	se	p value	beta	se	p value
11 week scan: Royston CRL z-score	-0.066	0.04	0.099	-0.081	0.039	0.04	0.088	0.046	0.056
11 week scan: Royston BPD z-score	-0.074	0.043	0.083	-0.076	0.042	0.073	-0.026	0.049	0.592
19 week scan: Royston BPD z-score	-0.023	0.032	0.472	-0.033	0.032	0.299	0.025	0.038	0.509
34 week scan: Royston BPD z-score	0.034	0.035	0.33	0.022	0.034	0.526	0.05	0.04	0.211
11 week scan: Royston HC z-score	-0.11	0.042	0.013	-0.1	0.042	0.016	-0.061	0.049	0.22
19 week scan: Royston HC z-score	-0.031	0.032	0.332	-0.035	0.031	0.266	0.03	0.037	0.41
34 week scan: Royston HC z-score	-0.011	0.034	0.74	-0.016	0.034	0.644	0.059	0.04	0.136
11 week scan: Royston AC z-score	-0.071	0.047	0.128	-0.083	0.047	0.076	-0.048	0.053	0.373
19 week scan: Royston AC z-score	-0.027	0.032	0.396	-0.03	0.031	0.332	0.047	0.036	0.201
34 week scan: Royston AC z-score	-0.022	0.033	0.51	-0.025	0.033	0.446	0.054	0.039	0.16
Birth weight z-score (also controlling for GA)	0.004	0.03	0.888	0.012	0.03	0.678	0.052	0.035	0.142

abdominal circumference ($p > 0.05$). Maternal pre-pregnancy BMI was significantly associated with head circumference and abdominal circumference ($p \leq 0.007$) but not with biparietal diameter.

Linear mixed-effect models for two measures of head size, namely biparietal diameter and head circumference z-score, measured at 11, 19 and 34 weeks gestation, showed that *FTO* genotype rs9939609 was strongly associated with the growth velocity of head size, as there was a significant interaction between genotype and gestational age ($p = 0.0009$ for biparietal diameter and $p = 0.014$ for head circumference). This demonstrates that *FTO* genotypes have different growth trajectories. When abdominal circumference z-score was used as the dependent variable, there was no association between the growth velocity of abdominal circumference and *FTO* genotype. The results from linear mixed-effect models analysing the rs1421085 genotype were very similar to those using the rs9939609 genotype due to the high LD between them (data not shown). When the *MC4R* genotype rs17782313 was used as a predictor in the longitudinal models there were no significant associations between this SNP and the growth velocity of biparietal diameter and abdominal circumference, but there was an association between *MC4R* and head circumference growth velocity ($p = 0.013$) across the three gestational ages of 11, 19 and 34 weeks.

Interactions between *FTO* genotype and sex, and between *FTO* genotype and maternal smoking were investigated but no significant interactions were found ($p > 0.05$).

3.3. *Placental FTO relative RNA level*

Placental *FTO* relative RNA level was available for 99 offspring (mean 1.23, sd 0.27).

No association was observed between *FTO* genotype and relative RNA levels of *FTO* in the placenta (assessed by ANOVA, p value = 0.914, Fig. 2).

Table 3 shows partial correlations, controlling for sex, of fetal anthropometric measurements with placental *FTO* relative gene expression. Neonatal measures were adjusted for sex, gestational age and mode of delivery. Several fetal anthropometric measurements appeared highly correlated with the *FTO* expression in the placenta (Table 3, Fig. 3). Head circumference at 34 weeks was significantly associated with placental *FTO* relative gene expression after Bonferroni correction and neonatal head circumference showed a borderline association.

We also attempted to measure the levels of *IRX3* in the term human placenta, but found that levels were too low to measure reliably.

Associations were also found between *FTO* mRNA expression and the expression of placental amino acid transporters. *FTO*

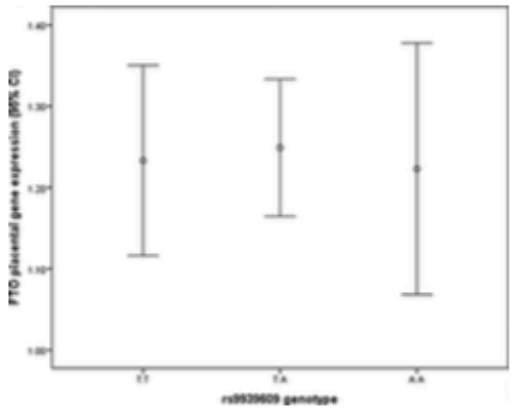

Fig. 2. There is no association between *FTO* genotype and expression of *FTO* in the placenta (ANOVA p value = 0.914).

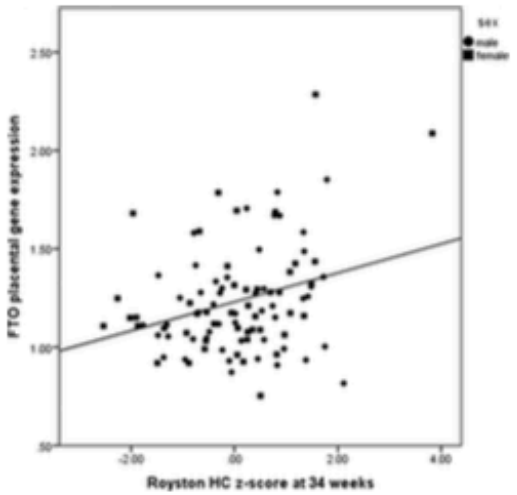

Fig. 3. The correlation between *FTO* relative RNA level in the placenta and 34 week Royston head circumference z-score (r = 0.324, p = 0.001, n = 98). Males were plotted using circles and females using squares.

expression was correlated with *ASCT2* (rho = 0.29, p = 0.004), *EAAT2* (rho = 0.22, p = 0.027) and *y*$^+$*LAT2* (rho = 0.37, p = 0.0002) mRNA expression.

4. Discussion

We have shown novel associations between *FTO* genotypes rs9939609 and rs1421085 and two measures of fetal head growth. From 11 to 34 weeks gestation fetuses with the homozygous *FTO* risk genotype (A:A or C:C) showed a higher velocity of biparietal diameter and head circumference growth in comparison with the other genotypes (T:A or T:C and T:T). Results were also in accordance with previous publications showing that maternal smoking is significantly associated with smaller fetal head size [30]. Trends were also identified in our cross-sectional analyses between the *FTO* SNPs and a SNP near *MC4R* and head circumference and crown-rump length, although these did not survive Bonferroni correction. For the above associations, the effect was in accordance with published literature for adults and babies [14,15,18] as the addition of each risk allele increased the measurements. We did not observe associations between the *MC4R* SNP and fetal growth trajectories of biparietal diameter and abdominal circumference, or between *FTO* SNPs and the fetal abdominal circumference growth trajectory.

Few authors have investigated the possible effect of *FTO* SNPs on fetal growth. Marsh et al. [31] reported that there was no evidence of any difference in fetal growth between the sexes and between rs9930609 genotype up to 28 weeks gestation. After 28 weeks gestation they observed a significant association between the rs9939609 A:A genotype and fetal growth restriction in non-smoking Australian mothers and fetal growth enhancement for mothers who smoked. This differs from our results as we did not observe a significant interaction between maternal smoking and genotype. However, the two sets of results are difficult to compare as our measurements were made by research staff following strict measurement protocols and we have considered the growth trajectory over all available gestational ages in the Southampton Women's Survey cohort; in contrast Marsh et al. used routinely collected data and analysed each trimester of pregnancy separately.

Placental function is an important determinant of fetal growth and may predispose to obesity later in life [32]. Our observations that *FTO* gene expression was correlated with birth weight are consistent with those of previous studies [33–35]. In addition we found novel associations between *FTO* gene expression and fetal growth parameters. However, placental *FTO* expression was not associated with either of the *FTO* genotypes in our SWS cohort,

Table 3
Partial correlations, controlling for sex, of anthropometric measurements and placental *FTO* relative RNA level

Variable	Correlation	Significance (2-tailed)	N
11 week scan: Royston CRL z-score	0.289	0.020	66
11 week scan: Royston BPD z-score	0.359	0.014	47
19 week scan: Royston BPD z-score	0.212	0.045	91
34 week scan: Royston BPD z-score	0.241	0.018	97
11 week scan: Royston HC z-score	0.205	0.172	47
19 week scan: Royston HC z-score	0.180	0.090	91
34 week scan: Royston HC z-score	0.324	0.001	98
11 week scan: Royston AC z-score	0.345	0.023	44
19 week scan: Royston AC z-score	0.179	0.091	91
34 week scan: Royston AC z-score	0.242	0.017	98
Birth weight (controlling for sex, GA and mode of delivery)	0.204	0.046	99
Neonatal HC (controlling for sex, GA and mode of delivery)	0.276	0.006	99
Neonatal AC (controlling for sex, GA and mode of delivery)	0.165	0.107	99

consistent with a previous report [34]. It is now thought that mutations in Intron 1 of the *FTO* gene control the expression of *IRX3* [20]. Our observation that FTO expression was independent of its genotype is consistent with the suggestion that the associations between FTO genotype and fetal growth are not mediated via FTO expression. If *FTO* is not regulated by genotype the question arises as to what is regulating *FTO* expression. *FTO* may be involved in nutrient sensing and regulate the mTOR pathway and, in the placenta, *FTO* gene expression may be related to maternal nutritional status. We observed that FTO gene expression was related to the expression of specific amino acid transporters in the placenta. As amino acid transfer is essential for fetal development this provides a potential mechanism by which FTO expression within the placenta may affect placental function and therefore fetal growth [36].

Consistent with the observation that *FTO* genotype is associated with fetal head growth; in humans a 'loss of function' mutation in the *FTO* gene has been found to induce postnatal growth retardation and malformations in the head and brain [37] Other recent studies have reported that carriers of common *FTO* gene polymorphisms show both a reduction in frontal lobe volume of the brain [38] and an impaired verbal fluency performance [39]. It was interesting that *FTO* genotype (thought to be controlling IRX3 gene expression) and *FTO* gene expression (which is independent of *FTO* genotype rs9939609) were both associated with fetal head growth in our study, however it is not clear whether there is a biological relationship underlying this. *FTO* knockout mice have altered head growth [40], but as knocking out the *FTO* gene also knocks out the *FTO* SNPs regulating *IRX3* it is not clear whether the effects of *FTO* knockout is due to the loss of *FTO* gene expression or the loss of regulation of the *IRX3* gene.

Fetal growth is a complex trait which is likely to be determined by multiple genetic [41] and environmental [42] factors. The cumulative effect of multiple variants could produce clinically relevant differences in growth. The detection of novel genetic variants associated with fetal growth has the potential to identify molecular mechanisms connected with growth and can yield insights of biological importance.

Author contributions

SJB contributed to the design of the study, performed the statistical analysis and interpretation of the results and drafted the article. SRC contributed to the statistical analysis, acquisition of data and interpretation of the results. MM contributed to acquisition of data, analysis and interpretation of data. JKC contributed to the design and interpretation of data. ASF contributed to the statistical analysis and interpretation of the data. CC contributed to the design, acquisition and interpretation of data. HMI contributed to acquisition of data, interpretation of data, revision and final approval of paper. JWH contributed to design, acquisition of data and interpretation of the data. RML contributed to sample collection, design and interpretation of the data. KMG contributed to design, analysis and interpretation of data. All authors reviewed and approved the final version of the article.

Conflict of interest

Keith Godfrey has received reimbursement for speaking at conferences sponsored by companies selling nutritional and pharmaceutical products. One of the research groups involved in this work are part of an academic consortium that has received funding from Abbott Nutrition, Nestec and Danone.

Ethical approval

The study was conducted according to the guidelines in the Declaration of Helsinki, and the Southampton and South West Hampshire Research Ethics Committee approved all procedures (276/97, 307/97).

Informed consent

Written informed consent was obtained from all participating women and by parents or guardians with parental responsibility on behalf of their children.

Acknowledgements

This work was supported by grants from the UK Medical Research Council (MC_U147585827); British Heart Foundation; Arthritis Research UK; National Osteoporosis Society; International Osteoporosis Foundation; Cohen Trust; National Institute for Health Research Musculoskeletal Biomedical Research Unit, University of Oxford; National Institute for Health Research Southampton Biomedical Research Centre, University of Southampton and University Hospital Southampton National Health Service Foundation Trust; and by the European Union's Seventh Framework Programme (FP7/2007–2013), project EarlyNutrition under grant agreement n°289346. The funders had no role in study design, data collection and analysis, decision to publish or preparation of manuscript.

We thank the mothers of the Southampton Women's Survey who gave us their time and acknowledge the work of the Southampton Women's Survey Study Group, and the team of dedicated research nurses and ancillary staff for their assistance.

Appendix A. Supplementary data

Supplementary data related to this article can be found at http://dx.doi.org/10.1016/j.placenta.2015.12.015.

References

[1] Organization WH, Childhood Overweight and Obesity. 2014. Available from: http://www.who.int/dietphysicalactivity/childhood/en/.
[2] C.J. Field, Early risk determinants and later health outcomes: implications for research prioritization and the food supply. Summary of the workshop, Am. J. Clin. Nutr. 89 (5) (2009) 1533s–1539s.
[3] H. Okubo, S.R. Crozier, N.C. Harvey, K.M. Godfrey, H.M. Inskip, C. Cooper, et al., Maternal dietary glycemic index and glycemic load in early pregnancy are associated with offspring adiposity in childhood: the Southampton Women's survey, Am. J. Clin. Nutr. 100 (2) (2014) 676–683.
[4] T.M. Frayling, N.J. Timpson, M.N. Weedon, E. Zeggini, R.M. Freathy, C.M. Lindgren, et al., A common variant in the FTO gene is associated with body mass index and predisposes to childhood and adult obesity, Science 316 (5826) (2007) 889–894.
[5] C. Dina, D. Meyre, S. Gallina, E. Durand, A. Korner, P. Jacobson, et al., Variation in FTO contributes to childhood obesity and severe adult obesity, Nat. Genet. 39 (6) (2007) 724–726.
[6] A. Scuteri, S. Sanna, W.M. Chen, M. Uda, G. Albai, J. Strait, et al., Genome-wide association scan shows genetic variants in the FTO gene are associated with obesity-related traits, PLoS Genet. 3 (7) (2007) e115.
[7] C. Bouchard, Childhood obesity: are genetic differences involved? Am. J. Clin. Nutr. 89 (5) (2009) 1494s–1501s.
[8] C. Bouchard, Defining the genetic architecture of the predisposition to obesity: a challenging but not insurmountable task, Am. J. Clin. Nutr. 91 (1) (2010) 5–6.
[9] C.M. Haworth, S. Carnell, E.L. Meaburn, O.S. Davis, R. Plomin, J. Wardle, Increasing heritability of BMI and stronger associations with the FTO gene over childhood, Obes. (Silver Spring, Md) 16 (12) (2008) 2663–2668.
[10] U. Sovio, D.O. Mook-Kanamori, N.M. Warrington, R. Lawrence, L. Briollais, C.N. Palmer, et al., Association between common variation at the FTO locus and changes in body mass index from infancy to late childhood: the complex nature of genetic association through growth and development, PLoS Genet. 7 (2) (2011) e1001307.

[11] J. Wardle, S. Carnell, C.M. Haworth, I.S. Farooqi, S. O'Rahilly, R. Plomin, Obesity associated genetic variation in FTO is associated with diminished satiety, J. Clin. Endocrinol. metabolism 93 (9) (2008) 3640–3643.
[12] T. Jess, E. Zimmermann, S.I. Kring, T. Berentzen, C. Holst, S. Toubro, et al., Impact on weight dynamics and general growth of the common FTO rs9939609: a longitudinal Danish cohort study, Int. J. Obes. 32 (9) (2008) 1388–1394.
[13] A. Lopez-Bermejo, C.J. Petry, M. Diaz, G. Sebastiani, F. de Zegher, D.B. Dunger, et al., The association between the FTO gene and fat mass in humans develops by the postnatal age of two weeks, J. Clin. Endocrinol. metabolism 93 (4) (2008) 1501–1505.
[14] R. Hardy, A.K. Wills, A. Wong, C.E. Elks, N.J. Wareham, R.J. Loos, et al., Life course variations in the associations between FTO and MC4R gene variants and body size, Hum. Mol. Genet. 19 (3) (2010) 545–552.
[15] L. Qi, P. Kraft, D.J. Hunter, F.B. Hu, The common obesity variant near MC4R gene is associated with higher intakes of total energy and dietary fat, weight change and diabetes risk in women, Hum. Mol. Genet. 17 (22) (2008) 3502–3508.
[16] N.J. Timpson, A. Sayers, G. Davey-Smith, J.H. Tobias, How does body fat influence bone mass in childhood? A mendelian randomization approach, JBone MinerRes. 24 (3) (2009) 522–533.
[17] F. Stutzmann, S. Cauchi, E. Durand, C. Calvacanti-Proenca, M. Pigeyre, A.L. Hartikainen, et al., Common genetic variation near MC4R is associated with eating behaviour patterns in European populations, Int. J. Obes. 33 (3) (2009) 373–378.
[18] C.J. Petry, A. Lopez-Bermejo, M. Diaz, G. Sebastiani, K.K. Ong, Z.F. de, et al., Association between a common variant near MC4R and change in body mass index develops by two weeks of age, Horm. Res. Paediatr. 73 (4) (2010) 275–280.
[19] G. Jia, Y. Fu, X. Zhao, Q. Dai, G. Zheng, Y. Yang, et al., N6-methyladenosine in nuclear RNA is a major substrate of the obesity-associated FTO, Nat. Chem. Biol. 7 (12) (2011) 885–887.
[20] S. Smemo, J.J. Tena, K.H. Kim, E.R. Gamazon, N.J. Sakabe, C. Gomez-Marin, et al., Obesity-associated variants within FTO form long-range functional connections with IRX3, Nature 507 (7492) (2014) 371–375.
[21] E. Robertshaw, K. Matsumoto, A. Lumsden, C. Kiecker, Irx3 and Pax6 establish differential competence for Shh-mediated induction of GABAergic and glutamatergic neurons of the thalamus, Proc. Natl. Acad. Sci. U. S. A. 110 (41) (2013) E3919–E3926.
[22] P. Gulati, M.K. Cheung, R. Antrobus, C.D. Church, H.P. Harding, Y.C. Tung, et al., Role for the obesity-related FTO gene in the cellular sensing of amino acids, Proc. Natl. Acad. Sci. U. S. A. 110 (7) (2013) 2557–2562.
[23] J.E. Cecil, R. Tavendale, P. Watt, M.M. Hetherington, C.N. Palmer, An obesity-associated FTO gene variant and increased energy intake in children, NEnglJMed 359 (24) (2008) 2558–2566.
[24] Q. Qi, T.O. Kilpelainen, M.K. Downer, T. Tanaka, C.E. Smith, I. Sluijs, et al., FTO genetic variants, dietary intake and body mass index: insights from 177 330 individuals, Hum. Mol. Genet. 23 (25) (2014) 6961–6972.
[25] H.M. Inskip, K.M. Godfrey, S.M. Robinson, C.M. Law, D.J. Barker, C. Cooper, Cohort profile: The Southampton Women's survey, IntJEpidemiol 35 (1) (2006) 42–48.
[26] P. Royston, Calculation of unconditional and conditional reference intervals for foetal size and growth from longitudinal measurements, StatMed 14 (13) (1995) 1417–1436.
[27] J.K. Cleal, P. Day, M.A. Hanson, R.M. Lewis, Measurement of housekeeping genes in human placenta, Placenta 30 (11) (2009) 1002–1003.
[28] N.M. Laird, J.H. Ware, Random-effects models for longitudinal data, Biometrics 38 (4) (1982) 963–974.
[29] K.A. Frazer, D.G. Ballinger, D.R. Cox, D.A. Hinds, L.L. Stuve, R.A. Gibbs, et al., A second generation human haplotype map of over 3.1 million SNPs, Nature 449 (7164) (2007) 851–861.
[30] R. Dobson, Smoking in Pregnancy Slows Growth of Baby's Head2007, 2007-03-08, 23:00:52. 499- p.
[31] J.A. Marsh, C.E. Pennell, N.M. Warrington, D. Mook-Kanamori, L. Briollais, S.J. Lye, et al., Fat mass and obesity-associated obesity-risk genotype is associated with lower foetal growth: an effect that is reversed in the offspring of smoking mothers, J. Dev. Orig. Health Dis. 3 (1) (2012) 10–20.
[32] R.M. Lewis, H. Demmelmair, R. Gaillard, K.M. Godfrey, S. Hauguel-de Mouzon, B. Huppertz, et al., The placental exposome: placental determinants of fetal adiposity and postnatal body composition, Ann. Nutr. metabolism 63 (3) (2013) 208–215.
[33] S. Mayeur, O. Cisse, A. Gabory, S. Barbaux, D. Vaiman, A. Vambergue, et al., Placental expression of the obesity-associated gene FTO is reduced by fetal growth restriction but not by macrosomia in rats and humans, J. Dev. Orig. Health Dis. 4 (2) (2013) 134–138.
[34] J. Bassols, A. Prats-Puig, M. Vazquez-Ruiz, M.M. Garcia-Gonzalez, M. Martinez-Pascual, P. Avelli, et al., Placental FTO expression relates to fetal growth, Int. J. Obes. 34 (9) (2010) 1365–1370.
[35] S.P. Sebert, M.A. Hyatt, L.L. Chan, M. Yiallourides, H.P. Fainberg, N. Patel, et al., Influence of prenatal nutrition and obesity on tissue specific fat mass and obesity-associated (FTO) gene expression, Reproduction 139 (1) (2010) 265–274.
[36] C.L. Paolini, A.M. Marconi, S. Ronzoni, M. Di Noio, P.V. Fennessey, G. Pardi, et al., Placental transport of leucine, phenylalanine, glycine, and proline in intrauterine growth-restricted pregnancies, J. Clin. Endocrinol. metabolism 86 (11) (2001) 5427–5432.
[37] S. Boissel, O. Reish, K. Proulx, H. Kawagoe-Takaki, B. Sedgwick, G.S. Yeo, et al., Loss-of-function mutation in the dioxygenase-encoding FTO gene causes severe growth retardation and multiple malformations, Am. J. Hum. Genet. 85 (1) (2009) 106–111.
[38] A.J. Ho, J.L. Stein, X. Hua, S. Lee, D.P. Hibar, A.D. Leow, et al., A commonly carried allele of the obesity-related FTO gene is associated with reduced brain volume in the healthy elderly, Proc. Natl. Acad. Sci. U. S. A. 107 (18) (2010) 8404–8409.
[39] C. Benedict, J.A. Jacobsson, E. Ronnemaa, M. Sallman-Almen, S. Brooks, B. Schultes, et al., The fat mass and obesity gene is linked to reduced verbal fluency in overweight and obese elderly men, Neurobiol. aging 32 (6) (2011) 1159 e1-5.
[40] X. Gao, Y.H. Shin, M. Li, F. Wang, Q. Tong, P. Zhang, The fat mass and obesity associated gene FTO functions in the brain to regulate postnatal growth in mice, PloS one 5 (11) (2010) e14005.
[41] M. Horikoshi, H. Yaghootkar, D.O. Mook-Kanamori, U. Sovio, H.R. Taal, B.J. Hennig, et al., New loci associated with birth weight identify genetic links between intrauterine growth and adult height and metabolism, Nat. Genet. 45 (1) (2013) 76–82.
[42] M. Hanson, K.M. Godfrey, K.A. Lillycrop, G.C. Burdge, P.D. Gluckman, Developmental plasticity and developmental origins of non-communicable disease: theoretical considerations and epigenetic mechanisms, Prog. biophys Mol. Biol. 106 (1) (2011) 272–280.

Appendix C Manufacturer protocols for RNA and DNA extraction kits

- RNazol® (SIGMA): http://www.sigmaaldrich.com/content/dam/sigma-aldrich/docs/Sigma/Bulletin/1/r4533bul.pdf
- miRNeasy kit (Qiagen): https://www.qiagen.com/us/resources/resourcedetail?id=632801fb-abc5-4e62-b954-ff51f126a34f&lang=en
- Quick-gDNA™ MiniPrep kit (Zymo Research): http://www.zymoresearch.com/downloads/dl/file/id/23/d3020i.pdf

List of References

1. Gauster, M., Desoye, G., Tötsch, M. & Hiden, U. The Placenta and Gestational Diabetes Mellitus. *Curr Diab Rep* **12**, 16-23 (2012).
2. Jansson, T. & Powell, T.L. Role of placental nutrient sensing in developmental programming. *Clinical obstetrics and gynecology* **56**, 591-601 (2013).
3. Barker, D.J. In utero programming of chronic disease. *Clinical science (London, England : 1979)* **95**, 115-128 (1998).
4. Barker, D.J. The origins of the developmental origins theory. *J Intern Med* **261**, 412-417 (2007).
5. Hanson, M.A. & D., G.P. Early Developmental Conditioning of Later Health and Disease: Physiology or Pathophysiology? *Physiol Rev* **94**, 1027-1076 (2014).
6. Barker, D.J.P. The Wellcome Foundation Lecture, 1994. The Fetal Origins of Adult Disease. *Proc Biol Sci* **262**, 37-43 (1995).
7. Godfrey, K.M., Gluckman, P.D. & Hanson, M.A. Developmental origins of metabolic disease: life course and intergenerational perspectives. *Trends Endocrinol Metab* **21**, 199-205 (2010).
8. Barker, D.J.P. & Osmond, C. Infant mortality, childhood nutrition, and ischaemic heart disease in England and Wales. *Lancet (London, England)* **327**, 1077-1081 (1986).
9. Barker, D.J., Winter, P.D., Osmond, C., Margetts, B. & Simmonds, S.J. Weight in infancy and death from ischaemic heart disease. *Lancet (London, England)* **2**, 577-580 (1989).
10. Barker, D.J., Bull, A.R., Osmond, C. & Simmonds, S.J. Fetal and placental size and risk of hypertension in adult life. *BMJ (Clinical research ed.)* **301**, 259-262 (1990).
11. Hales, C.N.*, et al.* Fetal and infant growth and impaired glucose tolerance at age 64. *BMJ (Clinical research ed.)* **303**, 1019-1022 (1991).
12. Hales, C.N. & Barker, D.J. Type 2 (non-insulin-dependent) diabetes mellitus: the thrifty phenotype hypothesis. *Diabetologia* **35**, 595-601 (1992).
13. Barker, D.J.P. The origins of the developmental origins theory. *J Intern Med* **261**, 412-417 (2007).
14. Roseboom, T., de Rooij, S. & Painter, R. The Dutch famine and its long-term consequences for adult health. *Early Hum Dev* **82**, 485-491 (2006).
15. Roseboom, T.J.*, et al.* Effects of prenatal exposure to the Dutch famine on adult disease in later life: an overview. *Mol Cell Endocrinol* **185**, 93-98 (2001).
16. Roseboom, T.J.*, et al.* Coronary heart disease after prenatal exposure to the Dutch famine, 1944–45. *Heart* **84**, 595-598 (2000).
17. Lopuhaä, C.E.*, et al.* Atopy, lung function, and obstructive airways disease after prenatal exposure to famine. *Thorax* **55**, 555-561 (2000).
18. Ravelli, A.C.J.*, et al.* Glucose tolerance in adults after prenatal exposure to famine. *Lancet (London, England)* **351**, 173-177 (1998).
19. Stanner, S.A. & Yudkin, J.S. Fetal programming and the Leningrad Siege study. *Twin research : the official journal of the International Society for Twin Studies* **4**, 287-292 (2001).
20. Dikensoy, E.*, et al.* The effect of Ramadan fasting on maternal serum lipids, cortisol levels and fetal development. *Arch Gynecol Obstet* **279**, 119-123 (2008).
21. Alwasel, S.H.*, et al.* Changes in Placental Size during Ramadan. *Placenta* **31**, 607-610 (2010).
22. Sakar, M.N.*, et al.* Ramadan fasting and pregnancy: implications for fetal development in summer season. *J Perinat Med* **43**, 319-323 (2015).
23. Inskip, H.M.*, et al.* Cohort profile: The Southampton Women's Survey. *Int J Epidemiol* **35**, 42-48 (2006).

24. Moon, R.J.*, et al.* Maternal Plasma Polyunsaturated Fatty Acid Status in Late Pregnancy Is Associated with Offspring Body Composition in Childhood. *J Clin Endocrinol Metab* **98**, 299-307 (2013).
25. Crozier, S.R.*, et al.* Maternal vitamin D status in pregnancy is associated with adiposity in the offspring: findings from the Southampton Women's Survey. *Am J Clin Nutr* **96**, 57-63 (2012).
26. Harvey, N.C.*, et al.* Intrauterine growth and postnatal skeletal development: findings from the Southampton Women's Survey. *Paediatr Perinat Epidemiol* **26**, 34-44 (2012).
27. Cleal, J.K.*, et al.* Placental amino acid transport may be regulated by maternal vitamin D and vitamin D-binding protein: results from the Southampton Women's Survey. *The British journal of nutrition* **113**, 1903-1910 (2015).
28. Holroyd, C.R.*, et al.* Placental size at 19 weeks predicts offspring bone mass at birth: Findings from the Southampton Women's Survey. *Placenta* **33**, 623-629.
29. Ozaki, T., Nishina, H., Hanson, M.A. & Poston, L. Dietary restriction in pregnant rats causes gender-related hypertension and vascular dysfunction in offspring. *The Journal of physiology* **530**, 141-152 (2001).
30. Brawley, L.*, et al.* Dietary protein restriction in pregnancy induces hypertension and vascular defects in rat male offspring. *Pediatr Res* **54**, 83-90 (2003).
31. Gonzalez, P.N.*, et al.* Chronic Protein Restriction in Mice Impacts Placental Function and Maternal Body Weight before Fetal Growth. *PLoS ONE* **11**, e0152227 (2016).
32. Jones, H.N.*, et al.* High-fat diet before and during pregnancy causes marked up-regulation of placental nutrient transport and fetal overgrowth in C57/BL6 mice. *FASEB J* **23**, 271-278 (2009).
33. Cagampang, F.R., Poore, K.R. & Hanson, M.A. Developmental origins of the metabolic syndrome: body clocks and stress responses. *Brain, behavior, and immunity* **25**, 214-220 (2011).
34. Jones, H.N., Powell, T.L. & Jansson, T. Regulation of placental nutrient transport--a review. *Placenta* **28**, 763-774 (2007).
35. Suarez, S.S. Chapter 3 - Gamete and Zygote Transport. in *Knobil and Neill's Physiology of Reproduction (Third Edition)* (ed. Wassarman, J.D.) 113-145 (Academic Press, St Louis, 2006).
36. Wu, G., Bazer, F.W., Cudd, T.A., Meininger, C.J. & Spencer, T.E. Maternal nutrition and fetal development. *J Nutr* **134**, 2169-2172 (2004).
37. SF, G. Developmental Biology. in *Early Mammalian Development*, Vol. 2016 (ed. 6th) (htttp://http://www.ncbi.nlm.nih.gov/book/NBK10052/, 2000).
38. Sharma, D., Shastri, S., Farahbakhsh, N. & Sharma, P. Intrauterine growth restriction - part 1. *The journal of maternal-fetal & neonatal medicine : the official journal of the European Association of Perinatal Medicine, the Federation of Asia and Oceania Perinatal Societies, the International Society of Perinatal Obstet*, 1-11 (2016).
39. Devaskar, S.U. & Chu, A. Intrauterine Growth Restriction: Hungry for an Answer. *Physiology (Bethesda, Md.)* **31**, 131-146 (2016).
40. Lewis, R.M., Cleal, J.K. & Hanson, M.A. Review: Placenta, evolution and lifelong health. *Placenta* **33 Suppl**, S28-32 (2012).
41. Cohen, E., Wong, F.Y., Horne, R.S. & Yiallourou, S.R. Intrauterine growth restriction: impact on cardiovascular development and function throughout infancy. *Pediatr Res* (2016).
42. W, H.O. *Promoting optimal fetal development* (World Health Organization, 2006).
43. Sayers, S.M., Lancaster, P.A.L. & Whitehead, C.L. Fetal Growth Restriction: Causes and Outcomes. in *Sexual and Reproductive Health: A Public Health Perspective* (ed. Look, P.V.) (Elsevier, 2014).
44. Gaccioli, F. & Lager, S. Placental Nutrient Transport and Intrauterine Growth Restriction. *Front Physiol* **7**, 40 (2016).

45. Norman, M. Low birth weight and the developing vascular tree: a systematic review. *Acta paediatrica (Oslo, Norway : 1992)* **97**, 1165-1172 (2008).
46. Iruretagoyena, J.I.*, et al.* Cardiac dysfunction is associated with altered sarcomere ultrastructure in intrauterine growth restriction. *Am J Obstet Gynecol* **210**, 550.e551-550.e557 (2014).
47. Valsamakis, G., Kanaka-Gantenbein, C., Malamitsi-Puchner, A. & Mastorakos, G. Causes of intrauterine growth restriction and the postnatal development of the metabolic syndrome. *Annals of the New York Academy of Sciences* **1092**, 138-147 (2006).
48. Langer, O. Fetal macrosomia: etiologic factors. *Clinical obstetrics and gynecology* **43**, 283-297 (2000).
49. Jolly, M.C., Sebire, N.J., Harris, J.P., Regan, L. & Robinson, S. Risk factors for macrosomia and its clinical consequences: a study of 350,311 pregnancies. *Eur J Obstet Gynecol Reprod Biol* **111**, 9-14 (2003).
50. Oken, E. & Gillman, M.W. Fetal Origins of Obesity. *Obes Res* **11**, 496-506 (2003).
51. Baird, J.*, et al.* Being big or growing fast: systematic review of size and growth in infancy and later obesity. *BMJ (Clinical research ed.)* **331**, 929 (2005).
52. Murphy, V.E., Smith, R., Giles, W.B. & Clifton, V.L. Endocrine Regulation of Human Fetal Growth: The Role of the Mother, Placenta, and Fetus. *Endocr Rev* **27**, 141-169 (2006).
53. Milani, S.*, et al.* Differences in Size at Birth Are Determined by Differences in Growth Velocity during Early Prenatal Life. *Pediatr Res* **57**, 205-210 (2005).
54. Polanl, P.E. Chromosomal and Other Genetic Influences on Birth Weight Variation. in *Ciba Foundation Symposium 27 - Size at Birth* 127-164 (John Wiley & Sons, Ltd, 2008).
55. Bleker, O.P., Buimer, M., van der Post, J.A. & van der Veen, F. Ted (G.J.) Kloosterman: on intrauterine growth. The significance of prenatal care. Studies on birth weight, placental weight and placental index. *Placenta* **27**, 1052-1054 (2006).
56. Carrera, J.M., Serra, B., Scazzochio, E. & Carrera, M. Regulating factors. in *Textbook of Perinatal Medicine, Second Edition* 1218-1228 (CRC Press, 2006).
57. Fowden, A.L. The role of insulin in fetal growth. *Early Hum Dev* **29**, 177-181 (1992).
58. Forhead, A.J. & Fowden, A.L. Thyroid hormones in fetal growth and prepartum maturation. *J Endocrinol* **221**, R87-R103 (2014).
59. Shields, B.M., Knight, B.A., Hill, A., Hattersley, A.T. & Vaidya, B. Fetal thyroid hormone level at birth is associated with fetal growth. *J Clin Endocrinol Metab* **96**, E934-938 (2011).
60. Allen, A.L., Fretz, P.B., Card, C.E. & Doige, C.E. The effects of partial thyroidectomy on the development of the equine fetus. *Equine veterinary journal* **30**, 53-59 (1998).
61. McIntosh, G.H.*, et al.* The effect of maternal and fetal thyroidectomy on fetal brain development in the sheep. *Neuropathology and applied neurobiology* **9**, 215-223 (1983).
62. Batchelor, D., Lewis, R., Breier, B., Gluckman, P. & Skinner, S. Fetal rat lung epithelium has a functional growth hormone receptor coupled to tyrosine kinase activity and insulin-like growth factor binding protein-2 production. *J Mol Endocrinol* **21**, 73-84 (1998).
63. Lewis, R.M., Poore, K.R. & Godfrey, K.M. The role of the placenta in the developmental origins of health and disease—Implications for practice. *Rev Gynaecol Perinatal Pract* **6**, 70-79 (2006).
64. Cross, J.C. Placental function in development and disease. *Reproduction, fertility, and development* **18**, 71-76 (2006).
65. Burton, G.J., Kaufmann, P. & Huppertz, B. Chapter 5 - Anatomy and Genesis of the Placenta. in *Knobil and Neill's Physiology of Reproduction (Third Edition)* (ed. Wassarman, J.D.) 189-243 (Academic Press, St Louis, 2006).

66. Verma, U. & Verma, N. An Overview of Development, Function and Diseases of the Placenta in *The placenta: development, function and diseases* (ed. Nicholson, R.) 1-30 (Nova Science publishers, 2013).
67. Mayhew, T.M. Stereology and the Placenta: Where's the Point? – A Review. *Placenta* **27**, S17-25 (2006).
68. Lager, S. & Powell, T.L. Regulation of Nutrient Transport across the Placenta. *J Pregnancy* **2012**, 14 (2012).
69. Gaccioli, F., Lager, S., Powell, T.L. & Jansson, T. Placental transport in response to altered maternal nutrition. *Journal of developmental origins of health and disease* **4**, 101-115 (2013).
70. Carter, A.M. Animal Models of Human Placentation – A Review. *Placenta* **28**, S41-S47 (2007).
71. Rossant, J. & Cross, J.C. Placental development: lessons from mouse mutants. *Nature reviews. Genetics* **2**, 538-548 (2001).
72. Watson, E.D. & Cross, J.C. Development of structures and transport functions in the mouse placenta. *Physiology (Bethesda, Md.)* **20**, 180-193 (2005).
73. Cross, J.C. How to make a placenta: Mechanisms of trophoblast cell differentiation in mice – A Review. *Placenta* **26**, S3-S9 (2005).
74. Simmons, D.G., Fortier, A.L. & Cross, J.C. Diverse subtypes and developmental origins of trophoblast giant cells in the mouse placenta. *Dev Biol* **304**, 567-578 (2007).
75. Evain-Brion, D. & Malassine, A. Human placenta as an endocrine organ. *Growth Horm IGF Res* **13**, S34 - 37 (2003).
76. Hunt, J.S., McIntire, R.H. & Petroff, M.G. Chapter 51 - Immunobiology of Human Pregnancy. in *Knobil and Neill's Physiology of Reproduction (Third Edition)* (ed. Wassarman, J.D.) 2759-2785 (Academic Press, St Louis, 2006).
77. Cleal, J.K.*, et al.* Facilitated transporters mediate net efflux of amino acids to the fetus across the basal membrane of the placental syncytiotrophoblast. *The Journal of physiology* **589**, 987-997 (2011).
78. Díaz, P., Powell, T.L. & Jansson, T. The Role of Placental Nutrient Sensing in Maternal-Fetal Resource Allocation. *Biol Reprod* **91**, 82 (2014).
79. Atkinson, D.E., Boyd, R.D.H. & Sibley, C.P. Chapter 52 - Placental Transfer. in *Knobil and Neill's Physiology of Reproduction (Third Edition)* (ed. Wassarman, J.D.) 2787-2846 (Academic Press, St Louis, 2006).
80. Illsley, N.P. Glucose transporters in the human placenta. *Placenta* **21**, 14-22 (2000).
81. Day, P.E., Cleal, J.K., Lofthouse, E.M., Hanson, M.A. & Lewis, R.M. What factors determine placental glucose transfer kinetics? *Placenta* **34**, 953-958 (2013).
82. Jansson, T., Cowley, E.A. & Illsley, N.P. Cellular localization of glucose transporter messenger RNA in human placenta. *Reproduction, fertility, and development* **7**, 1425-1430 (1995).
83. Jansson, T., Wennergren, M. & Illsley, N.P. Glucose transporter protein expression in human placenta throughout gestation and in intrauterine growth retardation. *J Clin Endocrinol Metab* **77**, 1554-1562 (1993).
84. Ericsson, A., Hamark, B., Powell, T.L. & Jansson, T. Glucose transporter isoform 4 is expressed in the syncytiotrophoblast of first trimester human placenta. *Human reproduction (Oxford, England)* **20**, 521-530 (2005).
85. Doege, H., Schurmann, A., Bahrenberg, G., Brauers, A. & Joost, H.G. GLUT8, a novel member of the sugar transport facilitator family with glucose transport activity. *The Journal of biological chemistry* **275**, 16275-16280 (2000).
86. Bibee, K.P., Illsley, N.P. & Moley, K.H. Asymmetric syncytial expression of GLUT9 splice variants in human term placenta and alterations in diabetic pregnancies. *Reproductive sciences (Thousand Oaks, Calif.)* **18**, 20-27 (2011).

87. Dawson, P.A*., et al.* Sequence and functional analysis of GLUT10: a glucose transporter in the Type 2 diabetes-linked region of chromosome 20q12-13.1. *Molecular genetics and metabolism* **74**, 186-199 (2001).
88. Cleal, J.K. & Lewis, R.M. The Mechanisms and Regulation of Placental Amino Acid Transport to the Human Foetus. *Journal of neuroendocrinology* **20**, 419-426 (2008).
89. Cetin, I*., et al.* Maternal and fetal amino acid concentrations in normal pregnancies and in pregnancies with gestational diabetes mellitus. *Am J Obstet Gynecol* **192**, 610-617 (2005).
90. Lewis, R.M*., et al.* Review: Modelling placental amino acid transfer − From transporters to placental function. *Placenta* **34**, S46-S51 (2013).
91. Desforges, M*., et al.* The SNAT4 isoform of the system A amino acid transporter is functional in human placental microvillous plasma membrane. *The Journal of physiology* **587**, 61-72 (2009).
92. Jansson, T. Amino Acid Transporters in the Human Placenta. *Pediatr Res* **49**, 141-147 (2001).
93. Matthews, J. Expression of Non-Organelle Glutamate Transporters to Support Peripheral Tissue Function. in *Glutamate Receptors in Peripheral Tissue: Excitatory Transmission Outside the CNS* (eds. Gill, S. & Pulido, O.) 47-75 (Springer US, 2005).
94. Day, P.E*., et al.* Partitioning of glutamine synthesised by the isolated perfused human placenta between the maternal and fetal circulations. *Placenta* **34**, 1223-1231 (2013).
95. Lofthouse, E.M. University of Southampton (2014).
96. Cariappa, R., Heath-Monnig, E. & Smith, C.H. Isoforms of amino acid transporters in placental syncytiotrophoblast: plasma membrane localization and potential role in maternal/fetal transport. *Placenta* **24**, 713-726 (2003).
97. Kudo, Y. & Boyd, C. Human placental amino acid transporter genes: expression and function. *Reproduction (Cambridge, England)* **124**, 593-600 (2002).
98. Lofthouse, E.M*., et al.* Glutamate cycling may drive organic anion transport on the basal membrane of human placental syncytiotrophoblast. *The Journal of physiology* **593**, 4549-4559 (2015).
99. Innis, S.M. Essential fatty acids in growth and development. *Progress in lipid research* **30**, 39-103 (1991).
100. Duttaroy, A.K. Transport of fatty acids across the human placenta: a review. *Progress in lipid research* **48**, 52-61 (2009).
101. Doege, H. & Stahl, A. Protein-mediated fatty acid uptake: novel insights from in vivo models. *Physiology (Bethesda, Md.)* **21**, 259-268 (2006).
102. Campbell, F.M., Taffesse, S., Gordon, M.J. & Dutta-Roy, A.K. Plasma membrane fatty-acid-binding protein in human placenta: identification and characterization. *Biochem Biophys Res Commun* **209**, 1011-1017 (1995).
103. Bonen, A., Chabowski, A., Luiken, J.J.F.P. & Glatz, J.F.C. Mechanisms and Regulation of Protein-Mediated Cellular Fatty Acid Uptake: Molecular, Biochemical, and Physiological Evidence. *Physiology* **22**, 15-28 (2007).
104. Haggarty, P. Placental Regulation of Fatty Acid Delivery and its Effect on Fetal Growth—A Review. *Placenta* **23**, S28-S38 (2002).
105. Dancis, J., Jansen, V. & Levitz, M. Transfer across perfused human placenta. IV. Effect of protein binding on free fatty acids. *Pediatr Res* **10**, 5-10 (1976).
106. Haggarty, P., Page, K., Abramovich, D.R., Ashton, J. & Brown, D. Long-chain polyunsaturated fatty acid transport across the perfused human placenta. *Placenta* **18**, 635-642 (1997).
107. Lewis, R.M., Hanson, M.A. & Burdge, G.C. Umbilical venous-arterial plasma composition differences suggest differential incorporation of fatty acids in NEFA and cholesteryl ester pools. *The British journal of nutrition* **106**, 463-467 (2011).

108. Edwards, D., Jones, C.J., Sibley, C.P. & Nelson, D.M. Paracellular permeability pathways in the human placenta: a quantitative and morphological study of maternal-fetal transfer of horseradish peroxidase. *Placenta* **14**, 63-73 (1993).
109. Erlebacher, A. Immunology of the maternal-fetal interface. *Annual review of immunology* **31**, 387-411 (2013).
110. Petraglia, F., Florio, P. & Torricelli, M. CHAPTER 53 - Placental Endocrine Function A2 - Neill, Jimmy D. in *Knobil and Neill's Physiology of Reproduction (Third Edition)* 2847-2897 (Academic Press, St Louis, 2006).
111. Petraglia, F., Lim, A.T. & Vale, W. Adenosine 3',5'-monophosphate, prostaglandins, and epinephrine stimulate the secretion of immunoreactive gonadotropin-releasing hormone from cultured human placental cells. *J Clin Endocrinol Metab* **65**, 1020-1025 (1987).
112. Petraglia, F., Vaughan, J. & Vale, W. Steroid hormones modulate the release of immunoreactive gonadotropin-releasing hormone from cultured human placental cells. *J Clin Endocrinol Metab* **70**, 1173-1178 (1990).
113. Barnea, E.R. & Kaplan, M. Spontaneous, gonadotropin-releasing hormone-induced, and progesterone-inhibited pulsatile secretion of human chorionic gonadotropin in the first trimester placenta in vitro. *J Clin Endocrinol Metab* **69**, 215-217 (1989).
114. Petraglia, F., Vaughan, J. & Vale, W. Inhibin and activin modulate the release of gonadotropin-releasing hormone, human chorionic gonadotropin, and progesterone from cultured human placental cells. *Proceedings of the National Academy of Sciences of the United States of America* **86**, 5114-5117 (1989).
115. Pepe, G.J. & Albrecht, E.D. Actions of placental and fetal adrenal steroid hormones in primate pregnancy. *Endocr Rev* **16**, 608-648 (1995).
116. Kumar, P. & Magon, N. Hormones in pregnancy. *Niger Med J* **53**, 179-183 (2012).
117. Mullis, P.E*., et al.* Aromatase deficiency in a female who is compound heterozygote for two new point mutations in the P450arom gene: impact of estrogens on hypergonadotropic hypogonadism, multicystic ovaries, and bone densitometry in childhood. *J Clin Endocrinol Metab* **82**, 1739-1745 (1997).
118. Ito, Y., Fisher, C.R., Conte, F.A., Grumbach, M.M. & Simpson, E.R. Molecular basis of aromatase deficiency in an adult female with sexual infantilism and polycystic ovaries. *Proceedings of the National Academy of Sciences of the United States of America* **90**, 11673-11677 (1993).
119. Sferruzzi-Perri, A.N. & Camm, E.J. The Programming Power of the Placenta. *Front Physiol* **7**(2016).
120. Jansson, N*., et al.* Maternal hormones linking maternal body mass index and dietary intake to birth weight. *Am J Clin Nutr* **87**, 1743-1749 (2008).
121. Belkacemi, L., Jelks, A., Chen, C.H., Ross, M.G. & Desai, M. Altered placental development in undernourished rats: role of maternal glucocorticoids. *Reprod Biol Endocrinol* **9**, 105 (2011).
122. Jansson, N*., et al.* Down-regulation of placental transport of amino acids precedes the development of intrauterine growth restriction in rats fed a low protein diet. *The Journal of physiology* **576**, 935-946 (2006).
123. Jansson, N*., et al.* Activation of Placental mTOR Signaling and Amino Acid Transporters in Obese Women Giving Birth to Large Babies. *J Clin Endocrinol Metab* **98**, 105-113 (2013).
124. Jansson, T., Ekstrand, Y., Bjorn, C., Wennergren, M. & Powell, T.L. Alterations in the activity of placental amino acid transporters in pregnancies complicated by diabetes. *Diabetes* **51**, 2214-2219 (2002).
125. Hayward, C.E*., et al.* Effect of maternal age and growth on placental nutrient transport: potential mechanisms for teenagers' predisposition to small-for-gestational-

age birth? *American journal of physiology. Endocrinology and metabolism* **302**, E233-242 (2012).
126. Ategbo, J.M.*, et al.* Modulation of adipokines and cytokines in gestational diabetes and macrosomia. *J Clin Endocrinol Metab* **91**, 4137-4143 (2006).
127. Lowe, L.P.*, et al.* Inflammatory mediators and glucose in pregnancy: results from a subset of the Hyperglycemia and Adverse Pregnancy Outcome (HAPO) Study. *J Clin Endocrinol Metab* **95**, 5427-5434 (2010).
128. Jones, H.N., Jansson, T. & Powell, T.L. IL-6 stimulates system A amino acid transporter activity in trophoblast cells through STAT3 and increased expression of SNAT2. *Am J Physiol Cell Physiol* **297**, C1228-1235 (2009).
129. Lager, S.*, et al.* Oleic acid stimulates system A amino acid transport in primary human trophoblast cells mediated by toll-like receptor 4. *J Lipid Res* **54**, 725-733 (2013).
130. Jones, H.N., Jansson, T. & Powell, T.L. Full-Length Adiponectin Attenuates Insulin Signaling and Inhibits Insulin-Stimulated Amino Acid Transport in Human Primary Trophoblast Cells. *Diabetes* **59**, 1161-1170 (2010).
131. Giovannelli, A., Greenwood, S.L., Desforges, M., Sibley, C.P. & Petraglia, F. Corticotrophin-releasing factor and urocortin inhibit system A activity in term human placental villous explants. *Placenta* **32**, 99-101 (2011).
132. Jansson, N., Greenwood, S.L., Johansson, B.R., Powell, T.L. & Jansson, T. Leptin stimulates the activity of the system A amino acid transporter in human placental villous fragments. *J Clin Endocrinol Metab* **88**, 1205-1211 (2003).
133. von Versen-Höynck, F., Rajakumar, A., Parrott, M.S. & Powers, R.W. Leptin Affects System A Amino Acid Transport Activity in the Human Placenta: Evidence for STAT3 Dependent Mechanisms. *Placenta* **30**, 361-367 (2009).
134. Vaughan, O.R., Sferruzzi-Perri, A.N. & Fowden, A.L. Maternal corticosterone regulates nutrient allocation to fetal growth in mice. *The Journal of physiology* **590**, 5529-5540 (2012).
135. Constancia, M.*, et al.* Placental-specific IGF-II is a major modulator of placental and fetal growth. *Nature* **417**, 945-948 (2002).
136. Strid, H., Care, A., Jansson, T. & Powell, T. Parathyroid hormone-related peptide (38-94) amide stimulates ATP-dependent calcium transport in the Basal plasma membrane of the human syncytiotrophoblast. *J Endocrinol* **175**, 517-524 (2002).
137. Strid, H., Bucht, E., Jansson, T., Wennergren, M. & Powell, T.L. ATP dependent Ca2+ transport across basal membrane of human syncytiotrophoblast in pregnancies complicated by intrauterine growth restriction or diabetes. *Placenta* **24**, 445-452 (2003).
138. Laplante, M. & Sabatini, David M. mTOR Signaling in Growth Control and Disease. *Cell* **149**, 274-293 (2012).
139. Roos, S., Lagerlöf, O., Wennergren, M., Powell, T.L. & Jansson, T. Regulation of amino acid transporters by glucose and growth factors in cultured primary human trophoblast cells is mediated by mTOR signaling. *Am J Physiol Cell Physiol* **297**, C723-C731 (2009).
140. Roos, S., Kanai, Y., Prasad, P.D., Powell, T.L. & Jansson, T. Regulation of placental amino acid transporter activity by mammalian target of rapamycin. *Am J Physiol Cell Physiol* **296**, C142-C150 (2009).
141. Roos, S.*, et al.* Mammalian target of rapamycin in the human placenta regulates leucine transport and is down-regulated in restricted fetal growth. *The Journal of physiology* **582**, 449-459 (2007).
142. Rosario, F.J., Kanai, Y., Powell, T.L. & Jansson, T. Mammalian target of rapamycin signalling modulates amino acid uptake by regulating transporter cell surface abundance in primary human trophoblast cells. *The Journal of physiology* **591**, 609-625 (2013).

143. Dimasuay, K.G., Boeuf, P., Powell, T.L. & Jansson, T. Placental Responses to Changes in the Maternal Environment Determine Fetal Growth. *Front Physiol* **7**(2016).
144. Hardie, D.G., Ross, F.A. & Hawley, S.A. AMPK: a nutrient and energy sensor that maintains energy homeostasis. *Nat Rev Mol Cell Biol* **13**, 251-262 (2012).
145. Ma, Y.*, et al.* Upregulation of growth signaling and nutrient transporters in cotyledons of early to mid-gestational nutrient restricted ewes. *Placenta* **32**, 255-263 (2011).
146. Gaccioli, F.*, et al.* Maternal Overweight Induced by a Diet with High Content of Saturated Fat Activates Placental mTOR and eIF2alpha Signaling and Increases Fetal Growth in Rats. *Biol Reprod* **89**, 96, 91-11 (2013).
147. Skeffington, K.L.*, et al.* Hypoxia, AMPK activation and uterine artery vasoreactivity. *The Journal of physiology* **594**, 1357-1369 (2016).
148. Kilberg, M.S., Shan, J. & Su, N. ATF4-dependent transcription mediates signaling of amino acid limitation. *Trends Endocrinol Metab* **20**, 436-443 (2009).
149. Strakovsky, R.S., Zhou, D. & Pan, Y.X. A low-protein diet during gestation in rats activates the placental mammalian amino acid response pathway and programs the growth capacity of offspring. *J Nutr* **140**, 2116-2120 (2010).
150. Yung, H.-w.*, et al.* Evidence of Placental Translation Inhibition and Endoplasmic Reticulum Stress in the Etiology of Human Intrauterine Growth Restriction. *Am j Pathol* **173**, 451-462 (2008).
151. Jansson, T., Aye, I.L. & Goberdhan, D.C. The emerging role of mTORC1 signaling in placental nutrient-sensing. *Placenta* **33** e23-29 (2012).
152. Dina, C.*, et al.* Variation in FTO contributes to childhood obesity and severe adult obesity. *Nat Genet* **39**, 724-726 (2007).
153. Gulati, P.*, et al.* Role for the obesity-related FTO gene in the cellular sensing of amino acids. *Proceedings of the National Academy of Sciences of the United States of America* **110**, 2557-2562 (2013).
154. Cheung, M.K., Gulati, P., O'Rahilly, S. & Yeo, G.S. FTO expression is regulated by availability of essential amino acids. *Int J Obes (Lond)* **37**, 744-747 (2013).
155. Jia, G.*, et al.* N6-methyladenosine in nuclear RNA is a major substrate of the obesity-associated FTO. *Nature chemical biology* **7**, 885-887 (2011).
156. Wang, X.*, et al.* N6-methyladenosine-dependent regulation of messenger RNA stability. *Nature* **505**, 117-120 (2014).
157. Bassols, J.*, et al.* Placental FTO expression relates to fetal growth. *Int J Obes (Lond)* **34**, 1365-1370 (2010).
158. Sébert, S.P.*, et al.* Influence of prenatal nutrition and obesity on tissue specific fat mass and obesity-associated (FTO) gene expression. *Reproduction (Cambridge, England)* **139**, 265-274 (2010).
159. Bass, J. & Takahashi, J.S. Circadian integration of metabolism and energetics. *Science* **330**, 1349-1354 (2010).
160. Ko, C.H. & Takahashi, J.S. Molecular components of the mammalian circadian clock. *Hum Mol Genet* **15** R271-277 (2006).
161. Albrecht, U. Invited review: regulation of mammalian circadian clock genes. *J Appl Physiol* **92**, 1348-1355 (2002).
162. Lee, C., Etchegaray, J.P., Cagampang, F.R., Loudon, A.S. & Reppert, S.M. Posttranslational mechanisms regulate the mammalian circadian clock. *Cell* **107**, 855-867 (2001).
163. Waddell, B.J., Wharfe, M.D., Crew, R.C. & Mark, P.J. A rhythmic placenta? Circadian variation, clock genes and placental function. *Placenta* **33**, 533-539 (2012).
164. Torres-Farfan, C.*, et al.* A circadian clock entrained by melatonin is ticking in the rat fetal adrenal. *Endocrinology* **152**, 1891-1900 (2011).
165. Nakagawa, T. & Guarente, L. Sirtuins at a glance. *J Cell Sci* **124**, 833-838 (2011).

166. Asher, G.*, et al.* SIRT1 regulates circadian clock gene expression through PER2 deacetylation. *Cell* **134**, 317-328 (2008).
167. Schwer, B. & Verdin, E. Conserved Metabolic Regulatory Functions of Sirtuins. *Cell Metabolism* **7**, 104-112 (2008).
168. Shoba, B.*, et al.* Function of Sirtuins in Biological Tissues. *Anat Rec (Hoboken)* **292**, 536-543 (2009).
169. Michan, S. & Sinclair, D. Sirtuins in mammals: insights into their biological function. *Biochem J* **404**, 1-13 (2007).
170. Nogueiras, R.*, et al.* Sirtuin 1 and Sirtuin 3: Physiological Modulators of Metabolism. *Physiol Rev* **92**, 1479-1514 (2012).
171. Houtkooper, R.H., Pirinen, E. & Auwerx, J. Sirtuins as regulators of metabolism and healthspan. *Nat Rev Mol Cell Biol* **13**, 225-238 (2012).
172. Matsuda, S., Kobayashi, M. & Kitagishi, Y. Expression and Function of PPARs in Placenta. *PPAR Res* **2013**, 7 (2013).
173. Toren, F., Chu-Xia, D. & Raul, M. Recent progress in the biology and physiology of sirtuins. *Nature* **460**, 587-591 (2009).
174. Sato, R. Sterol metabolism and SREBP activation. *Archives of biochemistry and biophysics* **501**, 177-181 (2010).
175. Saben, J.*, et al.* Maternal obesity is associated with a lipotoxic placental environment. *Placenta* **35**, 171-177 (2014).
176. Espenshade, P.J. SREBPs: sterol-regulated transcription factors. *J Cell Sci* **119**, 973-976 (2006).
177. Goldstein, J.L., DeBose-Boyd, R.A. & Brown, M.S. Protein sensors for membrane sterols. *Cell* **124**, 35-46 (2006).
178. Woollett, L.A. Where does fetal and embryonic cholesterol originate and what does it do? *Annu Rev Nutr* **28**, 97-114 (2008).
179. Bengoechea-Alonso, M.T. & Ericsson, J. SREBP in signal transduction: cholesterol metabolism and beyond. *Current opinion in cell biology* **19**, 215-222 (2007).
180. Marseille-Tremblay, C.*, et al.* Impact of maternal circulating cholesterol and gestational diabetes mellitus on lipid metabolism in human term placenta. *Molecular reproduction and development* **75**, 1054-1062 (2008).
181. Isganaitis, E.*, et al.* Accelerated postnatal growth increases lipogenic gene expression and adipocyte size in low-birth weight mice. *Diabetes* **58**, 1192-1200 (2009).
182. Lou, H.*, et al.* Assisted reproductive technologies impair the expression and methylation of insulin-induced gene 1 and sterol regulatory element-binding factor 1 in the fetus and placenta. *Fertility and sterility* **101**, 974-980.e972 (2014).
183. Clarson, L.H.*, et al.* Activity and expression of Na(+)-K(+)-ATPase in human placental cytotrophoblast cells in culture. *The Journal of physiology* **497**, 735-743 (1996).
184. Myren, M., Mose, T., Mathiesen, L. & Knudsen, L.E. The human placenta--an alternative for studying foetal exposure. *Toxicology in vitro : an international journal published in association with BIBRA* **21**, 1332-1340 (2007).
185. King, A., Thomas, L. & Bischof, P. Cell culture models of trophoblast II: trophoblast cell lines--a workshop report. *Placenta* **21** S113-119 (2000).
186. Hannan, N.J., Paiva, P., Dimitriadis, E. & Salamonsen, L.A. Models for study of human embryo implantation: choice of cell lines? *Biol Reprod* **82**, 235-245 (2010).
187. Vähäkangas, K. & Myllynen, P. Experimental methods to study human transplacental exposure to genotoxic agents. *Mutat Res* **608**, 129-135 (2006).
188. Simner, C.L. University of Southampton (2015).
189. Graham, F.L., Smiley, J., Russell, W.C. & Nairn, R. Characteristics of a Human Cell Line Transformed by DNA from Human Adenovirus Type 5. *The Journal of general virology* **36**, 59-72 (1977).

190. Durnin, J.V.G.A. & Womersley, J. Body fat assessed from total body density and its estimation from skinfold thickness: measurements on 481 men and women aged from 16 to 72 Years. *The British journal of nutrition* **32**, 77-97 (1974).
191. Crozier, S.R.*, et al.* Weight gain in pregnancy and childhood body composition: findings from the Southampton Women's Survey. *Am J Clin Nutr* **91**, 1745-1751 (2010).
192. Harvey, N.C.*, et al.* MAVIDOS Maternal Vitamin D Osteoporosis Study: study protocol for a randomized controlled trial. The MAVIDOS Study Group. *Trials* **13**, 13 (2012).
193. Janssen, A.B.*, et al.* Placental expression of imprinted genes varies with sampling site and mode of delivery. *Placenta* **36**, 790-795 (2015).
194. Gardosi J, F.A. GROW Customised Centile Calculator - GROW-CCC software v 6.7.5. (Gestation network).
195. Garber Md, P.A.J., Duncan Md, T.G., Goodman Md, A.M., Mills Rn, B.S.N.D.J. & Rohlf Md, J.L. Efficacy of Metformin in Type II Diabetes: Results of a Double-Blind, Placebo-controlled, Dose-Response Trial. *Am J Med* **103**, 491-497 (1997).
196. Tanaka, S. Derivation and culture of mouse trophoblast stem cells in vitro. *Methods in molecular biology (Clifton, N.J.)* **329**, 35-44 (2006).
197. VanGuilder, H.D., Vrana, K.E. & Freeman, W.M. Twenty-five years of quantitative PCR for gene expression analysis. *BioTechniques* **44**, 619-626 (2008).
198. Arya, M.*, et al.* Basic principles of real-time quantitative PCR. *Expert Rev Mol Diagn* **5**, 209-219 (2005).
199. Guescini, M., Sisti, D., Rocchi, M.B.L., Stocchi, L. & Stocchi, V. A new real-time PCR method to overcome significant quantitative inaccuracy due to slight amplification inhibition. *BMC Bioinformatics* **9**, 1-12 (2008).
200. Bustin, S.A.*, et al.* The MIQE Guidelines: Minimum Information for Publication of Quantitative Real-Time PCR Experiments. *Clin Chem* **55**, 611-622 (2009).
201. Cleal, J.K., Day, P., Hanson, M.A. & Lewis, R.M. Measurement of Housekeeping Genes in Human Placenta. *Placenta* **30**, 1002-1003 (2009).
202. Cleal, J.K., Day, P.L., Hanson, M.A. & Lewis, R.M. Sex Differences in the mRNA Levels of Housekeeping Genes in Human Placenta. *Placenta* **31**, 556-557 (2010).
203. Vandesompele, J.*, et al.* Accurate normalization of real-time quantitative RT-PCR data by geometric averaging of multiple internal control genes. *Genome biology* **3**, Research0034 (2002).
204. McClive, P.J. & Sinclair, A.H. Rapid DNA extraction and PCR-sexing of mouse embryos. *Molecular reproduction and development* **60**, 225-226 (2001).
205. Trapnell, C.*, et al.* Differential gene and transcript expression analysis of RNA-seq experiments with TopHat and Cufflinks. *Nature Protocols* **7**, 562-578 (2012).
206. Vlachos, I.S.*, et al.* DIANA-miRPath v3.0: deciphering microRNA function with experimental support. *Nucleic Acids Res* (2015).
207. Kohn, M.a.J., MS. . Sample size calculators. Sample size calculators for designing clinical research. Vol. 2016.
208. Heslehurst, N., Rankin, J., Wilkinson, J.R. & Summerbell, C.D. A nationally representative study of maternal obesity in England, UK: trends in incidence and demographic inequalities in 619 323 births, 1989-2007. *Int J Obes* **34**, 420-428 (2010).
209. King, J.C. Maternal Obesity, Metabolism, and Pregnancy Outcomes. *Annu Rev Nutr* **26**, 271-291 (2006).
210. Crowther, C.A.*, et al.* Effect of treatment of gestational diabetes mellitus on pregnancy outcomes. *The New England journal of medicine* **352**, 2477-2486 (2005).
211. George, A.*, et al.* Comparison of neonatal outcomes in women with gestational diabetes with moderate hyperglycaemia on metformin or glibenclamide--a randomised controlled trial. *The Australian & New Zealand journal of obstetrics & gynaecology* **55**, 47-52 (2015).

212. Balsells, M.*, et al.* Glibenclamide, metformin, and insulin for the treatment of gestational diabetes: a systematic review and meta-analysis. *BMJ (Clinical research ed.)* **350**, h102 (2015).
213. Lee, H.-y., Wei, D. & Loeken, M.R. Lack of metformin effect on mouse embryo AMPK activity: implications for metformin treatment during pregnancy. *Diabetes Metab Res Rev* **30**, 23-30 (2014).
214. Bruce, K.D.*, et al.* Maternal high-fat feeding primes steatohepatitis in adult mice offspring, involving mitochondrial dysfunction and altered lipogenesis gene expression. *Hepatology* **50**, 1796-1808 (2009).
215. Lanham, S.A.*, et al.* Maternal high-fat diet: effects on offspring bone structure. *Osteoporos Int* **21**, 1703-1714 (2010).
216. Barnea, M.*, et al.* Metformin affects the circadian clock and metabolic rhythms in a tissue-specific manner. *Biochim Biophys Acta* **1822**, 1796-1806 (2012).
217. Salomäki, H.*, et al.* Prenatal Metformin Exposure in Mice Programs the Metabolic Phenotype of the Offspring during a High Fat Diet at Adulthood. *PLoS ONE* **8**, e56594 (2013).
218. Berulava, T.*, et al.* FTO levels affect RNA modification and the transcriptome. *Eur J Hum Genet* **21**, 317-323 (2013).
219. Kennaway, D.J., Boden, M.J. & Varcoe, T.J. Circadian rhythms and fertility. *Mol Cell Endocrinol* **349**, 56-61 (2012).
220. Krämer, A., Green, J., Pollard, J. & Tugendreich, S. Causal Analysis Approaches in Ingenuity Pathway Analysis (IPA). *Bioinformatics* (2013).
221. Bruce, K.D.*, et al.* Altered cellular redox status, sirtuin abundance and clock gene expression in a mouse model of developmentally primed NASH. *Biochim Biophys Acta* **1861**, 584-593 (2016).
222. Rosario, F.J., Powell, T.L. & Jansson, T. Activation of placental insulin and mTOR signaling in a mouse model of maternal obesity associated with fetal overgrowth. *American journal of physiology. Regulatory, integrative and comparative physiology* **310**, R87-93 (2016).
223. Rena, G., Pearson, E.R. & Sakamoto, K. Molecular mechanism of action of metformin: old or new insights? *Diabetologia* **56**, 1898-1906 (2013).
224. Glueck, C.J.*, et al.* Height, weight, and motor-social development during the first 18 months of life in 126 infants born to 109 mothers with polycystic ovary syndrome who conceived on and continued metformin through pregnancy. *Human reproduction (Oxford, England)* **19**, 1323-1330 (2004).
225. Eyal, S.*, et al.* Pharmacokinetics of metformin during pregnancy. *Drug metabolism and disposition: the biological fate of chemicals* **38**, 833-840 (2010).
226. Spaulonci, C.P., Bernardes, L.S., Trindade, T.C., Zugaib, M. & Francisco, R.P. Randomized trial of metformin vs insulin in the management of gestational diabetes. *Am J Obstet Gynecol* **209**, 34.e31-37 (2013).
227. Rowan , J.A., Hague , W.M., Gao , W., Battin , M.R. & Moore , M.P. Metformin versus Insulin for the Treatment of Gestational Diabetes. *The New England journal of medicine* **358**, 2003-2015 (2008).
228. Niromanesh, S.*, et al.* Metformin compared with insulin in the management of gestational diabetes mellitus: a randomized clinical trial. *Diabetes research and clinical practice* **98**, 422-429 (2012).
229. Tertti, K.*, et al.* The role of organic cation transporters (OCTs) in the transfer of metformin in the dually perfused human placenta. *European journal of pharmaceutical sciences : official journal of the European Federation for Pharmaceutical Sciences* **39**, 76-81 (2010).

230. Kovo, M., Haroutiunian, S., Feldman, N., Hoffman, A. & Glezerman, M. Determination of metformin transfer across the human placenta using a dually perfused ex vivo placental cotyledon model. *Eur J Obstet Gynecol Reprod Biol* **136**, 29-33 (2008).
231. Staud, F. & Ceckova, M. Regulation of drug transporter expression and function in the placenta. *Expert opinion on drug metabolism & toxicology* **11**, 533-555 (2015).
232. Hemauer, S.J., Patrikeeva, S.L., Nanovskaya, T.N., Hankins, G.D. & Ahmed, M.S. Role of human placental apical membrane transporters in the efflux of glyburide, rosiglitazone, and metformin. *Am J Obstet Gynecol* **202**, 383.e381-387 (2010).
233. Musi, N.*, et al.* Metformin Increases AMP-Activated Protein Kinase Activity in Skeletal Muscle of Subjects With Type 2 Diabetes. *Diabetes* **51**, 2074 (2002).
234. Zhou, G.*, et al.* Role of AMP-activated protein kinase in mechanism of metformin action. *J Clin Invest* **108**, 1167-1174 (2001).
235. Hawley, S.A.*, et al.* Use of Cells Expressing γ Subunit Variants to Identify Diverse Mechanisms of AMPK Activation. *Cell Metab* **11**, 554-565 (2010).
236. Hundal, R.S.*, et al.* Mechanism by which metformin reduces glucose production in type 2 diabetes. *Diabetes* **49**, 2063-2069 (2000).
237. Pavan, B.*, et al.* Circadian clocks regulate adenylyl cyclase activity rhythms in human RPE cells. *Biochem Biophys Res Commun* **350**, 169-173 (2006).
238. Balsalobre, A., Damiola, F. & Schibler, U. A serum shock induces circadian gene expression in mammalian tissue culture cells. *Cell* **93**, 929-937 (1998).
239. Wolfe, D.*, et al.* Nutrient sensor-mediated programmed nonalcoholic fatty liver disease in low birthweight offspring. *Am J Obstet Gynecol* **207**, 308.e301-306 (2012).
240. Frayling, T.M.*, et al.* A Common Variant in the FTO Gene Is Associated with Body Mass Index and Predisposes to Childhood and Adult Obesity. *Science* **316**, 889-894 (2007).
241. Qi, L.*, et al.* Fat Mass–and Obesity-Associated (FTO) Gene Variant Is Associated With Obesity: Longitudinal Analyses in Two Cohort Studies and Functional Test. *Diabetes* **57**, 3145-3151 (2008).
242. Karasawa, S.*, et al.* Association of the common fat mass and obesity associated (FTO) gene polymorphism with obesity in a Japanese population. *Endocr J* **57**, 293-301 (2010).
243. Thorleifsson, G.*, et al.* Genome-wide association yields new sequence variants at seven loci that associate with measures of obesity. *Nat Genet* **41**, 18-24 (2009).
244. Chang, Y.-C.*, et al.* Common Variation in the Fat Mass and Obesity-Associated (FTO) Gene Confers Risk of Obesity and Modulates BMI in the Chinese Population. *Diabetes* **57**, 2245-2252 (2008).
245. Yeo, G.S.H. & O'Rahilly, S. Uncovering the biology of FTO. *Mol Metab* **1**, 32-36 (2012).
246. Fischer, J.*, et al.* Inactivation of the Fto gene protects from obesity. *Nature* **458**, 894-898 (2009).
247. Church, C.*, et al.* Overexpression of Fto leads to increased food intake and results in obesity. *Nat Genet* **42**, 1086-1092 (2010).
248. Barton, J.S.*, et al.* Variants in the FTO Gene significantly influence growth trajectories of fetal measurements in children of the Southampton Women's Survey *Placenta* **38**, 100-106 (2016).
249. López-Bermejo, A.*, et al.* The Association between the FTO Gene and Fat Mass in Humans Develops by the Postnatal Age of Two Weeks. *J Clin Endocrinol Metab* **93**, 1501-1505 (2008).
250. Smemo, S.*, et al.* Obesity-associated variants within FTO form long-range functional connections with IRX3. *Nature* **507**, 371-375 (2014).
251. Gerken, T.*, et al.* The Obesity-Associated FTO Gene Encodes a 2-Oxoglutarate-Dependent Nucleic Acid Demethylase. *Science* **318**, 1469-1472 (2007).
252. Jansson, T., Ekstrand, Y., Wennergren, M. & Powell, T.L. Placental glucose transport in gestational diabetes mellitus. *Am J Obstet Gynecol* **184**, 111-116 (2001).

253. Cecil, J.E., Tavendale, R., Watt, P., Hetherington, M.M. & Palmer, C.N.A. An Obesity-Associated FTO Gene Variant and Increased Energy Intake in Children. *New England Journal of Medicine* **359**, 2558-2566 (2008).
254. Pan, T. N6-methyl-adenosine modification in messenger and long non-coding RNA. *Trends Biochem Sci* **38**, 204-209 (2013).
255. Zhao, X.*, et al.* FTO-dependent demethylation of N6-methyladenosine regulates mRNA splicing and is required for adipogenesis. *Cell Res* **24**, 1403-1419 (2014).
256. Niu, Y.*, et al.* N6-methyl-adenosine (m6A) in RNA: an old modification with a novel epigenetic function. *Genomics, proteomics & bioinformatics* **11**, 8-17 (2013).
257. Alarcon, C.R., Lee, H., Goodarzi, H., Halberg, N. & Tavazoie, S.F. N6-methyladenosine marks primary microRNAs for processing. *Nature* **519**, 482-485 (2015).
258. Guttman, M. & Rinn, J.L. Modular regulatory principles of large non-coding RNAs. *Nature* **482**, 339-346 (2012).
259. Xu, C.*, et al.* Structural basis for selective binding of m6A RNA by the YTHDC1 YTH domain. *Nature chemical biology* **10**, 927-929 (2014).
260. Merkestein, M.*, et al.* FTO influences adipogenesis by regulating mitotic clonal expansion. *Nature communications* **6**, 6792 (2015).
261. Berulava, T., Rahmann, S., Rademacher, K., Klein-Hitpass, L. & Horsthemke, B. N6-adenosine methylation in MiRNAs. *PLoS ONE* **10**, e0118438 (2015).
262. Winter, J., Jung, S., Keller, S., Gregory, R.I. & Diederichs, S. Many roads to maturity: microRNA biogenesis pathways and their regulation. *Nat Cell Biol* **11**, 228-234 (2009).
263. Lofthouse, E.M.*, et al.* Phenylalanine transfer across the isolated perfused human placenta: an experimental and modeling investigation. *American journal of physiology. Regulatory, integrative and comparative physiology* **310**, R828 (2016).
264. Syngelaki, A.*, et al.* Metformin versus Placebo in Obese Pregnant Women without Diabetes Mellitus. *The New England journal of medicine* **374**, 434-443 (2016).
265. Sayed DA, T.H., Cagampang F, Byrne CD, Swales JG, Thomas P. The effect of maternal metformin treatment in murine obese pregnancy on fetal hepatic development. in *Physiology*, Vol. 31 PCB169 (Proceedings of physiological society, London, UK, 2014).